

**PHYSICO-CHEMICAL PROPERTIES OF
SOME POLY(METHYL
METHACRYLATE) BLENDS**

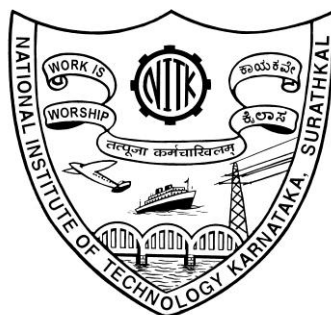
THESIS

Submitted in partial fulfillment of the requirements for the
degree of

DOCTOR OF PHILOSOPHY

by

SREEKANTHA JOIS H. S.



**DEPARTMENT OF CHEMISTRY
NATIONAL INSTITUTE OF TECHNOLOGY
KARNATAKA, SURATHKAL,
MANGALORE – 575025**

November, 2014

**PHYSICO-CHEMICAL PROPERTIES OF
SOME POLY(METHYL
METHACRYLATE) BLENDS**

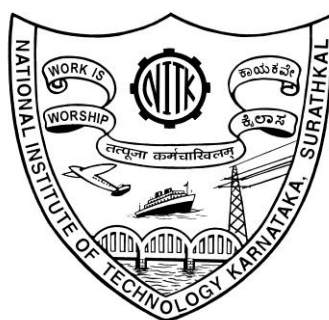
THESIS

Submitted in partial fulfillment of the requirements for the
degree of

DOCTOR OF PHILOSOPHY

by

SREEKANTHA JOIS H. S.



**DEPARTMENT OF CHEMISTRY
NATIONAL INSTITUTE OF TECHNOLOGY
KARNATAKA, SURATHKAL,
MANGALORE – 575025**

November, 2014

D E C L A R A T I O N

by the

Ph. D. RESEARCH SCHOLAR

I hereby declare that the Research Thesis entitled “**Physico-chemical properties of some Poly(methyl methacrylate) blends**” which is being submitted to the **National Institute of Technology Karnataka, Surathkal** in partial fulfilment of the requirements for the award of the Degree of **Doctor of Philosophy** in the department of **Chemistry** is a bonafide report of the research work carried out by me. The material contained in this Research Thesis has not been submitted to any University or Institution for the award of any degree.

Sreekantha Jois H. S.

(Reg. No.: **080827CY08F03**)

Department of Chemistry

National Institute of Technology Karnataka, Surathkal.

Place: NITK, Surathkal.

Date:

C E R T I F I C A T E

This is to certify that the Research Thesis entitled “**Physico-chemical properties of some Poly(methyl methacrylate) blends**” submitted by **Sreekantha Jois H. S.** (Register Number: **080827CY08F03**) as the record of the research work carried out by him, is accepted as the **Research Thesis** submission in partial fulfilment of the requirements for the award of degree of **Doctor of Philosophy**.

Prof. D. Krishna Bhat

Research Guide

Dept. of Chemistry, NITK, Surathkal.

(Name and Signature
with Date and Seal)

Chairman – DRPC
(Signature with Date and Seal)

DEDICATED TO

MY

PARENTS

AND

TEACHERS

ACKNOWLEDGEMENTS

First and foremost, I would like to thank my research supervisor Prof. D. Krishna Bhat, whose enthusiasm made the work a lot easier. His perfect balance between laboratory freedom and supervision, gave me a lot of liberty to pursue my own ideas and to work independently. I am fortunate enough to work under the guidance of a very helpful and understanding supervisor. I owe my deepest gratitude to him for his patience and belief in me.

I would like to thank my RPAC committee members, Dr. Arun M. Isloor, Department of Chemistry and Prof. Vijay Desai, Department of Mechanical Engineering, for spending their valuable time in evaluating my progress and providing thoughtful suggestions.

I sincerely thank the former Heads of the Department, Prof. A. Nithyananda Shetty, Prof. A. Vasudeva Adhikari and ex-HOD Prof. A. Chithranjan Hegde as well as the present Head of the Department, Prof. B. Ramachandra Bhat for providing me with the laboratory facilities. I am also thankful to Dr. D. Uday Kumar, Dr. Darshak R. Trivedi and Dr. Sib Sankar Mal for their moral support and help.

I am grateful to the non-teaching staff, Mrs. Kasthuri, Mr. Ashok, Mr. Pradeep, Mr. Harish, Mr. Prashanth, Ms. Shilpa Kunder, Ms. Swarna, Mrs. Sharmila and Mrs. Deepa who were prompt enough to lend me a helping hand at times of need.

I would like to thank NITK, Surathkal for providing me with Research Scholarship that provided the necessary financial support for this research.

I would like to thank all the Research Scholar friends for making my research days at NITK a memorable one. I whole heartedly thank each one of them and wish them success in their research work and all future endeavors.

I would like to thank each and every member of my family whose blessings and good wishes worked like a guiding lamp on the road leading to my goal.

Finally, I would like to thank all those who have directly or indirectly contributed for the completion for the completion of this research work.

Thank you

SREEKANTHA JOIS H. S.

ABSTRACT

In this thesis, studies on plasticized and non-plasticized polymer blends of Poly (methyl methacrylate) (PMMA) and Cellulose acetate (CA) and its derivatives with varying blend compositions prepared by solution casting method is presented. Miscibility, water uptake, ion exchange capacity (IEC), proton conductivity and dielectric properties of these blends have been studied. Dimethyl formamide (DMF) is used as solvent. Dimethyl phthalate (DMP), Diethyl phthalate (DEP), Dipropyl phthalate (DPP), Dibutyl phthalate (DBP) and Propylene carbonate (PC) have been used as plasticizers. Fourier transform infrared spectra (FTIR) and Differential scanning calorimetric (DSC) measurements have been used to analyze the miscibility of the plasticized and non-plasticized blends. Up to PMMA with CA and its derivatives with a composition of 50/50 for both plasticized and non-plasticized blends, water uptake amount of the blends showed an increasing trend. Ion exchange capacity for both plasticized and non-plasticized blends decreased with increase in PMMA content of the blends. The variations in the blend properties have been attributed to the presence of specific interactions and exchangeable groups in the blend system. Impedance analysis has been performed in order to calculate the blend conductivity. The proton conductivity of the plasticized and non-plasticized blends is in the order of $10^{-3} \text{ S cm}^{-1}$. The dielectric constant and dielectric loss measurements of the blends indicated the absence of any relaxation phenomenon in the blend system. Among the plasticized blend system, polymer blends with low percentage (2.5%, 5%, 7.5% and 10%) of PC, DMP, DEP, DPP and DBP have shown decreasing trend for water uptake test and an increasing trend for ion exchange capacity test as well as proton conductivity measurement. This attributes to the effect of plasticizers on the studied blend system.

Keywords: Polymer blends, PMMA, CA, miscibility, conductivity.

CONTENTS

Chapter 1

INTRODUCTION

1.1 POLYMER BLENDS	1
1.1.1 Factors in Miscibility and Immiscibility	2
1.1.2 Glass-transition Temperature	3
1.1.3 Dependences of Glass-transition Temperature	3
1.2 METHODOLOGY	4
1.2.1 Solution or Die Casting	4
1.3 CHARACTERIZATION TECHNIQUES	4
1.3.1 Spectral Properties	4
1.3.1.1 Infrared spectroscopy	4
1.3.2 Thermal Properties	5
1.3.2.1 Differential scanning calorimetry (DSC)	5
1.3.3 Electrochemical Impedance Spectroscopy	6
1.3.3.1 Proton conductivity mechanism	6
1.3.4 Electrical Properties	7
1.3.4.1 Dielectric constant	7
1.3.4.2 The complex dielectric constant and dielectric loss	9
1.4 COMPOUNDING OF POLYMERS	9
1.4.1 Plasticizers	10
1.4.2 Glass transition temperature and effect of plasticizers (plasticization)	10
1.5 A REVIEW OF LITERATURE	10
1.6 SCOPE OF THE WORK	28
1.7 OBJECTIVES	31
1.8 EXPERIMENTAL	32
1.8.1 Materials	32
1.8.1.1 Structure of PMMA	33
1.8.1.2 Structure of CA and its derivatives	33

1.8.1.3	Structures of plasticizers	33
1.8.2	Preparation of Blends	34
1.8.2.1	Preparation of non-plasticized blends	34
1.8.2.2	Preparation of plasticized blends	34
1.8.3	Membrane Characterization	35
1.8.3.1	Fourier transform infrared (FTIR) spectroscopic studies	35
1.8.3.2	Differential scanning calorimetry (DSC) studies	35
1.8.3.3	Water uptake	35
1.8.3.4	Ion exchange capacity measurements	35
1.8.3.5	Electrochemical impedance spectroscopy and proton conductivity measurement	36
1.8.3.6	Dielectric studies	36

Chapter 2

STUDIES ON NON-PLASTICIZED BLENDS OF PMMA WITH CA, CAP, CAB AND CAPH

2.1	A BRIEF ACCOUNT OF PMMA, CAP, CAB AND CAPH	39
2.1.1	Poly(methyl methacrylate) (PMMA) ($C_5H_8O_2$) _n	39
2.1.2	Cellulose acetate (CA)	40
2.1.3	Cellulose acetate propionate (CAP) ($C_{76}H_{114}O_{49}$)	41
2.1.4	Cellulose acetate butyrate (CAB) ($C_{84}H_{130}O_{49}$)	42
2.1.5	Cellulose acetate phthalate (CAPH) ($C_{116}H_{116}O_{64}$)	42
2.2	RESULTS AND DISCUSSION	44
2.2.1	Fourier Transform Infrared (FTIR) Spectroscopic Studies	44
2.2.2	Differential Scanning Calorimetry (DSC) Studies	45
2.2.3	Water Uptake	46
2.2.4	Ion Exchange Capacity (IEC) Measurements	47
2.2.5	Electrochemical Impedance Spectroscopy	47
2.2.5.1	Proton conductivity measurement	47

2.2.5.2	Temperature dependence of ionic conductivity	48
2.2.6	Dielectric Studies	49
2.3	FIGURES	50
2.4	TABLES	64

Chapter 3

STUDIES ON DIMETHYL PHTHALATE (DMP) PLASTICIZED BLENDS OF PMMA WITH CA, CAP, CAB AND CAPH

3.1	DIMETHYL PHTHALATE (DMP) PLASTICIZER	67
3.2	RESULTS AND DISCUSSION	68
3.2.1	Fourier Transform Infrared (FTIR) Spectroscopic Studies	68
3.2.2	Differential Scanning Calorimetry (DSC) Studies	69
3.2.3	Water Uptake	70
3.2.4	Ion Exchange Capacity (IEC) Measurements	72
3.2.5	Electrochemical Impedance Spectroscopy	72
3.2.5.1	Proton conductivity measurement	73
3.2.5.2	Temperature dependence of ionic conductivity	73
3.2.6	Dielectric Studies	74
3.3	FIGURES	76
3.4	TABLES	88

Chapter 4

STUDIES ON DIETHYL PHTHALATE (DEP) PLASTICIZED BLENDS OF PMMA WITH CA, CAP, CAB AND CAPH

4.1	DIETHYL PHTHALATE (DEP) PLASTICIZER	93
4.2	RESULTS AND DISCUSSION	93
4.2.1	Fourier Transform Infrared (FTIR) Spectroscopic Studies	93
4.2.2	Differential Scanning Calorimetry (DSC) Studies	95
4.2.3	Water Uptake	96

4.2.4	Ion Exchange Capacity (IEC) Measurements	97
4.2.5	Electrochemical Impedance Spectroscopy	98
4.2.5.1	Proton conductivity measurement	98
4.2.5.2	Temperature dependence of ionic conductivity	99
4.2.6	Dielectric Studies	100
4.3	FIGURES	101
4.4	TABLES	113

Chapter 5

STUDIES ON DIPROPYL PHTHALATE (DPP) PLASTICIZED BLENDS OF PMMA WITH CA, CAP, CAB AND CAPH

5.1	DIPROPYL PHTHALATE (DPP) PLASTICIZER	119
5.2	RESULTS AND DISCUSSION	119
5.2.1	Fourier Transform Infrared (FTIR) Spectroscopic Studies	119
5.2.2	Differential Scanning Calorimetry (DSC) Studies	121
5.2.3	Water Uptake	122
5.2.4	Ion Exchange Capacity (IEC) Measurements	123
5.2.5	Electrochemical Impedance Spectroscopy	123
5.2.5.1	Proton conductivity measurement	124
5.2.5.2	Temperature dependence of ionic conductivity	124
5.2.6	Dielectric Studies	125
5.3	FIGURES	127
5.4	TABLES	139

Chapter 6

STUDIES ON DIBUTYL PHTHALATE (DBP) PLASTICIZED BLENDS OF PMMA WITH CA, CAP, CAB AND CAPH

6.1	DIBUTYL PHTHALATE (DBP) PLASTICIZER	145
------------	--	------------

6.2	RESULTS AND DISCUSSION	145
6.2.1	Fourier Transform Infrared (FTIR) Spectroscopic Studies	145
6.2.2	Differential Scanning Calorimetry (DSC) Studies	147
6.2.3	Water Uptake	148
6.2.4	Ion Exchange Capacity (IEC) Measurements	149
6.2.5	Electrochemical Impedance Spectroscopy	150
6.2.5.1	Proton conductivity measurement	150
6.2.5.2	Temperature dependence of ionic conductivity	151
6.2.6	Dielectric Studies	152
6.3	FIGURES	153
6.4	TABLES	165

Chapter 7

STUDIES ON PROPYLENE CARBONATE (PC) PLASTICIZED BLENDS OF PMMA WITH CA, CAP, CAB AND CAPH

7.1	PROPYLENE CARBONATE (PC) PLASTICIZER	171
7.2	RESULTS AND DISCUSSION	172
7.2.1	Fourier Transform Infrared (FTIR) Spectroscopic Studies	172
7.2.2	Differential Scanning Calorimetry (DSC) Studies	173
7.2.3	Water Uptake	174
7.2.4	Ion Exchange Capacity (IEC) Measurements	175
7.2.5	Electrochemical Impedance Spectroscopy	176
7.2.5.1	Proton conductivity measurement	176
7.2.5.2	Temperature dependence of ionic conductivity	177
7.2.6	Dielectric Studies	178
7.3	FIGURES	179
7.4	TABLES	191

Chapter 8

SUMMARY, CONCLUSIONS AND SCOPE FOR FUTURE WORK

8.1 SUMMARY AND CONCLUSIONS 197

8.2 SCOPE OF THE FUTURE WORK 204

REFERENCES 205

LIST OF PUBLICATIONS 213

LIST OF CONFERENCE PRESENTATIONS 213

CURRICULUM VITAE 215

LIST OF ABBREVIATIONS

PMMA	Poly(methyl methacrylate)
CA	Cellulose acetate
CAP	Cellulose acetate propionate
CAB	Cellulose acetate butyrate
CAP, CAPH	Cellulose acetate hydrogen phthalate, Cellulose acetate phthalate
DMP	Dimethyl phthalate
DEP	Diethyl phthalate
DPP	Dipropyl phthalate
DBP	Dibutyl phthalate
PC	Propylene carbonate
EC	Ethylene carbonate
DMF	Dimethyl formamide
FTIR	Fourier transform infrared
DSC	Differential scanning calorimetry
LiBF ₄	Lithium tetrafluoroborate
LiClO ₄	Lithium perchlorate
Li ₂ B ₄ O ₇	Lithium tetraborate
PMA	Poly(methyl acrylate)
PVDF, PVdF	Poly(vinylidene fluoride)
PES	Poly(ethylene succinate)
PEG	Poly (ethylene) glycols
PVP	Poly vinyl pyrrolidone
PDLA	Poly lactides
DMTA	Dynamic mechanical analysis
DMC	Dimethyl carbonate
DEC	Diethyl carbonate
PVC	Poly(vinyl chloride)
PP	Polypropylene

SMA	Poly(styrene-co-maleic anhydride)
MA	Maleic anhydride
PEO	Poly(ethylene oxide)
PS	Polystyrene
PE	Polyethylene
PES	Polyethersulfone
PVP	Polyvinylpyrrolidone
EG	Exfoliated grapheme
THF	Tetra hydrofuran
SEM	Scanning electron microscopy
NMR	Nuclear magnetic resonance
TG	Thermogravimetry
DTA	Differential thermal analysis
XRD	X-ray diffraction
TEM	Transmission electron microscopy

Chapter 1

INTRODUCTION

Chapter 1 begins with introduction to polymers, polymer blends, methodology and characterization techniques. This chapter outlines a review of literature relevant to the polymer blends along with the scope and objectives of the present work. A brief account of the materials and methods employed in the present work has also been included at the end of this chapter.

A polymer is a giant or macro molecule formed by repeated union of several simple molecules called “monomers” (meaning, single part). The repeat units in a polymer chain are linked through strong covalent bonds. The properties of polymers are entirely different from those of its monomers (Billmeyer 1970).

Chemically, polymers are long-chain molecules of very high molecular weight, often measured in the hundreds of thousands. For this reason, the term “macromolecules” is frequently used when referring to polymeric materials (Sperling 2001).

The process by which the monomer molecules are linked to form a big polymer molecule is called “polymerization”. The length of the polymer chain is specified by the number of repeat units in the chain. This is called the “degree of polymerization” (DP). The molecular weight of the polymer is the product of the molecular weight of the repeat unit and the DP (Gowariker et al. 2008).

1.1 POLYMER BLENDS

Polymer blends are a key component of current polymer research and technology. This is fed in part by the ease of production of new materials by mixing and the diversity of properties that result. Mixtures of polymers are classified as polymer alloys, polymer blends and polymer composites. Utracki (2002) divided polymer blends into two categories: the “*immiscible*” polymer system, which is a polymer alloy, and the “*miscible*” polymer system, which is a polymer blend. On the other hand, a polymer mixed with a filler forms a polymer composite (Shonaik and Simon 1999). The composite materials are prepared by combining two or more substances, in which the desirable properties of each component is retained. Reinforced plastics are composites in

which a polymer is combined with a reinforcing agent, which may be organic or inorganic in nature (Kuriacose and Rajaram 1998).

The properties of polymer alloys, polymer blends and polymer composites depend on the quality of the dispersed phase, the microstructure of all phases, the adhesion and cohesion between phases, and the morphology of the system. Compatibility and molecular miscibility are two important properties of polymeric components.

There are polymers possessing several excellent properties such as high specific strength, dimensional stability, low creep, and good electrical and chemical properties. Therefore they are commonly used in electrical and electronic applications, automobiles, buildings and construction, industrial machinery and consumer products. However, issues of toughness, processibility and cost often hinder these high-performing plastics from becoming commercially useful. Blending is a simple, fast, effective and economical method of resolving the above mentioned problems and also provides a high performance-to-cost ratio.

In the past decade much attention has been given to the development of polymeric blends. Polymer blends offer the possibility of combining the unique properties of available materials and thus of producing materials with tailor-made properties, which often have advantages over the development of a completely new polymeric material

1.1.1 Factors in Miscibility and Immiscibility

A number of specific features may contribute to miscibility and/or immiscibility of polymer blends are listed below.

- Polarity
- Specific Group Attraction
- Molecular Weight
- Ratio
- Crystallinity (Shonaike and Simon 1999).

1.1.2 Glass-transition Temperature

The glass transition in non-crystalline polymers under ordinary experimental conditions occurs on cooling when the characteristic time of molecular motions responsible for structural rearrangements becomes longer than the timescale of the experiment. As a result, structural relaxation toward equilibrium is arrested below some temperature, T_g and the polymer is in the glassy state. The molecular motions responsible for structural relaxation in polymers involve only a small number of repeat units of each chain, and it is appropriate to refer to them henceforth as local segmental motions. In polymers, molecular motions involving more repeat units of each chain are possible and they contribute to viscoelastic properties over broad ranges. The molecular motions, and therefore a necessary condition for the former to contribute to observable viscoelastic properties of the polymer is mobility of the latter, which means that the temperature has to be higher than the glass-transition temperature, T_g . Thus, the glass transition is perhaps the most important factor that determines at any pressure and temperature the viscoelastic properties and applications of noncrystalline polymers. For example, if T_g is much higher than the temperature of application, the polymer is a hard glass and may be suitable for applications as engineering plastics. If T_g is sufficiently lower, the polymer is rubbery and may be used in the rubber industry (Mark et al. 2004). There is a temperature boundary for almost all amorphous polymers (and many crystalline polymers) only above which the substance remains soft, flexible and rubbery and below which it becomes hard, brittle and glassy. This temperature, below which a polymer is hard and above which it is soft, is called the “glass transition temperature”. The hard, brittle state is known as the glassy state and the soft flexible state as the rubbery or viscoelastic state (Gowariker et al. 2008).

1.1.3 Dependences of Glass-transition Temperature

The glass-transition temperature of a particular polymer depends on various controllable parameters such as

- Molecular Weight

- Diluents Concentration
- Blending
- Cross-linking
- Crystallinity
- Chain stiffness and internal plasticization
- Tacticity
- Pressure
- Polymer thin films
- Confinement in nanometer pores of glasses (Mark et al. 2004).

1.2 METHODOLOGY

1.2.1 Solution or Die Casting

Die casting is a relatively low cost process which consists of converting a liquid prepolymer to a solid object with a desired shape. The prepolymer compounded suitably with a curative and other ingredients is poured into a petridish, the later representing the die. The dish is then kept in an oven at an elevated temperature for a few hours to complete the cure reaction. During curing, the polymer block shrinks in size which helps in its removal from the die with ease. On cooling to room temperature, the solid product from the petridish is pulled out. The solid thus cast will have a shape identical to the interior of the petridish (Gowariker et al. 2008).

1.3 CHARACTERIZATION TECHNIQUES

1.3.1 Spectral Properties

1.3.1.1 *Infrared spectroscopy*: IR spectroscopy has been one of the most popular physical methods in the polymer characterization laboratory since it is useful in the elucidation of structures and the identification of organic and inorganic systems alike. The quantitative analysis of samples down to the pictogram quantities is straight forward for systems for which the spectra of the pure components are available. Yet, the most attractive

advantage of the method is the potential for a rapid multicomponent analysis to be carried out from a single measurement (spectrum), once the methodology has been calibrated.

IR spectroscopy is used extensively to investigate hydrogen bonding because the positions of the peaks for the X–H stretching mode are very sensitive to the extent of association. The unbounded X–H stretch gives rise to a relatively sharp peak, whereas, on formation of a hydrogen bond, X–H \cdots Y (where Y is the acceptor atom), the peak shifts to a lower wave number and becomes much broader. The downward shift is caused by the lengthening of the X–H bond, which results from the formation of hydrogen bonds. Hence formation of a stronger hydrogen bond will lengthen the X–H bond more and produce a shift to a lower wave number. Furthermore, a relationship between the position of the peak for the X–H group and the X–H \cdots Y bond distance (determined from crystallographic data) has been observed, whereby a lower frequency for the peak correlates with a shorter hydrogen bond distance (i.e. a stronger hydrogen bond and a longer X–H bond). IR spectroscopy can be used to measure the fraction of hydrogen bonded groups present as a function of composition and temperature (Mark et al. 2004).

1.3.2 Thermal Properties

Thermal analysis is a group of techniques in which a physical property of a substance is measured as a function of temperature whilst the substance is subjected to a controlled temperature program.

1.3.2.1 *Differential scanning calorimetry (DSC)*: A technique in which the difference in energy inputs into a substance and a reference material is measured as a function of temperature whilst the substance and reference material are subjected to a controlled temperature program. Two modes, power-compensation DSC and heat-flux DSC, can be distinguished, depending on the method of measurement used.

Usually, for the power-compensation DSC curve, heat flow rate should be plotted on the ordinate with endothermic reactions upwards and for the heat-flux DSC curve with endothermic reactions downwards (Hatakeyama and Liu 1998).

1.3.3 Electrochemical Impedance Spectroscopy

Impedance spectroscopy (IS) is a relatively new and powerful method of characterizing many of the electrical properties of materials and their interfaces with electronically conducting electrodes. It may be used to investigate the dynamics of bound or mobile charge in the bulk or interfacial regions of any kind of solid or liquid material: ionic, semiconducting, mixed electronic-ionic and even insulators (dielectrics).

There are three different types of electrical stimuli which are used in impedance spectroscopy. The most common and standard one, is to measure impedance by applying single-frequency voltage or current to the interface and measuring the phase shift and amplitude, or real and imaginary parts, of the resulting current at that frequency using either analog circuit or fast Fourier transform (FFT) analysis of the response. Commercial instruments are available which measure the impedance as a function of frequency automatically in the frequency ranges of about 1 mHz to 1 MHz and are easily interfaced to laboratory microcomputers. The advantages of this approach are the availability of these instruments and the ease of their use, as well as the fact that the experimentalist can achieve a better signal-to-noise ratio in the frequency range of most interest. In addition to these three approaches, one can combine them to generate other types of stimuli.

Any intrinsic property that influences the conductivity of an electrode-materials system, or an external stimulus, can be studied by impedance spectroscopy. The parameters derived from an impedance spectroscopy spectrum fall generally into two categories: (a) those pertinent only to the material itself, such as conductivity, dielectric constant, mobilities of charges, equilibrium concentrations of the charged species, and bulk generation-recombination rates; and (b) those pertinent to an electrode-material interface, such as adsorption-reaction rate constants, capacitance of the interface region, and diffusion coefficient of neutral species in the electrode itself (Barsoukov and Macdonald 2005).

1.3.3.1 *Proton conductivity mechanism*: Proton transfer phenomena follow two principal mechanisms where the proton remains shielded by electron density along its entire

diffusion path, so that in effect the momentary existence of a free proton is not seen. The most trivial case of proton migration requires the translational dynamics of bigger species, this is the chemical mechanism. In this mechanism the proton diffuses through the medium together with a “vehicle” (for example, with H₂O as H₃O⁺). The counter diffusion of unprotonated vehicles (H₂O) allows the net transport of protons. The observed conductivity, therefore, is directly dependant on the rate of vehicle diffusion.

In another principal mechanism, the vehicles show pronounced local dynamics but reside on their sites. The protons are transferred from one vehicle to the other by hydrogen bonds (proton hopping). Simultaneous reorganization of the proton environment, consisting or reorientation of individual species or even more extended ensembles, then leads in the formation of an uninterrupted path for proton migration. This mechanism is known as the Grotthus mechanism. This reorganization usually involves the reorientation of solvent dipoles (for example H₂O), which is an inherent part of establishing the proton diffusion pathway. The rates of proton transfer and reorganization of its environment affect directly this mechanism. All rates directly connected to the diffusion of protons. These two principal mechanisms essentially reflect the difference in nature of the hydrogen bonds formed between the protonated species and their environment.

In media which supports strong hydrogen bonding, the Grotthus mechanism is preferred, the vehicle mechanism is characteristic of species with weaker bonding. Consequently, Grotthus type mechanisms are progressively dominated by vehicle-type mechanisms with increasing temperature (Selvakumar 2009).

1.3.4 Electrical Properties

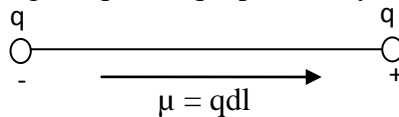
1.3.4.1 *Dielectric constant*: A dielectric material has interesting electrical properties because of the ability of an electric field to polarize the material to create electric dipoles. A dipole is an entity in which equal positive and negative charges are separated by a small distance; the electric dipole moment is given by

$$\mu = qdl \tag{1.1}$$

where q = charge

dl = distance between two charges

The electric dipole is a vector. In its simplest model, a dipole moment consists of two point charges of opposite sign, $+q$ and $-q$ separated by a distance.



Faraday first discovered the fundamental experimental result that the capacitance of a condenser is increased if the space between the conductors is filled with a dielectric material. If ' C_0 ' is the capacitance of the condenser with the region between the conductors evacuated and ' C ' its capacitance when the region is filled with a dielectric, then the ratio

$$C/C_0 = \epsilon_r \quad (1.2)$$

is found to be independent of the shape or the dimensions of the conductors and is solely a characteristic of the particular dielectric medium used. ' ϵ_r ' is called the *relative permittivity* or the *dielectric constant* of the medium. In the S.I. system of units the permittivity of the medium is defined as

$$\epsilon = \epsilon_0 \cdot \epsilon_r \quad (1.3)$$

where $\epsilon_0 = 8.854 \times 10^{-12} \text{ Fm}^{-1}$ and is an electric constant which represents the *permittivity* of vacuum while ' ϵ_r ' is the *relative permittivity* of the material. The term dielectric constant is sometimes used for both ' ϵ ' and ' ϵ_r '. Since this causes confusion, the terms *permittivity* and *relative permittivity* are to be preferred. The dielectric constant of a material is a macroscopic quantity that measures how effective an electric field is in polarizing the material.

Insulators or dielectrics are substances which do not possess free electric charges under ordinary circumstances. This does not mean that they cannot modify the electric field into which they are introduced. In fact the most important property of dielectrics is their ability to become polarized under the action of an external electric field. The atoms and molecules of dielectrics are influenced by an external field and hence the positive particles are pushed in the direction of the field while the negative particles in the

opposite direction from their equilibrium position. Hence dipoles are developed and they produce a field of their own. The process of producing electric dipoles out of neutral atoms and molecules is referred to as polarization.

1.3.4.2 *The complex dielectric constant and dielectric loss*: When a dielectric is subjected to an alternating field the polarization also varies periodically with time and so does the displacement. To describe this, two frequency dependent dielectric constants are introduced,

$$\epsilon_r' = D_0/E_0 \cos \delta \quad (1.4)$$

$$\epsilon_r'' = D_0/E_0 \sin \delta \quad (1.5)$$

where, D_0 and E_0 are electric flux density and electric field intensity, respectively.

Also,

$$\tan \delta = \epsilon_r'' / \epsilon_r' \quad (1.6)$$

Because both ϵ_r' and ϵ_r'' are frequency dependent, the phase angle ' δ ' is also frequency dependent.

The energy losses are thus proportional to $\sin \delta$ since $\epsilon_r'' = (D_0/E_0) \sin \delta$. For this reason $\sin \delta$ is called the '*loss factor*' and ' δ ' is the '*loss angle*'. For small values of ' δ ', $\tan \delta$ is called as the loss factor because $\tan \delta \approx \sin \delta \approx \delta$.

The dielectric loss at low frequencies is mainly due to d.c. resistivity. But at high frequencies the dielectric loss is mostly due to dipole rotations or to ionic transitions from the lower energy states to higher energy states. Because of the upward transition, the energy is absorbed from the applied field (Pillai 2006).

1.4 COMPOUNDING OF POLYMERS

Polymers in their pure form, as obtained from the manufacturing plants after isolation and purification, are called "virgin" polymers or "virgin" resins. Barring a few (e.g. polystyrene, polyethylene), virgin polymers, as such, may not be amenable for processing straightaway. The process involving incorporation of ingredients such as plasticizers, vulcanizing agents, curatives, stabilizers, fillers, coloring agents, flame

retardants and lubricants into the virgin polymer is known as “compounding” of the polymers (Gowariker et al. 2008).

1.4.1 Plasticizers: Plasticizers are small molecules added to soften a polymer by lowering its glass transition temperature or reducing its crystallinity or melting temperature (Sperling 2001).

1.4.2 Glass transition temperature and effect of plasticizers (plasticization):

Plasticizers are low molecular weight non-volatile substances, which when added to a polymer, improve its workability, flexibility, stability, processibility and, hence, utility. The plasticizer substantially reduces the brittleness of many amorphous polymers because its addition even in small quantities markedly reduces the T_g of the polymer. This effect is due to the reduction in cohesive forces of attraction between polymer chains. Plasticizer molecules, being relatively small in size compared to polymer molecules, penetrate into the polymer matrix and establish polar attractive forces between it and the chain segments. These attractive forces reduce the cohesive forces between the polymer chains and increase the segmental mobility, thereby reducing the T_g value (Gowariker et al. 2008 and Shonaike and Simon 1999).

1.5 A REVIEW OF LITERATURE

Literature survey indicates that a good number of studies have been done on polymer blends of a variety of polymers under different composition and conditions.

Salazar et al. (1991) have prepared amorphous films of poly(vinylidene fluoride) (PVDF) – poly(methyl methacrylate) (PMMA) by initial precipitation from a solvent and rapid solidification at ≈ 15 °C from the molten state. Different compositions of PVDF/PMMA blends were prepared. X – ray scattering analysis suggests that mixture of the two components throughout the composition range studied occurs at a molecular level. The T_g and the predictions of Gordon and Taylor (Gordon and Taylor 1952), revealed that the depression of microhardness was caused by the shift of T_g towards

lower temperatures. The effect of PVDF molecules was to act as a softening agent within the PMMA component.

Torres and Ramos (1994) have prepared binary blends of PVDF with cellulose acetate butyrate (CAB) and were characterized by using DSC, WAXS and FTIR spectroscopy. This system was proved to be partially miscible, showing a significant decrease on the thermal parameters (ΔH_f and T_m) as well as on the crystallinity index (CI) of PVDF with CAB content on the second DSC run.

Buchanan et al. (1997) studied the relationship between blend miscibility and biodegradation of cellulose acetate and poly(ethylene succinate) blends. The miscibility of cellulose acetate (CA) and poly(ethylene succinate) (PES) has been investigated using a variety of thermal techniques and by solid – state ^{13}C NMR spectroscopy. A combination of thermal and NMR analysis suggests that these blends are not fully miscible on a 2.5 to 5 nm scale. Investigation of the biodegradation of the blend components and of the blends revealed that PES degraded relatively rapidly and that CA degraded slowly.

Yoshida (1997) has reported the conformational formation and crystallization dynamics of miscible PVDF/at-PMMA and PVDF/iso-PMMA polymer blends from the molten state by the simultaneous DSC/FT-IR measurements.

Blends of amorphous and crystalline polylactides (PDLA and PLLA) with poly(methyl methacrylate) (PMMA) and poly(methyl acrylate) (PMA) have been prepared. Thermal behaviour and miscibility of these blends along the entire composition interval were studied by differential scanning calorimetry (d.s.c.). The results were compared with those obtained by dynamic mechanical analysis (DMTA). Only one T_g was found in PDLA/PMA and PDLA/PMMA blends, indicating a high degree of miscibility in both systems. Nevertheless, the PDLA/PMMA blend presented enlargements of the T_g width at high PMMA contents (Eguiburu et al. 1998).

Rao et al. (1999) studied the specific interaction between CAP and PMMA, and CAP forms a compatible blend with PMMA in the entire composition range. The compatibility of the system may be due to the formation of a hydrogen bond between the

carbonyl group of PMMA and the free hydroxyl group of CAP. DSC results have shown the miscibility of the blends.

Thermally reversible ionically conducting gel electrolytes, comprising blends of atactic and isotactic poly(methyl methacrylate) (PMMA), lithium salt and an organic solvent, have been prepared and characterized. Due to association between isotactic PMMA (i-PMMA) and syndiotactic sequences of atactic PMMA (a-PMMA) strong gels are formed in solvents which ordinarily do not form gels with high molecular weight a-PMMA, namely, dimethyl carbonate (DMC) and diethyl carbonate (DEC). The plot of the dependence of the elastic moduli on the fraction of i-PMMA passes through a maximum at ~1:1 molar ratio between isotactic and syndiotactic fractions of a-PMMA. However, the conductivity of the gels is invariant to the ratio of i-PMMA and a-PMMA. Thus, a gel with a typical polymer content of 15–20 wt %, 1 M lithium salt, and a ratio of i-PMMA to a-PMMA of about 1:3 has an ionic conductivity in the range of 1×10^{-3} – 4×10^{-3} S cm⁻¹ and possesses a dynamic elastic modulus one order of magnitude higher than the electrolytes containing only atactic PMMA. This modulus is obtained at values of the frequency between 0.01 and 100 radians, so that even under static conditions the gels do not flow and exhibit reversible elasticity to approximately 100 % elongation. Thermal mechanical analysis and calorimetry of these gels show that the physical crosslinks formed by stereocomplexed syndiotactic and isotactic triads melt in the range of 65–85 °C depending on the nature of the solvent and lithium salt. The fact that these gel electrolytes are thermoreversible makes them readily processable. After melt casting they form transparent dimensionally stable, self supporting films (Yarovoy et al. 1999).

Karlou and Schneider (2000) have investigated poly(vinyl chloride)/poly(methyl methacrylate) (PVC/PMMA) blends by comparative p-V-T and DSC measurements. The study was concentrated on the glass transition range of the blends, and it was found that the blends are characterized by a single glass transition temperature suggesting miscibility of the blend components. It was shown that the glass transition of the blends increases with both increasing heating rate and pressure.

Chand and Vashushtha (2000) have developed a new type of fly ash (FA) filled polypropylene/poly(methyl methacrylate) (PP/PMMA) blend. Structural and thermal properties of FA filled PP/PMMA blend system have been determined and analyzed by SEM, TG and DTA respectively. Strength of FA filled and unfilled PP/PMMA blends were determined at room temperature by tensile testing machine.

Stephan et al. (2000) studied ionic conductivities of plasticized poly(vinylchloride) (PVC)/poly(methylmethacrylate) (PMMA) blend electrolyte films containing two different lithium salts, viz., lithium tetrafluoroborate (LiBF_4) and lithium perchlorate (LiClO_4) using the AC impedance technique at 25 °C, 40 °C, 50 °C and 60 °C. A mixture of ethylene carbonate (EC) and propylene carbonate (PC) is used as the plasticizer. Pure PMMA and PMMA-rich phases exhibited better conductivity. The variation of ionic conductivity for different plasticizer contents and for different lithium salts is reported. The variation in film morphology is examined by scanning electron microscopic examination. Finally, the existence of ion-ion pairs has been identified using Fourier Transform Infrared analysis (FT-IR) measurements.

Rao et al. (2000) have investigated the miscibility characteristics of cellulose acetate hydrogen phthalate (CAP) and poly(vinyl pyrrolidone) (PVP) by solution viscometric, ultrasonic, and differential scanning calorimetric (DSC) methods. From viscosity measurements, Krigbaum and Wall polymer-polymer interaction parameter Δb was evaluated. Ultrasonic velocity and adiabatic compressibility have been plotted versus blend composition and are found to be linear. Variation of T_g with composition follows Gordon-Taylor equation. T_g values have also been calculated from the Fox equation (Fox 1956). The results obtained reveal that CAP forms a miscible blend with PVP in the entire composition range. Compatibility may be due to the formation of hydrogen bonding between the carbonyl group of PVP and the free-hydroxyl group of CAP. Compatibility has also been confirmed from dielectric measurements.

Rajendran and Uma (2000) studied the preparation and characterization of composite polymer electrolytes of PVC-PMMA- LiBF_4 -DBP for different concentrations of ZrO_2 have been investigated. FTIR studies indicate complex formation between the

polymers, salt and plasticizer. The electrical conductivity values measured by a.c. impedance spectroscopy are found to depend upon the ZrO_2 concentration. The temperature dependence of the conductivity of the polymer films seems to obey the VTF relation. The conductivity values are presented in $10^{-3} \text{ S cm}^{-1}$.

Artyushkova et al. (2001) have published correlative x-ray photoelectron spectroscopy (XPS) and Fourier transform infrared (FTIR) studies of the complex heterogeneous structure of 50/50 poly(vinyl chloride) (PVC)/poly(methyl methacrylate) (PMMA) polymer blends. The comparable lateral resolution and parallel (real-time) imaging capabilities of both techniques allow for a direct comparison of surface (XPS) and bulk (FTIR) measurements of polymer blends.

Park et al. (2001) have studied a new binder system consisting of cellulose acetate butyrate (CAB) and poly(ethylene glycol) (PEG) with various molecular weights. CAB and PEGs with various molecular weights had good compatibility. The blends exhibited low enough viscosity to make homogeneous feed stock for the injection molding.

Rajendran and Mahendran (2001) have prepared blend based polymer electrolytes composed of poly(methyl methacrylate) (PMMA), poly(vinyl alcohol) (PVA) and LiClO_4 using solvent casting technique. The polymer films were characterized by XRD and FTIR studies to determine the molecular environment for the conducting ions. These polymer films have been investigated in terms of ionic conductivity using the results of impedance studies. Plasticizer used is dimethyl phthalate (DMP).

Hou and Siow (2001) have studied the electrochemical characteristics of plasticized polymer electrolytes based on poly(acrylonitrile-butadiene-styrene) (ABS) and poly(methyl methacrylate) (PMMA) blends. The ionic conductivity of the polymer electrolyte with an ABS/PMMA ratio of 6/4 and a plasticizer (EC/PC = ethylene carbonate/propylene carbonate) content of 60 % was highest when the LiClO_4 content was 4.8 %. The properties of the electrode interface in contact with the polymer electrolyte were investigated.

The lithium salt (x) ($x = \text{LiAsF}_6, \text{LiPF}_6$) was complexed with a blend PVC/PMMA and plasticized with a combination of EC and PC. The electrolyte films were prepared

using doctor blade method and subjected to ionic conductivity measurements. The films were also subjected to TG - DTA and FT-IR analysis. The effect of salt on ionic conductivity is discussed (Kalyanasundaram et al. 2001).

Shafee et al. (2001) have prepared the blends of PHB with CAB by solution casting from chloroform solutions at different compositions. The miscibility, crystallization behavior and phase structure were investigated using DSC, optical microscopy and SAXS. CAB/PHB blends were found to be miscible in the melt state as evidenced by the deduction of a single T_g for each composition.

Saq'an et al. (2001) have studied the optical and dielectric properties of prepared polyvinylchloride/atactic polymethylmethacrylate (PVA/ α -PMMA) blends as a function of applied field frequency and PMMA content. The observed optical energy gaps and the energy gap tails were determined from the measured absorption spectra. It was found that the applied frequency and the α -PMMA concentration have some effects on the physical parameters such as the optical energy gap, the glass transition temperature (T_g), the dielectric constant, and the refractive index. Correlation between the determined optical energy gaps and the measured T_g is presented. The observed changes in these physical parameters are due to structural changes in the amorphous domains, impurities and space charge within the interfaces in the mixed phases.

Miyashita et al. (2002) have prepared binary blend films of cellulose acetate (CA) with flexible synthetic polymers including poly(vinyl acetate) (PVAc), poly(N-vinyl pyrrolidone) (PVP), and poly(N-vinyl pyrrolidone-co-vinyl acetate) [P(VP-co-VAc)] from mixed polymer solutions by solvent evaporation. FT-IR measurements for the miscible blends revealed the presence of hydrogen-bonding interactions and assumed to largely contribute to the good miscibility.

Ramesh et al. (2002) studied the miscibility of PVC blends (PVC/PMMA and PVC/PEO). Experiments using viscosimetry and DSC were performed. The presence of attractive forces among polymers was evaluated. Viscosimetric and thermal analysis showed that the PVC/PMMA and PVC/PEO blends are miscible.

Mahendran and Rajendran (2003) prepared blend based polymer electrolytes composed of PMMA, PVdF, Lithium salt (LiX) ($X = \text{ClO}_4, \text{BF}_4$ and CF_3SO_3) and DMP are prepared using solvent casting technique. The films have been characterized using XRD, FTIR, Thermal and SEM studies; the effect of complexing salt and temperature on ionic conductivity is also discussed.

Uma et al. (2003) have prepared thin film of poly (vinylchloride) and poly (methylnethacrylate) blend polymer electrolytes plasticized with a combination of DBP and Li_2SO_4 salts by solution casting technique. The prepared films were subjected to a.c. impedance measurements as a function of temperature ranging from 304-373 K. The maximum conductivity at 304 K was found to be $1.24 \times 10^{-8} \text{ Scm}^{-1}$ for PVC-PMMA- Li_2SO_4 -DBP (7.5-17.5-5-70 mole-%). Temperature dependence studies on the ionic conductivity in the PVC-PMMA- Li_2SO_4 -DBP system suggest that the ion conduction follows the Williams-Landel-Ferry (WLF) mechanism, which is further confirmed by Vogel-Tamman-Fulcher (VTF) plots. XRD, FTIR, SEM and thermal studies revealed complex formation.

The amount of water absorption of poly(methyl methacrylate) (PMMA) containing 0, 1, 3 and 5 wt % of an adhesive monomer, 4-methacryloxyethyl trimellitic anhydride (4-META), was measured at 7 °C, 37 °C and 60 °C. After the water uptake reached equilibrium in specimens, they were desorbed to obtain a constant value and the absorption process was repeated. Mass changes in the second desorption were recorded for the storage temperatures of 37 °C and 60 °C. Multiple regression analyses were conducted on three independent variables, 4-META concentration, storage temperature and absorption–desorption cycle. A statistically significant relationship was found between the maximum water uptake and 4-META concentration, while there was no relationship between the maximum water uptake and diffusion coefficient obtained using the Fick's law. The negative relationship in the latter did not support the free space theory. The significant and positive relationship between the maximum water uptake and 4-META concentration demonstrates that water molecules diffuse through the formation of a hydrogen bond at polar sites. The maximum water uptake was not influenced by

temperature, while the diffusion coefficient increased with the rise in temperature. The activation energy was 41–47 and 50–53 kJ/mol in the first and second absorption tests, respectively (Unemoria et al. 2003).

Mijovic et al. (2004) have studied the property-morphology relationships in polymethylmethacrylate/polyvinylidene fluoride (PMMA/PVDF) blends. All blends were compounded in a twin-screw extruder and then processed by injection molding. Mechanical properties of blends of various compositions were studied by dynamic mechanical and impact strength measurements. The presence of crystalline regions in blends was determined by Differential Scanning Calorimetry (DSC). Morphology of fracture surfaces of blends was studied by Spinning Electron Microscopy (SEM). PMMA/PVDF blends were found to form compatible mixtures over a wide range of blend composition. Changes in dynamic mechanical properties upon annealing were found to be a direct function of blend morphology. Electron microscopic evidence showed no signs of phase separation. DSC measurements detected crystalline regions in all blends containing 40 percent or more (by weight) PVDF.

Bichuch et al. (2004) Mechanical properties, optical transmission, surface topography, and dielectric loss are studied for films formed by blends of polymers of vinyl chloride and methyl methacrylate with their copolymers. the goal of this study was to examine in detail blends of VC and MMA homopolymers with VC/MMA copolymer.

Mahendran et al. (2005) have reported the transport properties of gel type ionic conducting membranes consisting of poly(methyl methacrylate) (PMMA), poly(vinylidene fluoride) (PVDF), lithium perchlorate (LiClO_4) as a salt and dioctyl phthalate (DOP), dibutyl phthalate (DBP), dimethyl phthalate (DMP) or diethyl phthalate (DEP) as plasticizer. The polymer films were characterized by XRD, thermal, FTIR and impedance spectroscopic studies.

Song et al. (2005) have introduced a new binder system, containing ternary polymer blends of poly(methyl methacrylate) (PMMA), cellulose acetate butyrate (CAB) and polyethylene glycol (PEG) for the powder injection molding of stainless steel powders, to improve the mechanical strength. The binders of some CAB/PEG blends

were easily processed by injection molding due to low viscosity. Some CAB/PEG binder exhibited cracks and deformation during the solvent extraction. When the PMMA was added to CAB/PEG binder, the feed stocks could be injection molded and showed significantly improved mechanical properties such as flexural modulus.

Nicotera et al. (2005) have prepared blend ionic conducting membranes formed by poly(methyl methacrylate) (PMMA)/poly(vinylidene fluoride) (PVDF), lithium perchlorate (LiClO_4) as a salt and a mixture of ethylene carbonate (EC) – propylene carbonate (PC) as plasticizer and are characterized by impedance spectroscopy and dynamic rheological experiments.

Oldak et al. (2005) have studied the photo- and bio- degradation processes in polyethylene (PE), cellulose and their blends. PE, Cellulose and their blends with different compositions were exposed to UV radiation or composted in soil for bio-degradation. Both types of degradation were carried out under laboratory conditions. The course of degradation processes has been studied using ATR-FTIR and Raman spectroscopies. There are practically no changes in spectra of photo- or bio-degraded pure PE and cellulose powders. Prolonged UV exposure leads to efficient photo-oxidation of blends studied.

Osman et al. (2005) have synthesized poly(methyl methacrylate)/poly(ethylene oxide) (PMMA/PEO) based polymer electrolytes using the solution cast technique. Four systems of PMMA/PEO blends based polymer electrolytes films with ethylene carbonate (EC) as plasticizer; lithium hexafluorophosphate (LiPF_6) systems were investigated. The films were characterized by impedance spectroscopy and FTIR. The FTIR spectra show the complexation occurring between polymers, plasticizer and lithium salt. The FTIR results give further insight in the conductivity enhancement of PMMA/PEO blends based polymer electrolytes.

Li et al. (2006) have studied the glass transition temperatures (T_g) of the poly(methyl methacrylate) and poly(styrene-co-maleic anhydride) (PMMA/SMA) blends plotted versus composition. The samples of all compositions showed only a single T_g . Blends exhibiting a single T_g are regarded as miscible which the immiscible ones are

characterized by two distinct values of T_g , corresponding to the two phases. The composition dependence of the T_g can be described by the Gordon – Taylor - Kwei empirical equation.

Olmos and Benito (2006) have chosen poly(methyl methacrylate) as an additive for an epoxy system. FT-IR spectroscopy (near, FT-NIR, and medium, FT-MIR, ranges) and steady-state fluorescence spectroscopy were used to monitor the epoxy cure reaction and the induced phase separation in a PMMA (2 % w/w)-modified diepoxy-diamine model system.

Tanwar et al. (2006) studied that the conductivity of PMMA can be increased by using a suitable dopant material. All the doped films show better conductivity as compared to pure PMMA films. The increase in conductivity was accounted due to creation of additional hopping sites for the charge carriers in doped samples. Hopping process was the probable mechanism of conduction phenomenon.

High polymer blends Polymethyl methacrylate (PMMA) with cellulose acetate (CA) and Cellulose acetate phthalate (CAP) of varying blend compositions have been prepared to study their biodegradation behavior and blend miscibility. Films of PMMA-CA and PMMA-CAP blends have been prepared by solution casting using Acetone and Dimethyl formamide (DMF) as solvents respectively. Degradation analysis was done by weight loss method and degradability increased with the increase in CA and CAP content in the blend compositions. Miscibility of the blends may be due to the formation of hydrogen bond between the carbonyl group of PMMA and the free hydroxyl group of CA and CAP (Bhat and Kumar 2006).

Adoor et al. (2006) have investigated the blend miscibility of poly(vinyl alcohol) and poly(methyl methacrylate) in N,N-dimethylformamide solution by viscosity, density, ultrasonic velocity, refractive index, and UV and fluorescence spectra studies. Differential scanning calorimetry and scanning electron microscopy were used to confirm the blend miscibility in the solid state. Blends were compatible when the concentration of poly(vinyl alcohol) was greater than 60 wt %.

Macossay et al. (2007) have studied the effect of needle diameter on the resulting electrospun poly(methyl methacrylate) (PMMA) average nanofiber diameter for three different needle gauges. The resulting nanofibers were observed and analyzed by scanning electron microscopy (SEM), suggesting a lack of correlation between the needle diameter used and the resulting average nanofiber diameter. Thermogravimetric analysis (TGA) indicated an increase in the thermal stability of PMMA nanofibers when compared to powdered PMMA, while differential scanning calorimetry (DSC) studies evidenced lower glass transition temperatures (T_g) for PMMA nanofibers in the first heating cycle.

Schroeder et al. (2007) have studied thermoset materials obtained from styrene/vinyl ester resins of different molecular weights modified with poly(methyl methacrylate) (PMMA). Scanning electron microscopy and transmission electron microscopy micrographs of the fracture surfaces allowed the determination of a two-phase morphology of the modified networks. Depending on the molecular weight of the vinyl ester oligomer, the initial content of the PMMA additive, and the selected curing temperature, different morphologies were obtained.

Othman et al. (2007) has prepared five systems of samples by the solution casting technique. These are the plasticized poly(methyl methacrylate) (PMMA-EC) system, the LiCF_3SO_3 salted-poly(methyl methacrylate) (PMMA- LiCF_3SO_3) system, the LiBF_4 salted-poly(methyl methacrylate) (PMMA- LiBF_4) system, the LiCF_3SO_3 salted-poly(methyl methacrylate) containing a fixed amount of plasticizer ([PMMA-EC]- LiCF_3SO_3) system, and the LiBF_4 salted-poly(methyl methacrylate) containing a fixed amount of plasticizer ([PMMA-EC]- LiBF_4) system. The conductivities of the films from each system are characterized by impedance spectroscopy. The increase in conductivity is due to the increase in number of mobile ions, and decrease in conductivity is attributed to ion association. The increase and decrease in the number of ions can be implied from the dielectric constant, ϵ_r -frequency plots. The conductivity-temperature studies are carried out in the temperature range between 303 and 373 K. The results show that the conductivity is increased when the temperature is increased and obeys Arrhenius rule.

Selvakumar and Bhat (2008) studied the miscibility behavior of PMMA and CAB blends in DMF in the temperature range 303-323 K. The results indicated that the blends are miscible in the entire composition range between 303-323 K. The FTIR study of the blend films also indicated the presence of specific interactions such as hydrogen bonding, supporting the results of solution studies.

Structure and properties for binary blends composed of biomass-based cellulose acetate propionate (CAP) and poly(epichlorohydrin) (PECH) have been studied. It was found from the dynamic mechanical measurements that mutual dissolution takes place to some degree with remaining CAP-rich and PECH-rich regions in the blends. As a result of the interdiffusion, leading to fine morphology, the blends exhibit high level of optical transparency although the individual pure components have different refractive index. Furthermore, the mechanical toughness of CAP, which is one of the most serious problems for CAP, is considerably improved by blending PECH. This will have a great impact on industries because the blend technique widens the application of CAP (Yamaguchi and Masuzawa 2008).

Ketotifen was immobilized in cellulose acetate propionate (CAP) membranes and in cellulose acetate butyrate (CAB) membranes. The characteristics of each system were evaluated under a range of experimental conditions. The topography and uniformity of the membranes was assessed using scanning electron microscopy. The release characteristics associated with Ketotifen were monitored spectrophotometrically. The swelling capacity of the membranes was evaluated and attributed to the combined effects of diffusion and of complex dissociation, during swelling. The materials produced were able to provide controlled release of Ketotifen due to their controlled swelling behavior and adequate release properties. The results showed that the release of Ketotifen from the CAB membranes is higher but the release from the CAP membranes is more uniform (Sobral et al. 2008).

Selvakumar and Bhat (2008) have investigated the possibility of producing a biodegradable polymer electrolyte based on cellulose acetate (CA) with varied concentration of LiClO_4 for use in supercapacitors. The successful doping of the CA

films has been analyzed by FTIR and DSC measurements of the LiClO₄ doped CA films. The ionic conductivity of the films increased with increase in salt content and the maximum ionic conductivity obtained for the solid polymer electrolyte at room temperature was $4.9 \times 10^{-3} \Omega^{-1}$ for CA with 16 % LiClO₄. The biodegradation of the solid polymer electrolyte films have been tested by soil burial, degradation in activated sludge, and degradation in buffer medium methods. The extent of biodegradation in the films has been measured by AC Impedance spectroscopy and weight loss calculations. The study indicated sufficient biodegradability of the materials. A p/p polypyrrole supercapacitor has been fabricated and its electrochemical characteristics and performance have been studied. The supercapacitor showed a fairly good specific capacitance of 90 F g⁻¹ and a time constant of 1 s.

Durães et al. (2008) reports the thermal and structural changes promoted by Buriti (*Mauritia flexuosa* L.) oil incorporation into polystyrene (PS) and poly(methyl methacrylate) (PMMA) matrices. Buriti oil, which was used due to its high-carotene content has a good thermal stability and can provide some stability to PS and PMMA as it was shown by TG and TMA data. DSC results showed that both PMMA and PS-based materials were plasticized by the oil and demonstrated that they are immiscible materials. SEM images depict the materials' morphology.

Chang and Woo (2009) have studied the effect of a miscible polymeric diluent on complex formation between isotactic and syndiotactic poly(methyl methacrylate). Formation of a stereocomplex structure in a blend of isotactic and syndiotactic poly(methyl methacrylate)s (iPMMA/sPMMA) was found to be significantly enhanced by introducing a mutual miscible diluent of poly(ethylene oxide) (PEO) in the blend, even when prepared using a kinetically hindered noncomplexing CHCl₃ solvent. Mechanisms and influencing factors, such as thermal treatment, annealing temperature, annealing time, or PEO content in blends, on structures of stereocomplexes in the ternary iPMMA/sPMMA/PEO blends are discussed. FT-IR characterization provided evidence of weak interactions between PEO and the stereocomplex of PMMA.

The miscibility behavior of PMMA and PEG blends in THF has been studied in the temperature range 298-313K. The miscibility has been analyzed by solution viscosity, ultrasonic velocity, and refractive index measurement of the blend solutions. The FTIR studies of the blend films also indicated the presence of weak specific interactions supporting the results of solution studies (Selvakumar et al. 2009).

Rajendran et al. (2009) have studied PVAc-based polymer electrolytes prepared by solvent casting technique. The complex formation in PVAc-PMMA-PC-LiClO₄ system has been confirmed from XRD and FTIR studies. All the electrolytes show appreciable conductivity even at room temperature.

Solid polymer blend electrolytes based on PVAc-PMMA-LiClO₄ in different compositions are prepared by solution-casting technique. The complexation of the developed polymer electrolyte is confirmed using FTIR and XRD studies. The ionic conductivity of the developed films was measured by AC impedance technique. The thermal stability was observed for the films from TG/DTA analysis (Rajendran et al. 2010).

Deka and Kumar (2010) have investigated a novel polymer electrolyte based on poly(methyl methacrylate) (PMMA)/layered lithium trivanadate (LiV₃O₈) nanocomposite. X-ray diffraction (XRD) study shows that d-spacing is increased from 6.3±0.1 Å to 12.8±0.1 Å upon intercalation of the polymer into the layered LiV₃O₈. Room temperature ionic conductivity of the obtained nanocomposite gel polymer electrolyte is found to be superior to that of conventional PMMA-based gel polymer electrolyte. Enhancement in ionic conductivity of the nanocomposite gel electrolyte is attributed to the formation of a two-dimensional channel as a result of decreased interaction between Li⁺ and V₃O₈⁻ layers as confirmed by FTIR. SEM results show aggregation of nanocomposite particles resulting from extension of some of the polymer chains from interlayer to the edge providing paths for Li⁺ ion transport. Interfacial stability of nanocomposite gel electrolyte is also found to be better than that of the conventional PMMA-based gel polymer electrolyte.

The domains of time and space generally covered by full atomistic simulation (AS) to represent the glass transition temperature, T_g , are very small. Physical interpretations of the phenomena occurring at this transition are inevitably limited. To specifically address such limitation, behavior of the heat capacity that accounts for the freezing of the degrees of freedom as temperature is decreased, is investigated. The selected polymer is poly(methyl methacrylate) since it offers the opportunity to exhibit a different T_g according to the tacticity of its chain. AS and experimental data are thus compared to a theoretical model that takes into account three contributions to the leap in the heat capacity occurring at T_g . The comparison discloses that an excellent agreement is obtained between simulated and experimental contributions from vibrations and free volume. However, from an AS viewpoint changes in the conformation weakly contribute to this leap. Despite this discrepancy local contributions to the glass transition as predicted by atomistic simulation, are sufficient to determine T_g (Soldera et al. 2010).

Polymer electrolyte membranes, comprising of poly(methyl methacrylate) (PMMA), lithium tetraborate ($\text{Li}_2\text{B}_4\text{O}_7$) as salt and dibutyl phthalate (DBP) as plasticizer were prepared using a solution casting method. The incorporation of DBP enhanced the ionic conductivity of the polymer electrolyte. The polymer electrolyte containing 70 wt. % of poly(methyl methacrylate)–lithium tetraborate and 30 wt. % of DBP presents the highest ionic conductivity of 1.58×10^{-7} S/cm. The temperature dependence of ionic conductivity study showed that these polymer electrolytes obey Vogel–Tamman–Fulcher (VTF) type behavior. Thermogravimetric analysis (TGA) was employed to analyse the thermal stability of the polymer electrolytes. Fourier transform infrared (FTIR) studies confirmed the complexation between poly(methyl methacrylate), lithium tetraborate and DBP (Ramesh and Chao 2011).

Puls et al. (2011) highlights that CA polymer based consumer products have good potential for environmental degradation. There is also potential for increasing the degradation with accelerated disintegration by redesigning commercial products.

Kumar and Bhat (2011) have studied the miscibility behavior of PVDF and CA blends in DMF in the temperature range 303-323K. The miscibility has been analyzed by

solution viscosity, ultrasonic velocity and refractive index measurement of the blend solutions. The FTIR study of the blend films also indicated the presence of weak specific interactions supporting the results of solution studies.

Badmapriya and Rajalakshmi (2011) have optimized the properties of new polymeric films based on blends of cellulose acetate and guar gum. Cellulose acetate, a water-insoluble polymer can protect the core from the small intestinal pH and act as a reservoir type system. Variation in the guar gum:cellulose acetate blends were made thereby highly efficient and easy application tools were identified altering the membrane's properties.

IPN-type composites consisting of cellulose acetate (CA) and poly(methyl methacrylate; PMMA) were successfully synthesized in film form. In this synthesis, a mercapto group (SH)-containing CA, CA-MA, was prepared in advance by esterification of CA with mercaptoacetic acid, and then intercomponent cross-linking between CA-MA and PMMA was attained by thiol-ene polymerization of methyl methacrylate (MMA) onto the CA-MA substrate. For comparison, polymer synthesis was also attempted to produce a semi-IPN type of composites comprising CA and cross-linked PMMA, via copolymerization of MMA and ethylene glycol dimethacrylate as cross-linker in a homogeneous system containing CA solute. Thermal and mechanical properties of thus obtained polymer composites were investigated by differential scanning calorimetry, dynamic mechanical analysis, and a tensile test, in correlation with the mixing state of the essentially immiscible cellulosic and methacrylate polymer components. It was shown that the specific IPN technique using thiol-ene reactions usually resulted in a much better compatibility-enhanced polymer composite, which exhibited a higher tensile strength and even an outstanding ductility without parallel in any film sample of CA, PMMA, and their physical blends (Aoki et al. 2011).

Jeon et al. (2012) deals with the preparation, structural characterization, and physical performances of composites composed of biomass-based cellulose acetate propionate (CAP) and exfoliated graphene (EG). Structural features, thermal stability, mechanical modulus, and electrical resistivity of CAP/EG composites are investigated as

a function of EG content. SEM and X-ray diffraction data demonstrate that graphene platelets of EG are well dispersed and exfoliated in the CAP matrix. Thermo-oxidative stability of CAP/EG composites under active oxygen gas condition is improved substantially due to the gas barrier effect of graphene platelets of EG dispersed in the CAP matrix. Dynamic mechanical modulus of the composites is also enhanced significantly with increasing the EG content. The electrical volume resistivity of CAP/EG composites prepared by melt-compounding is decreased dramatically.

The nanosheet of graphene was chemically modified by long alkyl chain for enhanced compatibility with polymer matrix and graphene/poly(methyl methacrylate) (PMMA) nanocomposites with homogeneous dispersion of the nanosheets and enhanced nanofiller-matrix interfacial interaction were fabricated via a facile in-situ bulk polymerization. The nanocomposites were characterized by X-ray diffraction, Fourier transform infrared spectroscopy, Scanning electron microscopy and thermogravimetry (Yuan et al. 2012).

All-cellulose composite fibers were produced by electrospinning dispersions containing cellulose acetate (CA) and cellulose nanocrystals (CNCs). Precursor polymer matrices were obtained after dispersion of CA with different degrees of substitution in a binary mixture of organic solvents. The obtained fibers of CA loaded with CNCs had typical widths in the nano- and micro-scale and presented a glass transition temperature of 145 °C. The CA component was converted to cellulose by using alkaline hydrolysis to yield all-cellulose composite fibers that preserved the original morphology of the precursor system. Together with Fourier transform infrared spectroscopy fingerprints the thermal behavior of the all-cellulose composite fibers indicated complete conversion of cellulose acetate to regenerated cellulose. Noticeable changes in the thermal, surface and chemical properties were observed upon deacetylation. Not only the thermal transitions of cellulose acetate disappeared but the initial water contact angle of the web was reduced drastically (Vallejos et al. 2012).

The hydrogen bond interactions and dynamics of the poly (methyl methacrylate) (PMMA) and poly(4-vinyl phenol) (PVPh) polymer blends were studied by a variety of

advanced solid-state NMR techniques. The possible hydrogen bond interactions between the carbonyl group of PMMA and hydroxyl group of PVPh were successfully elucidated by two-dimensional ^1H - ^1H spin-exchange ^{13}C - ^1H heteronuclear chemical-shift correlation (HETCOR) NMR experiment. The ^{13}C 2D separation of undistorted powder patterns by effortless recoupling (SUPER) experiments combined with quantum chemical calculations for the theoretical predictions of chemical-shift anisotropy (CSA) parameters were utilized to investigate the intermolecular hydrogen-bonding interactions and molecular conformation of the blends. ^{13}C - ^1H PISEMA (polarization inversion and spin-exchange at magic angle) experiments at different temperatures were used to reveal the heterogeneous dynamics resulting from the cooperative motion associated with the hydrogen bond interaction. PISEMA analysis shows that the motion of aromatic group in PVPh is affected by the rotating motions of methyl in PMMA (Fu et al. 2013).

Cellulose acetate (CA) with a degree of substitution (DS) of 2.5 has been plasticized using eco-friendly plasticizers such as triacetin, tripropionin, triethyl citrate, tributyl citrate, tributyl 2-acetyl citrate and poly(ethylene glycol) of low molecular weight. Thermo-mechanical properties and hydrophilicity of the modified CA have been measured and correlated with the content and nature of the plasticizer used and compared with unplasticized CA. The increase in toughening and the change in the hydrophilicity by the plasticization were evaluated in terms of aging and weathering stability under accelerated conditions. Samples were exposed to UV-degradation with water spray periods. The treated samples were removed periodically and characterized by several analytical techniques. The results are discussed with particular emphasis toward the effects of plasticization on enhancement of the degradation rate of CA. The plasticization of CA triggered an increase of the weight loss between 50 and 90 %, where low molecular weight plasticizers were shown to be more effective. A right balance between hydrophilicity and plasticization efficiency (reduction of T_g) is needed to increase the degradation rate of CA (Quintana et al. 2013).

1.6 SCOPE OF THE WORK

In the modern era, polymers have led to the invention of new materials and hence occupy a major place in the materials field. In characteristics and application prospects polymers offer novelty and versatility, which is not found in any other kind of materials. Extensive use of these polymers has also resulted in marked increase of municipal and industrial waste throughout the world. In developing countries, environmental pollution by polymers has assumed dangerous proportions. As a result, attempts have been made to solve these problems by including biodegradability into these polymers in everyday use through slight modifications of their structures or blending them with biodegradable materials. The development of biodegradable polymer blend with an optimum balance of physical properties and biodegradable properties is of importance to relieve environmental problems like waste disposal.

The importance of blending has increased recently because it has become a useful approach for the preparation of materials with new desirable properties that are absent in the component polymers. The blending of polymers may result in reduction of basic cost and improved processing and also may enable properties of importance to be maximized. However, manifestation of these properties of polymer blends depends upon the miscibility of the components and structure. The basis of polymer-polymer miscibility may arise from any specific interaction, such as hydrogen bonding, dipole-dipole forces or charge transfer interactions in the system. The miscibility studies of polymer blend systems are of great significance for engineering applications of polymers. They also provide substantial information on the processes involving polymer production and their uses. Polymer dissolution also plays a key role in many industrial applications and an understanding of the dissolution process allows for the optimization of design and processing conditions as well as selection of a suitable solvent. Hence it is of interest to identify and to study the specific interactions and the miscibility aspects of the polymer blend systems.

Keeping these points in view, in the present study an investigation of the miscibility behaviors of some selected polymers has been undertaken. An attempt to

develop and study some new biodegradable polymer blends has also been made. The polymers used for the study mainly belong to the class of commodity polymers. The selection of commodity polymers for the purpose is with an intention of their end use as eco-friendly packaging materials. Naturally available polymer materials such as cellulose acetate and its derivatives have been used for the preparation of biodegradable polymer blends with poly(methyl methacrylate) so as to make use of renewable resources.

Poly(methyl methacrylate) (PMMA), is both a thermoplastic and transparent plastic, is especially known for its exceptional optical properties. This uncrystallized polymer shows remarkable transparency. PMMA at ambient temperature is hard, rigid, and brittle with little elongation. PMMA is hygroscopic and, under extreme conditions, the water absorbed will act as a plasticizer and will modify the properties of the material. Its creep is fairly limited. When critical stress is exceeded, PMMA is subject to crazing. This phenomenon is even accentuated in the presence of corrosive agents (alcohol, gasoline etc.). It is resistant to inorganic acids and alkalis but is attacked by a wide range of organic solvents. Resistance to shock is relatively low and the polymer is brittle. This resistance can be improved by adding an anti-shock agent. PMMA resists scratching to a good degree under normal conditions of use. However, when cleaned frequently or used in a dusty environment, it could be scratched. PMMAs are easily polished. It is often used as an alternative to glass and is preferred for many applications because of its moderate properties, easy handling, easy processing and low cost.

The basic raw material used to manufacture cellulose acetate polymer is purified plant derived cellulose. Cellulose is modified with raw materials containing acetyl groups to form cellulose acetate polymers. The unique properties of cellulose acetate enable a great variety of end-use applications. It can be used as fabrics, films, filters etc. They are also useful in separation technology, molded goods and plastics. Some special applications of cellulose acetates are ink reservoirs, medical wound dressings, hygiene products and specialty papers. This polymer does not persist long term and can be degraded under a variety of mechanisms like biodegradability, chemical degradation, photo degradation and disintegration.

Phthalates are by far the most widely used plasticizers, primarily to make soft and flexible polyvinyl chloride for the applications in the industry of automotive, building and construction material, cable, flooring, medical device and toys. Minor quantity of phthalates is used in adhesives, caulk, sealants and paint to improve work performance. Small molecule phthalates are used as solvents in perfumes to provide longer linger longer and in nail polish to prevent chipping. They are also used as ingredients of insect repellents, as solvents in lacquer and pesticides, and as dye carrier. They are used as textile lubricating agents and as solid rocket propellants. A wide range of phthalates of varying chain length and structure provides each adequate properties and cost-effective for various processing and mechanical requirements.

Phthalate plasticizers have been found to be a health concern when found in direct contact with bodily fluids. Studies performed on laboratory animals have shown that there is direct evidence that certain phthalate plasticizers have a carcinogenic effect in vivo. Because they are readily miscible in organic solvents like plasma and saliva, humans have a chance of ingesting or absorbing them during common medical procedures. It is believed that once they are absorbed they are stored in the fatty tissue of humans, and therefore can be teratogenic. There is also little known about the body's ability to metabolize them once they are ingested or absorbed.

Review of literature reveals that the preparation and characterization of polymer blends with different morphology, and using different additives to the polymer matrix in preparing different polymer blends and composites for various applications were not much explored. In light of the above, preparation of polymer blends gains its importance. By adding plasticizers, the polymer blends render plasticity, also addition to enhanced ionic conductivity.

In view of this, it is proposed to prepare high polymer blends of PMMA with biodegradable polymers by solution casting method with and without plasticizers. During the preparation of PMMA and cellulose acetate and its derivatives blends Dimethyl phthalate (DMP), Diethyl phthalate (DEP), Dipropyl phthalate (DPP), Dibutyl phthalate (DBP) and Propylene carbonate (PC) are used as plasticizers. It has been planned to

prepare low percentage of plasticized blends in view of health and to avoid toxicity effects. The properties of these blends and composites are studied by thermal, spectral and electrochemical methods. The objectives of the present research work are listed below.

1.7 OBJECTIVES

1. To prepare non-plasticized blends of Poly(methyl methacrylate) (PMMA) with Cellulose derivatives namely, Cellulose acetate (CA), Cellulose acetate propionate (CAP), Cellulose acetate butyrate (CAB) and Cellulose acetate phthalate (CAPH).
2. To prepare low percentage (2.5 %, 5 %, 7.5 % and 10 %) plasticized blends of PMMA with Cellulose derivatives like CA, CAP, CAB and CAPH with plasticizers such as Dimethyl phthalate (DMP), Diethyl phthalate (DEP), Dipropyl phthalate (DPP), Dibutyl phthalate (DPP) and Propylene carbonate (PC).
3. To study the miscibility of the plasticized and non-plasticized blends by Fourier transform infrared (FTIR) spectroscopy and Differential scanning calorimetry (DSC).
4. To study the membrane properties such as water uptake and ion exchange capacity (IEC) of the plasticized and non-plasticized blends.
5. To study the conductivity and dielectric properties of the plasticized and non-plasticized blends using AC impedance spectroscopy.

The thesis comprises of eight chapters. **Chapter 1** gives a brief introduction to polymer blends and methodology. A review of literature on polymer blends, scope and objectives of the present research work and a brief account of materials and methods used in the present work have also been included in this chapter.

Chapter 2 provides the miscibility, water uptake, ion exchange capacity, conductivity and dielectric studies of non-plasticized blends of PMMA with CA, CAP, CAB and CAPH. This chapter describes the different characterization techniques such as

FTIR and DSC to confirm the miscibility of the non-plasticized blends. Membrane behaviors were studied by water uptake and ion exchange capacity tests. The proton conductivity and dielectric studies have been calculated with the help of electrochemical impedance spectroscopy measurement.

Chapter 3, 4, 5, 6 and 7 deals with miscibility, water uptake, ion exchange capacity, conductivity and dielectric studies of dimethyl phthalate (DMP), diethyl phthalate (DEP), dipropyl phthalate (DPP), dibutyl phthalate (DBP) and propylene carbonate (PC) plasticized blends of PMMA with CA, CAP, CAB and CAPH respectively. The percentage amounts of plasticizers used in all these blends are, 2.5, 5, 7.5 and 10. The miscibility of the plasticized blends has been analyzed characterization techniques such as FTIR and DSC. Water uptake and ion exchange capacity tests have been incorporated to study the membrane behavior. The electrochemical impedance spectroscopy measurements have been done to calculate proton conductivity and dielectric studies of the prepared plasticized blends.

Chapter 8 outlines the summary and conclusions of the present study along with the scope for the future work.

1.8 EXPERIMENTAL

1.8.1 Materials

Polymers tested in this work were obtained from commercial sources and were used as received. PMMA, with MW=1,20,000; CA, with MW=52,000; CAP, with MN=75,000; CAB, with MN=70,000 and CAPH, with MW=2534.12 were supplied by Sigma Aldrich. Dimethyl formamide (DMF) was used as solvent supplied by Merck. The plasticizers used were DMP, with MW=194.18; DEP, with MW=222.24; DPP, with MW=250.29; DBP, with MW=278.34 and PC, with MW=102.09 obtained from Sigma Aldrich and was used as received.

1.8.1.1 Structure of PMMA

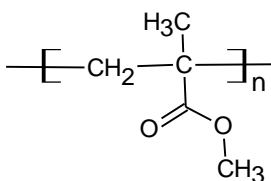


Figure 1.1 Structure of PMMA.

1.8.1.2 Structure of CA and its derivatives

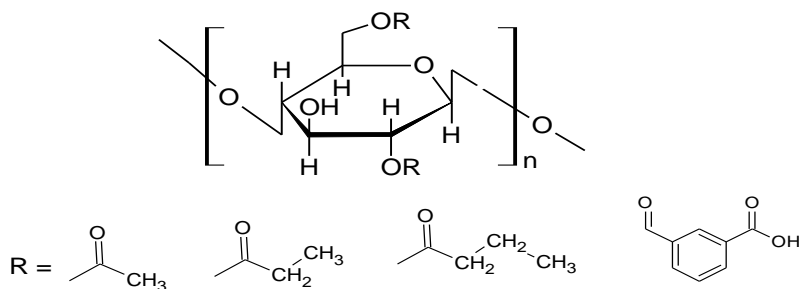


Figure 1.2 Structure of CA and its derivatives.

1.8.1.3 Structures of plasticizers

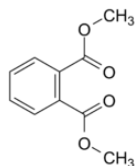


Figure 1.3 Structure of DMP.

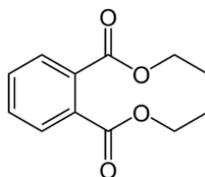


Figure 1.4 Structure of DEP.

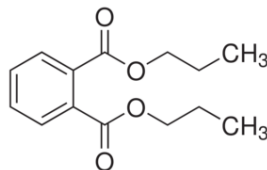


Figure 1.5 Structure of DPP.

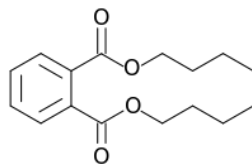


Figure 1.6 Structure of DBP.

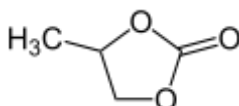


Figure 1.7 Structure of PC.

1.8.2 Preparation of Blends

1.8.2.1 Preparation of non-plasticized blends

Blends of non-plasticized PMMA with Cellulose acetate and its derivatives were prepared by die casting or solution casting. The % (w/v) stock solutions of PMMA and CA and its derivatives were prepared in DMF by stirring for 24 hours. The solution mixtures thus prepared were stirred for three hours for uniform mixing. They were then poured into Teflon petri dishes and the solvent was allowed to evaporate at 60 °C for 72 h in a vacuum oven for drying. The dried films were taken out from the vacuum oven and stored in a vacuum desiccator.

1.8.2.2 Preparation of plasticized blends

Blends of 2.5 %, 5 %, 7.5 % and 10 % DMP, DEP, DPP, DBP and PC plasticized PMMA with Cellulose acetate and its derivatives were prepared by die casting or solution casting. The % (w/v) stock solutions of PMMA and CA and its derivatives with respective plasticizers were prepared in DMF by stirring for 24 hours. The solution mixtures thus prepared were stirred for three hours for uniform mixing. They were then poured into Teflon petri dishes and the solvent was allowed to evaporate at 60 °C for 144 h in a vacuum oven for drying. The dried films were taken out from vacuum oven and stored in a vacuum desiccator.

1.8.3 Membrane Characterization

1.8.3.1 Fourier transform infrared (FTIR) spectroscopic studies

FTIR spectra of the pure polymers and blends (non-plasticized and plasticized) were scanned in the range between 4000 and 400 cm^{-1} on a NICOLET AVATAR 330 FTIR-ATR spectrophotometer.

1.8.3.2 Differential scanning calorimetry (DSC) studies

DSC thermograms of pure polymers and blends (non-plasticized and plasticized) were obtained on a SHIMADZU DSC-60. The sample of 4 to 4.5 mg in weight was sealed in an aluminium pan and measurements were performed over the temperature range of ambient to 250 $^{\circ}\text{C}$ at the heating rate of 10 $^{\circ}\text{Cmin}^{-1}$ under nitrogen gas flow.

1.8.3.3 Water uptake

The water uptake in the pure polymers and blends (non-plasticized and plasticized) were measured by immersing the blends into deionised water at room temperature for 24 h. Then the blends were taken out, wiped with tissue paper, and immediately weighed on a balance. Triplicates were run for each blend to get the satisfactory reproducibility. The water uptake in the blends, W , was calculated by

$$W = \frac{W_{wet} - W_{dry}}{W_{dry}} \quad (1.7)$$

where W_{dry} and W_{wet} are the weight of dry and corresponding water absorbed membranes, respectively.

1.8.3.4 Ion exchange capacity measurements

Ion exchange capacity (IEC) indicates the number of milliequivalents (mequiv.) of ions in 1 g of the dry polymer blend. To determine the ion exchange capacity, blends of similar weight were soaked in 50 mL of 0.01 N sodium hydroxide (NaOH) solution for 24 h at ambient temperature. After 24 h, 10 mL of the solution was titrated with 0.01N sulphuric acid (H_2SO_4), using a phenolphthalein indicator. IEC was calculated by

$$IEC = \frac{(B - P) \times 0.01 \times 5}{m} \quad (1.8)$$

where IEC is ion exchange capacity (in mequivg^{-1}), B is amount of sulphuric acid used to

neutralize blank sample solution in mL. P is amount of H_2SO_4 used to neutralize the blend soaked solution used in the study in mL, 0.01 is normality of the H_2SO_4 . Here, 5 is the factor corresponding to the ratio of the amount of NaOH used to soak the blend/s to the amount used for titration, and m is the mass of the polymer blend in g.

1.8.3.5 *Electrochemical impedance spectroscopy and proton conductivity measurement*

The AC impedance spectra of the membranes were recorded in the frequency range between 0.01 Hz and 100000 Hz with amplitude of 5 mV using AUTOLAB Electrochemical System (Eco Chemie BV, Netherlands) over the temperature range of 30 °C to 70 °C. Proton conductivity measurements were performed on the membranes in a typical two-electrode cell by AC impedance technique. The conductivity cell composed of two copper electrodes of 2 cm × 2 cm dimensions. The blend sample was sandwiched between the two copper electrodes fixed in a Teflon block and kept in a closed glass container. 1M NaCl solution was used as an electrolyte. The cell was kept at each measuring temperature for a minimum of 60 min to ensure thermal equilibration of the sample at the temperature before measurement. The resistance value associated with the blend conductivity was determined from the high frequency intercept of the impedance with the real axis. The blend conductivity was calculated from the membrane resistance, R , using the following equation:

$$\sigma = L/RA \quad (1.9)$$

where σ is the proton conductivity of blend (in Scm^{-1}), L is the thickness (in cm) and A is the area of the blend (in cm^2).

1.8.3.6 *Dielectric studies*

Complex impedance data, Z^* can be represented by its real, Z_R and imaginary, Z_I parts by the relation:

$$Z^* = Z_R + jZ_I \quad (1.10)$$

The relationships between complex impedance, admittance, permittivity and electrical modulus can be found elsewhere.

The equations for the dielectric constant, ϵ_R and the dielectric loss, ϵ_I , can be shown as

$$\varepsilon_R = \frac{Z_I}{\omega C_0 (Z_R^2 + Z_I^2)} \quad (1.11)$$

$$\varepsilon_I = \frac{Z_R}{\omega C_0 (Z_R^2 + Z_I^2)} \quad (1.12)$$

Here $C_0 = \frac{\varepsilon_0 A}{t}$ and ε_0 is the permittivity of the free space, A is the electrolyte-electrode contact area and t is the thickness of the sample and $\omega=2\pi f$, f being the frequency in Hz.

Chapter 2

STUDIES ON NON-PLASTICIZED BLENDS OF PMMA WITH CA, CAP, CAB AND CAPH

Chapter 2 describes the study of non-plasticized blends of PMMA with CA derivatives. This chapter also gives a brief account of component polymers which are used in the present work.

2.1 A BRIEF ACCOUNT OF PMMA, CA, CAP, CAB AND CAPH

2.1.1 Poly (methyl methacrylate) (PMMA) (C₅H₈O₂)_n

PMMA (Acrylic) is a thermoplastic and transparent plastic. Plexiglass and Lucite are the two of the most common names. It is also commonly known as Acrylic glass, Acrylic, Perspex or Plexiglas.

It is prepared by radical polymerization in bulk or suspension. It is a colourless transparent plastic with an excellent outdoor life and good strength. It is amorphous by nature, owing to the presence of bulky side groups in the molecules. It is resistant to many chemicals but soluble in organic solvents such as ketones, chlorinated hydrocarbons and esters. It can be thermally depolymerised to yield back the entire quantity of monomer. Optical clarity is the main feature of this plastic. In many applications, it is an excellent substitute for glass. It has good mechanical properties. However, compared to glass, it has poor scratch resistance. It is used to make attractive signboards and durable lenses for automobile lighting. It is also used in buildings for decorative purposes (Gowariker et al. 2008).

Properties of PMMA: Good weatherability, clear/colourable-excellent clarity, good insulation properties, UV resistant, good abrasion resistance, good stiffness, low smoke emission, low water absorption.

Uses of PMMA

- Industrial uses: water tank liner, hand-held computer case, liquid chemical pump, conveyor rollers, soap dispensers hatch covers, bumper guards
- Automotive industry: lenses of exterior lights, trunk release handles, master cylinder dashboard lighting
- Consumer products: aquariums, motorcycle helmet lenses, paint, furniture, picture framing, umbrella clamps, cell phone antennas, bicycle air pumps, AV wall outlets, visors etc.

- Medical applications: lens implants, hard contact lenses, dentures, fillings.

2.1.2 Cellulose acetate (CA)

CA is the acetate ester of cellulose. It is produced by the action of acetic anhydride on cellulose catalyzed by sulfuric acid or perchloric acid. The final polymer contains 40 wt % of acetyl groups. It is used as a film base in photography, as a component in some adhesives, and as a frame material for eyeglasses. It is also used as a synthetic fiber and in the manufacture of cigarette filters and playing cards.

The Federal Trade Commission definition for acetate fiber is “A manufactured fiber in which the fiber-forming substance is cellulose acetate, where not less than 92 percent of the hydroxyl groups are acetylated, the term triacetate may be used as a generic description of the fiber.”

Acetate is derived from cellulose by deconstructing wood pulp into purified fluffy white cellulose. In order to get a good product special qualities of pulps dissolving pulps are used. A common problem with these is that the reactivity of the cellulose is uneven. The cellulose is reacted with acetic acid and acetic anhydride in the presence of sulfuric acid. It is then put through a controlled, partial hydrolysis to remove the sulfate and a sufficient number of acetate groups to give the product the desired properties. The anhydroglucose unit is the fundamental repeating structure of cellulose and has three hydroxyl groups which can react to form acetate esters. The most common form of cellulose acetate fiber has an acetate group on approximately two of every three hydroxyls. This cellulose diacetate is known as secondary acetate, or simply as acetate. After it is formed, cellulose acetate is dissolved in acetone into a viscous resin for extrusion through spinnerets. As the filaments emerge, the solvent is evaporated in warm air via dry spinning, producing fine cellulose acetate fibers.

Properties of CA: Cellulose acetate is cellulosic and thermoplastic. It shows the properties of selective absorption and removal of low levels of certain organic chemicals. Cellulose acetate can be easily bonded with plasticizers, heat, and pressure. It is soluble in many common solvents including acetone and other organic solvents and can be modified to be soluble in alternative solvents like water. It is hydrophilic with good liquid

transport and excellent absorption. In textile applications, it provides comfort and absorbency, but also loses strength when wet. Acetate fibers are hypoallergenic. It can be easily composted or incinerated. It can be dyed, however special dyes and pigments are required since acetate does not accept dyes ordinarily used for cotton and rayon. Acetate fibers are resistant to mold and mildew. It is easily weakened by strong alkaline solutions and strong oxidizing agents.

Uses of CA:

- Cellulose acetate is widely used to make buttons, sunglasses, linings, blouses, dresses, wedding and party attire, home furnishings, draperies, upholstery and slip covers.
- Industrially, it is used to make cigarette and other filters, ink reservoirs for fiber tip pens.
- It is used to make high absorbency products like diapers and surgical products.
- The original Lego bricks were manufactured from cellulose acetate from 1949 to 1963.
- Its use is common in Award Ribbon: Rosettes for equestrian events, dog/cat shows, corporate awards, and advertising and identification products all use cellulose acetate ribbon.
- KEM brand playing cards are made of cellulose acetate. It is used at the World Series of Poker and in many poker rooms at major casinos (Gowariker et al. 2008).

2.1.3 Cellulose acetate propionate (CAP) (C₇₆H₁₁₄O₄₉)

CAP is a mixed cellulose ester. It is produced by the action of acetic acid on propionic acid catalyzed by organic acids. The final polymer contains 2.5 wt % acetyl and 46 wt % propionyl groups.

Properties of CAP: CAP properties are intermediate between CA and CAB. They resemble CA in many performance properties and are similar to CAB in solubility and compatibility. Like acetates, the propionates have low odor and thus can be used where this is a requirement. Propionate esters can be used effectively to disperse pigments.

Propionates are also stable to ultraviolet light and do not react with dyes, fluorescent colors or metallic pigments.

Uses of CAP: In printing inks and clear overprint varnishes because of its wide solubility in ink solvents, compatibility with other resins used in printing inks. It is useful in plastic coatings, paper coatings and various reprographic processes.

2.1.4 Cellulose acetate butyrate (CAB) (C₈₄H₁₃₀O₄₉)

CAB is a cellulosic and thermoplastic, commonly known as butyrate. It is made by the esterification of cellulose with a mixture of acetic anhydride and butyric anhydride. The esterification is controlled in such a way that the final polymer contains 13.5 wt % of acetyl and 37 wt % of butyl groups.

Properties of CAB: It is resistant to ultraviolet rays. It has high impact strength, good dimensional stability, excellent compatibility with plasticizers and much lower moisture absorption, as compared to cellulose acetate. CAB has better weathering characteristics than Cellulose acetate or Cellulose propionate. It is also tougher than Cellulose acetate, transparent and glossy surface finish.

Uses of CAB: Tool handles, panels for illuminated signs, steering wheels, goggles, bathroom fittings, decorative trim for cars and consumer durables, drawing stencils, pens, pneumatic system traps, blister packaging, laminating with Aluminium foil (Gowariker et al. 2008).

2.1.5 Cellulose acetate phthalate (CAPH) (C₁₁₆H₁₁₆O₆₄)

CAPH is also known as cellacefate or Cellacephate or Cellulose Acetate 1,2 - Benzene Dicarboxylate, is a commonly used polymer phthalate in the formulation of pharmaceuticals, such as the enteric coating of tablets or capsules and for controlled release formulations. It is a cellulose polymer where about half of the hydroxyls are esterified with acetyls, a quarter is esterified with one or two carboxyls of a phthalic acid, and the last rest is unchanged. It is a hygroscopic white to off-white free-flowing powder, granules, or flakes. It is tasteless and odorless, though may have a weak odor of acetic acid. Its main use in pharmaceuticals is with enteric formulations. It can be used together with other coating agents, e.g. ethyl cellulose. Cellulose acetate phthalate is commonly

plasticized with diethyl phthalate, a hydrophobic compound, or triethyl citrate, a hydrophilic compound; other compatible plasticizers are various phthalates, triacetin, dibutyl tartrate, glycerol, propylene glycol, tripropionin, triacetin citrate, acetylated monoglycerides, etc.

The most common way to prepare cellulose acetate phthalate consists of the reaction of a partially substituted cellulose acetate (CA) with phthalic anhydride in the presence of an organic solvent and a basic catalyst. The organic solvents widely used as reaction media for the phthaloylation of cellulose acetate are acetic acid, acetone, or pyridine. The basic catalysts employed are anhydrous sodium acetate when using acetic acid, amines when using acetone, and the organic solvent itself when using pyridine as reaction medium.

Properties of CAPH: CAPH has been used for several decades as a pharmaceutical excipient due to its solubility dependent on the pH of the aqueous media. Enteric coatings based on CAPH are resistant to acidic gastric fluids, but easily soluble in mildly basic medium of the intestine. The degree of substitution (DS) mainly determines the pH sensitive solubility of CAPH (as other properties of this mixed ester) namely the average number of substituent groups bound to an anhydroglucose unit (AGU), as well as by the molar ratio (acetyl and phthaloyl groups). These two structural characteristics of the polymer are dependent on the method employed for its synthesis.

Uses of CAPH:

- Film coating of tablets
- Enteric coating of tablets
- Sustained release
- Delayed release
- Pallate coating material
- Recently, CAPH's potential to inhibit infections by human immunodeficiency virus type 1 (HIV-1) and several herpes viruses in vitro have been investigated.

2.2 RESULTS AND DISCUSSION

2.2.1 Fourier Transform Infrared (FTIR) Spectroscopic Studies

FTIR spectroscopy is used to confirm the presence of hydrogen bonding and the miscibility of the blends in the solid state. In comparison with the typical chemical changes, the changes in energies, bond lengths and electron densities with the formation of hydrogen bonds are actually quite small in magnitude and FTIR spectroscopy is preferred method since it is very sensitive to the formation of the hydrogen bond (He et al. 2004). If the groups involved in the hydrogen bond formation in a blend system are carbonyl and hydroxyl moieties, then the vibration frequencies of both the groups are expected to show a red shift due to hydrogen bond formation compared with the non-interacting group frequencies.

FTIR spectra of pure PMMA, PMMA/CA 50/50 blend and pure CA were shown in Figure 2.1, Figure 2.2 and Figure 2.3 respectively. The carbonyl frequency of pure CA (Figure 2.3) at 1736.4 cm^{-1} decreased to 1723.1 cm^{-1} in the PMMA/CA 50/50 blend (Figure 2.2). Similarly, FTIR spectra of PMMA/CAP 50/50 blend and pure CAP were shown in Figure 2.4 and Figure 2.5 respectively. The carbonyl frequency of pure CAP (Figure 2.5) at 1736.4 cm^{-1} decreased to 1729.9 cm^{-1} in the PMMA/CAP 50/50 blend (Figure 2.4). FTIR spectra of PMMA/CAB 50/50 blend and pure CAB were shown in Figure 2.6 and Figure 2.7 respectively. The carbonyl frequency of pure CAB (Figure 2.7) at 1740.4 cm^{-1} decreased to 1731.3 cm^{-1} in the PMMA/CAB 50/50 blend (Figure 2.6). FTIR spectra of PMMA/CAPh 50/50 blend and pure CAPh were shown in Figure 2.8 and Figure 2.9 respectively. The carbonyl frequency of pure CAPh (Figure 2.9) at 1721.8 cm^{-1} decreased to 1721.6 cm^{-1} in the PMMA/CAPh 50/50 blend (Figure 2.8). Such shift in the specific vibration frequencies are ascribed to the formation of a weak hydrogen bond between component polymers in the blend. This can also be contributing to the miscibility of the blends.

The strong and broad band at around 3475.2 cm^{-1} and 3610.3 cm^{-1} in pure CA (Figure 2.3) and PMMA/CA 50/50 blend (Figure 2.2), 3482.0 cm^{-1} and 3473.5 cm^{-1} in pure CAP (Figure 2.5) and PMMA/CAP 50/50 blend (Figure 2.4), 3602.8 cm^{-1} and

3486.7 cm⁻¹ in pure CAB (Figure 2.7) and PMMA/CAB 50/50 blend (Figure 2.6), 3465.4 cm⁻¹ and 3428.4 cm⁻¹ in pure CAPH (Figure 2.9) and PMMA/CAPH 50/50 blend (Figure 2.8), respectively, corresponded to the -OH stretching vibrations of hydroxyl groups. The intensity of the broad band decreased after blending, indicating that part of the -OH groups are involved in the hydrogen bond formation. These results indicate that specific interactions such as the hydrogen bonding forces exist in the blends and this is leading to the miscibility of the blends.

2.2.2 Differential Scanning Calorimetry (DSC) Studies

Miscibility of blends has been widely discussed in the literature. One of the standard methods employed to understand the miscibility of polymer blends is Differential Scanning Calorimetry (DSC). The DSC thermograms of pure polymers and CA derivatives blends are shown in Figure 2.10, Figure 2.11, Figure 2.12 and Figure 2.13 respectively.

In the figures, (a) is 0/100, (b) is 30/70, (c) is 50/50, (d) is 70/30 and (e) is 100/0 blend compositions. From Figure 2.10 to Figure 2.13, it can be seen that the T_g for pure CA, CAP, CAB, CAPH and PMMA are 191.78 °C, 141.8 °C, 133.63 °C, 145.59 °C and 107.46 °C respectively. It is interesting to note here that the thermograms for the blends (Figure 2.10 to Figure 2.13) exhibited single T_g and its value lies intermediate to the T_g values of pure PMMA and pure CA derivatives. Further, the T_g values of the blend films decreased regularly on increase of PMMA content in the blends. Such a systematic variation of T_g in the blends is indicative of miscibility of the components in the blends.

A number of theoretical equations have been proposed for estimating the glass transition temperature of blend films from the properties of the pure components. Gordon-Taylor equation (Gordon and Taylor 1952) (Eq. (2.1)) and Fox equation (Fox 1956) (Eq. (2.2)) are the frequently used expressions for predicting the glass transition temperature of amorphous polymer blends:

$$Tg^b = \frac{W_1 Tg_1 + kW_2 Tg_2}{W_1 + kW_2} \quad (2.1)$$

$$\frac{1}{Tg^b} = \frac{W_1}{Tg_1} + \frac{W_2}{Tg_2} \quad (2.2)$$

where T_g^b is glass transition temperature (T_g) of the blend, T_{g1} and T_{g2} are the glass transition temperatures of the pure components, PMMA and CA derivatives respectively. W_1 and W_2 are weight fraction of components, PMMA and CA derivatives respectively. k is a fitting parameter and the examination data is best fitted by this equation with $k = 0.24, 0.24, 2.4$ and 0.34 respectively for PMMA/CA, PMMA/CAP, PMMA/CAB and PMMA/CAPh blends. This result supports that, blends have high miscibility in the amorphous state. The thermal properties of the PMMA/CA, PMMA/CAP, PMMA/CAB and PMMA/CAPh blends are presented in Table 2.1, Table 2.2, Table 2.3 and Table 2.4 respectively. The blends show a positive deviation from Fox equation implying an intermolecular interaction between the polymers.

2.2.3 Water Uptake

The relationship between water uptake against PMMA content in the PMMA/CA, PMMA/CAP, PMMA/CAB and PMMA/CAPh blends are shown in Figure 2.14, Figure 2.15, Figure 2.16 and Figure 2.17 respectively.

As seen from the figures, the water uptake for pure CA is 0.99 wt %, CAP is 1.1 wt %, CAB is 1.39 wt % and CAPh is 1.6 wt %. The water uptake of the blends increased up to 50 wt % of PMMA concentration. The maximum water uptake of 6.73 %, 7.65 %, 7.69 % and 7.78 % was observed for the PMMA/CA, PMMA/CAP, PMMA/CAB and PMMA/CAPh blends with 50 wt % PMMA. The water absorption decreased on addition of further amounts of PMMA. In general, an increase in water uptake indicates the presence of voids in the polymer structure. The increase in water uptake in the blends up to 50 wt % of PMMA indicates that the blends are being formed with gradual increase in the void volume in the blends. The film appears slightly cloudy after water absorption. And this is maximum in the case of 50 % CA blend film. At this composition the structure of the blend formed may be with maximum amount of void spaces. The hydrogen bonding between the components of the blends at this composition may be facilitating this specific feature. At other compositions the component polymers

may be blending in a gradually more compact structured pattern with reduction in void volumes and hence in turn reducing the water absorption.

2.2.4 Ion Exchange Capacity (IEC) Measurements

Ion exchange capacity (IEC) provides an indirect approximation for the ion exchangeable groups present in the pure and blend polymers which are responsible for proton conduction. The IEC values for pure and PMMA/CA derivatives blends are shown graphically in Figure 2.18, Figure 2.19, Figure 2.20 and Figure 2.21.

From the figure it can be seen that the IEC values decreases for the blends with an increase in PMMA content. It is known that CA derivatives has exchangeable –OH groups. Hence it is evident that when PMMA content of the blend is increased, the number of replaceable sites available in the blend would decrease and hence the decrease in the IEC of the blends.

2.2.5 Electrochemical Impedance Spectroscopy

Electrochemical impedance spectroscopy is, recently, being widely applied in determining various material properties, prime among which are permittivity and conductivity. Figure 2.22, Figure 2.23, Figure 2.24 and Figure 2.25 shows AC impedance spectra (Cole-Cole or Nyquist plots) of 50/50 PMMA/CA, PMMA/CAP, PMMA/CAB and PMMA/CAPh blends at different temperatures, respectively.

The impedance responses are typical of the electrolytes where the bulk resistance is the major contribution to the total resistance and only a minor contribution from grain boundary resistance. The straight lines inclined towards the real-axis representing the electrolyte electrode double layer capacitance behavior are obtained for all the samples over the whole range of frequency evaluated.

2.2.5.1 Proton conductivity measurement

The variation of conductivity of the blends with temperature and room temperature conductivity of the blends are shown in Figure 2.26, Figure 2.27, Figure 2.28 and Figure 2.29 respectively. It has been observed that at 30 °C, among the polyblends the blends with PMMA/CA, PMMA/CAP, PMMA/CAB and PMMA/CAPh 10/90 composition showed the highest proton conductivity value of $2.11 \times 10^{-3} \text{ S cm}^{-1}$, $2.46 \times$

$10^{-3} \text{ S cm}^{-1}$, $2.52 \times 10^{-3} \text{ S cm}^{-1}$ and $2.71 \times 10^{-3} \text{ S cm}^{-1}$, respectively. The proton conductivity increased as the temperature is increased in the measured temperature range between 30 °C to 70 °C. Also, it has been found from impedance plots that as the temperature is increased, the bulk resistance R decreased resulting in an increase in the value of proton conductivity. This may be mainly due to the fact that at higher temperature, there is an enhancement in the ion movement, favoring conductivity.

2.2.5.2 Temperature dependence of ionic conductivity

It has been found that the increase in temperature, for all compositions, increases the proton conductivity of the blend film. The increase in the proton conductivity is may be mainly due to the fact that an increase in temperature increases the mobility of ions. Further, the vibrational motion of the polymer backbone and side chains, which becomes more vigorous with increase in temperature can also facilitate the conduction of ions. The increased amplitude of vibration brings the coordination sites closer to one another enabling the ions to hop from the occupied site to the unoccupied site with lesser energy required. Increase in amplitude of vibration of the polymer backbone and side chains can also increase the fraction of free volume in the polymer electrolyte system (Aziz et al. 2010). Druger et al. (1983) and Druger et al. (1985) have attributed the change in conductivity with temperature in solid polymer electrolyte to hopping model, which results in an increase in the free volume of the system. The hopping model either permits the ions to hop from one site to another site or provides a pathway for ions to move. In other words, this facilitates translational motion of the ions. From this, it is clear that the ionic motion is due to translational motion/hopping facilitated by the polymer. The nonexistence of any unusual variation of conductivity indicates the existence of overall amorphous region (Aziz et al. 2010). This implies that coupling of the ion movement with the amorphous nature of the polymer is facilitating the conductivity in the blends.

Electrical conduction is a thermally activated process and follows the Arrhenius law

$$\sigma = \sigma_o \exp\left[-\frac{E_a}{kT}\right] \quad (2.3)$$

where, σ is the conductivity at a particular temperature, σ_0 is the pre-exponential factor, k is the Boltzmann's constant, and T is the absolute temperature. As there is no sudden change in the value of conductivity with temperature it may be inferred that these blends do not undergo any phase transitions within the temperature range studied. The variation of conductivity of the studied blends with composition at room temperature shows that conductivity increased with increase in CA content in the blends. The overall trend is similar to that of IEC variation of the blends. A steep change in conductivity of the blends in the middle range of composition is also observed which is unlike that of IEC variation. It may also be recalled here that the water uptake behavior also showed a different pattern in this region of composition. Hence the observed conductivity pattern of the blends may be attributed to the combined effects formation of specific structural features due to hydrogen bonding and variation of exchangeable group content in the blends which are facilitating the ion hopping through the polymer structure.

2.2.6 Dielectric Studies

The conductivity behavior of polymer electrolyte can be understood from dielectric studies (Ramesh et al. 2002). The dielectric constant is a measure of stored charge. The variations of dielectric constant and dielectric loss with frequency at different temperatures have been shown in Figure 2.30, Figure 2.31, Figure 2.32 and Figure 2.33 respectively.

There are no appreciable relaxation peaks observed in the frequency range employed in this study. Both dielectric constant and dielectric loss rise sharply at low frequencies indicating that electrode polarization and space charge effects have occurred confirming non-debye dependence (Qian et al. 2001 and Govindaraj et al. 1995). On the other hand, at high frequencies, periodic reversal of the electric field occurs so fast that there is no excess ion diffusion in the direction of the field. Polarization due to charge accumulation decreases, leading to the observed decrease in dielectric constant and dielectric loss (Ramesh and Arof 2001). The dielectric constant and dielectric loss increases at higher temperatures due to the higher charge carrier density. As the temperature increases, the degree of salt dissociation and re-dissociation of ion

aggregates increases resulting in the increase in number of free ions or charge carrier density.

2.3 FIGURES

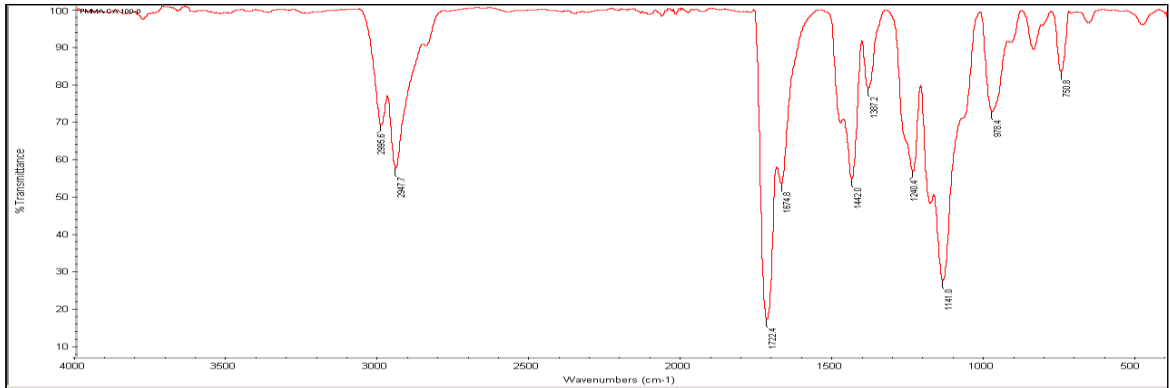


Figure 2.1 FTIR Spectrum of pure PMMA.

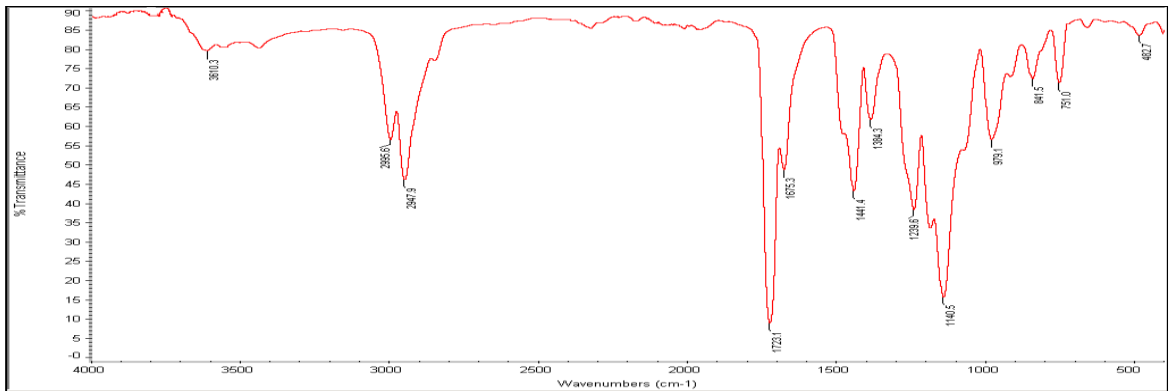


Figure 2.2 FTIR Spectrum of PMMA (50 %) - CA (50 %) blend.

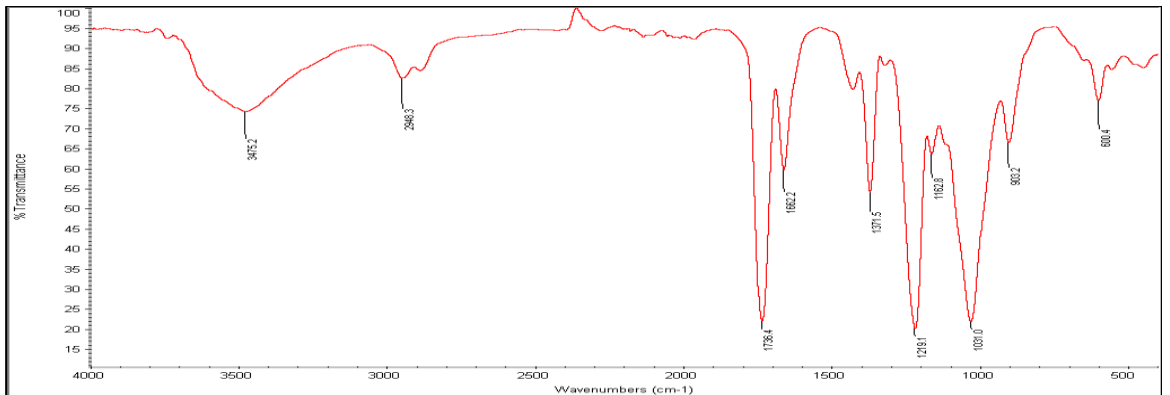


Figure 2.3 FTIR Spectrum of pure CA.

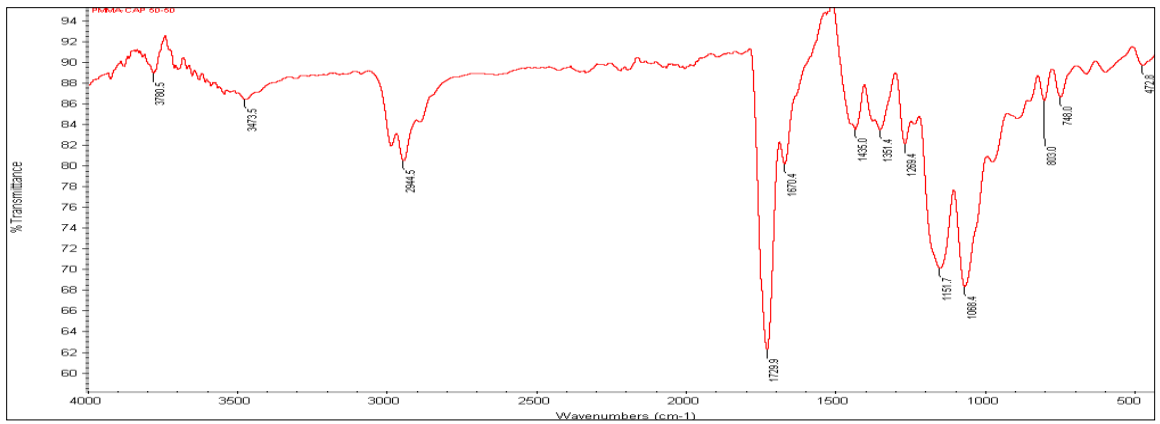


Figure 2.4 FTIR Spectrum of PMMA (50 %) - CAP (50 %) blend.

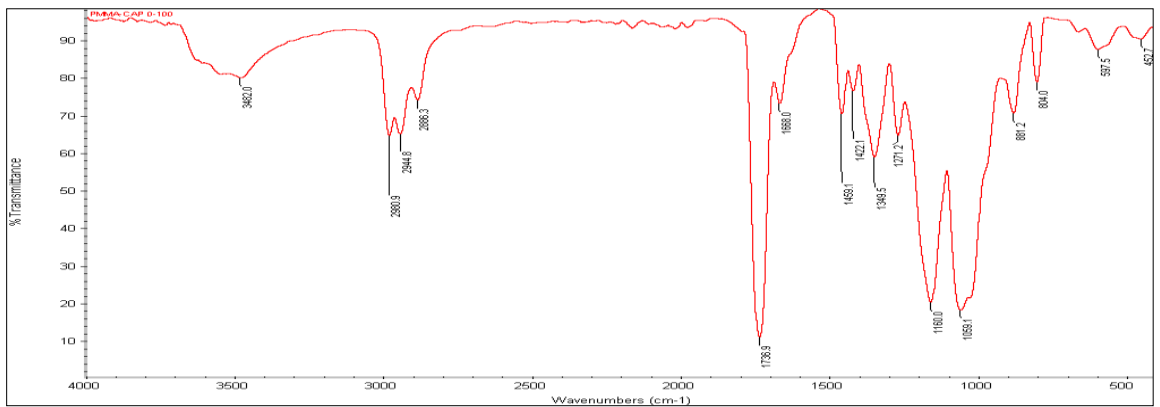


Figure 2.5 FTIR Spectrum of pure CAP.

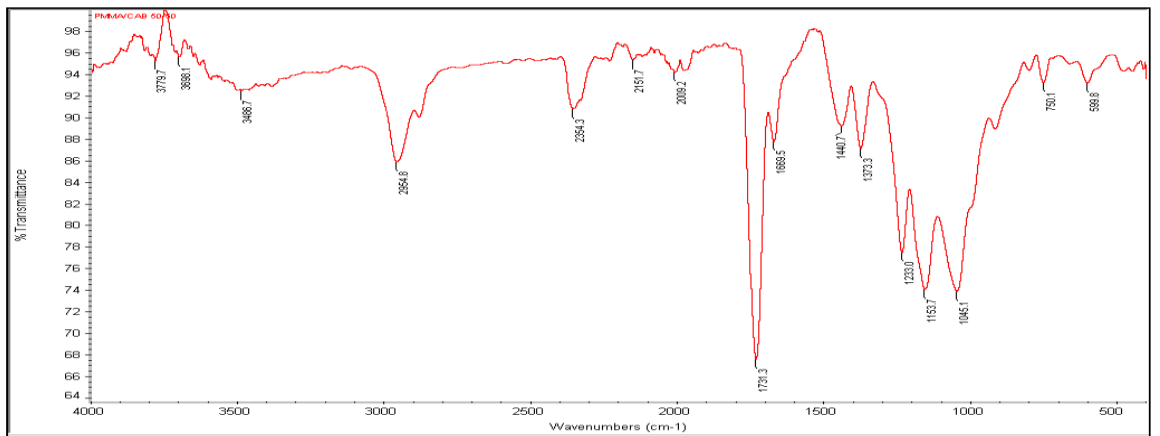


Figure 2.6 FTIR Spectrum of PMMA (50 %) - CAB (50 %) blend.

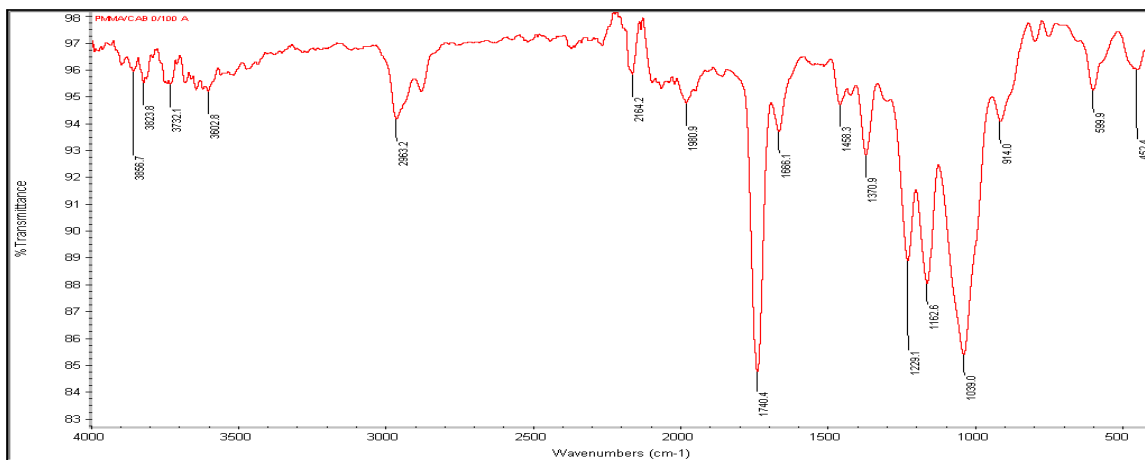


Figure 2.7 FTIR Spectrum of pure CAB.

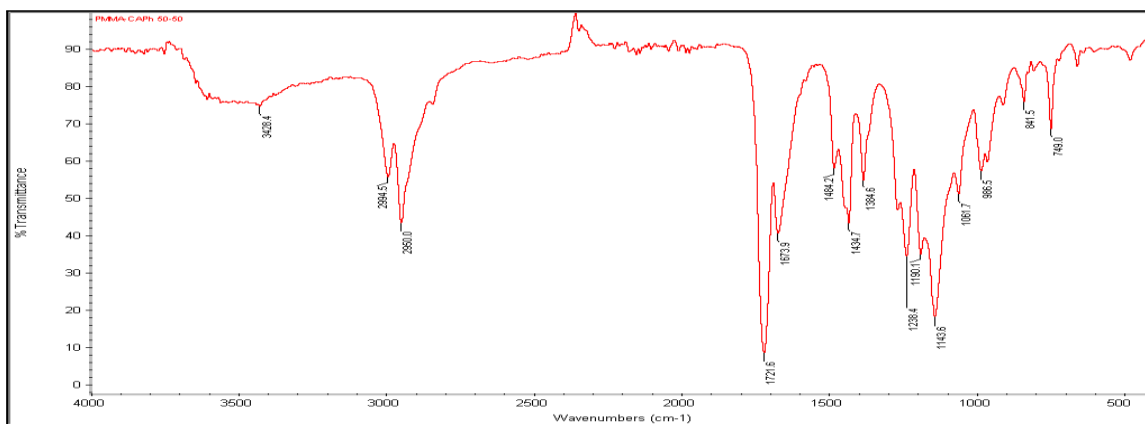


Figure 2.8 FTIR Spectrum of PMMA (50 %) – CAPH (50 %) blend.

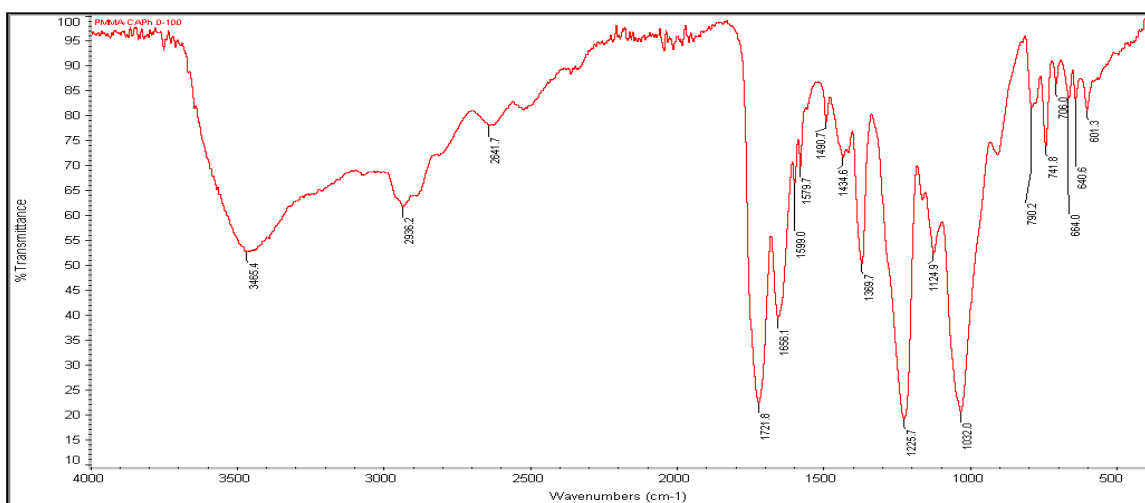


Figure 2.9 FTIR Spectrum of pure CAPH.

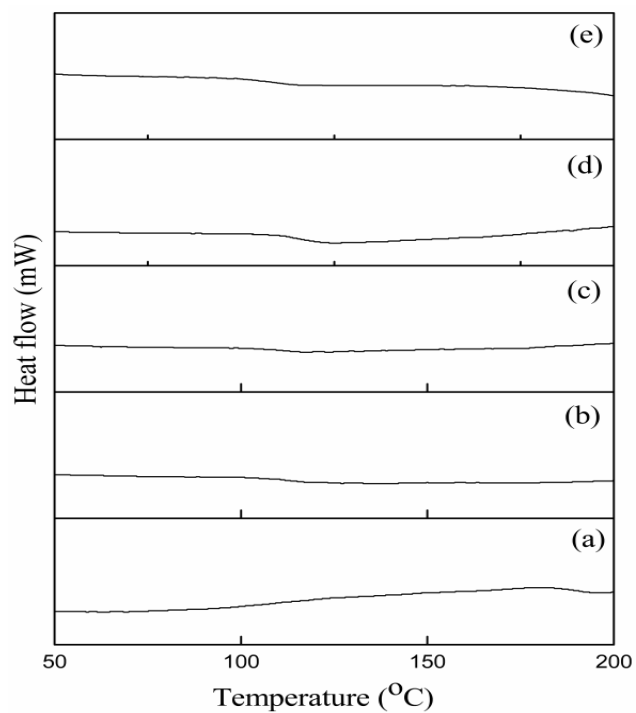


Figure 2.10 DSC scans of (a) 0/100, (b) 30/70, (c) 50/50, (d) 70/30 and (e) 100/0 PMMA/CA blends.

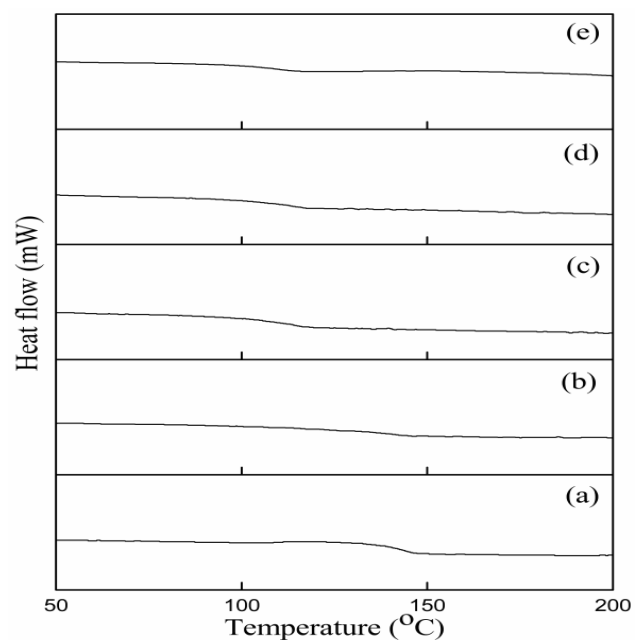


Figure 2.11 DSC scans of (a) 0/100, (b) 30/70, (c) 50/50, (d) 70/30 and (e) 100/0 PMMA/CAP blends.

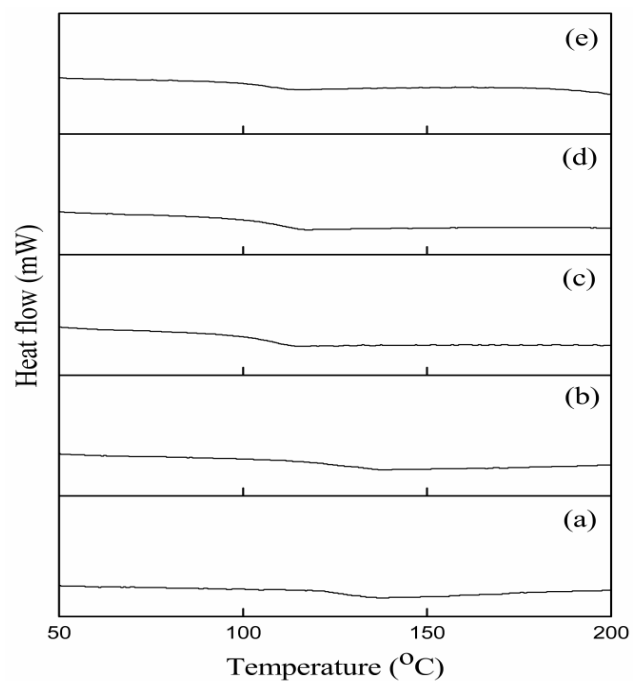


Figure 2.12 DSC scans of (a) 0/100, (b) 30/70, (c) 50/50, (d) 70/30 and (e) 100/0 PMMA/CAB blends.

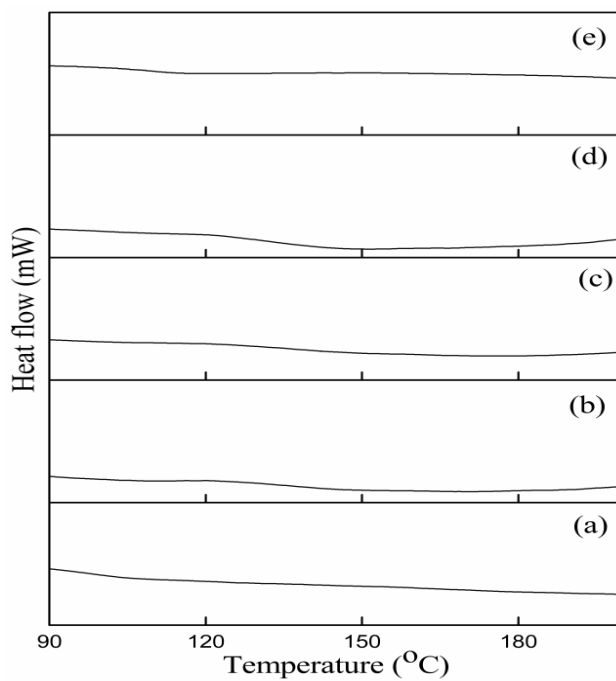


Figure 2.13 DSC scans of (a) 0/100, (b) 30/70, (c) 50/50, (d) 70/30 and (e) 100/0 PMMA/CAPh blends.

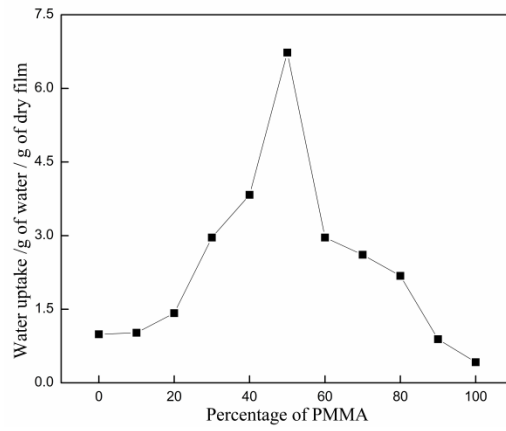


Figure 2.14 Water absorption by PMMA/CA blends.

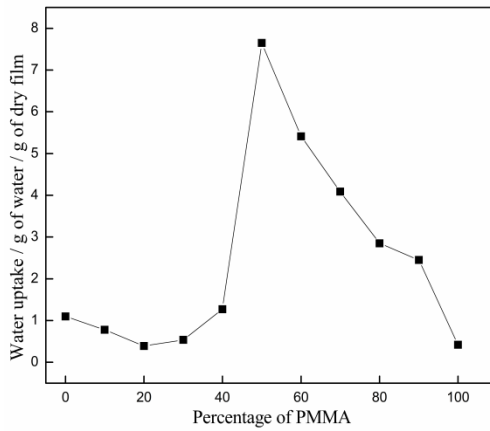


Figure 2.15 Water absorption by PMMA/CAP blends.

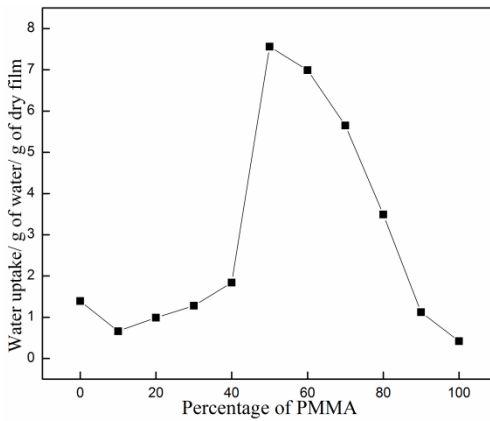


Figure 2.16 Water absorption by PMMA/CAB blends.

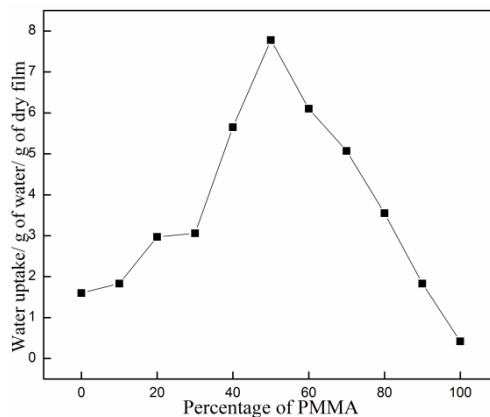


Figure 2.17 Water absorption by PMMA/CAPh blends.

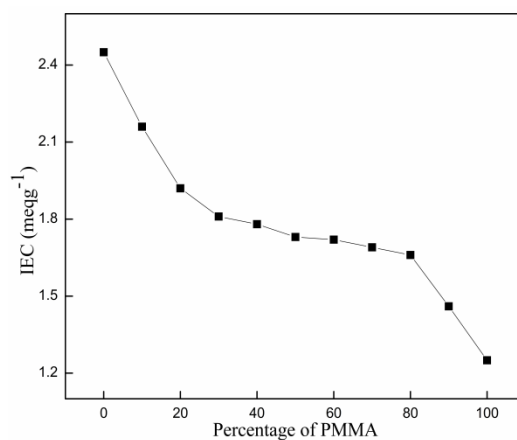


Figure 2.18 The change of IEC values in the PMMA/CA blends.

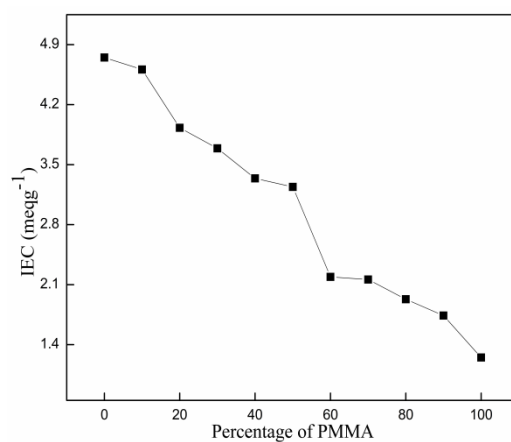


Figure 2.19 The change of IEC values in the PMMA/CAP blends.

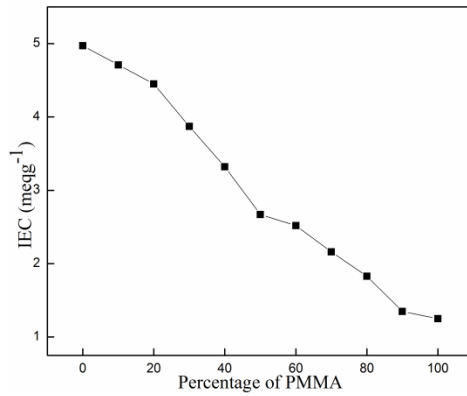


Figure 2.20 The change of IEC values in the PMMA/CAB blends.

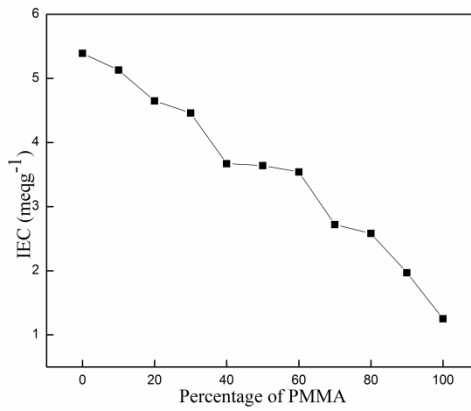


Figure 2.21 The change of IEC values in the PMMA/CAPh blends.

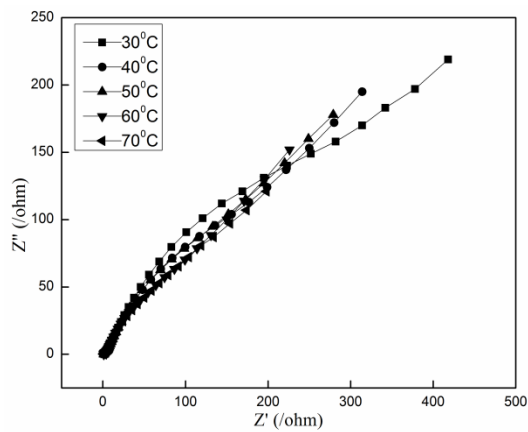


Figure 2.22 AC impedance spectrum of 50/50 PMMACA blend at different temperatures.

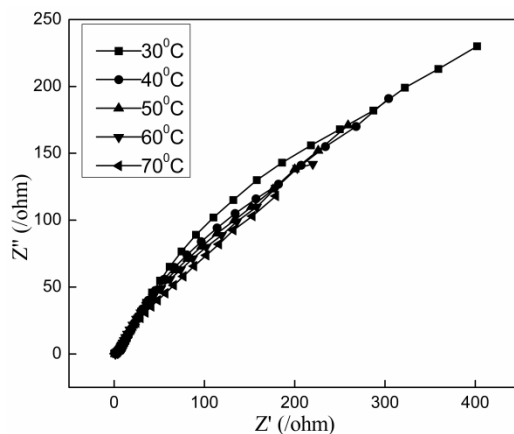


Figure 2.23 AC impedance spectrum of 50/50 PMMA/CAP blend at different temperatures.

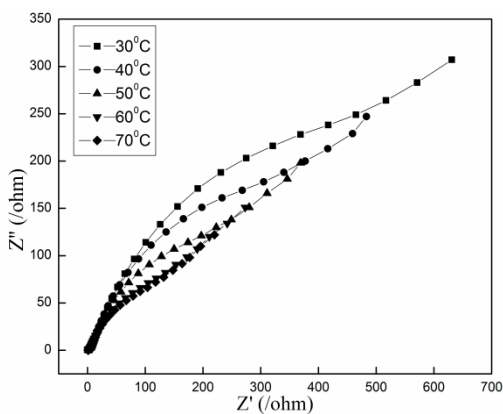


Figure 2.24 AC impedance spectrum of 50/50 PMMA/CAB blend at different temperatures.

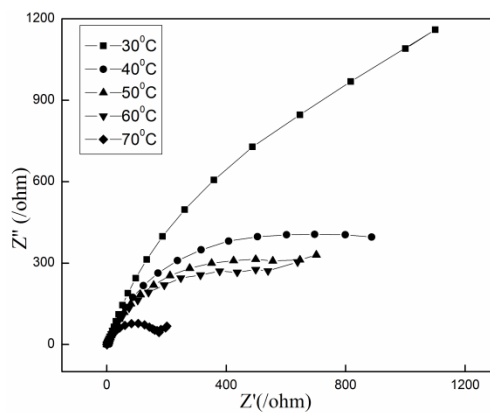


Figure 2.25 AC impedance spectrum of 50/50 PMMA/CAPh blend at different temperatures.

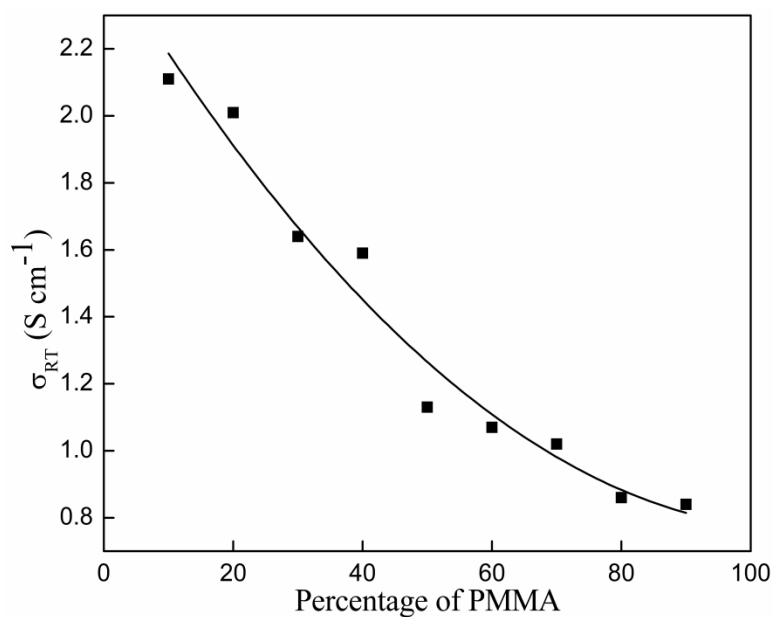
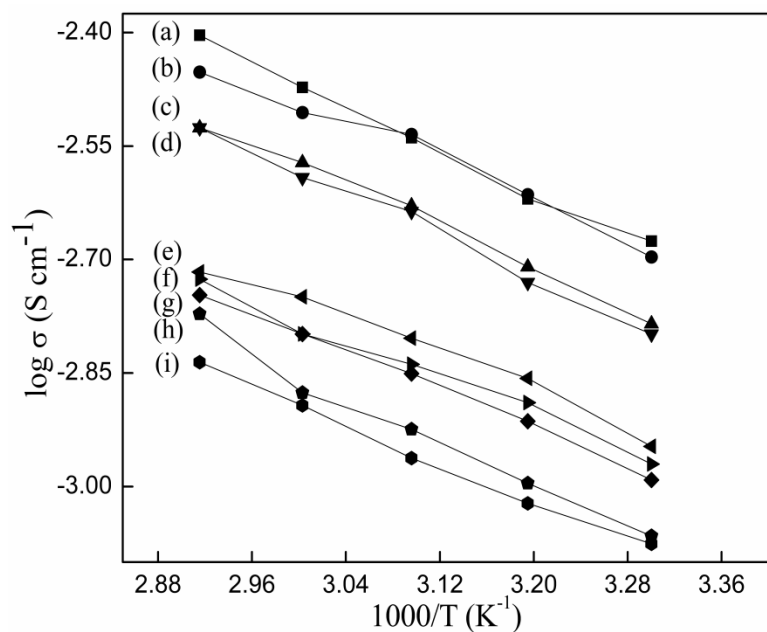


Figure 2.26 (x) Arrhenius plots for conductivity σ of (a) 10/90, (b) 20/80, (c) 30/70, (d) 40/60, (e) 50/50, (f) 60/40, (g) 70/30, (h) 80/20, (i) 90/10 PMMA/CA blends. (y) Room temperature conductivity values of PMMA/CA blends.

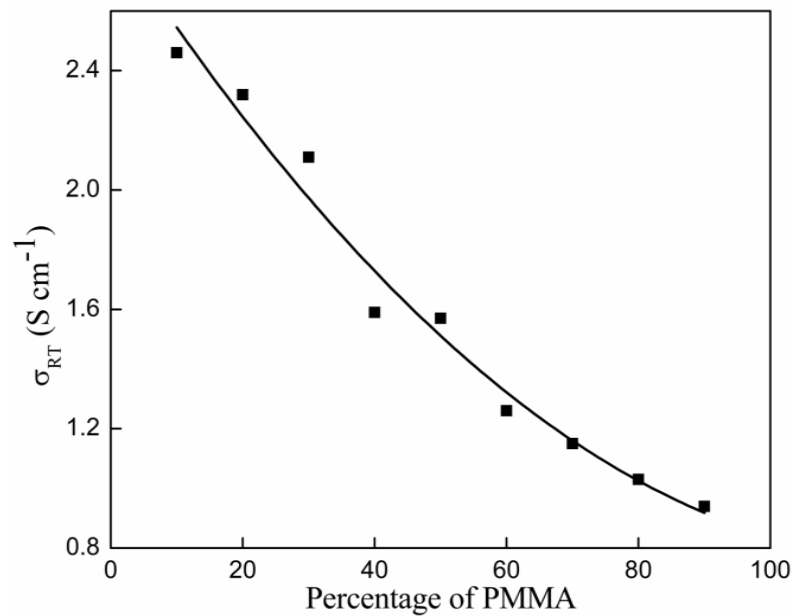
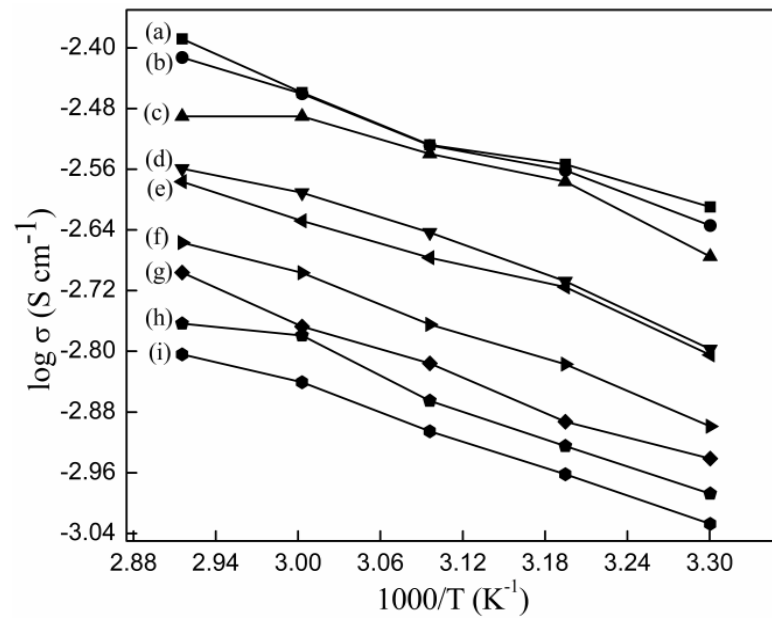


Figure 2.27 (x) Arrhenius plots for conductivity σ of (a) 10/90, (b) 20/80, (c) 30/70, (d) 40/60, (e) 50/50, (f) 60/40, (g) 70/30, (h) 80/20, (i) 90/10 PMMA/CAP blends. (y) Room temperature conductivity values of PMMA/CAP blends.

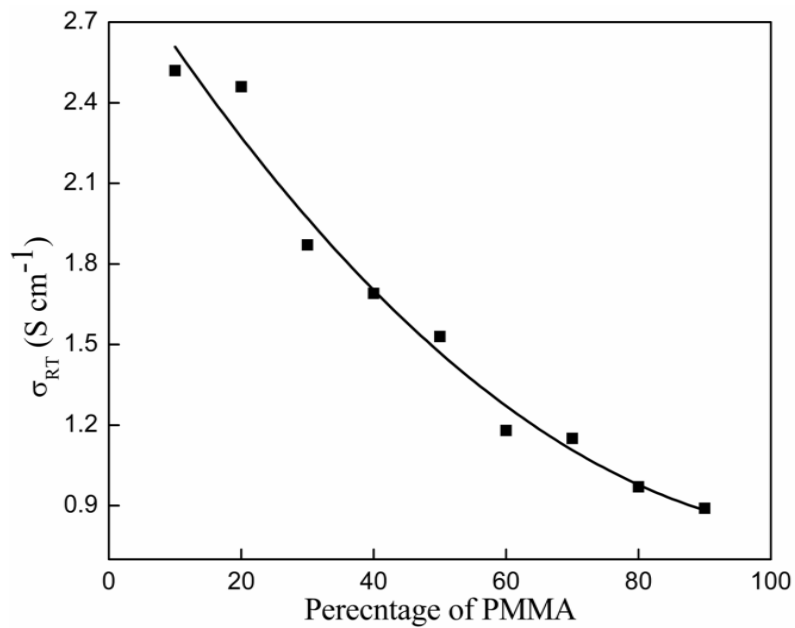
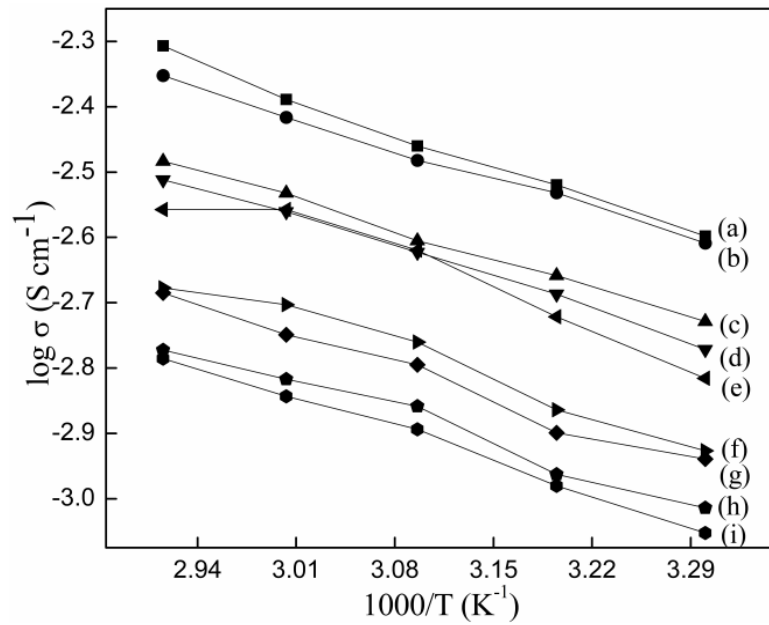


Figure 2.28 (x) Arrhenius plots for conductivity σ of (a) 10/90, (b) 20/80, (c) 30/70, (d) 40/60, (e) 50/50, (f) 60/40, (g) 70/30, (h) 80/20, (i) 90/10 PMMA/CAB blends. (y) Room temperature conductivity values of PMMA/CAB blends.

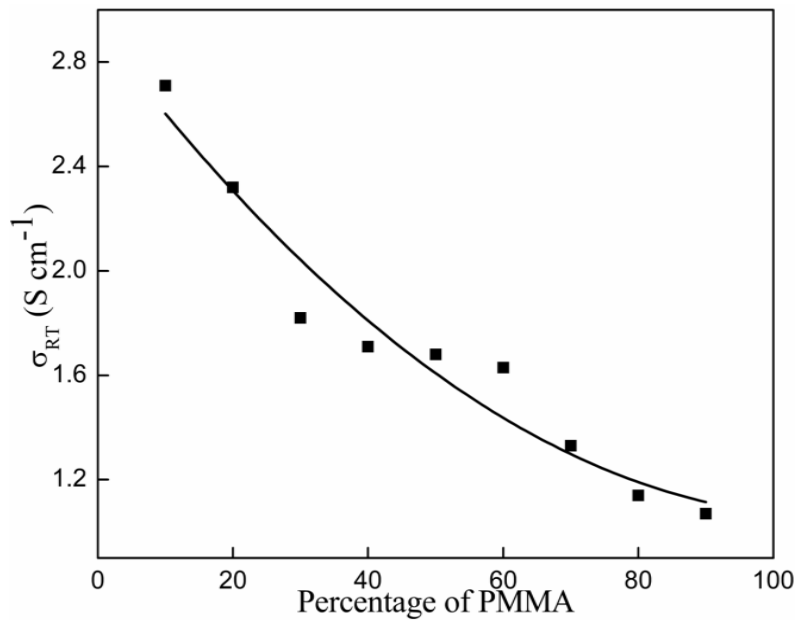
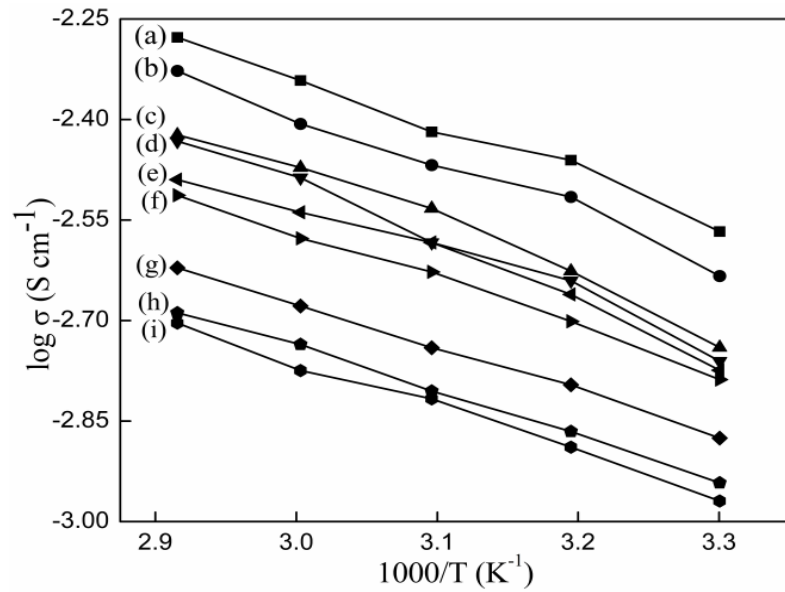


Figure 2.29 (x) Arrhenius plots for conductivity σ of (a) 10/90, (b) 20/80, (c) 30/70, (d) 40/60, (e) 50/50, (f) 60/40, (g) 70/30, (h) 80/20, (i) 90/10 PMMA/CAPh blends. (y) Room temperature conductivity values of PMMA/CAPh blends.

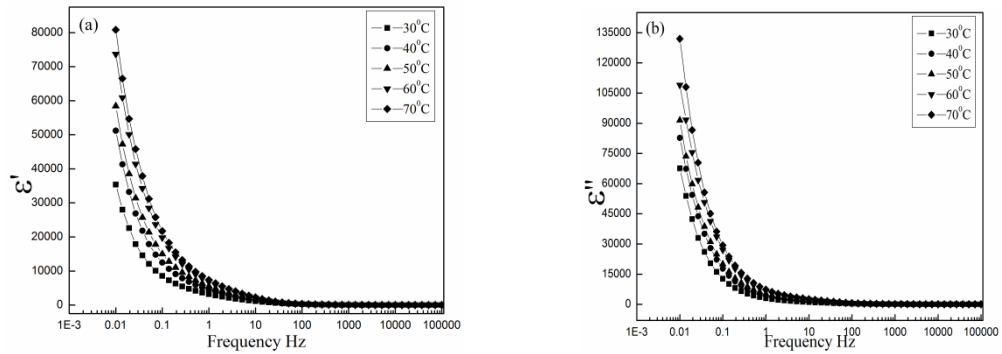


Figure 2.30 Variations of dielectric constant (a) and dielectric loss (b) with frequency at different temperatures for PMMA/CA 50/50 blend.

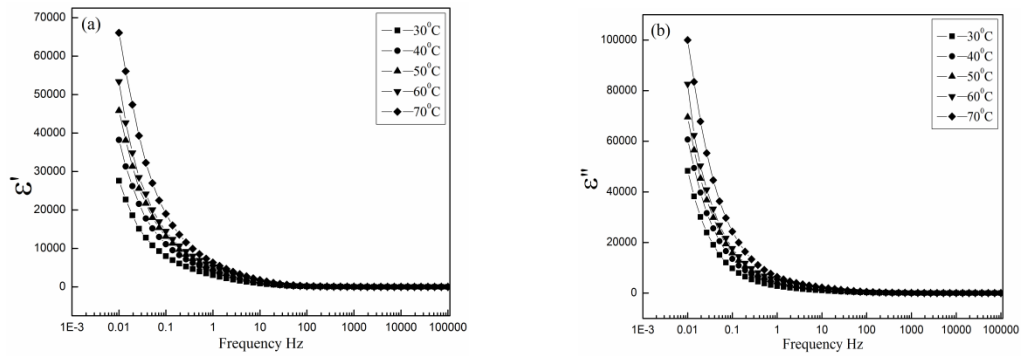


Figure 2.31 Variations of dielectric constant (a) and dielectric loss (b) with frequency at different temperatures for PMMA/CAP 50/50 blend.

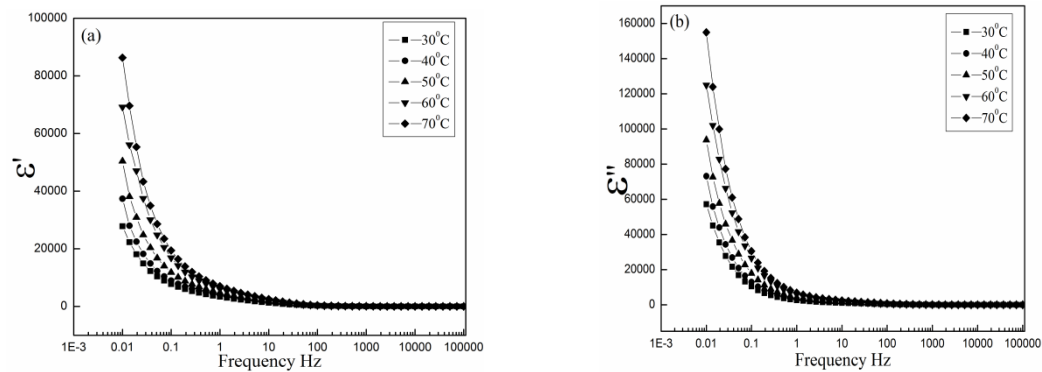


Figure 2.32 Variations of dielectric constant (a) and dielectric loss (b) with frequency at different temperatures for PMMA/CAB 50/50 blend.

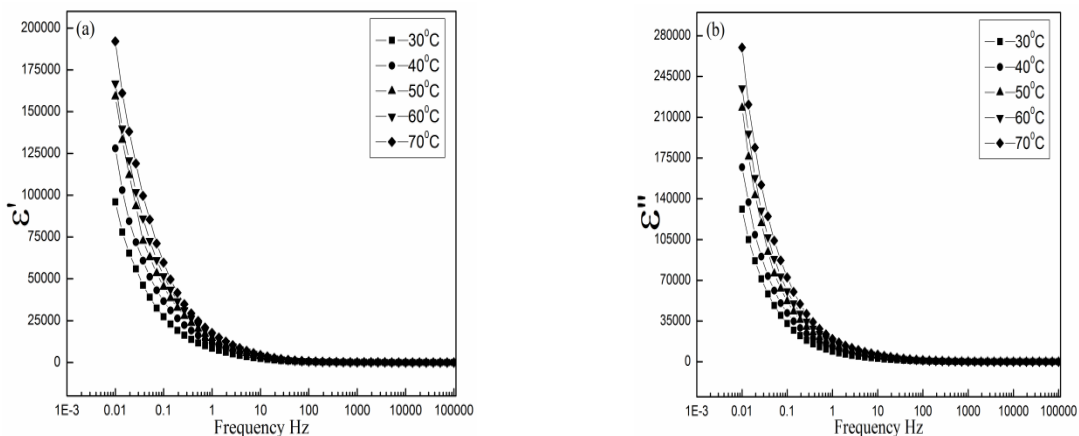


Figure 2.33 Variations of dielectric constant (a) and dielectric loss (b) with frequency at different temperatures for PMMA/CAPh 50/50 blend.

2.4 TABLES

Table 2.1 Thermal properties of PMMA/CA blends.

Sample	PMMA (wt %)	T _g (°C)	Fox equation	Gordon-Taylor equation
0/100	0	191.78	191.78	191.78
10/90	10	190.27	177.83	165.09
20/80	20	182.97	165.77	148.76
30/70	30	128.19	155.24	137.73
40/60	40	125.92	145.97	129.78
50/50	50	115.15	137.74	123.78
60/40	60	113.61	130.39	119.09
70/30	70	111.80	123.79	115.32
80/20	80	111.34	117.82	112.23
90/10	90	111.24	112.40	109.65
100/0	100	107.46	107.46	107.46

Table 2.2 Thermal properties of PMMA/CAP blends.

Sample	PMMA (wt %)	T_g (°C)	Fox equation	Gordon-Taylor equation
0/100	0	141.80	141.80	141.80
10/90	10	140.99	137.41	137.42
20/80	20	139.66	133.28	133.30
30/70	30	138.67	129.39	129.42
40/60	40	134.65	125.73	125.75
50/50	50	118.91	122.26	122.29
60/40	60	113.74	118.97	119.01
70/30	70	112.33	115.88	115.89
80/20	80	112.15	112.93	112.94
90/10	90	111.17	110.13	110.13
100/0	100	107.46	107.46	107.46

Table 2.3 Thermal properties of PMMA/CAB blends.

Sample	PMMA (wt %)	T_g (°C)	Fox equation	Gordon-Taylor equation
0/100	0	133.63	133.63	133.63
10/90	10	126.59	130.45	128.12
20/80	20	124.66	127.42	123.82
30/70	30	121.42	124.53	120.36
40/60	40	115.55	121.77	117.53
50/50	50	115.53	119.12	115.16
60/40	60	113.92	116.59	113.15
70/30	70	109.76	114.17	111.43
80/20	80	108.88	111.84	109.93
90/10	90	108.47	109.61	108.62
100/0	100	107.46	107.46	107.46

Table 2.4 Thermal properties of PMMA/CAPh blends.

Sample	PMMA (wt %)	T_g (°C)	Fox equation	Gordon-Taylor equation
0/100	0	145.59	145.59	145.59
10/90	10	145.10	140.60	144.20
20/80	20	142.25	135.94	142.60
30/70	30	140.67	131.58	140.74
40/60	40	138.90	127.49	138.54
50/50	50	138.23	123.65	135.92
60/40	60	134.32	120.03	132.71
70/30	70	132.95	116.62	128.72
80/20	80	119.00	113.39	123.62
90/10	90	109.23	110.35	116.85
100/0	100	107.46	107.46	107.46

Chapter 3

STUDIES ON DIMETHYL PHTHALATE (DMP) PLASTICIZED BLENDS OF PMMA WITH CA, CAP, CAB AND CPh

Chapter 3 presents and discusses the results of the studies on PMMA-CA derivatives blends plasticized with varying amounts of dimethyl phthalate (DMP) plasticizer. A brief note of the DMP plasticizer has also been included in this chapter.

3.1 DIMETHYL PHTHALATE (DMP) PLASTICIZER

Dimethyl phthalate is a phthalate plasticizer. It is the methyl ester of phthalic acid. Dimethyl phthalate is an ectoparasiticide and has many other uses, including in solid rocket propellants, plastics, and insect repellents. DMP is used as a solvent and plasticizer for cellulose acetate and cellulose acetate-butyrate formulations.

Properties:

Physical properties	
Molecular formula	C ₁₀ H ₁₀ O ₄
Molecular mass	194.18
Density	1.19 g/cm ³
Boiling point	283-284 °C
Dielectric constant	8.11

Uses:

- Used in insect and mosquito repellent.
- As solvenrapic films and sheets, blister packaging and tape applications in formulation of organic peroxide.
- As a plasticizers in poly vinyl acetate and rubber.
- Dissolves with many natural resins, Glyceryl-phthalate resin and may be used with coumarone resins.
- As additive in polysulfides rubber to reduce shear strength and for easy mixing.
- Used in manufacturing of celluloid.
- As solvent in nitrocellulose and cellulose acetate in varnishes/lacquers.

3.2 RESULTS AND DISCUSSION

3.2.1 Fourier Transform Infrared (FTIR) Spectroscopic Studies

FTIR spectra of 50/50 PMMA/CA blend plasticized with 2.5%, 5%, 7.5% and 10 % DMP are shown in Figure 3.1, Figure 3.2, Figure 3.3 and Figure 3.4 respectively. The FTIR stretching frequencies of PMMA/CA, PMMA/CAP, PMMA/CAB and PMMA/CAPh blends plasticized with DMP are given in Table 3.1. Carbonyl frequency of 0/100 PMMA/CA blend with 2.5 % DMP at 1734.7 cm^{-1} decreased to 1726.1 cm^{-1} in 50/50 PMMA/CA blend with 2.5 % DMP. Similarly, the carbonyl frequency of 0/100 PMMA/CA blend with 5 % DMP at 1734.9 cm^{-1} decreased to 1728.8 cm^{-1} in 50/50 PMMA/CA blend with 5 % DMP, the carbonyl frequency of 0/100 PMMA/CA blend with 7.5 % DMP at 1733.9 cm^{-1} decreased to 1723.9 cm^{-1} in 50/50 PMMA/CA blend with 7.5 % DMP and carbonyl frequency of 0/100 PMMA/CA blend with 10 % DMP at 1734.4 cm^{-1} decreased to 1723.4 cm^{-1} in 50/50 PMMA/CA blend with 10 % DMP.

The carbonyl frequency of 0/100 PMMA/CAP blend with 2.5 % DMP at 1736.9 cm^{-1} decreased to 1723.7 cm^{-1} in 50/50 PMMA/CAP blend with 2.5 % DMP. Similarly, the carbonyl frequency of 0/100 PMMA/CAP blend with 5 % DMP at 1736.1 cm^{-1} decreased to 1723.9 cm^{-1} in 50/50 PMMA/CAP blend with 5 % DMP, the carbonyl frequency of 0/100 PMMA/CAP blend with 7.5 % DMP at 1735.9 cm^{-1} decreased to 1723.1 cm^{-1} in 50/50 PMMA/CAP blend with 7.5 % DMP and carbonyl frequency of 0/100 PMMA/CAP blend with 10 % DMP at 1735.0 cm^{-1} decreased to 1723.4 cm^{-1} in 50/50 PMMA/CAP blend with 10 % DMP.

The carbonyl frequency of 0/100 PMMA/CAB blend with 2.5 % DMP at 1737.1 cm^{-1} decreased to 1723.4 cm^{-1} in 50/50 PMMA/CAB blend with 2.5 % DMP. Similarly, the carbonyl frequency of 0/100 PMMA/CAB blend with 5 % DMP at 1736.6 cm^{-1} decreased to 1723.1 cm^{-1} in 50/50 PMMA/CAB blend with 5 % DMP, the carbonyl frequency of 0/100 PMMA/CAB blend with 7.5 % DMP at 1736.3 cm^{-1} decreased to 1723.4 cm^{-1} in 50/50 PMMA/CAB blend with 7.5 % DMP and the carbonyl frequency of 0/100 PMMA/CAB blend with 10 % DMP at 1736.3 cm^{-1} decreased to 1723.2 cm^{-1} in 50/50 PMMA/CAB blend with 10 % DMP.

The carbonyl frequency of 0/100 PMMA/CAPh blend with 2.5 % DMP at 1669.1 cm^{-1} shifted to 1715.5 cm^{-1} in 50/50 PMMA/CAPh blend with 2.5 % DMP. Similarly, the carbonyl frequency of 0/100 PMMA/CAPh blend with 5 % DMP at 1660.1 cm^{-1} shifted to 1665.4 cm^{-1} in 50/50 PMMA/CAPh blend with 5 % DMP, the carbonyl frequency of 0/100 PMMA/CAPh blend with 7.5 % DMP at 1660.8 cm^{-1} shifted to 1718.4 cm^{-1} in 50/50 PMMA/CAPh blend with 7.5 % DMP and the carbonyl frequency of 0/100 PMMA/CAPh blend with 10 % DMP at 1658.9 cm^{-1} shifted to 1721.7 cm^{-1} in 50/50 PMMA/CAPh blend with 10 % DMP (Table 3.1).

Such shift in the specific vibration frequencies are ascribed to the formation of a weak hydrogen bond between component polymers in the blend. This can also be contributing to the miscibility of the blends.

The -OH stretching vibrations of hydroxyl groups occurred as broad band at 3469.5 cm^{-1} and 3446.3 cm^{-1} in 0/100 PMMA/CA blend with 2.5 % DMP and 50/50 PMMA/CA blend with 2.5 % DMP respectively. Similarly, the -OH stretching vibrations of hydroxyl groups in the case of other blends with varying compositions are given in Tables 3.1.

The intensity of the broad band decreased after blending, indicating that part of the -OH groups are involved in the hydrogen bond formation. These results indicate that specific interactions such as the hydrogen bonding forces exist in the blends and this is leading to the miscibility of the blends.

3.2.2 Differential Scanning Calorimetry (DSC) Studies

Miscibility of blends has been widely discussed in the literature. One of the standard methods employed to understand the miscibility of polymer blends is Differential Scanning Calorimetry (DSC). The DSC thermograms of 2.5 %, 5 %, 7.5 % and 10 % DMP plasticized 50/50 PMMA/CA blends are shown in Figure 3.5 (a), Figure 3.5 (b), Figure 3.5 (c) and Figure 3.5 (d) respectively.

From Figure 3.5 (a) to Figure 3.5 (d), it can be seen that the T_g for 2.5 %, 5 %, 7.5 % and 10 % DMP plasticized 50/50 PMMA/CA blends are 113.83 °C, 113.49 °C, 113.35 °C and 112.62 °C respectively. It is interesting to note here that the thermograms for the

blends (Figure 3.5 (a) to Figure 3.5 (d)) exhibited single T_g and its value lies intermediate to the T_g values of 2.5 %, 5 %, 7.5 % and 10 % DMP plasticized pure PMMA and pure CA derivatives respectively. Further, the T_g values of the blend films decreased regularly on increase of PMMA content in the blends. Such a systematic variation of T_g in the blends is indicative of miscibility of the components in the blends.

A number of theoretical equations have been proposed for estimating the glass transition temperature of blend films from the properties of the pure components. Gordon-Taylor equation (Gordon and Taylor 1952) (Eq. (2.1)) and Fox equation (Fox 1956) (Eq. (2.2)) are the frequently used expressions for predicting the glass transition temperature of amorphous polymer blends.

The examination data is best fitted by this equation with $k = 0.15, 0.15, 0.15$ and 0.10 respectively for 2.5 %, 5 %, 7.5 % and 10 % DMP plasticized PMMA/CA blends. This result supports that, blends have high miscibility in the amorphous state. The thermal properties of 2.5 %, 5 %, 7.5 % and 10 % DMP plasticized PMMA/CA, PMMA/CAP, PMMA/CAB and PMMA/CAPh blends have shown single T_g and are presented in Table 3.2. Hence it can be concluded that all the blends studied are miscible in the entire composition range. The blends show a positive deviation from Fox equation implying an intermolecular interaction between the polymers.

3.2.3 Water Uptake

The water uptake capacity of the polymer blend films have been calculated using the equation 1.7. The plots of water uptake against DMP content in the PMMA/CA, PMMA/CAP, PMMA/CAB and PMMA/CAPh blends with 2.5 %, 5 %, 7.5 % and 10 % DMP plasticizer are shown in Figure 3.6, Figure 3.7, Figure 3.8 and Figure 3.9 respectively.

As seen from the figures, the water uptake for 0/100 PMMA/CA, PMMA/CAP, PMMA/CAB and PMMA/CAPh blends with 2.5 % DMP are 0.95 wt %, 1.05 wt %, 1.32 wt % and 1.56 wt % respectively. The water uptake of the blends increased up to 50 wt % of CA derivatives concentration. The maximum water uptake was observed for the blends with 50/50 PMMA/CA, PMMA/CAP, PMMA/CAB and PMMA/CAPh blends

with 2.5 % DMP are 6.26 wt %, 7.60 wt %, 7.63 wt % and 7.69 wt % respectively, which decrease on addition of further PMMA.

The water uptake for 0/100 PMMA/CA, PMMA/CAP, PMMA/CAB and PMMA/CAPh blends with 5 % DMP are 0.94 wt %, 1.05 wt %, 1.31 wt % and 1.51 wt % respectively. The water uptake of the blends increased up to 50 wt % of CA derivatives concentration. The maximum water uptake was observed for the blends with 50/50 PMMA/CA, PMMA/CAP, PMMA/CAB and PMMA/CAPh blends with 5 % DMP are 6.00 wt %, 7.50 wt %, 7.56 wt % and 7.63 wt % respectively, which decrease on addition of further PMMA.

The water uptake for 0/100 PMMA/CA, PMMA/CAP, PMMA/CAB and PMMA/CAPh blends with 7.5 % DMP are 0.94 wt %, 1.04 wt %, 1.31 wt % and 1.51 wt % respectively. The water uptake of the blends increased up to 50 wt % of CA derivatives concentration. The maximum water uptake was observed for the blends with 50/50 PMMA/CA, PMMA/CAP, PMMA/CAB and PMMA/CAPh blends with 7.5 % DMP are 5.82 wt %, 7.43 wt %, 7.56 wt % and 7.57 wt % respectively, which decrease on addition of further PMMA.

The water uptake for 0/100 PMMA/CA, PMMA/CAP, PMMA/CAB and PMMA/CAPh blends with 10 % DMP are 0.93 wt %, 1.04 wt %, 1.30 wt % and 1.51 wt % respectively. The water uptake of the blends increased up to 50 wt % of CA derivatives concentration. The maximum water uptake was observed for the blends with 50/50 PMMA/CA, PMMA/CAP, PMMA/CAB and PMMA/CAPh blends with 10 % DMP are 5.82 wt %, 7.29 wt %, 7.40 wt % and 7.49 wt % respectively, which decrease on addition of further PMMA.

In general, an increase in water uptake indicates the presence of voids in the polymer structure. The increase in water uptake in the blends up to 50 wt % of PMMA indicates that the blends are being formed with gradual increase in the void volume in the blends. The film appears slightly cloudy after water absorption. And this is maximum in the case of 50 % CA blend film. At this composition the structure of the blend formed may be with maximum amount of void spaces. The hydrogen bonding between the

components of the blends at this composition may be facilitating this specific feature. At other compositions the component polymers may be blending in a gradually more compact structured pattern with reduction in void volumes and hence in turn reducing the water absorption.

3.2.4 Ion Exchange Capacity (IEC) Measurements

Ion exchange capacity (IEC) provides an indirect approximation for the ion exchangeable groups present in the pure and blend polymers which are responsible for proton conduction. The IEC values for 2.5 %, 5 %, 7.5 % and 10 % DMP plasticized pure and PMMA/CA, PMMA/CAP, PMMA/CAB and PMMA/CAPh blends are shown graphically in Figure 3.10, Figure 3.11, Figure 3.12 and Figure 3.13, respectively.

From the figure it can be seen that the IEC values decreases for the blends with an increase in PMMA content. It is known that CA derivatives has exchangeable –OH groups. Hence it is evident that when PMMA content of the blend is increased, the number of replaceable sites available in the blend would decrease and hence the decrease in the IEC of the blends.

3.2.5 Electrochemical Impedance Spectroscopy

Electrochemical Impedance spectroscopy is recently being widely applied in determining various material properties, prime among which are permittivity and conductivity. Figure 3.14, Figure 3.15, Figure 3.16 and Figure 3.17 shows AC impedance spectra (Cole-Cole or Nyquist plots) of 2.5 %, 5 %, 7.5 % and 10 % DMP plasticized 50/50 PMMA/CA blends at different temperatures, respectively.

The impedance responses are typical of the electrolytes where the bulk resistance is the major contribution to the total resistance and only a minor contribution from grain boundary resistance. The straight lines inclined towards the real-axis representing the electrolyte electrode double layer capacitance behavior are obtained for all the samples over the whole range of frequency evaluated. AC impedance spectra of 2.5 %, 5 %, 7.5 % and 10 % DMP plasticized 50/50 PMMA/CAP, PMMA/CAB and PMMA/CAPh blends at different temperatures, respectively have shown the similar trend for electrochemical impedance spectra.

3.2.5.1 Proton conductivity measurement

The variation of conductivity of the blends with temperature and room temperature conductivity of the blends are shown in Figure 3.18, Figure 3.19, Figure 3.20 and Figure 3.21 respectively. It has been observed that at 30 °C, among the polyblends studied the blends with 2.5 % DMP plasticized PMMA/CA, PMMA/CAP, PMMA/CAB and PMMA/CAPh 30/70 composition showed the highest proton conductivity value of $1.84 \times 10^{-3} \text{ S cm}^{-1}$, $2.39 \times 10^{-3} \text{ S cm}^{-1}$, $2.41 \times 10^{-3} \text{ S cm}^{-1}$ and $2.53 \times 10^{-3} \text{ S cm}^{-1}$, respectively. The proton conductivity increased as the temperature is increased in the measured temperature range between 30 °C to 70 °C. Also, it has been found from impedance plots that as the temperature is increased, the bulk resistance R decreased resulting in an increase in the value of proton conductivity. This may be mainly due to the fact that at higher temperature, there is an enhancement in the ion movement, favoring conductivity. Proton conductivity measurement of 5 %, 7.5 % and 10 % DMP plasticized 50/50 PMMA/CAP, PMMA/CAB and PMMA/CAPh blends at different temperatures respectively have shown the similar trend.

3.2.5.2 Temperature dependence of ionic conductivity

It has been found that the proton conductivity of the blend film increased with increasing temperature for all compositions. This may be mainly due to the fact that an increase in temperature increases the mobility of ions and this in turn increases the conductivity. Further, the vibrational motion of the polymer backbone and side chains, which becomes more vigorous with increase in temperature can also facilitate the conduction of ions. The increased amplitude of vibration brings the coordination sites closer to one another enabling the ions to hop from the occupied site to the unoccupied site with lesser energy required. Increase in amplitude of vibration of the polymer backbone and side chains can also increase the fraction of free volume in the polymer electrolyte system (Aziz et al. 2010). Druger et al. (1983) and Druger et al. (1985) have attributed the change in conductivity with temperature in solid polymer electrolyte to hopping model, which results in an increase in the free volume of the system. The hopping model either permits the ions to hop from one site to another or provides a

pathway for ions to move. In other words, this facilitates translational motion of the ions. From this, it is clear that the ionic motion is due to translational motion/hopping facilitated by the polymer. The nonexistence of any unusual variation of conductivity indicates the existence of overall amorphous region (Aziz et al. 2010). This implies that coupling of the ion movement with the amorphous nature of the polymer is facilitating the conductivity in the blends.

Electrical conduction is a thermally activated process and follows the Arrhenius law

$$\sigma = \sigma_0 \exp\left[-\frac{E_a}{kT}\right] \quad (2.3)$$

where, σ is the conductivity at a particular temperature, σ_0 is the pre-exponential factor, k is the Boltzmann's constant, and T is the absolute temperature. As there is no sudden change in the value of conductivity with temperature it may be inferred that these blends do not undergo any phase transitions within the temperature range studied. The variation of conductivity of the studied blends with composition at room temperature shows that conductivity increased with increase in CA content in the blends. The overall trend is similar to that of IEC variation of the blends. A steep change in conductivity of the blends in the middle range of composition is also observed which is unlike that of IEC variation. It may also be recalled here that the water uptake behavior also showed a different pattern in this region of composition. Hence the observed conductivity pattern of the blends may be attributed to the combined effects formation of specific structural features due to hydrogen bonding and variation of exchangeable group content in the blends which are facilitating the ion hopping through the polymer structure.

3.2.6 Dielectric Studies

The dielectric constant and loss of the films have been calculated using the equations 1.11 and 1.12 respectively. The conductivity behavior of polymer electrolyte can be understood from dielectric studies (Ramesh et al. 2002). The dielectric constant is a measure of stored charge. The variations of dielectric constant and dielectric loss with frequency at different temperatures have been shown in Figure 3.22, Figure 3.23, Figure 3.24 and Figure 3.25 respectively, for 2.5 %, 5 %, 7.5 % and 10 % DMP plasticized

50/50 PMMA/CA blends. Similar trends have also been seen for 2.5 %, 5 %, 7.5 % and 10 % DMP plasticized 50/50 PMMA/CAP, PMMA/CAB and PMMA/CAPh blends at different temperatures.

There are no appreciable relaxation peaks observed in the frequency range employed in this study. Both dielectric constant and dielectric loss rise sharply at low frequencies indicating that electrode polarization and space charge effects have occurred confirming non-debye dependence (Qian et al. 2001 and Govindaraj et al. 1995). On the other hand, at high frequencies, periodic reversal of the electric field occurs so fast that there is no excess ion diffusion in the direction of the field. Polarization due to charge accumulation decreases, leading to the observed decrease in dielectric constant and dielectric loss (Ramesh and Arof 2001). The dielectric constant and dielectric loss increase at higher temperatures due to the higher charge carrier density. As temperature increases, the degree of salt dissociation and redissociation of ion aggregates increases resulting in the increase in number of free ions or charge carrier density.

With increasing plasticizer content and for a fixed frequency, the conductivity value of the polymer blends increases. This shows that the plasticizer has increased the conductivity of the polymer blends. Therefore the number of mobile ions in the sample increases and since the conductivity is proportional to the number of mobile ions, the conductivity is therefore increased. It is quite obvious that salt is the agent responsible for conductivity of the polymer blends as other components of the blends do not have such species. The role of the plasticizer here is to increase the mobility of the ions so that the conductivity of polymer blend increases. Alternatively, plasticization can also increase ionic mobility by reducing the potential barrier to ionic motion as a result of the decreasing cation-anion coordination of the salt. Since no significant relaxation peaks have been observed in the dielectric constant and dielectric loss-frequency spectrum, it is inferred that the bulk electrolyte does not contribute much towards conductivity enhancement. This indicates that the polymer blends have shown conductivity due to hopping mechanism.

3.3 FIGURES

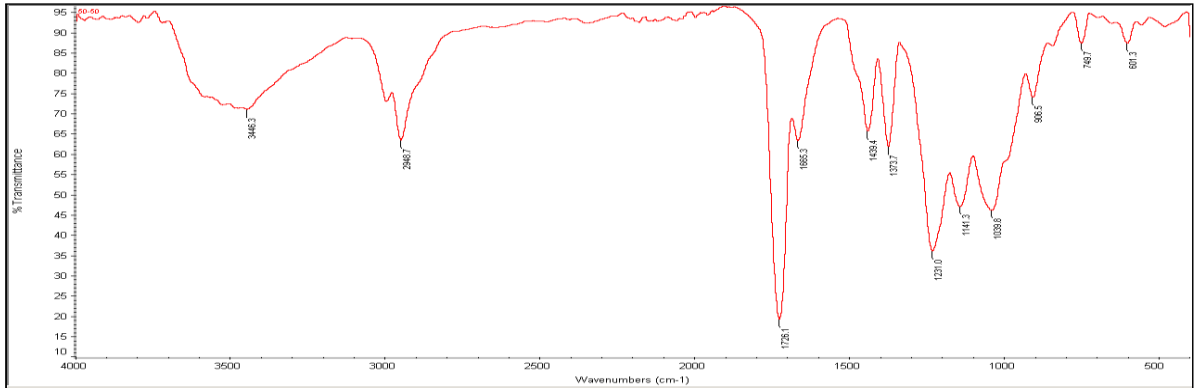


Figure 3.1 FTIR Spectrum of 2.5 % DMP plasticized 50/50 PMMA/CA blend.

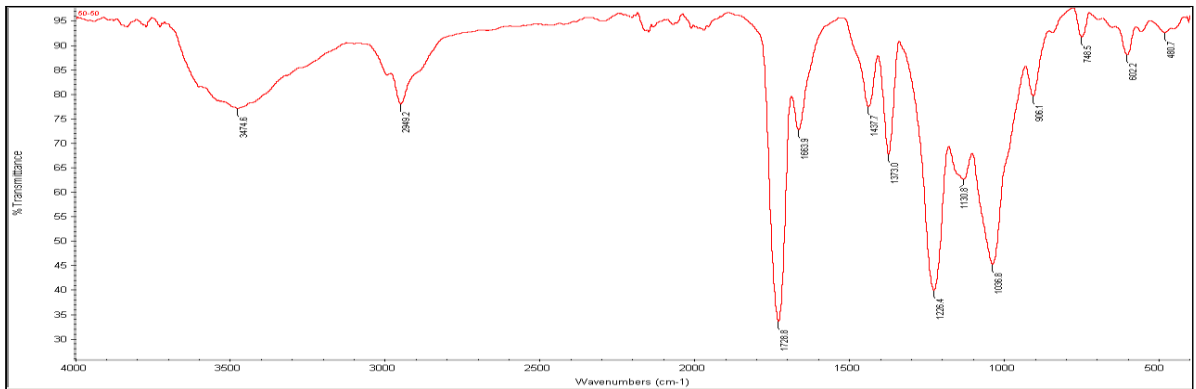


Figure 3.2 FTIR Spectrum of 5 % DMP plasticized 50/50 PMMA/CA blend.

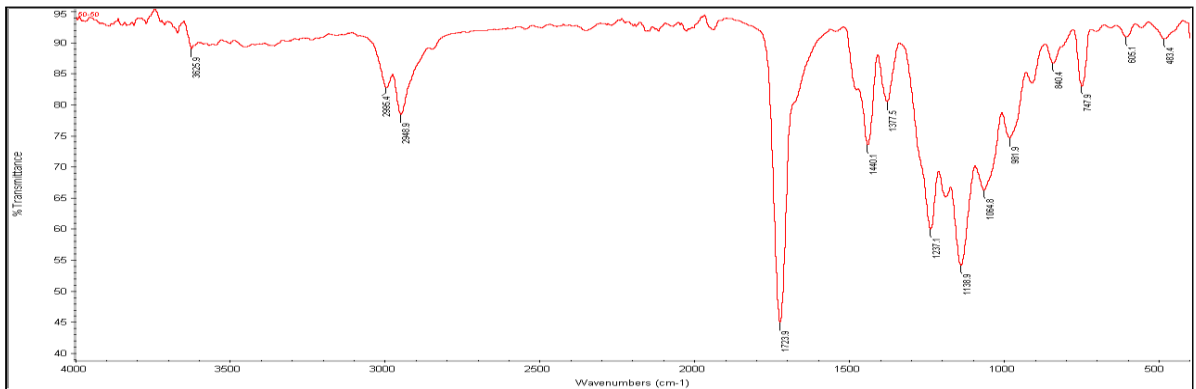


Figure 3.3 FTIR Spectrum of 7.5 % DMP plasticized 50/50 PMMA/CA blend.

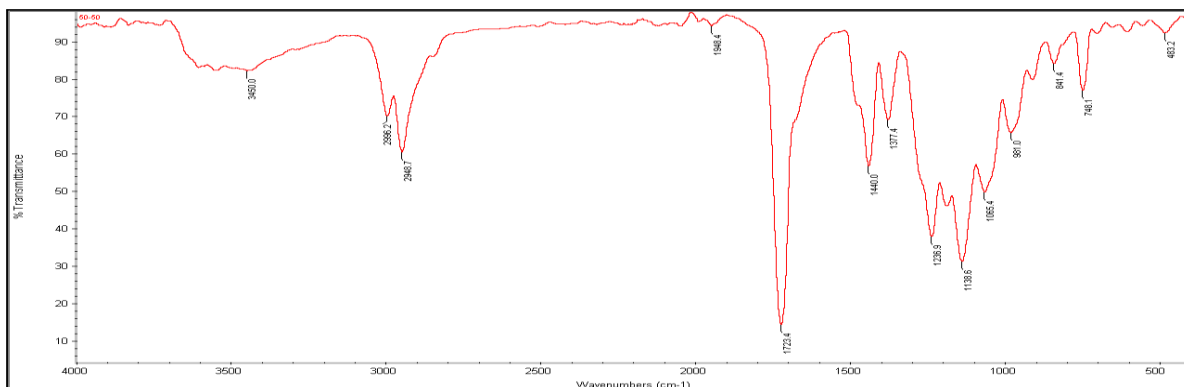


Figure 3.4 FTIR Spectrum of 10 % DMP plasticized 50/50 PMMA/CA blend.

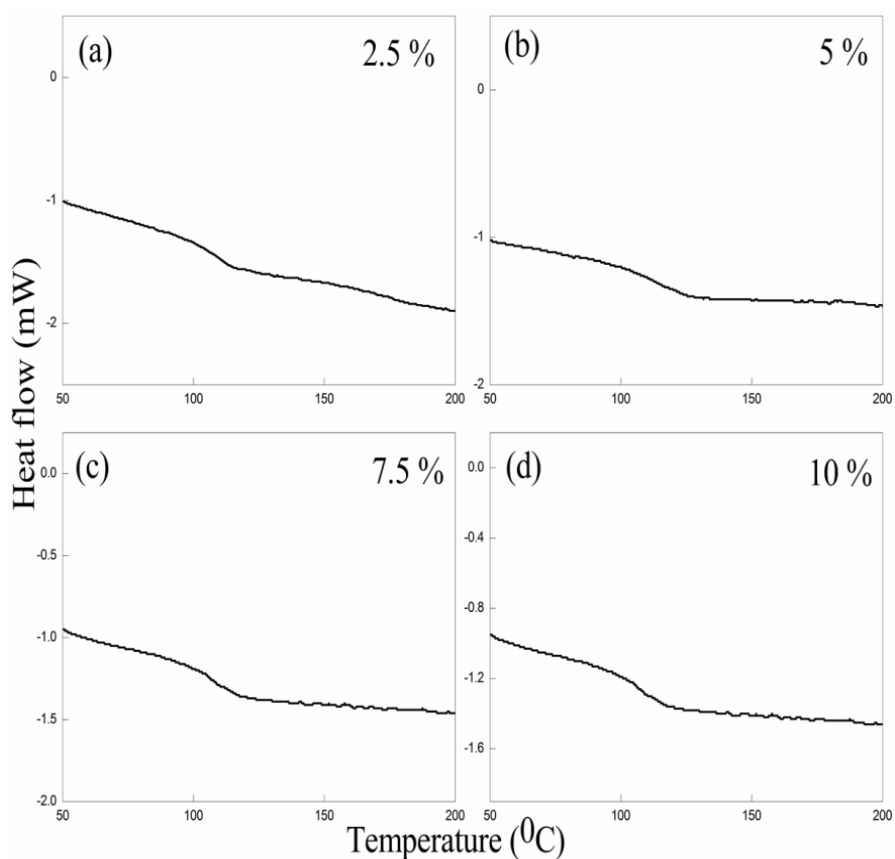


Figure 3.5 (a), (b), (c) and (d) DSC scans of 2.5 %, 5 %, 7.5 % and 10 % DMP plasticized 50/50 PMMA/CA blends.

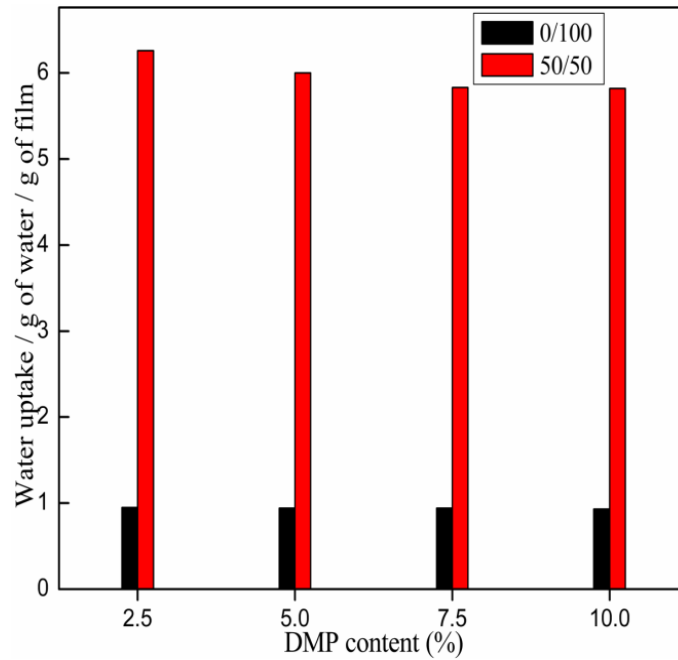


Figure 3.6 Water absorption by 2.5 %, 5 %, 7.5 % and 10 % DMP plasticized 0/100 and 50/50 PMMA/CA blends.

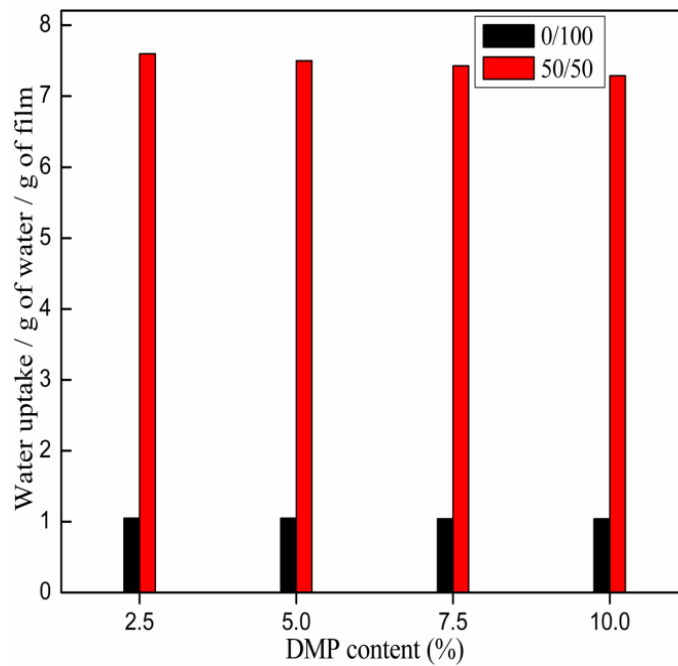


Figure 3.7 Water absorption by 2.5 %, 5 %, 7.5 % and 10 % DMP plasticized 0/100 and 50/50 PMMA/CAP blends.

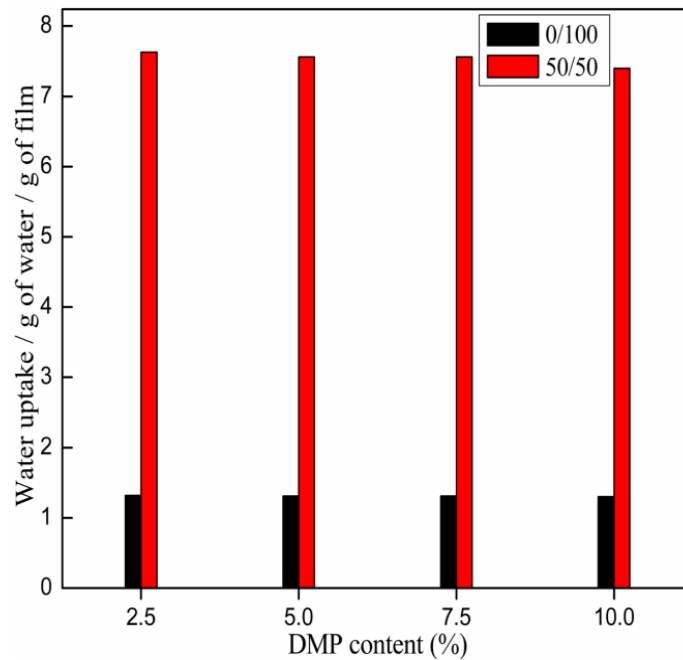


Figure 3.8 Water absorption by 2.5 %, 5 %, 7.5 % and 10 % DMP plasticized 0/100 and 50/50 PMMA/CAB blends.

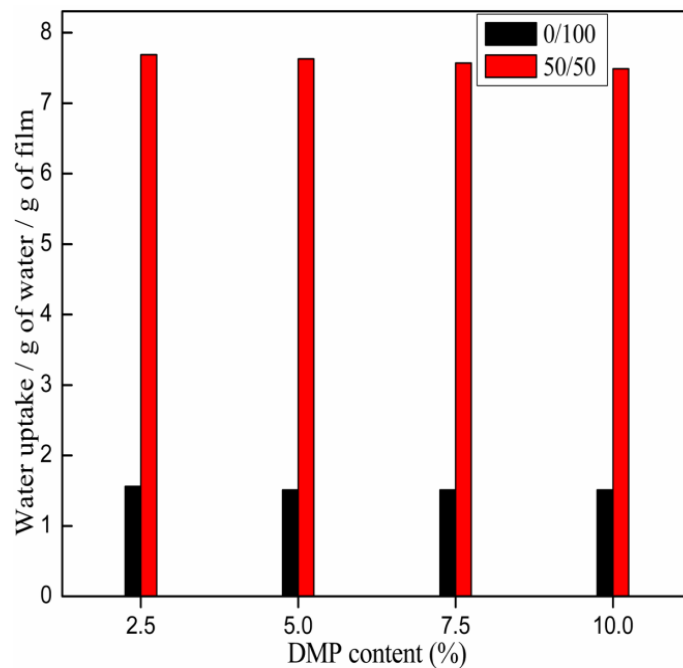


Figure 3.9 Water absorption by 2.5 %, 5 %, 7.5 % and 10 % DMP plasticized 0/100 and 50/50 PMMA/CAPh blends.

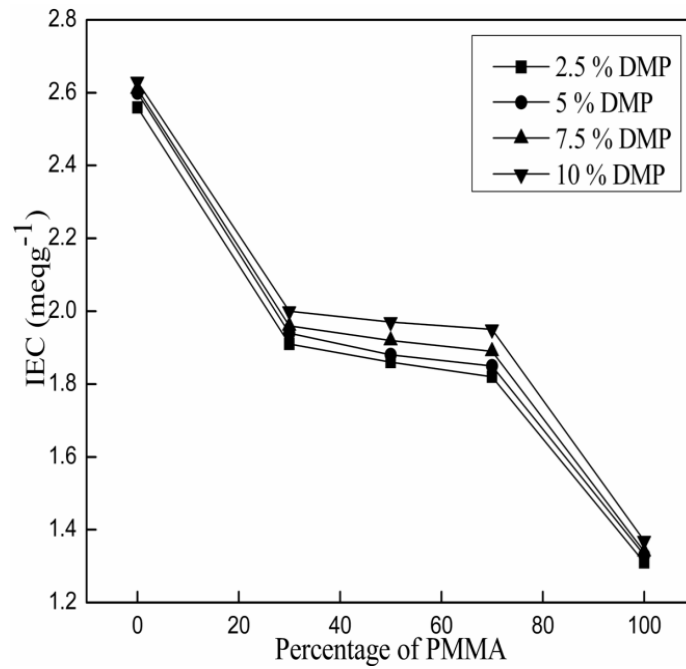


Figure 3.10 The change of IEC values in 2.5 %, 5 %, 7.5 % and 10 % DMP plasticized PMMA/CA blends.

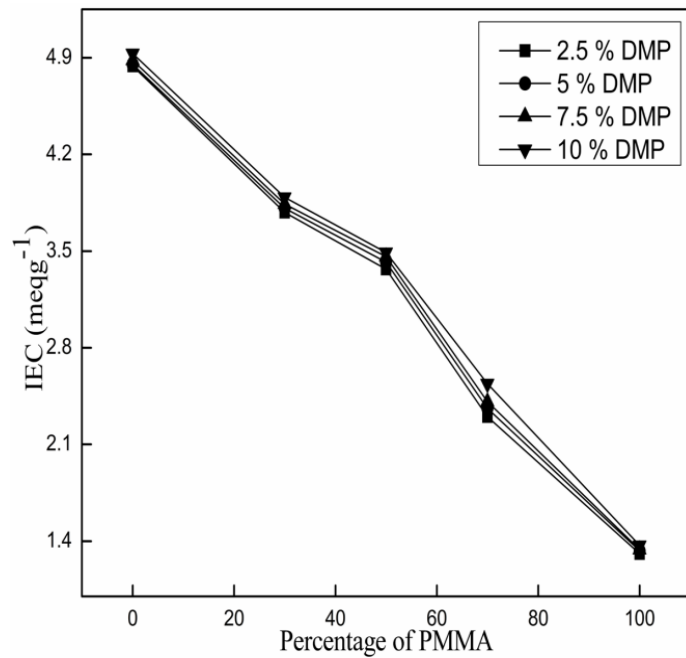


Figure 3.11 The change of IEC values in 2.5 %, 5 %, 7.5 % and 10 % DMP plasticized PMMA/CAP blends.

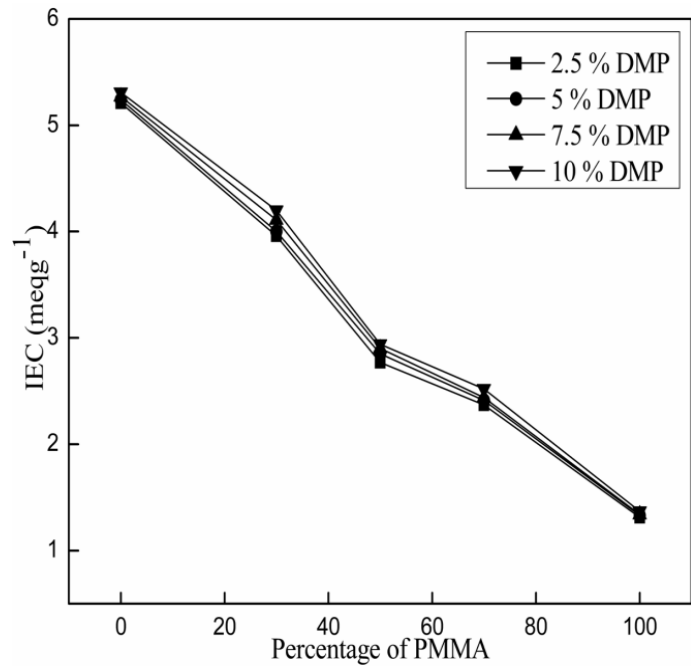


Figure 3.12 The change of IEC values in 2.5 %, 5 %, 7.5 % and 10 % DMP plasticized PMMA/CAB blends.

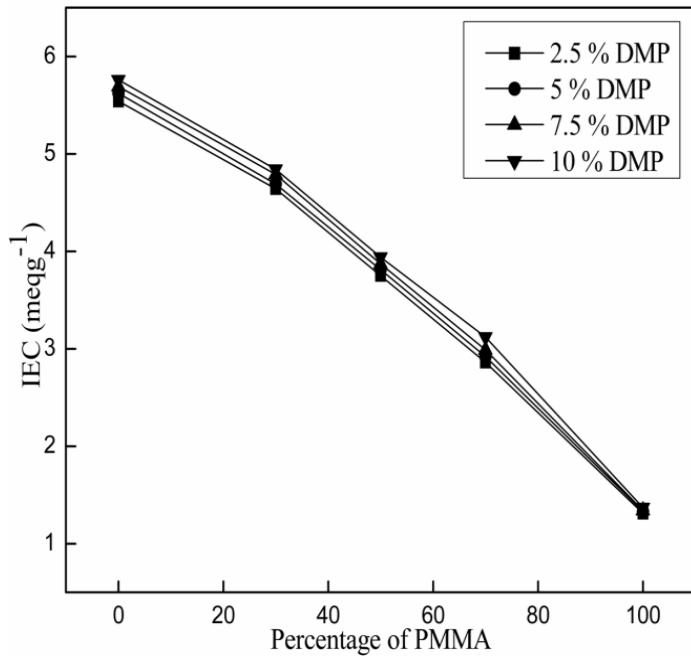


Figure 3.13 The change of IEC values in 2.5 %, 5 %, 7.5 % and 10 % DMP plasticized PMMA/CAPh blends.

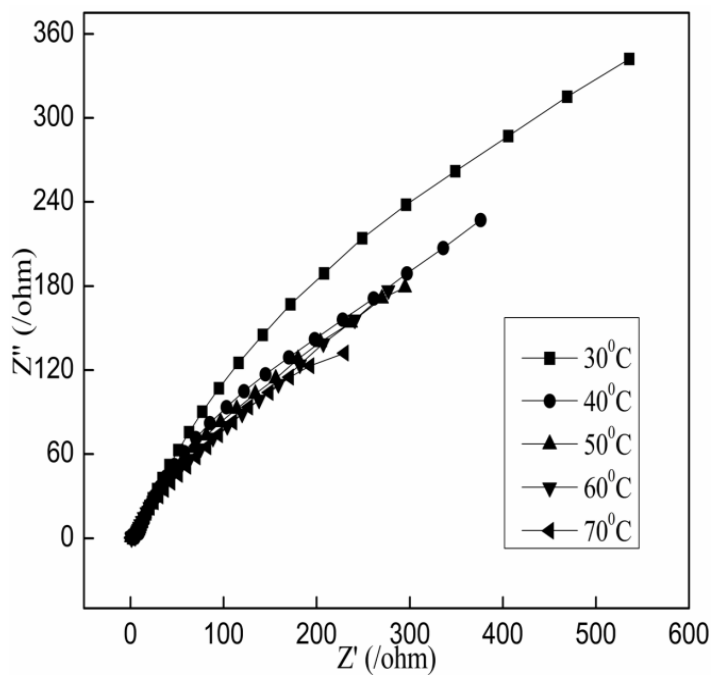


Figure 3.14 AC impedance spectrum of 2.5 % DMP plasticized 50/50 PMMA/CA blend at different temperatures.

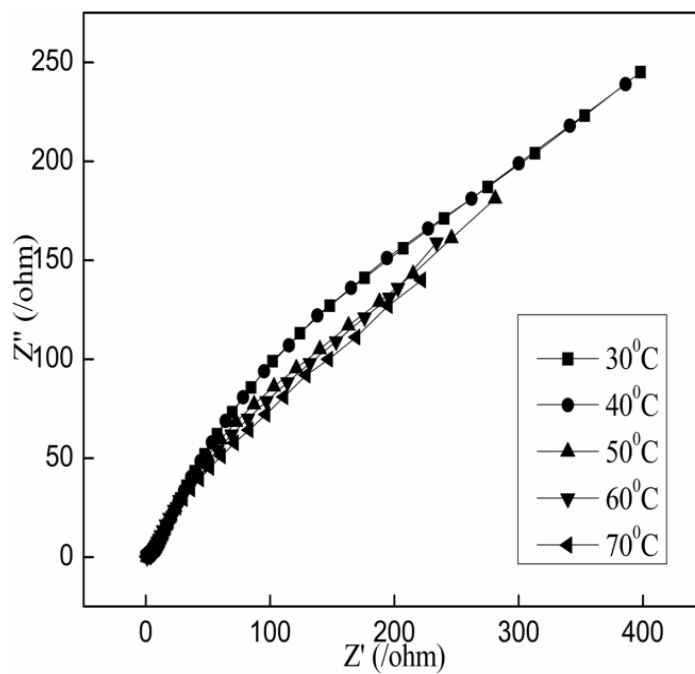


Figure 3.15 AC impedance spectrum of 5 % DMP plasticized 50/50 PMMA/CA blend at different temperatures.

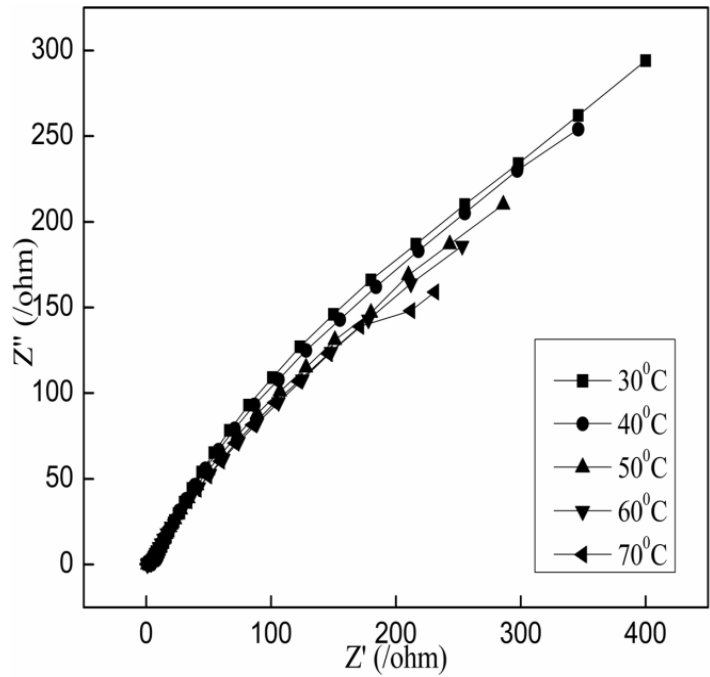


Figure 3.16 AC impedance spectrum of 7.5 % DMP plasticized 50/50 PMMA/CA blend at different temperatures.

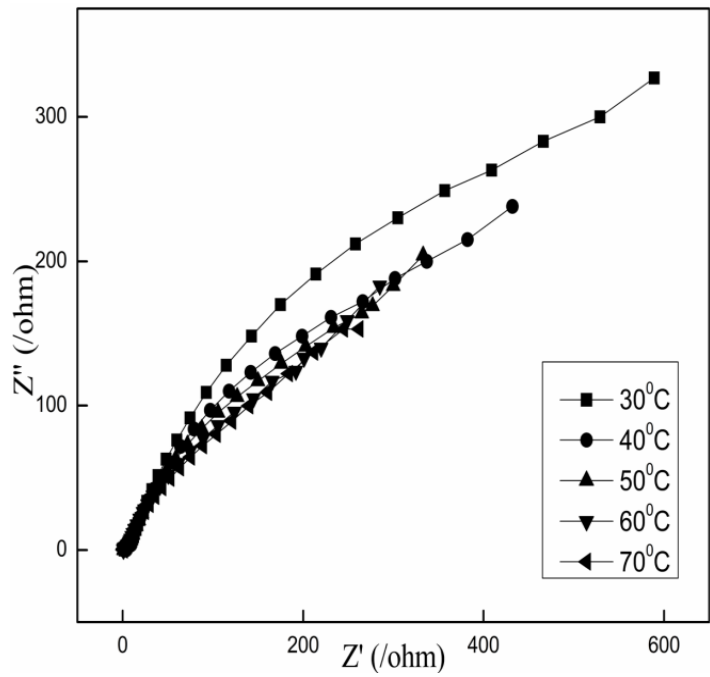


Figure 3.17 AC impedance spectrum of 10 % DMP plasticized 50/50 PMMA/CA blend at different temperatures.

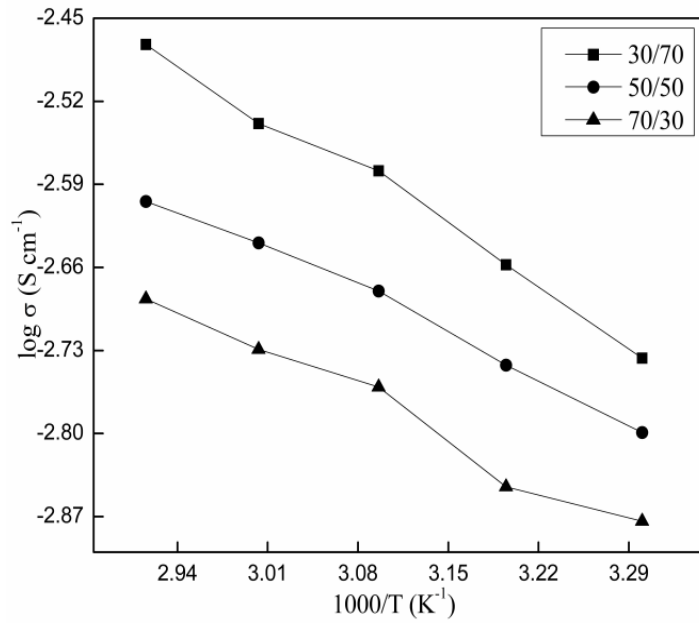


Figure 3.18 Arrhenius plots for conductivity σ of 2.5 % DMP plasticized PMMA/CA blends.

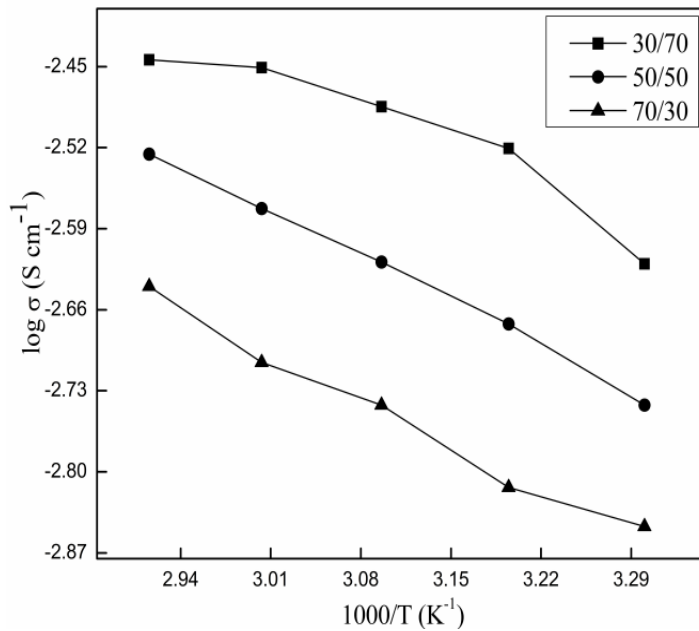


Figure 3.19 Arrhenius plots for conductivity σ of 2.5 % DMP plasticized PMMA/CAP blends.

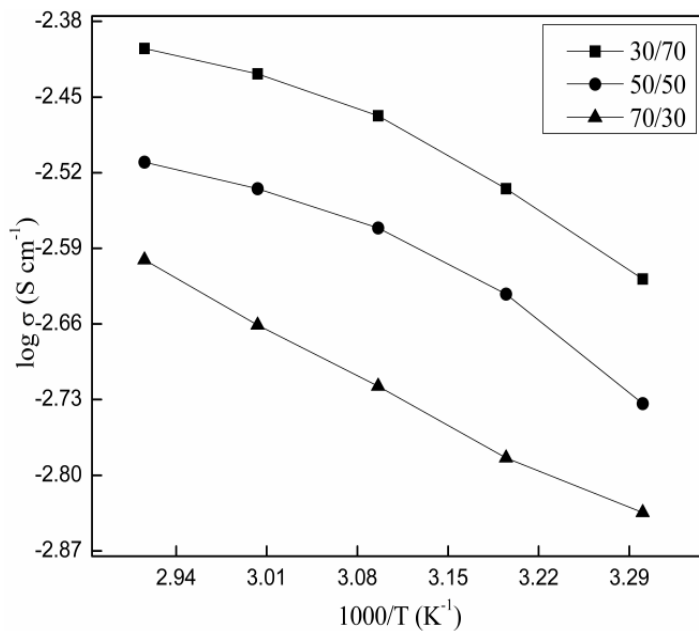


Figure 3.20 Arrhenius plots for conductivity σ of 2.5 % DMP plasticized PMMA/CAB blends.

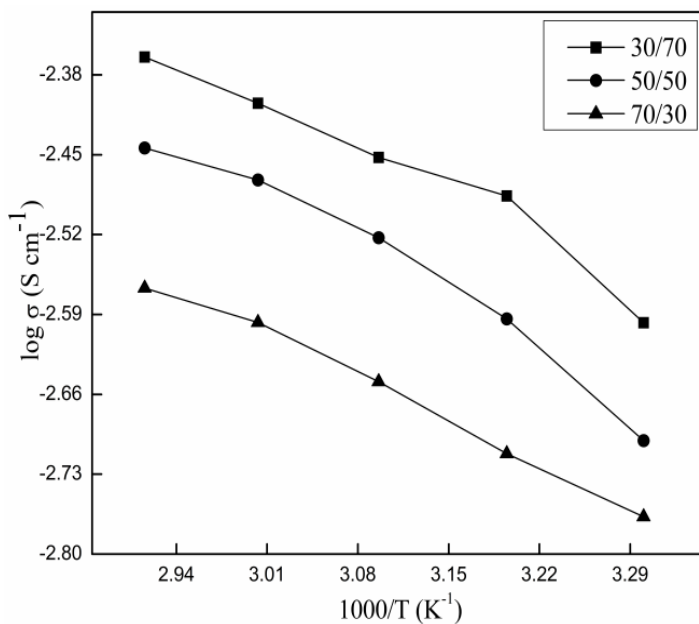


Figure 3.21 Arrhenius plots for conductivity σ of 2.5 % DMP plasticized PMMA/CAPh blends.

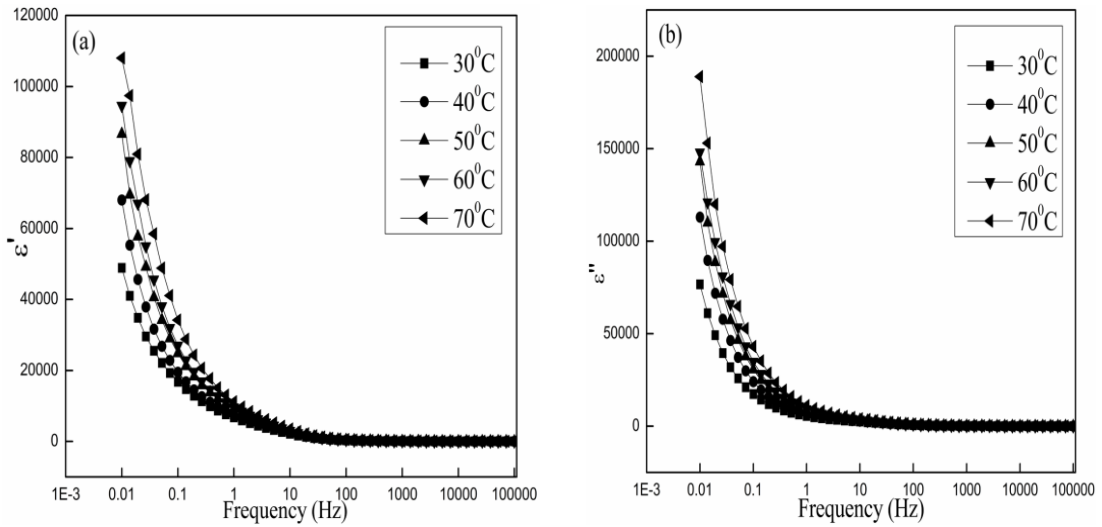


Figure 3.22 Variations of dielectric constant (a) and dielectric loss (b) with frequency at different temperatures for 2.5 % DMP plasticized 50/50 PMMA/CA blend.

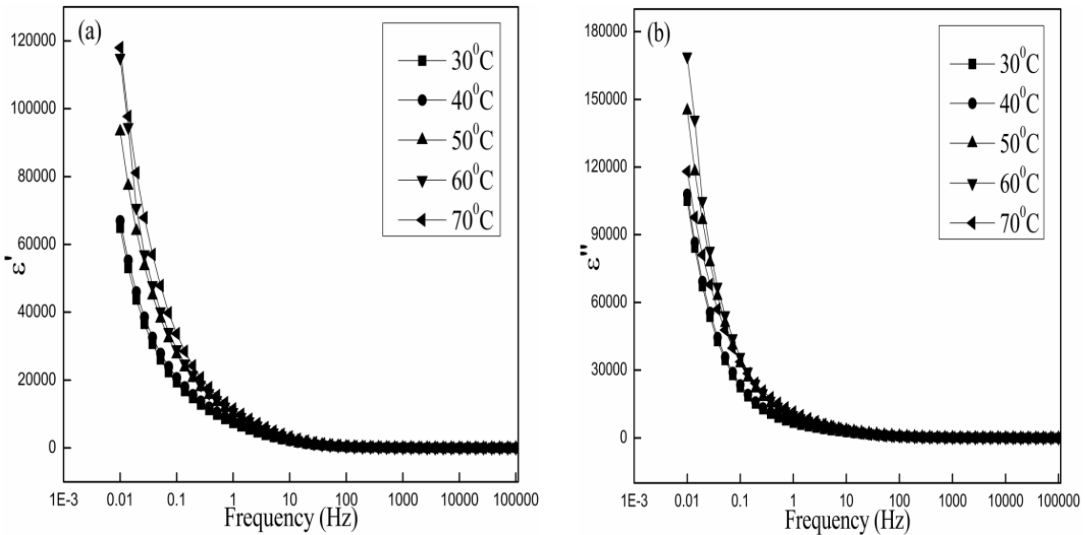


Figure 3.23 Variations of dielectric constant (a) and dielectric loss (b) with frequency at different temperatures for 5 % DMP plasticized 50/50 PMMA/CA blend.

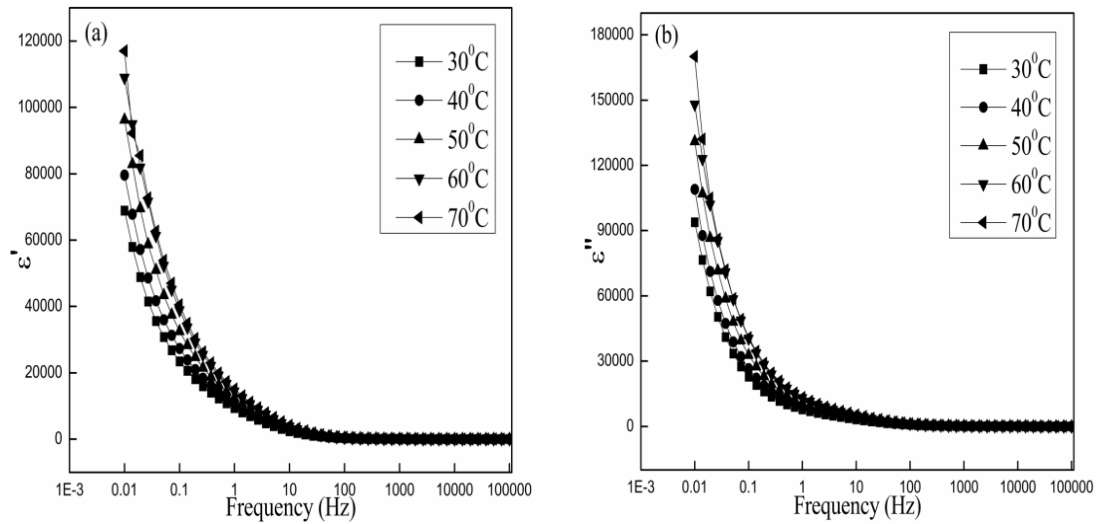


Figure 3.24 Variations of dielectric constant (a) and dielectric loss (b) with frequency at different temperatures for 7.5 % DMP plasticized 50/50 PMMA/CA blend.

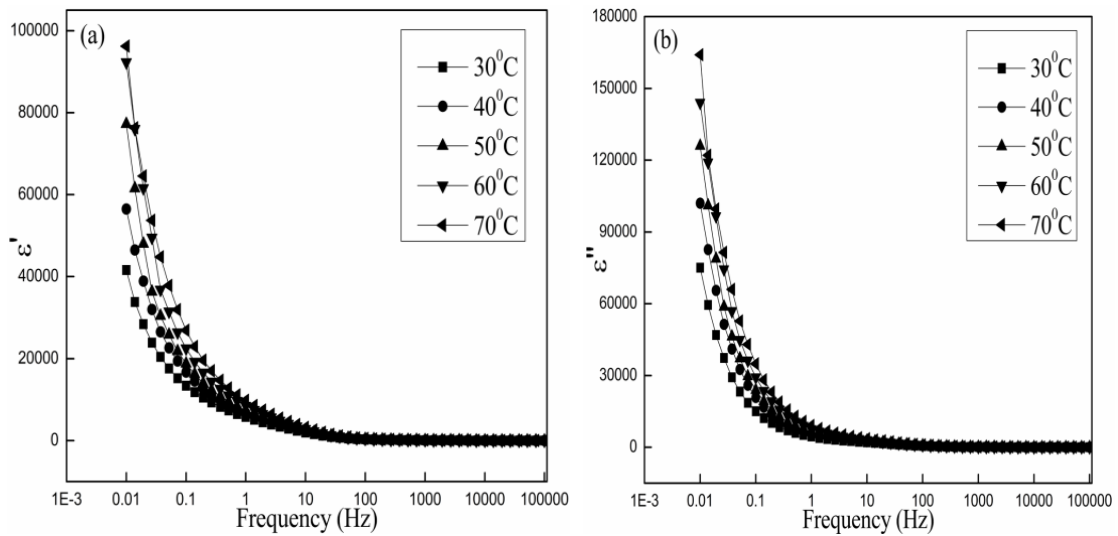


Figure 3.25 Variations of dielectric constant (a) and dielectric loss (b) with frequency at different temperatures for 10 % DMP plasticized 50/50 PMMA/CA blend.

3.4 TABLES

Table 3.1 IR stretching frequencies of DMP plasticized PMMA/CA, PMMA/CAP, PMMA/CAB and PMMA/CAPh blends.

PMMA/CA 2.5 DMP	-CO Stretching Frequencies	-OH Stretching Frequencies
0/100	1734.7	3469.5
50/50	1726.1	3446.3
PMMA/CA 5 DMP		
0/100	1734.9	3470.0
50/50	1728.8	3474.6
PMMA/CA 7.5 DMP		
0/100	1733.9	3466.4
50/50	1723.9	3625.9
PMMA/CA 10 DMP		
0/100	1734.4	3474.3
50/50	1723.4	3450.0
PMMA/CAP 2.5 DMP		
0/100	1736.9	3472.3
50/50	1723.7	3615.8
PMMA/CAP 5 DMP		
0/100	1736.1	3477.2
50/50	1723.9	3455.4
PMMA/CAP 7.5 DMP		
0/100	1735.9	3484.9
50/50	1723.1	3564.6
PMMA/CAP 10 DMP		
0/100	1735.0	3492.4
50/50	1723.4	3436.5
PMMA/CAB 2.5 DMP		
0/100	1737.1	3479.0
50/50	1723.4	3442.0
PMMA/CAB 5 DMP		
0/100	1736.6	3476.0
50/50	1723.1	3437.6

PMMA/CAB 7.5 DMP		
0/100	1736.3	3474.9
50/50	1723.4	3445.5
PMMA/CAB 10 DMP		
0/100	1736.3	3474.7
50/50	1723.2	3441.6
PMMA/CAPh 2.5 DMP		
0/100	1669.1	3417.8
50/50	1715.5	3399.7
PMMA/CAPh 5 DMP		
0/100	1660.1	3424.6
50/50	1665.4	3426.0
PMMA/CAPh 7.5 DMP		
0/100	1660.8	3404.8
50/50	1718.4	3416.3
PMMA/CAPh 10 DMP		
0/100	1658.9	3417.4
50/50	1721.7	3531.9

Table 3.2 Thermal properties of 2.5 %, 5 %, 7.5 % and 10 % DMP plasticized PMMA/CA, PMMA/CAP, PMMA/CAB and PMMA/CAPh blends.

Sample	T _g (°C)	Fox equation	k values	Gordon-Taylor equation
PMMA/CA 2.5 DMP				
0/100	177.55	177.55		177.55
30/70	122.64	147.86		124.82
50/50	113.83	133.03	0.15	115.65
70/30	110.49	120.90		110.66
100/0	106.36	106.36		106.36
PMMA/CA 5 DMP				
0/100	176.12	176.12		176.12
30/70	122.59	147.06		124.31
50/50	113.49	132.49	0.15	115.30
70/30	110.17	120.54		110.40
100/0	106.18	106.18		106.18
PMMA/CA 7.5 DMP				
0/100	173.78	173.78		173.78
30/70	122.44	145.86		123.64
50/50	113.35	131.75	0.15	114.92
70/30	109.54	120.13		110.18
100/0	106.09	106.09		106.09
PMMA/CA 10 DMP				
0/100	172.94	172.94		172.94
30/70	122.01	145.35		118.60
50/50	112.62	131.38	0.1	112.01
70/30	107.92	119.85		108.67
100/0	105.92	105.92		105.92
PMMA/CAP 2.5 DMP				
0/100	135.70	135.70		135.70
30/70	135.59	125.33		124.04
50/50	117.77	119.25	0.65	117.92
70/30	111.13	113.74		112.75
100/0	106.36	106.36		106.36
PMMA/CAP 5 DMP				
0/100	135.52	135.52		135.52
30/70	134.70	125.15	0.6	123.30
50/50	117.15	119.07		117.18

70/30	110.67	113.56		112.18
100/0	106.18	106.18		106.18
PMMA/CAP 7.5 DMP				
0/100	135.39	135.39		135.39
30/70	134.49	125.03		121.87
50/50	115.88	118.96	0.5	115.86
70/30	109.59	113.46		111.26
100/0	106.09	106.09		106.09
PMMA/CAP 10 DMP				
0/100	135.07	135.07		135.07
30/70	134.13	124.77		121.17
50/50	115.21	118.73	0.47	115.24
70/30	108.45	113.25		110.81
100/0	105.92	105.92		105.92
PMMA/CAB 2.5 DMP				
0/100	130.12	130.12		130.12
30/70	119.74	121.95		117.83
50/50	113.27	117.05	0.4	113.15
70/30	108.14	112.52		109.84
100/0	106.36	106.36		106.36
PMMA/CAB 5 DMP				
0/100	130.01	130.01		130.01
30/70	119.25	121.81		117.97
50/50	113.20	116.89	0.42	113.23
70/30	107.79	112.36		109.82
100/0	106.18	106.18		106.18
PMMA/CAB 7.5 DMP				
0/100	129.43	129.43		129.43
30/70	118.15	121.42		117.91
50/50	112.94	116.60	0.44	113.22
70/30	107.10	112.16		109.79
100/0	106.09	106.09		106.06
PMMA/CAB 10 DMP				
0/100	128.98	128.98		128.98
30/70	117.65	121.07		117.47
50/50	112.38	116.32	0.43	112.85
70/30	106.92	111.92		109.51
100/0	105.92	105.92		105.92

PMMA/CAPh 2.5 DMP

0/100	140.10	140.10		140.10
30/70	138.47	127.93		138.10
50/50	135.86	120.92	6.8	135.77
70/30	131.14	114.64		131.48
100/0	106.36	106.36		106.36

PMMA/CAPh 5 DMP

0/100	139.80	139.80		139.80
30/70	137.69	127.67		137.81
50/50	135.57	120.69	6.8	135.49
70/30	130.66	114.44		131.21
100/0	106.18	106.18		106.18

PMMA/CAPh 7.5 DMP

0/100	139.50	139.50		139.50
30/70	136.60	127.46		137.20
50/50	134.28	120.52	5.8	134.59
70/30	130.38	114.30		129.92
100/0	106.09	106.09		106.09

PMMA/CAPh 10 DMP

0/100	139.00	139.00		139.00
30/70	136.20	127.09		136.24
50/50	133.16	120.23	4.7	133.20
70/30	128.84	114.06		128.03
100/0	105.92	105.92		105.92

Chapter 4

STUDIES ON DIETHYL PHTHALATE (DEP) PLASTICIZED BLENDS OF PMMA WITH CA, CAP, CAB AND CPh

Chapter 4 deals with the study of diethyl phthalate (DEP) plasticized blends of PMMA-CA derivatives.

4.1 DIETHYL PHTHALATE (DEP) PLASTICIZER

Diethyl phthalate is a phthalate ester, namely the diethyl ester of phthalic acid. It is a clear substance that is liquid at room temperature and is only slightly more dense than liquid water. It has a faint, disagreeable odor and can be transferred from the plastics that contain it.

Properties:

Physical properties	
Molecular formula	$C_{12}H_{14}O_4$
Molecular mass	222.24
Density	1.12 g/cm ³ at 20 °C
Boiling point	295 °C
Dielectric constant	7.13

Uses:

Since the compound is a suitable solvent for many organic molecules, it is often used to bind cosmetics and fragrances. Other industrial uses include plasticizers, detergent bases, aerosol sprays, incense sticks and as a fixative in the manufacture of perfumes, attars, etc. Diethyl phthalate plasticizer is also used in the processing of Cellulose Acetates. DEP is also used as a denaturant for Ethyl Alcohol.

4.2 RESULTS AND DISCUSSION

4.2.1 Fourier Transform Infrared (FTIR) Spectroscopic Studies

FTIR spectra of 50/50 PMMA/CA blend plasticized with 2.5%, 5%, 7.5% and 10 % DEP are shown in Figure 4.1, Figure 4.2, Figure 4.3 and Figure 4.4 respectively. The FTIR stretching frequencies of PMMA/CA, PMMA/CAP, PMMA/CAB and PMMA/CAPh blends plasticized with DEP are also given in Tables 4.1. Carbonyl frequency of 0/100 PMMA/CA blend with 2.5 % DEP at 1730.2 cm⁻¹ decreased to

1723.5 cm^{-1} in 50/50 PMMA/CA blend with 2.5 % DMP. Similarly, the carbonyl frequency of 0/100 PMMA/CA blend with 5 % DEP at 1733.7 cm^{-1} decreased to 1723.8 cm^{-1} in 50/50 PMMA/CA blend with 5 % DEP, the carbonyl frequency of 0/100 PMMA/CA blend with 7.5 % DEP at 1733.9 cm^{-1} decreased to 1723.6 cm^{-1} in 50/50 PMMA/CA blend with 7.5 % DEP and 0/100 PMMA/CA blend with 10 % DEP at 1734.0 cm^{-1} decreased to 1722.9 cm^{-1} in 50/50 PMMA/CA blend with 10 % DEP.

The carbonyl frequency of 0/100 PMMA/CAP blend with 2.5 % DEP at 1737.2 cm^{-1} decreased to 1723.3 cm^{-1} in 50/50 PMMA/CAP blend with 2.5 % DEP. Similarly, the carbonyl frequency of 0/100 PMMA/CAP blend with 5 % DEP at 1737.4 cm^{-1} decreased to 1723.0 cm^{-1} in 50/50 PMMA/CAP blend with 5 % DEP, the carbonyl frequency of 0/100 PMMA/CAP blend with 7.5 % DEP at 1737.3 cm^{-1} decreased to 1723.9 cm^{-1} in 50/50 PMMA/CAP blend with 7.5 % DEP and the carbonyl frequency of 0/100 PMMA/CAP blend with 10 % DEP at 1737.4 cm^{-1} decreased to 1723.0 cm^{-1} in 50/50 PMMA/CAP blend with 10 % DEP.

The carbonyl frequency of 0/100 PMMA/CAB blend with 2.5 % DEP at 1738.0 cm^{-1} decreased to 1722.9 cm^{-1} in 50/50 PMMA/CAB blend with 2.5 % DEP. Similarly, the carbonyl frequency of 0/100 PMMA/CAB blend with 5 % DEP at 1738.0 cm^{-1} decreased to 1722.5 cm^{-1} in 50/50 PMMA/CAB blend with 5 % DEP, the carbonyl frequency at 0/100 PMMA/CAB blend with 7.5 % DEP at 1737.7 cm^{-1} decreased to 1726.7 cm^{-1} in 50/50 PMMA/CAB blend with 7.5 % DEP and the carbonyl frequency of 0/100 PMMA/CAB blend with 10 % DEP at 1738.4 cm^{-1} decreased to 1723.2 cm^{-1} in 50/50 PMMA/CAB blend with 10 % DEP.

The carbonyl frequency of 0/100 PMMA/CAPh blend with 2.5 % DEP at 1655.1 cm^{-1} shifted to 1713.8 cm^{-1} in 50/50 PMMA/CAPh blend with 2.5 % DEP. Similarly, the carbonyl frequency of 0/100 PMMA/CAPh blend with 5 % DEP at 1660.3 cm^{-1} shifted to 1668.5 cm^{-1} in 50/50 PMMA/CAPh blend with 5 % DEP, the carbonyl frequency of 0/100 PMMA/CAPh blend with 7.5 % DEP at 1659.9 cm^{-1} shifted to 1657.2 cm^{-1} in 50/50 PMMA/CAPh blend with 7.5 % DEP and the carbonyl frequency of 0/100

PMMA/CAPh blend with 10 % DEP at 1661.8 cm^{-1} shifted to 1718.6 cm^{-1} in 50/50 PMMA/CAPh blend with 10 % DEP.

Such shift in the specific vibration frequencies are ascribed to the formation of a weak hydrogen bond between component polymers in the blend. This can also be contributing to the miscibility of the blends.

The -OH stretching vibrations of hydroxyl groups occurred as broad band at 3491.2 cm^{-1} and 3563.1 cm^{-1} in 0/100 PMMA/CA blend with 2.5 % DEP and 50/50 PMMA/CA blend with 2.5 % DEP respectively. Similarly, the -OH stretching vibrations of hydroxyl groups in the case of other blends with varying compositions are given in Tables 4.1.

The intensity of the broad band decreased after blending, indicating that part of the -OH groups are involved in the hydrogen bond formation. These results indicate that specific interactions such as the hydrogen bonding forces exist in the blends and this is leading to the miscibility of the blends.

4.2.2 Differential Scanning Calorimetry (DSC) Studies

The DSC thermograms of 2.5 %, 5 %, 7.5 % and 10 % DEP plasticized 50/50 PMMA/CA blends are shown in Figure 4.5 (a), Figure 4.5 (b), Figure 4.5 (c) and Figure 4.5 (d) respectively.

From Figure 4.5 (a) to Figure 4.5 (d), it can be seen that the T_g for 2.5 %, 5 %, 7.5 % and 10 % DEP plasticized 50/50 PMMA/CA blends are $114.35\text{ }^\circ\text{C}$, $113.94\text{ }^\circ\text{C}$, $113.56\text{ }^\circ\text{C}$ and $113.01\text{ }^\circ\text{C}$ respectively. It is interesting to note here that the thermograms for the blends (Figure 4.5 (a) to Figure 4.5 (d)) exhibited single T_g and its value lies intermediate to the T_g values of 2.5 %, 5 %, 7.5 % and 10 % DEP plasticized pure PMMA and pure CA derivatives respectively. Further, the T_g values of the blend films decreased regularly on increase of PMMA content in the blends. Such a systematic variation of T_g in the blends is indicative of miscibility of the components in the blends.

Theoretical equations like Eq. (2.1) and Eq. (2.2) have been proposed for estimating the glass transition temperature of blend films from the properties of pure

components and also to predict the glass transition temperature of amorphous polymer blends.

The examination data is best fitted by this equation with $k = 0.13, 0.13, 0.12$ and 0.10 respectively for 2.5 %, 5 %, 7.5 % and 10 % DEP plasticized PMMA/CA blends. This result supports that, blends have high miscibility in the amorphous state. The thermal properties of 2.5 %, 5 %, 7.5 % and 10 % DEP plasticized PMMA/CA, PMMA/CAP, PMMA/CAB and PMMA/CAPh blends have shown single T_g and are presented in Table 4.2. Hence it can be concluded that all the blends studied are miscible in the entire composition range. The blends show a positive deviation from Fox equation implying an intermolecular interaction between the polymers.

4.2.3 Water Uptake

The water uptake capacity of the polymer blend films have been calculated using the equation 1.7. The plots of water uptake against DEP content in the PMMA/CA, PMMA/CAP, PMMA/CAB and PMMA/CAPh blends with 2.5 %, 5 %, 7.5 % and 10 % of DEP plasticizer are shown in Figure 4.6, Figure 4.7, Figure 4.8 and Figure 4.9, respectively.

As seen from the figures, the water uptake for 0/100 PMMA/CA, PMMA/CAP, PMMA/CAB and PMMA/CAPh blends with 2.5 % DEP are 0.94 wt %, 1.03 wt %, 1.30 wt % and 1.51 wt % respectively. The water uptake of the blends increased up to 50 wt % of CA derivatives concentration. The maximum water uptake was observed for the blends with 50/50 PMMA/CA, PMMA/CAP, PMMA/CAB and PMMA/CAPh blends with 2.5 % DEP are 5.94 wt %, 7.46 wt %, 7.63 wt % and 7.66 wt % respectively, which decrease on addition of further PMMA.

The water uptake for 0/100 PMMA/CA, PMMA/CAP, PMMA/CAB and PMMA/CAPh blends with 5 % DEP are 0.93 wt %, 1.03 wt %, 1.29 wt % and 1.51 wt % respectively. The water uptake of the blends increased up to 50 wt % of CA derivatives concentration. The maximum water uptake was observed for the blends with 50/50 PMMA/CA, PMMA/CAP, PMMA/CAB and PMMA/CAPh blends with 5 % DEP are

5.79 wt %, 7.33 wt %, 7.51 wt % and 7.59 wt % respectively, which decrease on addition of further PMMA.

The water uptake for 0/100 PMMA/CA, PMMA/CAP, PMMA/CAB and PMMA/CAPh blends with 7.5 % DEP are 0.91 wt %, 1.03 wt %, 1.27 wt % and 1.49 wt % respectively. The water uptake of the blends increased up to 50 wt % of CA derivatives concentration. The maximum water uptake was observed for the blends with 50/50 PMMA/CA, PMMA/CAP, PMMA/CAB and PMMA/CAPh blends with 7.5 % DEP are 5.73 wt %, 7.21 wt %, 7.36 wt % and 7.43 wt % respectively, which decrease on addition of further PMMA.

The water uptake for 0/100 PMMA/CA, PMMA/CAP, PMMA/CAB and PMMA/CAPh blends with 10 % DEP are 0.88 wt %, 1.01 wt %, 1.21 wt % and 1.48 wt % respectively. The water uptake of the blends increased up to 50 wt % of CA derivatives concentration. The maximum water uptake was observed for the blends with 50/50 PMMA/CA, PMMA/CAP, PMMA/CAB and PMMA/CAPh blends with 10 % DEP are 5.65 wt %, 7.13 wt %, 7.36 wt % and 7.37 wt % respectively, which decrease on addition of further PMMA.

The prepared polymer blends have shown a maximum water uptake in the 50 wt. % of PMMA indicating the presence of void volume in the blends and further decrease in the water uptake due to the compact structured pattern with reduction in void volumes has been discussed in chapter 3, section 3.2.3 of the thesis.

4.2.4 Ion Exchange Capacity (IEC) Measurements

Ion exchange capacity (IEC) provides an indirect approximation for the ion exchangeable groups present in the pure and blend polymers which are responsible for proton conduction. The IEC values for 2.5 %, 5 %, 7.5 % and 10 % DEP plasticized pure and PMMA/CA, PMMA/CAP, PMMA/CAB and PMMA/CAPh blends are shown graphically in Figure 4.10, Figure 4.11, Figure 4.12 and Figure 4.13.

From the figure it can be seen that the IEC values decreases for the blends with an increase in PMMA content. It is known that CA derivatives has exchangeable –OH groups. Hence it is evident that when PMMA content of the blend is increased, the

number of replaceable sites available in the blend would decrease and hence the decrease in the IEC of the blends.

4.2.5 Electrochemical Impedance Spectroscopy

Electrochemical Impedance spectroscopy is recently being widely applied in determining various material properties, prime among which are permittivity and conductivity. Figure 4.14, Figure 4.15, Figure 4.16 and Figure 4.17 shows AC impedance spectra (Cole-Cole or Nyquist plots) of 2.5 %, 5 %, 7.5 % and 10 % DEP plasticized 50/50 PMMA/CA blends at different temperatures, respectively.

The impedance responses due to the bulk resistance of the electrolyte and electrolyte-electrode double layer capacitance behavior of the samples over the whole range of frequency evaluated has been discussed in the chapter 3, section 3.2.5 of the thesis. AC impedance spectra of 2.5 %, 5 %, 7.5 % and 10 % DEP plasticized 50/50 PMMA/CAP, PMMA/CAB and PMMA/CAPh blends at different temperatures, respectively have shown the similar trend for electrochemical impedance spectra.

4.2.5.1 Proton conductivity measurement

The variation of conductivity of the blends with temperature and room temperature conductivity of the blends are shown in Figure 4.18, Figure 4.19, Figure 4.20 and Figure 4.21 respectively. It has been observed that at 30 °C, among the polyblends studied the blends with 2.5 % DEP plasticized PMMA/CA, PMMA/CAP, PMMA/CAB and PMMA/CAPh 30/70 composition showed the highest proton conductivity value of $1.71 \times 10^{-3} \text{ S cm}^{-1}$, $2.28 \times 10^{-3} \text{ S cm}^{-1}$, $2.29 \times 10^{-3} \text{ S cm}^{-1}$ and $2.39 \times 10^{-3} \text{ S cm}^{-1}$, respectively. The proton conductivity increased as the temperature is increased in the measured temperature range between 30 °C to 70 °C. Also, it has been found from impedance plots that as the temperature is increased, the bulk resistance R decreased resulting in an increase in the value of proton conductivity. This may be mainly due to the fact that at higher temperature, there is an enhancement in the ion movement, favoring conductivity. Proton conductivity measurement of 5 %, 7.5 % and 10 % DEP plasticized 50/50 PMMA/CAP, PMMA/CAB and PMMA/CAPh blends at different temperatures respectively have shown the similar trend.

4.2.5.2 Temperature dependence of ionic conductivity

It has been found that the proton conductivity of the blend film increased with increasing temperature for all compositions. This may be mainly due to the fact that an increase in temperature increases the mobility of ions and this in turn increases the conductivity. Further, the vibrational motion of the polymer backbone and side chains, which becomes more vigorous with increase in temperature can also facilitate the conduction of ions. The increased amplitude of vibration brings the coordination sites closer to one another enabling the ions to hop from the occupied site to the unoccupied site with lesser energy required. Increase in amplitude of vibration of the polymer backbone and side chains can also increase the fraction of free volume in the polymer electrolyte system (Aziz et al. 2010). Druger et al. (1983) and Druger et al. (1985) have attributed the change in conductivity with temperature in solid polymer electrolyte to hopping model, which results in an increase in the free volume of the system. The hopping model either permits the ions to hop from one site to another or provides a pathway for ions to move. In other words, this facilitates translational motion of the ions. From this, it is clear that the ionic motion is due to translational motion/hopping facilitated by the polymer. The nonexistence of any unusual variation of conductivity indicates the existence of overall amorphous region (Aziz et al. 2010). This implies that coupling of the ion movement with the amorphous nature of the polymer is facilitating the conductivity in the blends.

Electrical conduction is a thermally activated process and follows the Arrhenius law

$$\sigma = \sigma_0 \exp\left[-\frac{E_a}{kT}\right] \quad (2.3)$$

where, σ is the conductivity at a particular temperature, σ_0 is the pre-exponential factor, k is the Boltzmann's constant, and T is the absolute temperature. As there is no sudden change in the value of conductivity with temperature it may be inferred that these blends do not undergo any phase transitions within the temperature range studied. The conductivity has been discussed on the basis of the increase in the CA contents along

with the ion exchange capacity and water absorption facilitating the ion hopping through the polymer structure has been detailed in chapter 3, section 3.2.5.2 of the thesis.

4.2.6 Dielectric Studies

The dielectric constant and loss of the films have been calculated using the equations 1.11 and 1.12 respectively. The conductivity behavior of polymer electrolyte can be understood from dielectric studies (Ramesh et al. 2002). The dielectric constant is a measure of stored charge. The variations of dielectric constant and dielectric loss with frequency at different temperatures have been shown in Figure 4.22, Figure 4.23, Figure 4.24 and Figure 4.25 respectively, for 2.5 %, 5 %, 7.5 % and 10 % DEP plasticized 50/50 PMMA/CA blends. Similar trends have also been seen for 2.5 %, 5 %, 7.5 % and 10 % DEP plasticized 50/50 PMMA/CAP, PMMA/CAB and PMMA/CAPh blends at different temperatures.

There are no appreciable relaxation peaks observed, indicating the electrode polarization and space charge effects have occurred confirming non-debye dependence; the increase in dielectric constant and dielectric loss at higher temperatures due to the higher charge carrier density and conductivity of the polymer blends due to hopping mechanism has been discussed in the chapter 3, section 3.2.6 in the thesis.

4.3 FIGURES

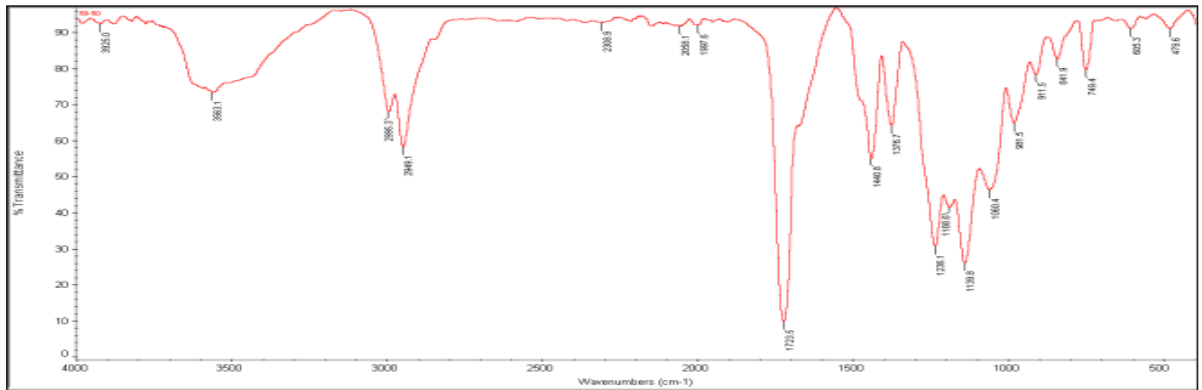


Figure 4.1 FTIR Spectrum of 2.5 % DEP plasticized 50/50 PMMA/CA blend.

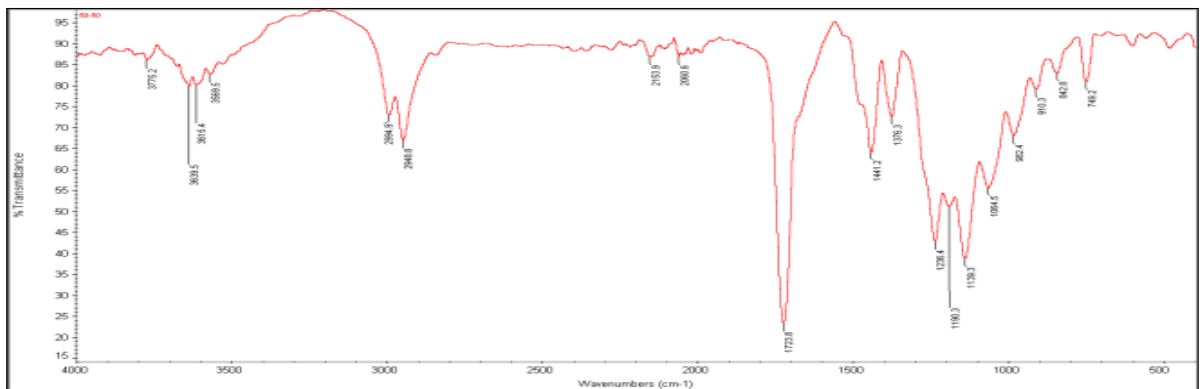


Figure 4.2 FTIR Spectrum of 5 % DEP plasticized 50/50 PMMA/CA blend.

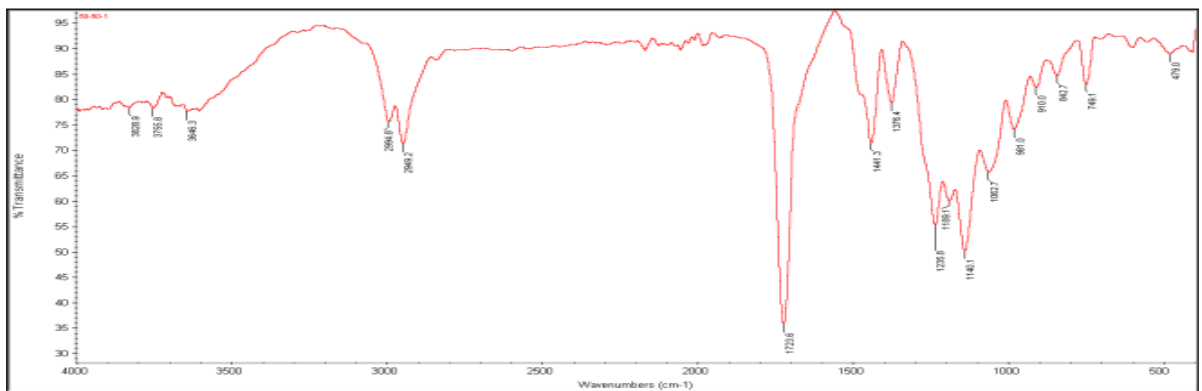


Figure 4.3 FTIR Spectrum of 7.5 % DEP plasticized 50/50 PMMA/CA blend.

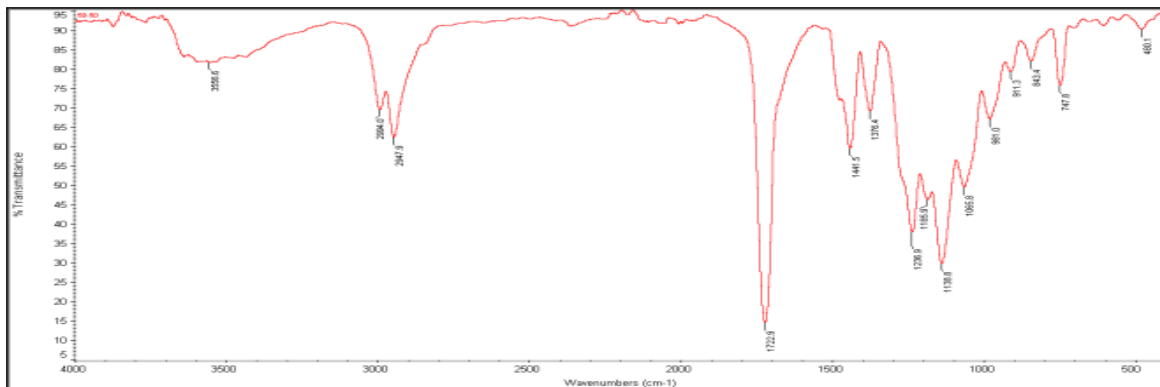


Figure 4.4 FTIR Spectrum of 10 % DEP plasticized 50/50 PMMA/CA blend.

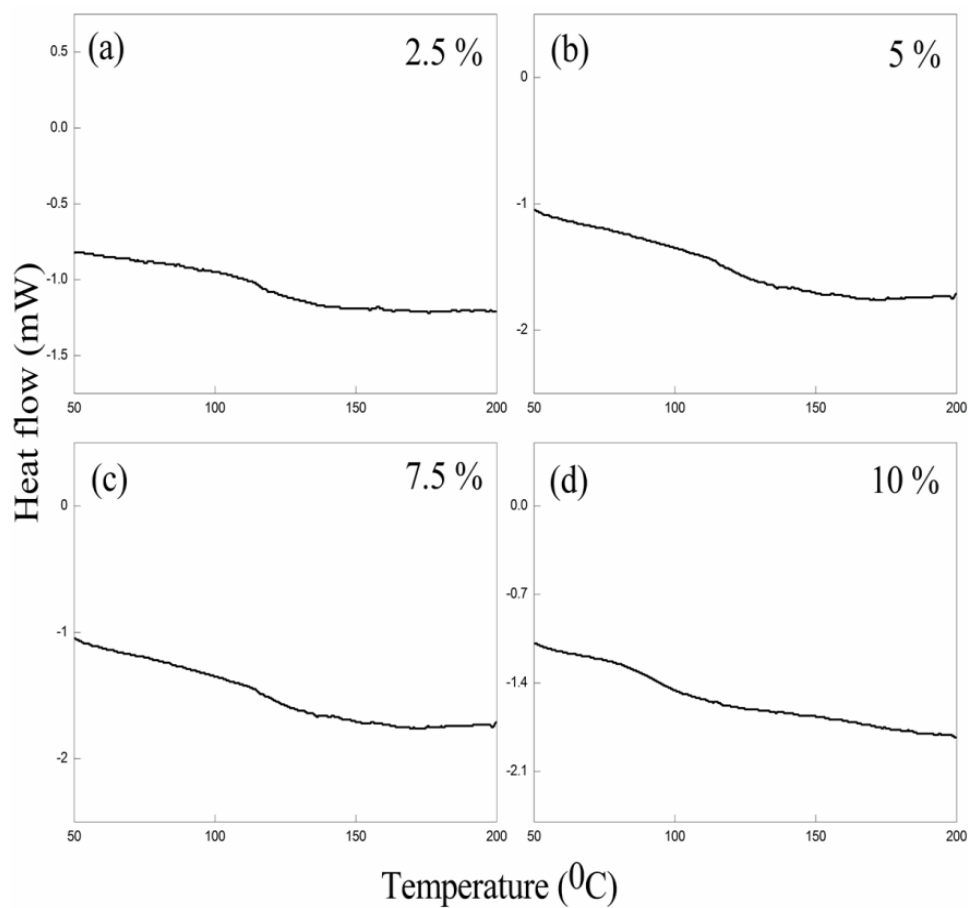


Figure 4.5 (a), (b), (c) and (d) DSC scans of 2.5 %, 5 %, 7.5 % and 10 % DEP plasticized 50/50 PMMA/CA blends.

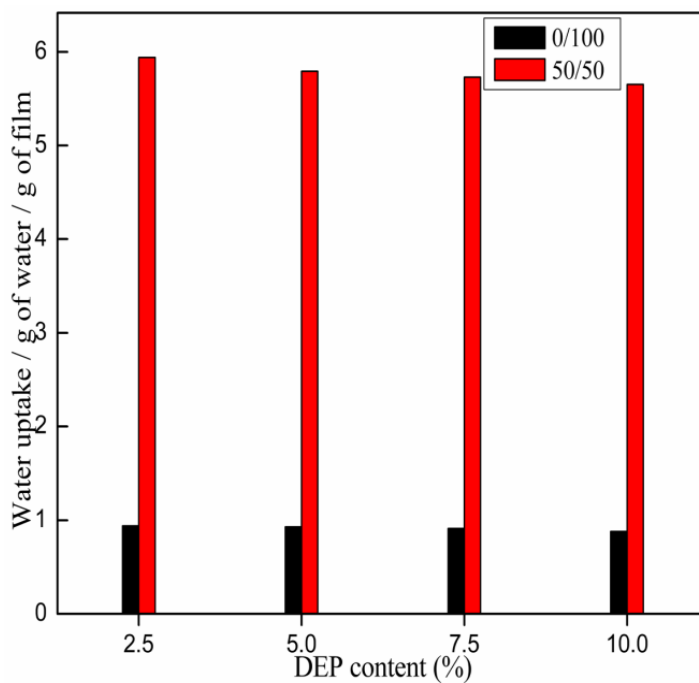


Figure 4.6 Water absorption by 2.5 %, 5 %, 7.5 % and 10 % DEP plasticized 0/100 and 50/50 PMMA/CA blends.

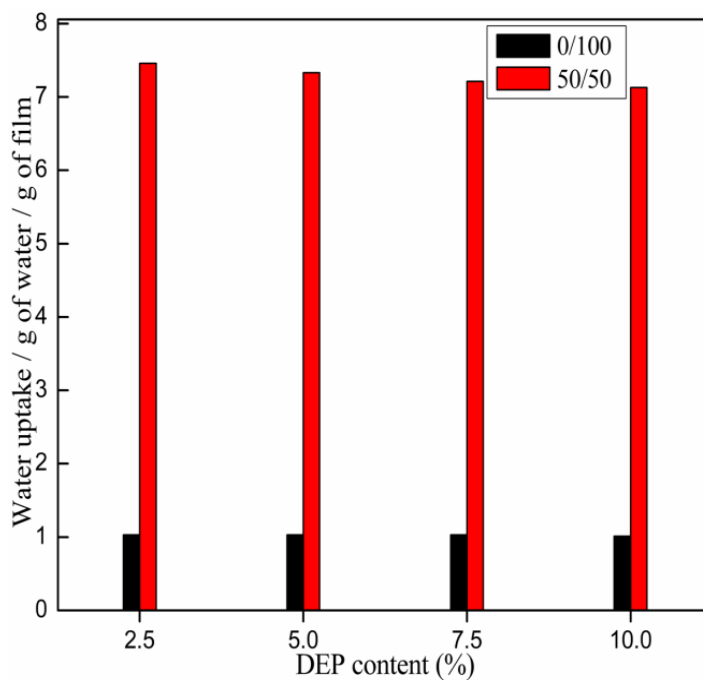


Figure 4.7 Water absorption by 2.5 %, 5 %, 7.5 % and 10 % DEP plasticized 0/100 and 50/50 PMMA/CAP blends.

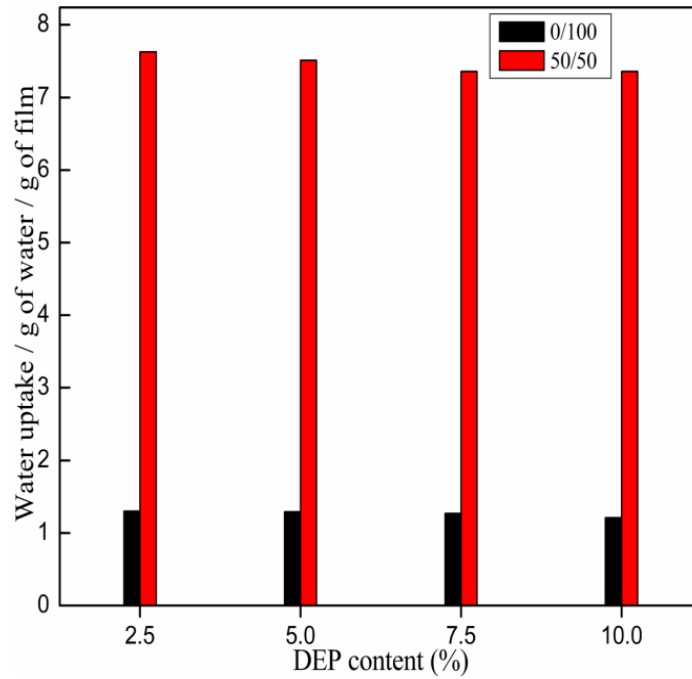


Figure 4.8 Water absorption by 2.5 %, 5 %, 7.5 % and 10 % DEP plasticized 0/100 and 50/50 PMMA/CAB blends.

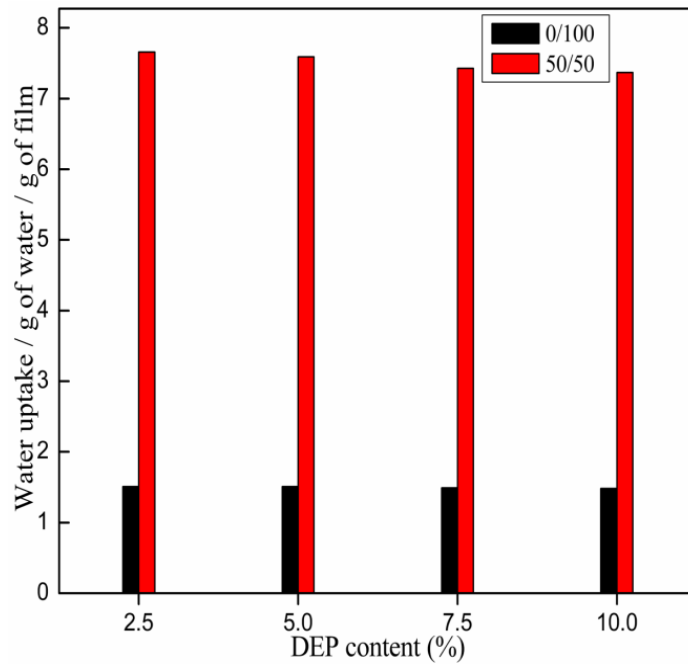


Figure 4.9 Water absorption by 2.5 %, 5 %, 7.5 % and 10 % DEP plasticized 0/100 and 50/50 PMMA/CAPh blends.

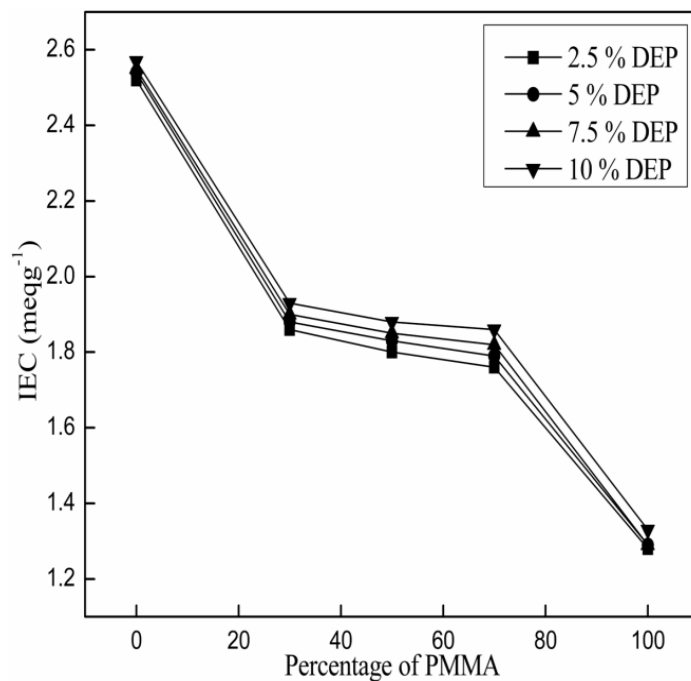


Figure 4.10 The change of IEC values in 2.5 %, 5 %, 7.5 % and 10 % DEP plasticized PMMA/CA blends.

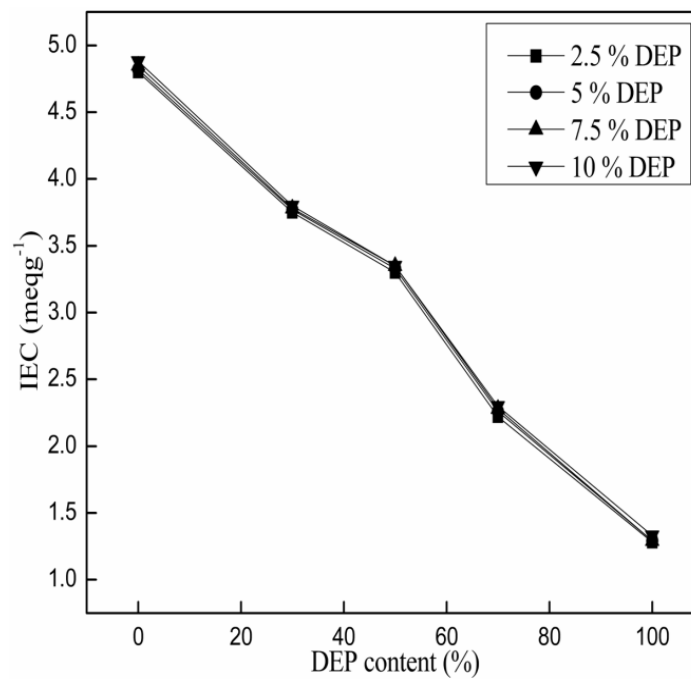


Figure 4.11 The change of IEC values in 2.5 %, 5 %, 7.5 % and 10 % DEP plasticized PMMA/CAP blends.

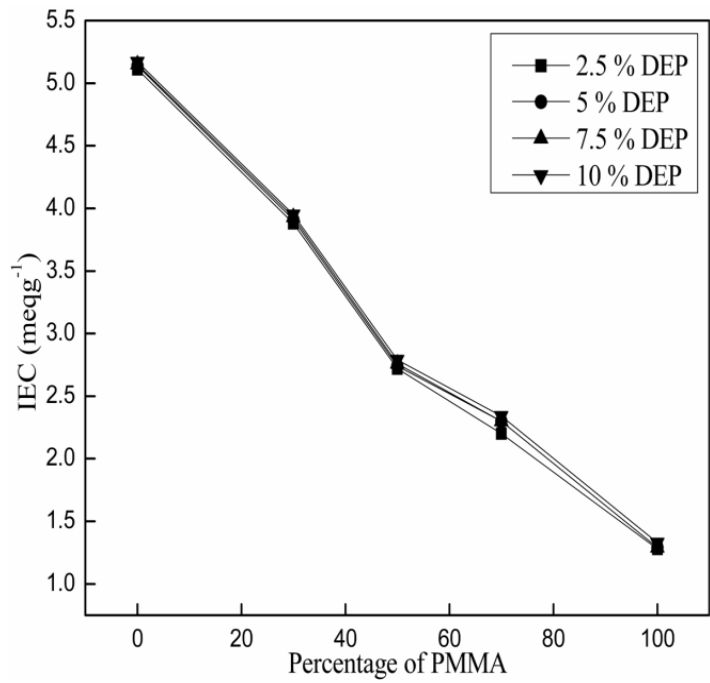


Figure 4.12 The change of IEC values in 2.5 %, 5 %, 7.5 % and 10 % DEP plasticized PMMA/CAB blends.

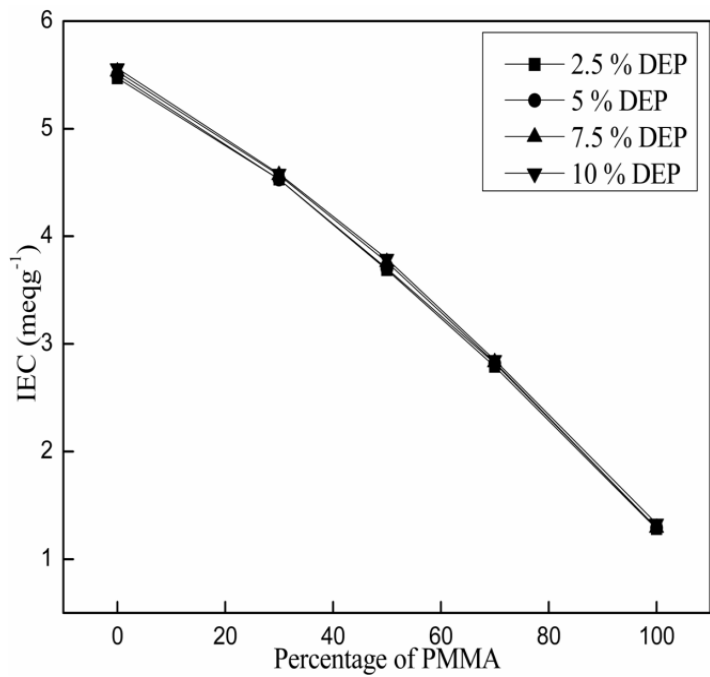


Figure 4.13 The change of IEC values in 2.5 %, 5 %, 7.5 % and 10 % DEP plasticized PMMA/CAPh blends.

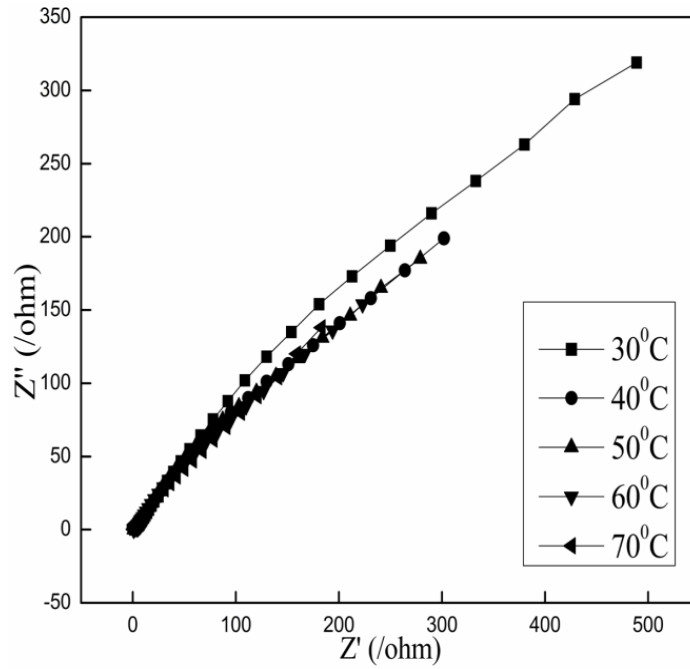


Figure 4.14 AC impedance spectrum of 2.5 % DEP plasticized 50/50 PMMA/CA blend at different temperatures.

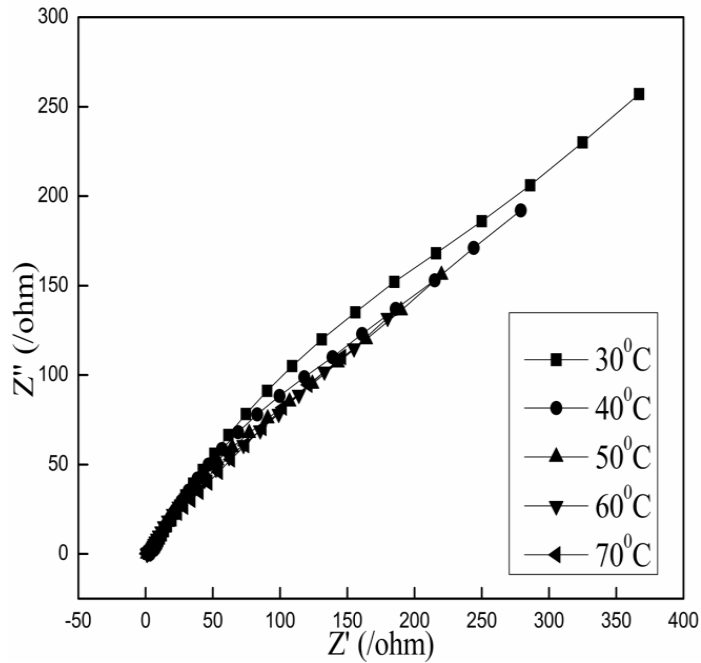


Figure 4.15 AC impedance spectrum of 5 % DEP plasticized 50/50 PMMA/CA blend at different temperatures.

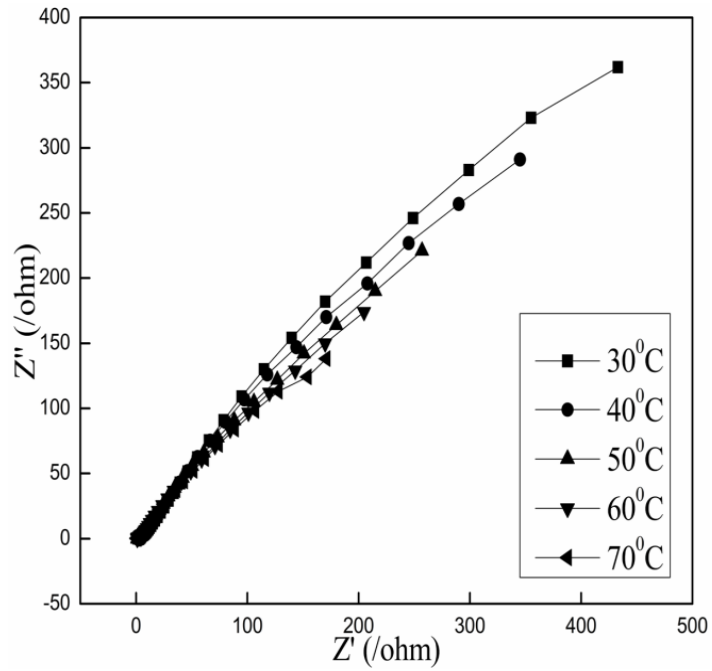


Figure 4.16 AC impedance spectrum of 7.5 % DEP plasticized 50/50 PMMA/CA blend at different temperatures.

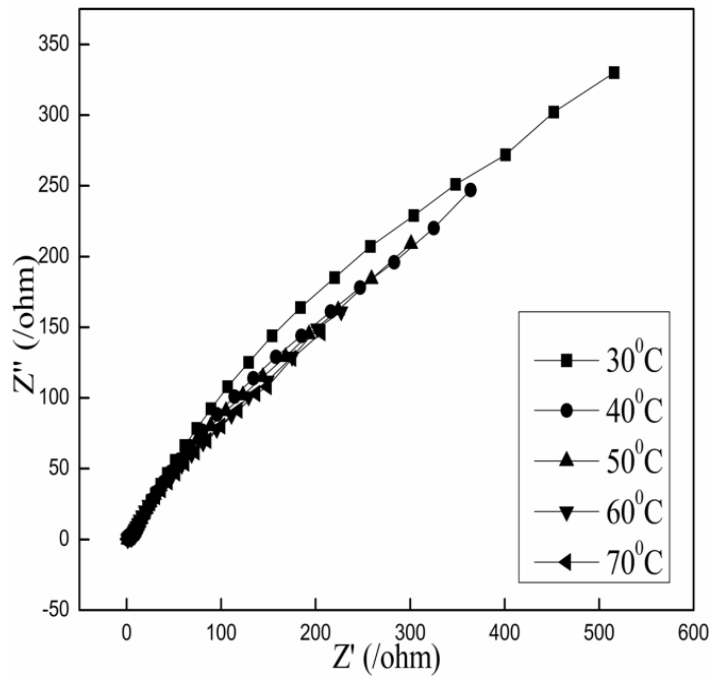


Figure 4.17 AC impedance spectrum of 10 % DEP plasticized 50/50 PMMA/CA blend at different temperatures.

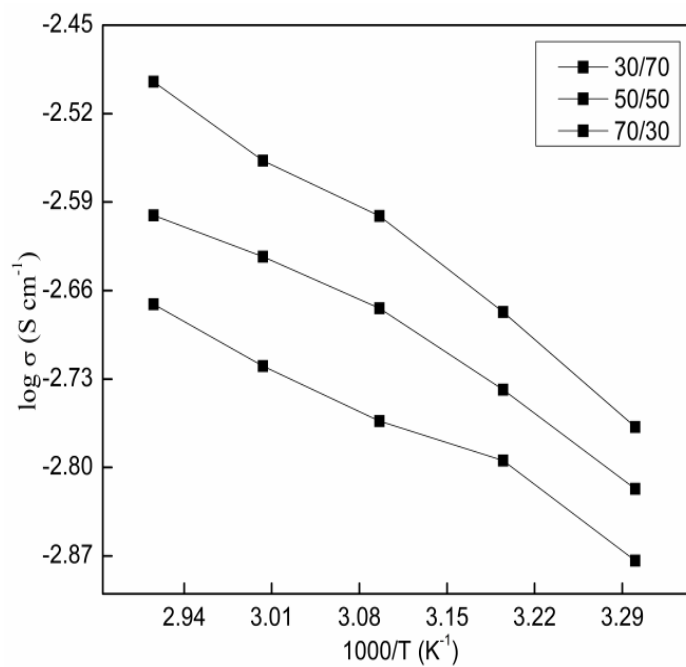


Figure 4.18 Arrhenius plots for conductivity σ of 2.5 % DEP plasticized PMMA/CA blends.

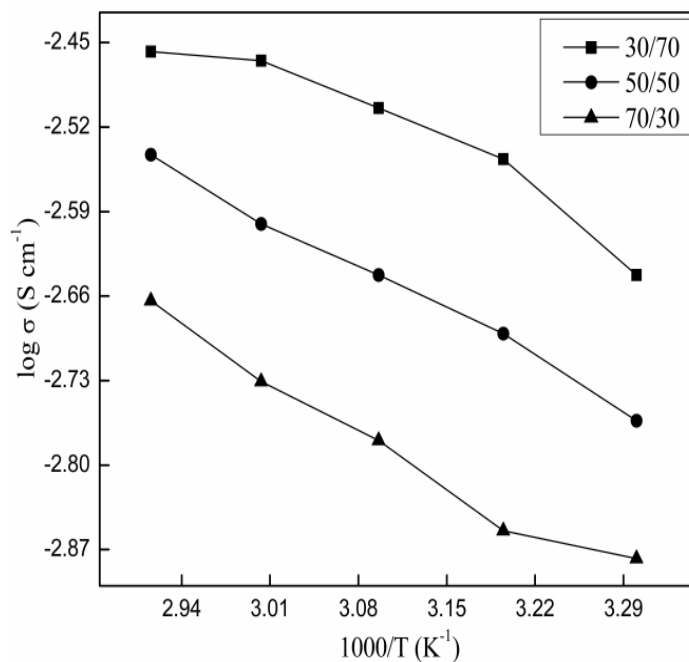


Figure 4.19 Arrhenius plots for conductivity σ of 2.5 % DEP plasticized PMMA/CAP blends.

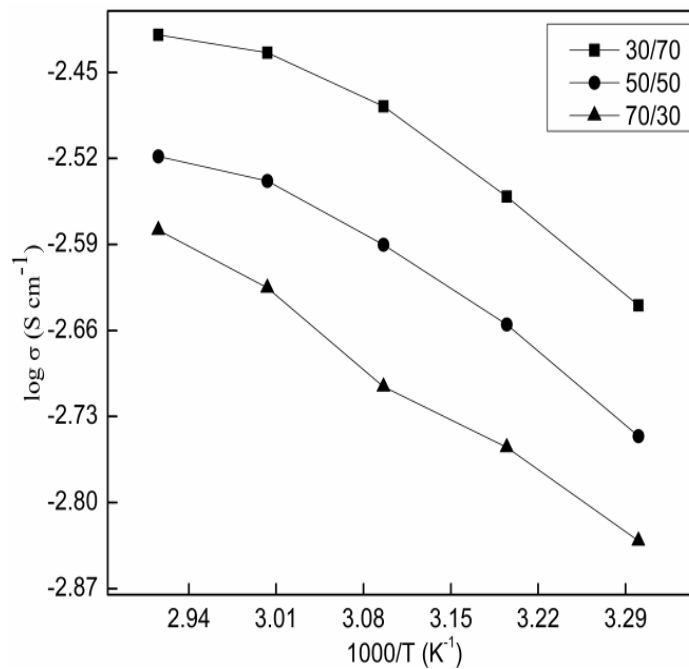


Figure 4.20 Arrhenius plots for conductivity σ of 2.5 % DEP plasticized PMMA/CAB blends.

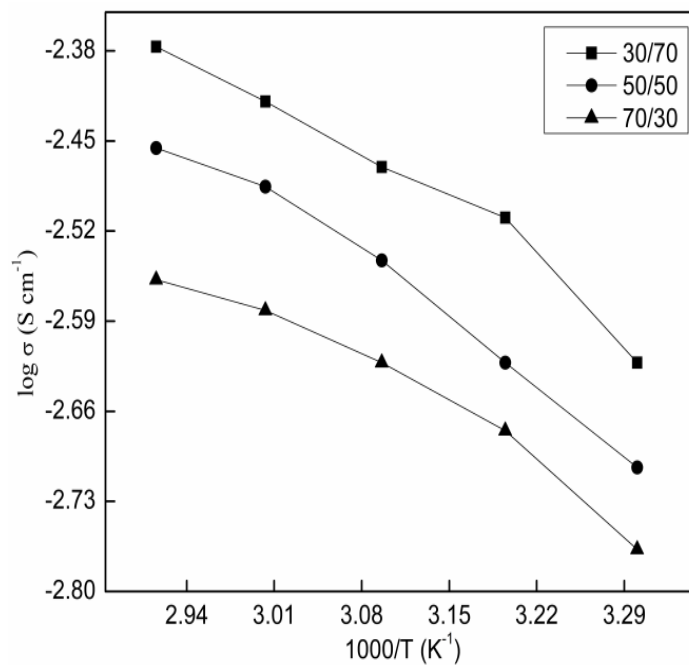


Figure 4.21 Arrhenius plots for conductivity σ of 2.5 % DEP plasticized PMMA/CAPh blends.

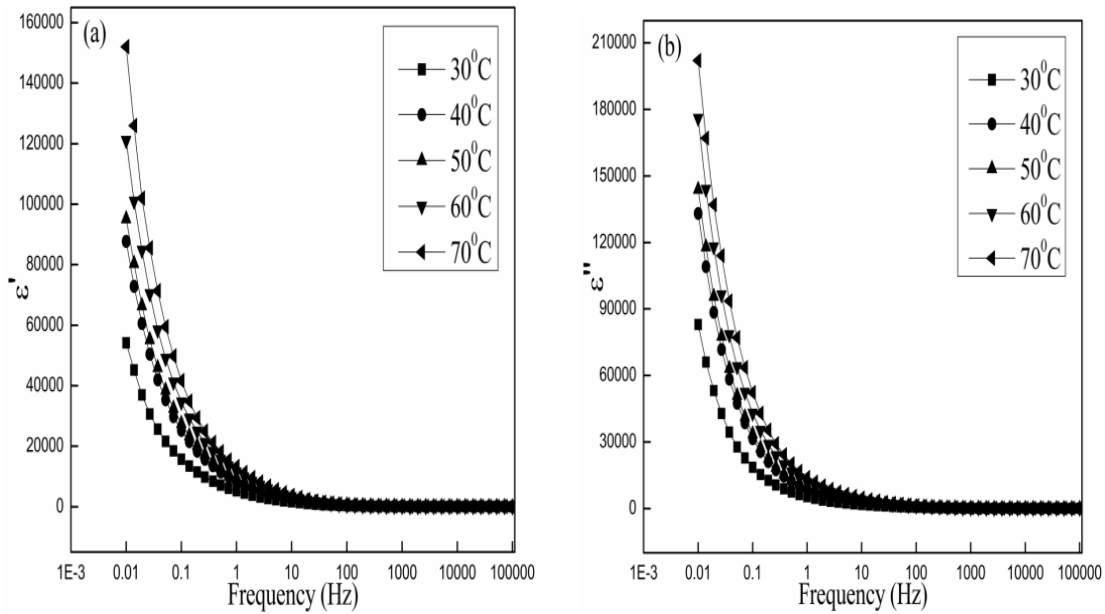


Figure 4.22 Variations of dielectric constant (a) and dielectric loss (b) with frequency at different temperatures for 2.5 % DEP plasticized 50/50 PMMA/CA blend.

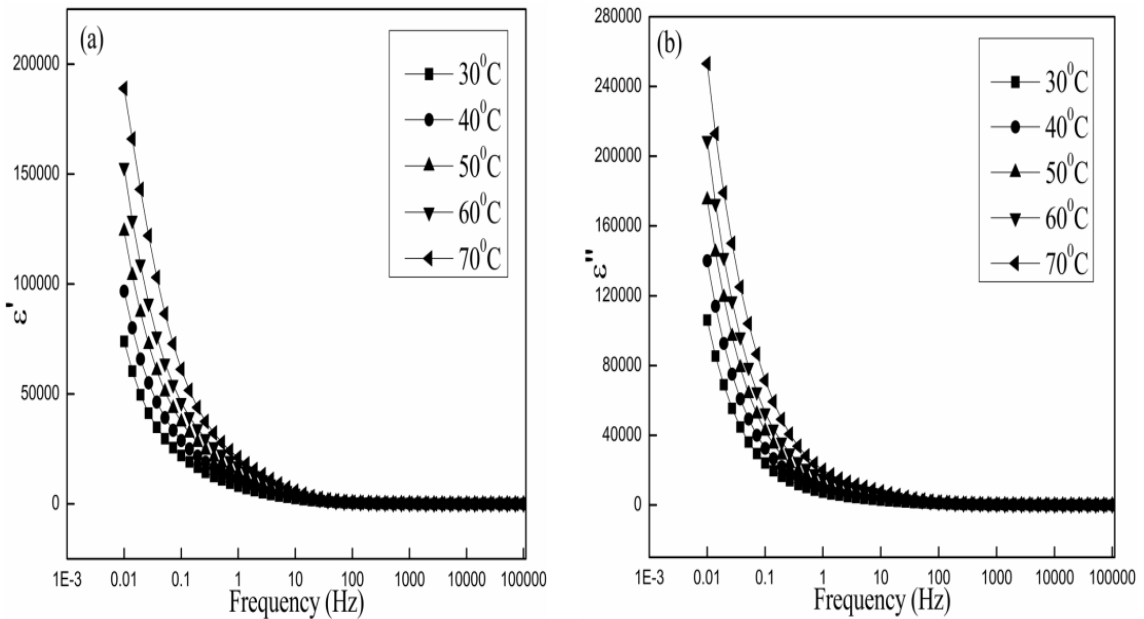


Figure 4.23 Variations of dielectric constant (a) and dielectric loss (b) with frequency at different temperatures for 5 % DEP plasticized 50/50 PMMA/CA blend.

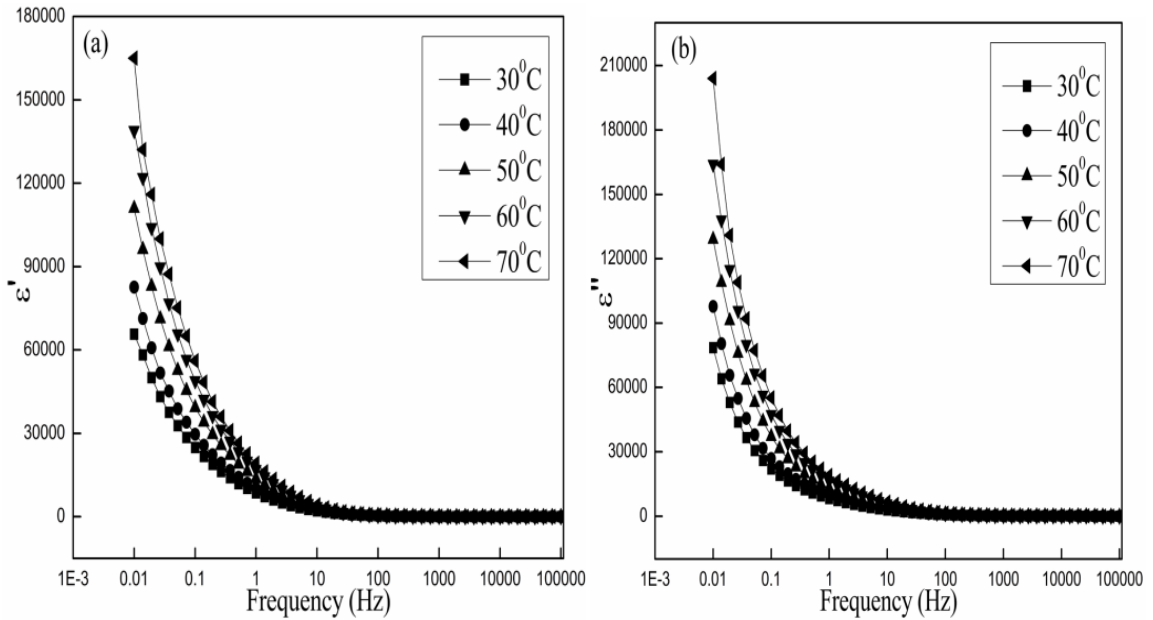


Figure 4.24 Variations of dielectric constant (a) and dielectric loss (b) with frequency at different temperatures for 7.5 % DEP plasticized 50/50 PMMA/CA blend.

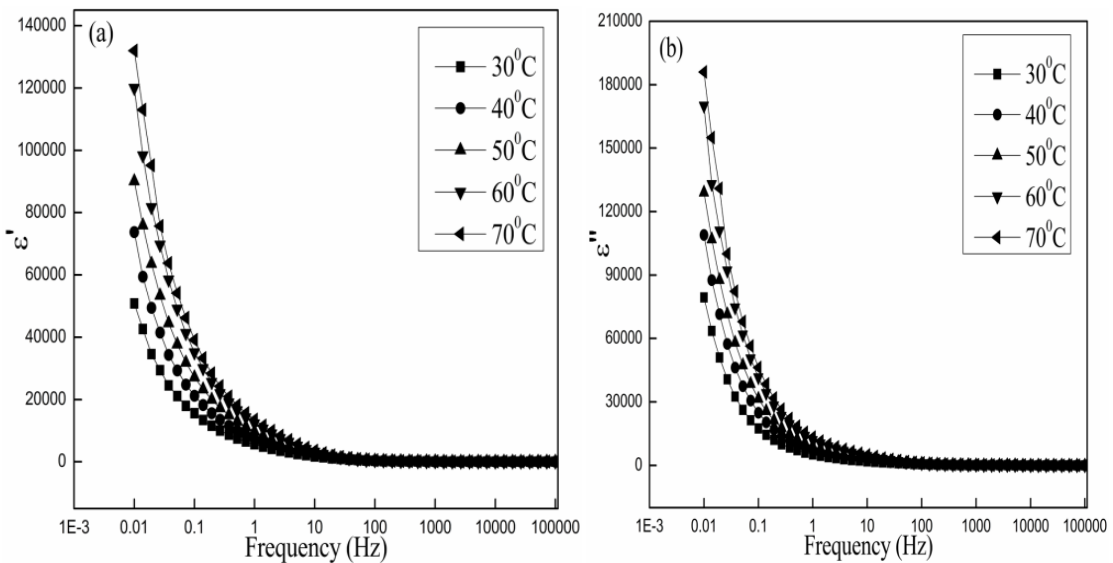


Figure 4.25 Variations of dielectric constant (a) and dielectric loss (b) with frequency at different temperatures for 10 % DEP plasticized 50/50 PMMA/CA blend.

4.4 TABLES

Table 4.1 IR stretching frequencies of DEP plasticized PMMA/CA, PMMA/CAP, PMMA/CAB and PMMA/CAPh blends.

PMMA/CA 2.5 DEP	-CO Stretching Frequencies	-OH Stretching Frequencies
0/100	1730.2	3491.2
50/50	1723.5	3563.1
PMMA/CA 5 DEP		
0/100	1733.7	3489.4
50/50	1723.8	3615.4
PMMA/CA 7.5 DEP		
0/100	1733.9	3473.6
50/50	1723.6	3646.3
PMMA/CA 10 DEP		
0/100	1734.0	3485.6
50/50	1722.9	3556.6
PMMA/CAP 2.5 DEP		
0/100	1737.2	3550.9
50/50	1723.3	3627.5
PMMA/CAP 5 DEP		
0/100	1737.4	3493.8
50/50	1723.0	3569.6
PMMA/CAP 7.5 DEP		
0/100	1737.3	3476.1
50/50	1723.9	3547.9
PMMA/CAP 10 DEP		
0/100	1737.4	3485.2
50/50	1723.0	3547.7
PMMA/CAB 2.5 DEP		
0/100	1738.0	3482.8
50/50	1722.9	3430.9
PMMA/CAB 5 DEP		
0/100	1738.0	3488.4
50/50	1722.5	3540.2

PMMA/CAB 7.5 DEP

0/100	1737.7	3503.5
50/50	1726.7	3484.6

PMMA/CAB 10 DEP

0/100	1738.4	3479.8
50/50	1723.2	3439.2

PMMA/CAPh 2.5 DEP

0/100	1655.1	3415.4
50/50	1713.8	3434.7

PMMA/CAPh 5 DEP

0/100	1660.3	3396.5
50/50	1668.5	3436.3

PMMA/CAPh 7.5 DEP

0/100	1659.9	3394.9
50/50	1657.2	3392.9

PMMA/CAPh 10 DEP

0/100	1661.8	3444.6
50/50	1718.6	3385.5

Table 4.2 Thermal properties of 2.5 %, 5 %, 7.5 % and 10 % DEP plasticized PMMA/CA, PMMA/CAP, PMMA/CAB and PMMA/CAPh blends.

Sample	T_g (°C)	Fox equation	k values	Gordon-Taylor equation
PMMA/CA 2.5 DEP				
0/100	179.44	179.44		179.44
30/70	123.60	148.90		123.53
50/50	114.35	133.72	0.13	114.95
70/30	111.09	121.35		110.42
100/0	106.57	106.57		106.57
PMMA/CA 5 DEP				
0/100	178.69	178.69		178.69
30/70	123.50	148.52		123.33
50/50	113.94	133.49	0.13	114.84
70/30	110.99	121.22		110.35
100/0	106.54	106.54		106.54
PMMA/CA 7.5 DEP				
0/100	178.58	178.58		178.58
30/70	123.20	148.43		122.26
50/50	113.56	133.42	0.12	114.21
70/30	110.01	121.16		110.02
100/0	106.49	106.49		106.49
PMMA/CA 10 DEP				
0/100	178.53	178.53		178.53
30/70	123.13	148.40		120.11
50/50	113.01	133.40	0.10	113.03
70/30	108.64	121.15		109.44
100/0	106.48	106.48		106.48
PMMA/CAP 2.5 DEP				
0/100	137.17	137.17		137.17
30/70	136.15	126.29		124.42
50/50	118.03	119.95	0.6	118.05
70/30	111.59	114.21		112.83
100/0	106.57	106.57		106.57
PMMA/CAP 5 DEP				
0/100	136.43	136.43		136.43
30/70	135.28	125.84		123.47
50/50	117.24	119.65	0.56	117.27
70/30	111.33	114.04		112.33

100/0	106.54	106.54		106.54
PMMA/CAP 7.5 DEP				
0/100	136.35	136.35		136.35
30/70	135.07	125.77		122.57
50/50	116.36	119.58	0.5	116.44
70/30	110.14	113.98		111.76
100/0	106.49	106.49		106.49
PMMA/CAP 10 DEP				
0/100	135.85	135.85		135.85
30/70	134.82	125.47		121.84
50/50	115.81	119.39	0.47	115.87
70/30	109.31	113.87		111.40
100/0	106.48	106.48		106.48
PMMA/CAB 2.5 DEP				
0/100	131.44	131.44		131.44
30/70	119.87	122.84		118.58
50/50	113.70	117.71	0.4	113.68
70/30	108.58	112.98		110.21
100/0	106.57	106.57		106.57
PMMA/CAB 5 DEP				
0/100	131.31	131.31		131.31
30/70	119.59	122.75		118.50
50/50	113.64	117.64	0.4	113.62
70/30	108.29	112.93		110.16
100/0	106.54	106.54		106.54
PMMA/CAB 7.5 DEP				
0/100	130.82	130.82		130.82
30/70	118.96	122.43		118.24
50/50	113.46	117.41	0.4	113.44
70/30	107.38	112.78		110.05
100/0	106.49	106.49		106.49
PMMA/CAB 10 DEP				
0/100	130.38	130.38		130.38
30/70	118.16	122.15		118.02
50/50	113.20	117.22	0.4	113.31
70/30	107.08	112.68		109.98
100/0	106.48	106.48		106.48

PMMA/CAPh 2.5 DEP				
0/100	141.99	141.99		141.99
30/70	138.66	129.12		139.43
50/50	136.47	121.76	5.5	136.54
70/30	131.66	115.19		131.44
100/0	106.57	106.57		106.57
PMMA/CAPh 5 DEP				
0/100	141.50	141.50		141.50
30/70	138.12	128.82		138.93
50/50	135.78	121.56	5.4	136.04
70/30	131.18	115.07		130.95
100/0	106.54	106.54		106.54
PMMA/CAPh 7.5 DEP				
0/100	141.20	141.20		141.20
30/70	137.50	128.62		138.12
50/50	134.60	121.41	4.4	134.77
70/30	130.68	114.97		129.17
100/0	106.49	106.49		106.49
PMMA/CAPh 10 DEP				
0/100	140.50	140.50		140.50
30/70	137.46	128.21		137.60
50/50	133.58	121.15	4.6	134.43
70/30	129.17	114.82		129.05
100/0	106.48	106.48		106.48

Chapter 5

STUDIES ON DIPROPYL PHTHALATE (DPP) PLASTICIZED BLENDS OF PMMA WITH CA, CAP, CAB AND CPh

Chapter 5 describes the study of dipropyl phthalate (DPP) plasticized blends of PMMA-CA derivatives. A brief note on DPP plasticizer has also been included in this chapter.

5.1 DIPROPYL PHTHALATE (DPP) PLASTICIZER

Dipropyl phthalate is a phthalate ester. It is a clear, colorless liquid at room temperature. It is stable under ordinary conditions of use and storage.

Properties:

Physical properties	
Molecular formula	C ₁₄ H ₁₈ O ₄
Molecular mass	250.29
Density	1.078 g/cm ³ at 25 °C
Boiling point	317.5 °C

Uses: Used as a plasticizer.

5.2 RESULTS AND DISCUSSION

5.2.1 Fourier Transform Infrared (FTIR) Spectroscopic Studies

FTIR spectra of 50/50 PMMA/CA blend plasticized with 2.5%, 5%, 7.5% and 10 % DPP are shown in Figure 5.1, Figure 5.2, Figure 5.3 and Figure 5.4 respectively. The FTIR stretching frequencies of PMMA/CA, PMMA/CAP, PMMA/CAB and PMMA/CAPh blends plasticized with DPP are also given in Tables 5.1. Carbonyl frequency of 0/100 PMMA/CA blend with 2.5 % DPP at 1730.3 cm⁻¹ decreased to 1722.3 cm⁻¹ in 50/50 PMMA/CA blend with 2.5 % DPP. Similarly, the carbonyl frequency of 0/100 PMMA/CA blend with 5 % DPP at 1732.1 cm⁻¹ decreased to 1723.1 cm⁻¹ in 50/50 PMMA/CA blend with 5 % DPP, the carbonyl frequency of 0/100 PMMA/CA blend with 7.5 % DPP at 1732.9 cm⁻¹ decreased to 1722.8 cm⁻¹ in 50/50 PMMA/CA blend with 7.5 % DPP and 0/100 PMMA/CA blend with 10 % DPP at 1732.2 cm⁻¹ decreased to 1725.6 cm⁻¹ in 50/50 PMMA/CA blend with 10 % DPP.

The carbonyl frequency of 0/100 PMMA/CAP blend with 2.5 % DPP at 1736.4 cm⁻¹ decreased to 1722.8 cm⁻¹ in 50/50 PMMA/CAP blend with 2.5 % DPP. Similarly,

the carbonyl frequency of 0/100 PMMA/CAP blend with 5 % DPP at 1736.5 cm^{-1} decreased to 1724.8 cm^{-1} in 50/50 PMMA/CAP blend with 5 % DPP, the carbonyl frequency of 0/100 PMMA/CAP blend with 7.5 % DPP at 1737.9 cm^{-1} decreased to 1723.7 cm^{-1} in 50/50 PMMA/CAP blend with 7.5 % DPP and the carbonyl frequency of 0/100 PMMA/CAP blend with 10 % DPP at 1736.5 cm^{-1} decreased to 1724.9 cm^{-1} in 50/50 PMMA/CAP blend with 10 % DPP.

The carbonyl frequency of 0/100 PMMA/CAB blend with 2.5 % DPP at 1737.3 cm^{-1} decreased to 1722.5 cm^{-1} in 50/50 PMMA/CAB blend with 2.5 % DPP. Similarly, the carbonyl frequency of 0/100 PMMA/CAB blend with 5 % DPP at 1736.9 cm^{-1} decreased to 1723.5 cm^{-1} in 50/50 PMMA/CAB blend with 5 % DPP, the carbonyl frequency at 0/100 PMMA/CAB blend with 7.5 % DPP at 1737.2 cm^{-1} decreased to 1722.7 cm^{-1} in 50/50 PMMA/CAB blend with 7.5 % DPP and the carbonyl frequency of 0/100 PMMA/CAB blend with 10 % DPP at 1737.1 cm^{-1} decreased to 1723.0 cm^{-1} in 50/50 PMMA/CAB blend with 10 % DPP.

The carbonyl frequency of 0/100 PMMA/CAPh blend with 2.5 % DPP at 1659.6 cm^{-1} shifted to 1718.8 cm^{-1} in 50/50 PMMA/CAPh blend with 2.5 % DPP. Similarly, the carbonyl frequency of 0/100 PMMA/CAPh blend with 5 % DPP at 1652.4 cm^{-1} shifted to 1718.3 cm^{-1} in 50/50 PMMA/CAPh blend with 5 % DPP, the carbonyl frequency of 0/100 PMMA/CAPh blend with 7.5 % DPP at 1658.5 cm^{-1} shifted to 1719.6 cm^{-1} in 50/50 PMMA/CAPh blend with 7.5 % DPP and the carbonyl frequency of 0/100 PMMA/CAPh blend with 10 % DPP at 1653.5 cm^{-1} shifted to 1720.0 cm^{-1} in 50/50 PMMA/CAPh blend with 10 % DPP.

Such shift in the specific vibration frequencies are ascribed to the formation of a weak hydrogen bond between component polymers in the blend. This can also be contributing to the miscibility of the blends.

The -OH stretching vibrations of hydroxyl groups occurred as broad band at 3440.3 cm^{-1} and 3444.9 cm^{-1} in 0/100 PMMA/CA blend with 2.5 % DPP and 50/50 PMMA/CA blend with 2.5 % DPP respectively. Similarly, the -OH stretching vibrations

of hydroxyl groups in the case of other blends with varying compositions are given in Tables 5.1.

The intensity of the broad band decreased after blending, indicating that part of the –OH groups are involved in the hydrogen bond formation. These results indicate that specific interactions such as the hydrogen bonding forces exist in the blends and this is leading to the miscibility of the blends.

5.2.2 Differential Scanning Calorimetry (DSC) Studies

The DSC thermograms of 2.5 %, 5 %, 7.5 % and 10 % DPP plasticized 50/50 PMMA/CA blends are shown in Figure 5.5 (a), Figure 5.5 (b), Figure 5.5 (c) and Figure 5.5 (d) respectively.

From Figure 5.5 (a) to Figure 5.5 (d), it can be seen that the T_g for 2.5 %, 5 %, 7.5 % and 10 % DEP plasticized 50/50 PMMA/CA blends are 114.56 °C, 114.25 °C, 114.00 °C and 113.22 °C respectively. It is interesting to note here that the thermograms for the blends (Figure 5.5 (a) to Figure 5.5 (d)) exhibited single T_g and its value lies intermediate to the T_g values of 2.5 %, 5 %, 7.5 % and 10 % DPP plasticized pure PMMA and pure CA derivatives respectively. Further, the T_g values of the blend films decreased regularly on increase of PMMA content in the blends. Such a systematic variation of T_g in the blends is indicative of miscibility of the components in the blends.

For estimating the glass transition temperature of blend films from the properties of pure components and also predicting the glass transition temperature of amorphous polymer blends, theoretical equations like Eq. (2.1) and Eq. (2.2) have been proposed.

The examination data is best fitted by this equation with $k = 0.12, 0.12, 0.12$ and 0.10 respectively for 2.5 %, 5 %, 7.5 % and 10 % DPP plasticized PMMA/CA blends. This result supports that, blends have high miscibility in the amorphous state. The thermal properties of 2.5 %, 5 %, 7.5 % and 10 % DPP plasticized PMMA/CA, PMMA/CAP, PMMA/CAB and PMMA/CAPh blends have shown single T_g and are presented in Table 5.2. Hence it can be concluded that all the blends studied are miscible in the entire composition range. The blends show a positive deviation from Fox equation implying an intermolecular interaction between the polymers.

5.2.3 Water Uptake

The water uptake capacity of the polymer blend films have been calculated using the equation 1.7. The plots of water uptake against DPP content in the PMMA/CA, PMMA/CAP, PMMA/CAB and PMMA/CAPh blends with 2.5 %, 5 %, 7.5 % and 10 % of DPP plasticizer are shown in Figure 5.6, Figure 5.7, Figure 5.8 and Figure 5.9, respectively.

As seen from the figures, the water uptake for 0/100 PMMA/CA, PMMA/CAP, PMMA/CAB and PMMA/CAPh blends with 2.5 % DPP are 0.86 wt %, 1.01 wt %, 1.20 wt % and 1.48 wt % respectively. The water uptake of the blends increased up to 50 wt % of CA derivatives concentration. The maximum water uptake was observed for the blends with 50/50 PMMA/CA, PMMA/CAP, PMMA/CAB and PMMA/CAPh blends with 2.5 % DPP are 5.65 wt %, 7.40 wt %, 7.49 wt % and 7.66 wt % respectively, which decrease on addition of further PMMA.

The water uptake for 0/100 PMMA/CA, PMMA/CAP, PMMA/CAB and PMMA/CAPh blends with 5 % DPP are 0.86 wt %, 1.00 wt %, 1.20 wt % and 1.47 wt % respectively. The water uptake of the blends increased up to 50 wt % of CA derivatives concentration. The maximum water uptake was observed for the blends with 50/50 PMMA/CA, PMMA/CAP, PMMA/CAB and PMMA/CAPh blends with 5 % DPP are 5.65 wt %, 7.21 wt %, 7.40 wt % and 7.59 wt % respectively, which decrease on addition of further PMMA.

The water uptake for 0/100 PMMA/CA, PMMA/CAP, PMMA/CAB and PMMA/CAPh blends with 7.5 % DPP are 0.86 wt %, 1.00 wt %, 1.20 wt % and 1.47 wt % respectively. The water uptake of the blends increased up to 50 wt % of CA derivatives concentration. The maximum water uptake was observed for the blends with 50/50 PMMA/CA, PMMA/CAP, PMMA/CAB and PMMA/CAPh blends with 7.5 % DPP are 5.60 wt %, 7.17 wt %, 7.29 wt % and 7.43 wt % respectively, which decrease on addition of further PMMA.

The water uptake for 0/100 PMMA/CA, PMMA/CAP, PMMA/CAB and PMMA/CAPh blends with 10 % DPP are 0.85 wt %, 1.00 wt %, 1.19 wt % and 1.47 wt

% respectively. The water uptake of the blends increased up to 50 wt % of CA derivatives concentration. The maximum water uptake was observed for the blends with 50/50 PMMA/CA, PMMA/CAP, PMMA/CAB and PMMA/CAPh blends with 10 % DPP are 5.40 wt %, 6.77 wt %, 7.10 wt % and 7.37 wt % respectively, which decrease on addition of further PMMA.

The prepared polymer blends have shown a maximum water uptake in the 50 wt. % of PMMA indicating the presence of void volume in the blends and further decrease in the water uptake due to the compact structured pattern with reduction in void volumes has been discussed in chapter 3, section 3.2.3 of the thesis.

5.2.4 Ion Exchange Capacity (IEC) Measurements

Ion exchange capacity (IEC) provides an indirect approximation for the ion exchangeable groups present in the pure and blend polymers which are responsible for proton conduction. The IEC values for 2.5 %, 5 %, 7.5 % and 10 % DPP plasticized pure and PMMA/CA derivatives blends are shown graphically in Figure 5.10 Figure 5.11, Figure 5.12 and Figure 5.13.

From the figure it can be seen that the IEC values decreases for the blends with an increase in PMMA content. It is known that CA derivatives has exchangeable –OH groups. Hence it is evident that when PMMA content of the blend is increased, the number of replaceable sites available in the blend would decrease and hence the decrease in the IEC of the blends.

5.2.5 Electrochemical Impedance Spectroscopy

Electrochemical Impedance spectroscopy is recently being widely applied in determining various material properties, prime among which are permittivity and conductivity. Figure 5.14, Figure 5.15, Figure 5.16 and Figure 5.17 shows AC impedance spectra (Cole-Cole or Nyquist plots) of 2.5 %, 5 %, 7.5 % and 10 % DPP plasticized 50/50 PMMA/CA blends at different temperatures, respectively.

The impedance responses due to the bulk resistance of the electrolyte and electrolyte-electrode double layer capacitance behavior of the samples over the whole range of frequency evaluated has been discussed in the chapter 3, section 3.2.5 of the

thesis. AC impedance spectra of 2.5 %, 5 %, 7.5 % and 10 % DPP plasticized 50/50 PMMA/CAP, PMMA/CAB and PMMA/CAPh blends at different temperatures, respectively have shown the similar trend for electrochemical impedance spectra.

5.2.5.1 Proton conductivity measurement

The variation of conductivity of the blends with temperature and room temperature conductivity of the blends are shown in Figure 5.18, Figure 5.19, Figure 5.20 and Figure 5.21 respectively. It has been observed that at 30 °C, among the polyblends studied the blends with 2.5 % DPP plasticized PMMA/CA, PMMA/CAP, PMMA/CAB and PMMA/CAPh 30/70 composition showed the highest proton conductivity value of $1.67 \times 10^{-3} \text{ S cm}^{-1}$, $2.18 \times 10^{-3} \text{ S cm}^{-1}$, $2.19 \times 10^{-3} \text{ S cm}^{-1}$ and $2.26 \times 10^{-3} \text{ S cm}^{-1}$, respectively. The proton conductivity increased as the temperature is increased in the measured temperature range between 30 °C to 70 °C. Also, it has been found from impedance plots that as the temperature is increased, the bulk resistance R decreased resulting in an increase in the value of proton conductivity. This may be mainly due to the fact that at higher temperature, there is an enhancement in the ion movement, favoring conductivity. Proton conductivity measurement of 5 %, 7.5 % and 10 % DPP plasticized 50/50 PMMA/CAP, PMMA/CAB and PMMA/CAPh blends at different temperatures respectively have shown the similar trend.

5.2.5.2 Temperature dependence of ionic conductivity

It has been found that the proton conductivity of the blend film increased with increasing temperature for all compositions. This may be mainly due to the fact that an increase in temperature increases the mobility of ions and this in turn increases the conductivity. Further, the vibrational motion of the polymer backbone and side chains, which becomes more vigorous with increase in temperature can also facilitate the conduction of ions. The increased amplitude of vibration brings the coordination sites closer to one another enabling the ions to hop from the occupied site to the unoccupied site with lesser energy required. Increase in amplitude of vibration of the polymer backbone and side chains can also increase the fraction of free volume in the polymer electrolyte system (Aziz et al. 2010). Druger et al. (1983) and Druger et al. (1985) have

attributed the change in conductivity with temperature in solid polymer electrolyte to hopping model, which results in an increase in the free volume of the system. The hopping model either permits the ions to hop from one site to another or provides a pathway for ions to move. In other words, this facilitates translational motion of the ions. From this, it is clear that the ionic motion is due to translational motion/hopping facilitated by the polymer. The nonexistence of any unusual variation of conductivity indicates the existence of overall amorphous region (Aziz et al. 2010). This implies that coupling of the ion movement with the amorphous nature of the polymer is facilitating the conductivity in the blends.

Electrical conduction is a thermally activated process and follows the Arrhenius law

$$\sigma = \sigma_0 \exp\left[-\frac{E_a}{kT}\right] \quad (2.3)$$

where, σ is the conductivity at a particular temperature, σ_0 is the pre-exponential factor, k is the Boltzmann's constant, and T is the absolute temperature. As there is no sudden change in the value of conductivity with temperature it may be inferred that these blends do not undergo any phase transitions within the temperature range studied. The conductivity has been discussed on the basis of the increase in the CA contents along with the ion exchange capacity and water absorption facilitating the ion hopping through the polymer structure has been detailed in chapter 3, section 3.2.5.2 of the thesis.

5.2.6 Dielectric Studies

The dielectric constant and loss of the films have been calculated using the equations 1.11 and 1.12 respectively. The conductivity behavior of polymer electrolyte can be understood from dielectric studies (Ramesh et al. 2002). The dielectric constant is a measure of stored charge. The variations of dielectric constant and dielectric loss with frequency at different temperatures have been shown in Figure 5.22, Figure 5.23, Figure 5.24 and Figure 5.25 respectively, for 2.5 %, 5 %, 7.5 % and 10 % DPP plasticized 50/50 PMMA/CA blends. Similar trends have also been seen for 2.5 %, 5 %, 7.5 % and 10 % DPP plasticized 50/50 PMMA/CAP, PMMA/CAB and PMMA/CAPh blends at different temperatures.

There are no appreciable relaxation peaks observed, indicating the electrode polarization and space charge effects have occurred confirming non-debye dependence; the increase in dielectric constant and dielectric loss at higher temperatures due to the higher charge carrier density and conductivity of the polymer blends due to hopping mechanism has been discussed in the chapter 3, section 3.2.6 in the thesis.

5.3 FIGURES

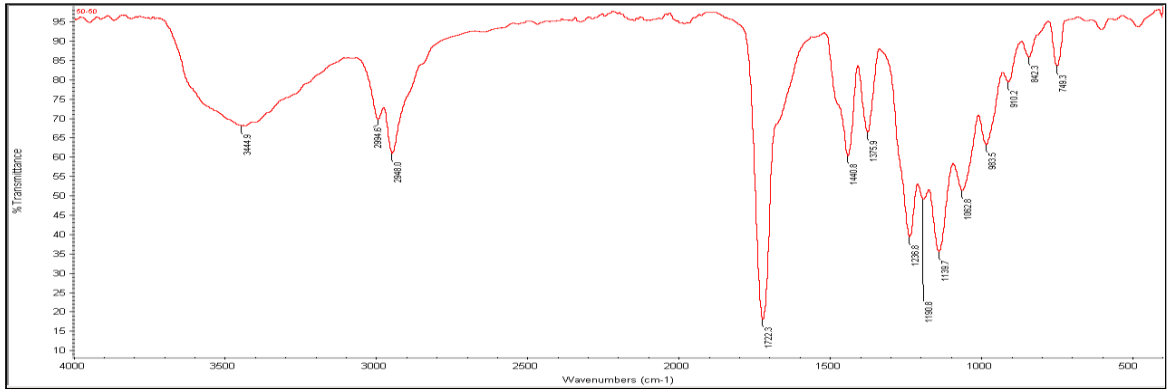


Figure 5.1 FTIR Spectrum of 2.5 % DPP plasticized 50/50 PMMA/CA blend.

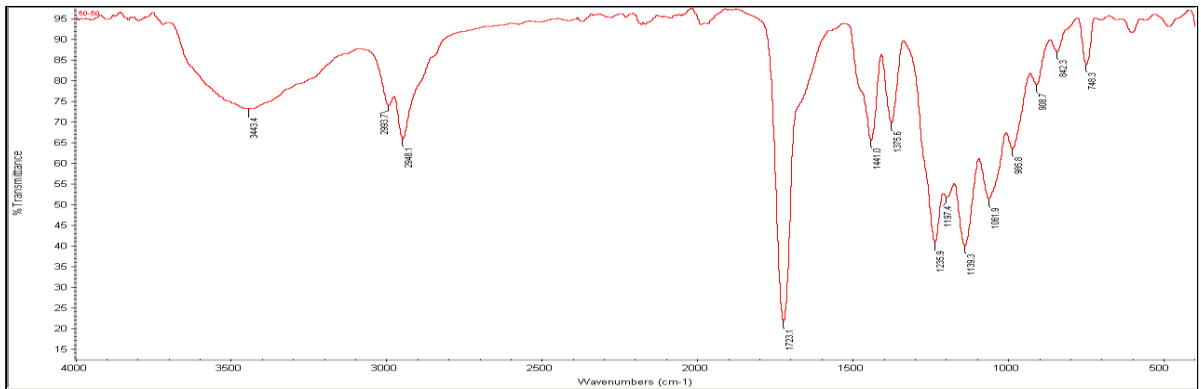


Figure 5.2 FTIR Spectrum of 5 % DPP plasticized 50/50 PMMA/CA blend.

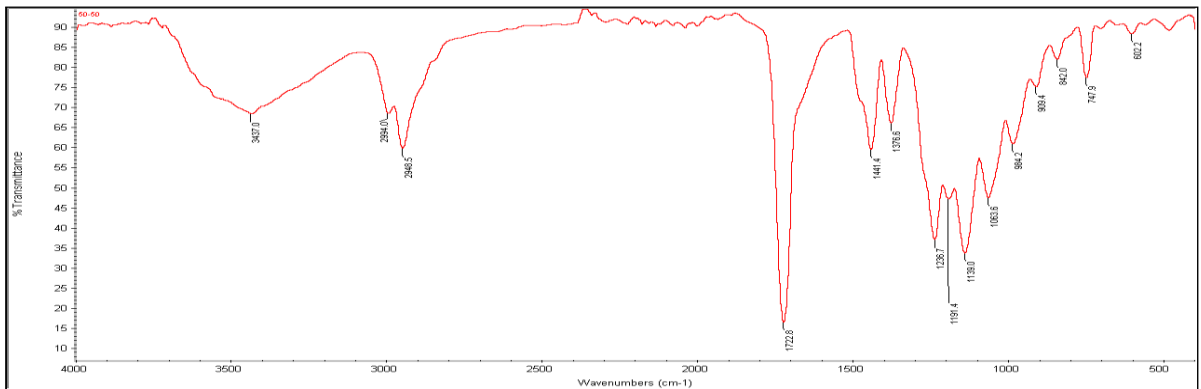


Figure 5.3 FTIR Spectrum of 7.5 % DPP plasticized 50/50 PMMA/CA blend.

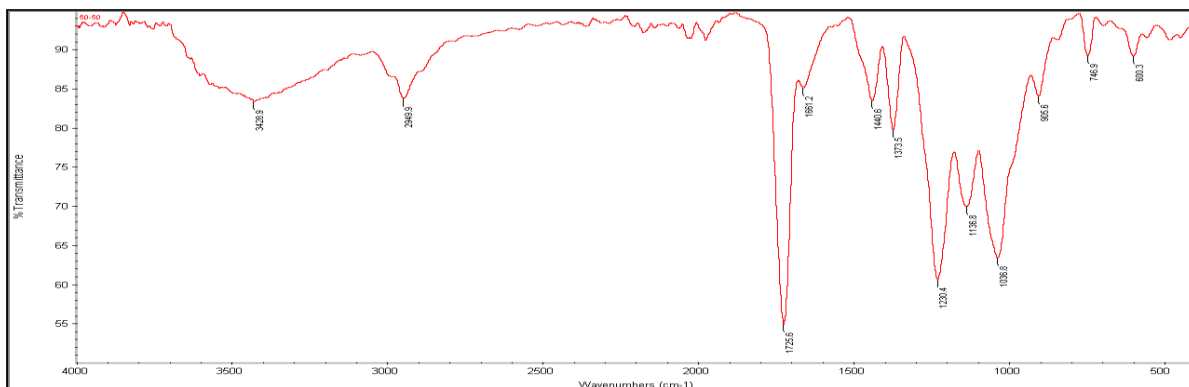


Figure 5.4 FTIR Spectrum of 10 % DPP plasticized 50/50 PMMA/CA blend.

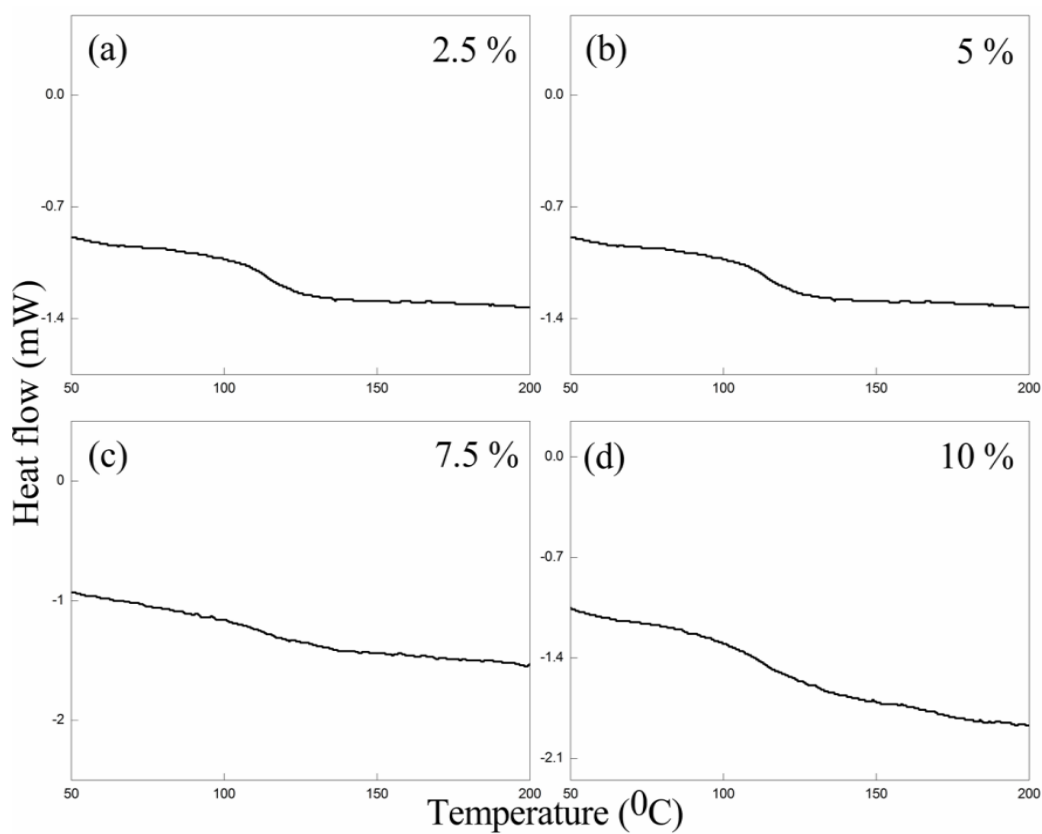


Figure 5.5 (a), (b), (c) and (d) DSC scans of 2.5 %, 5 %, 7.5 % and 10 % DPP plasticized 50/50 PMMA/CA blends.

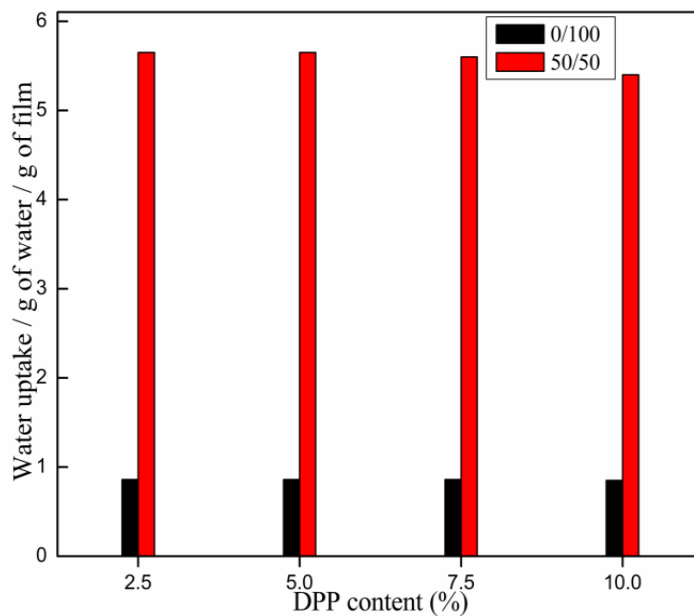


Figure 5.6 Water absorption by 2.5 %, 5 %, 7.5 % and 10 % DPP plasticized 0/100 and 50/50 PMMA/CA blends.

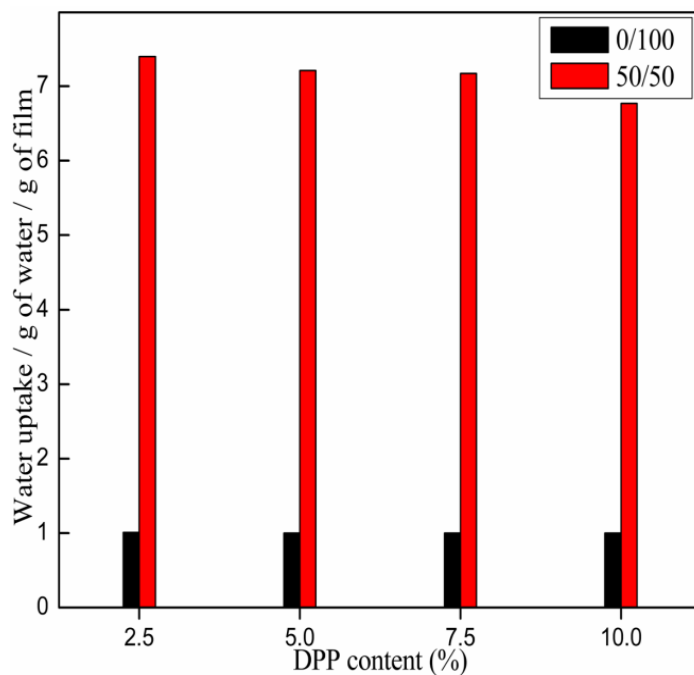


Figure 5.7 Water absorption by 2.5 %, 5 %, 7.5 % and 10 % DPP plasticized 0/100 and 50/50 PMMA/CAP blends.

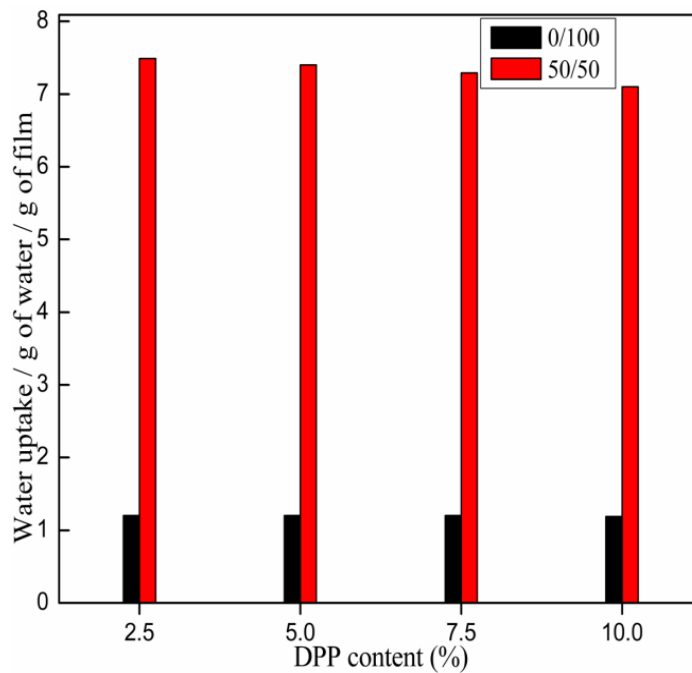


Figure 5.8 Water absorption by 2.5 %, 5 %, 7.5 % and 10 % DPP plasticized 0/100 and 50/50 PMMA/CAB blends.

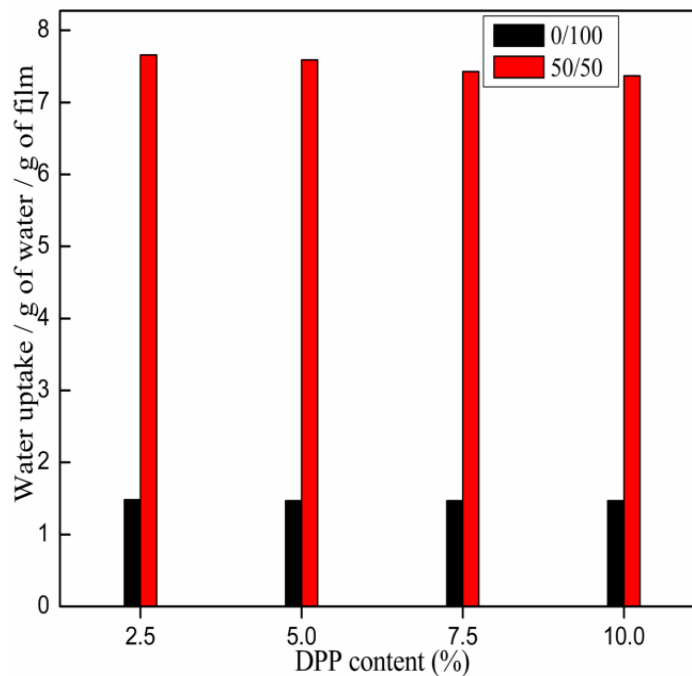


Figure 5.9 Water absorption by 2.5 %, 5 %, 7.5 % and 10 % DPP plasticized 0/100 and 50/50 PMMA/CAPh blends.

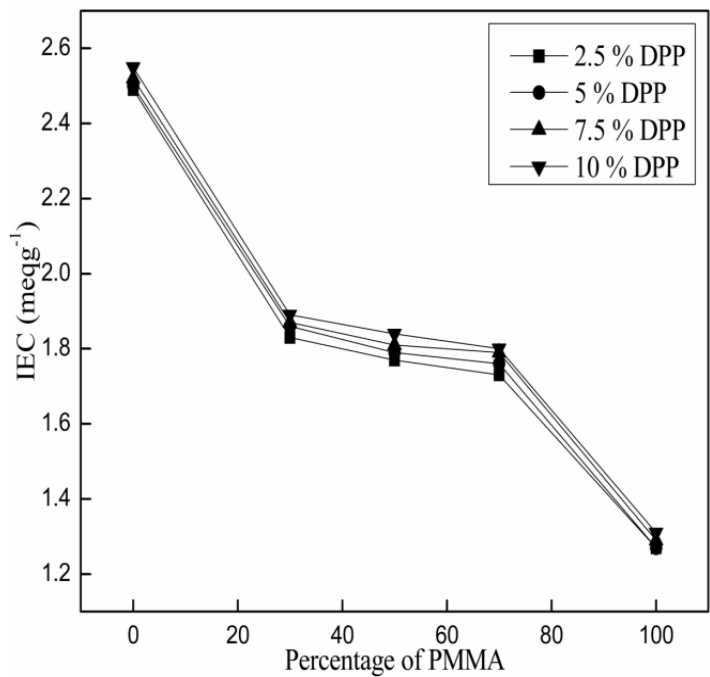


Figure 5.10 The change of IEC values in 2.5 %, 5 %, 7.5 % and 10 % DPP plasticized PMMA/CA blends.

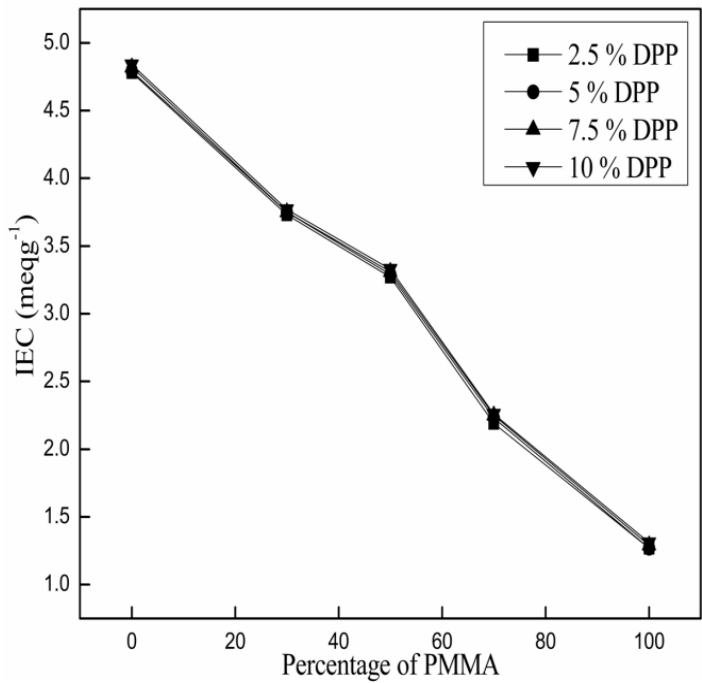


Figure 5.11 The change of IEC values in 2.5 %, 5 %, 7.5 % and 10 % DPP plasticized PMMA/CAP blends.

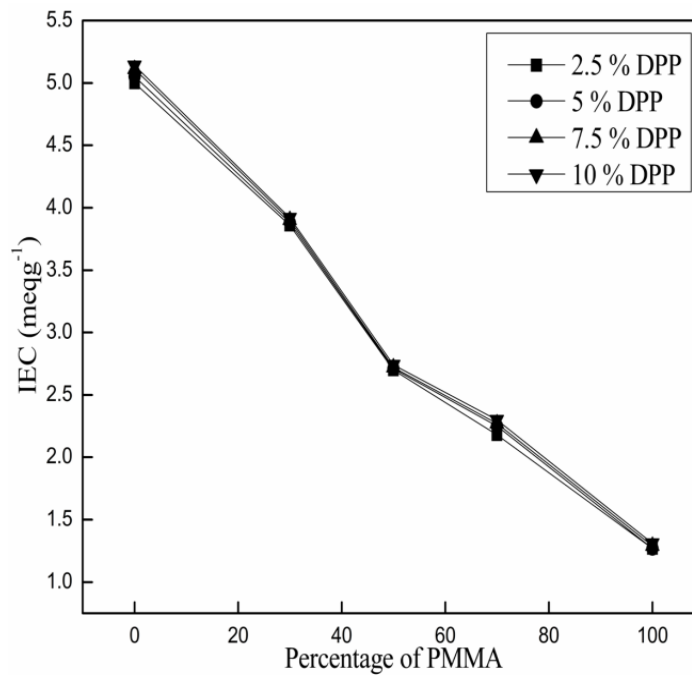


Figure 5.12 The change of IEC values in 2.5 %, 5 %, 7.5 % and 10 % DPP plasticized PMMA/CAB blends.

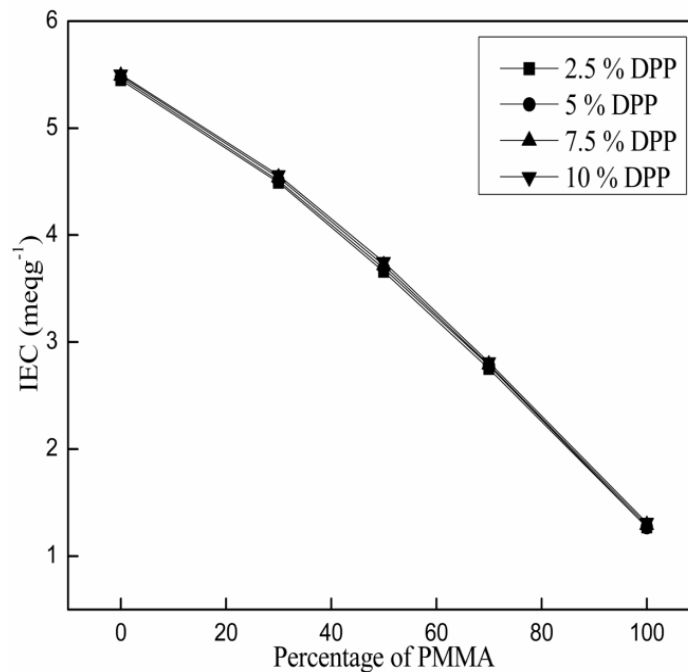


Figure 5.13 The change of IEC values in 2.5 %, 5 %, 7.5 % and 10 % DPP plasticized PMMA/CAPh blends.

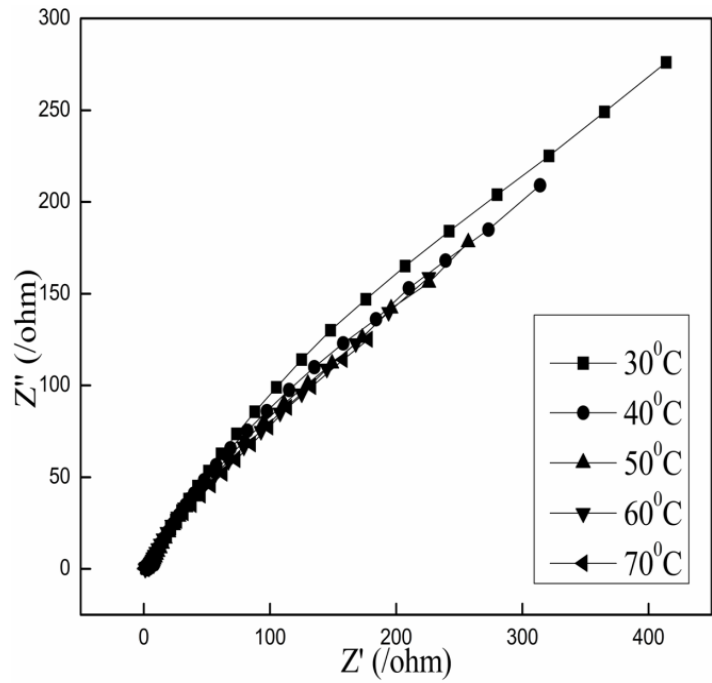


Figure 5.14 AC impedance spectrum of 2.5 % DPP plasticized 50/50 PMMA/CA blend at different temperatures.

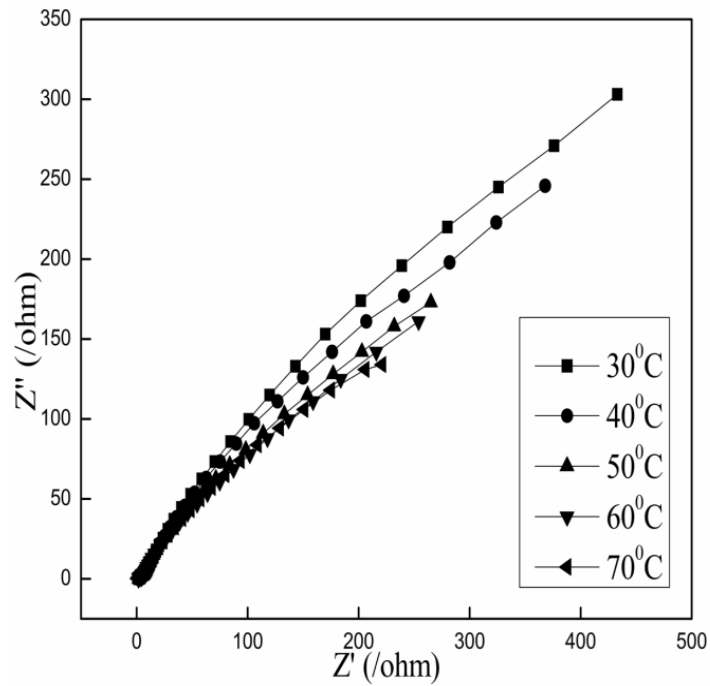


Figure 5.15 AC impedance spectrum of 5 % DPP plasticized 50/50 PMMA/CA blend at different temperatures.

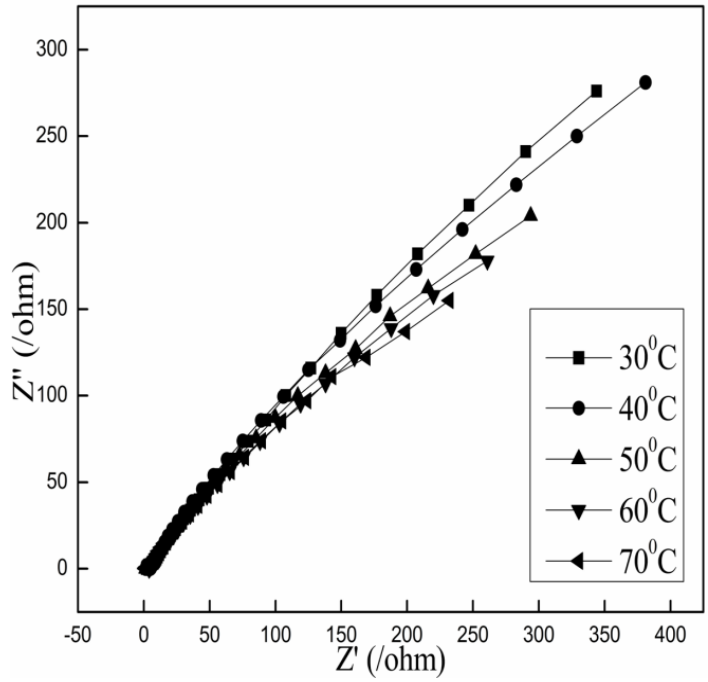


Figure 5.16 AC impedance spectrum of 7.5 % DPP plasticized 50/50 PMMA/CA blend at different temperatures.

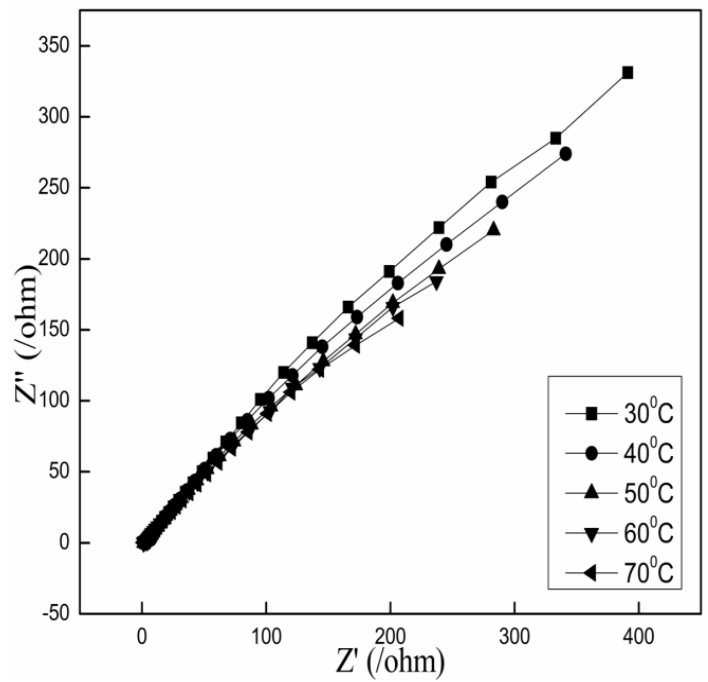


Figure 5.17 AC impedance spectrum of 10 % DPP plasticized 50/50 PMMA/CA blend at different temperatures.

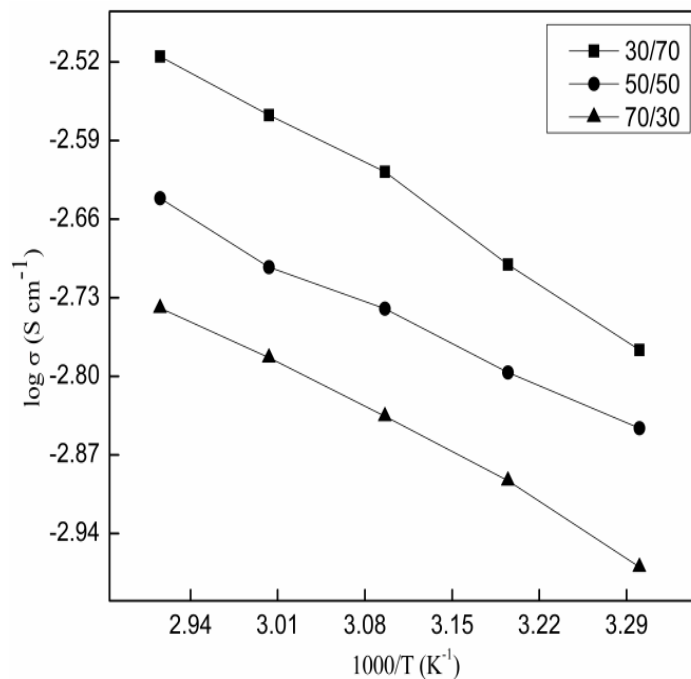


Figure 5.18 Arrhenius plots for conductivity σ of 2.5 % DPP plasticized PMMA/CA blends.

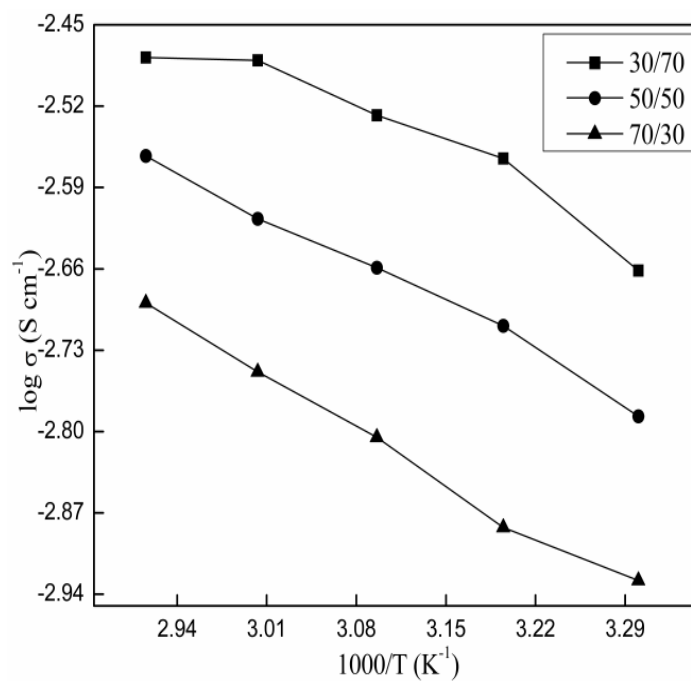


Figure 5.19 Arrhenius plots for conductivity σ of 2.5 % DPP plasticized PMMA/CAP blends.

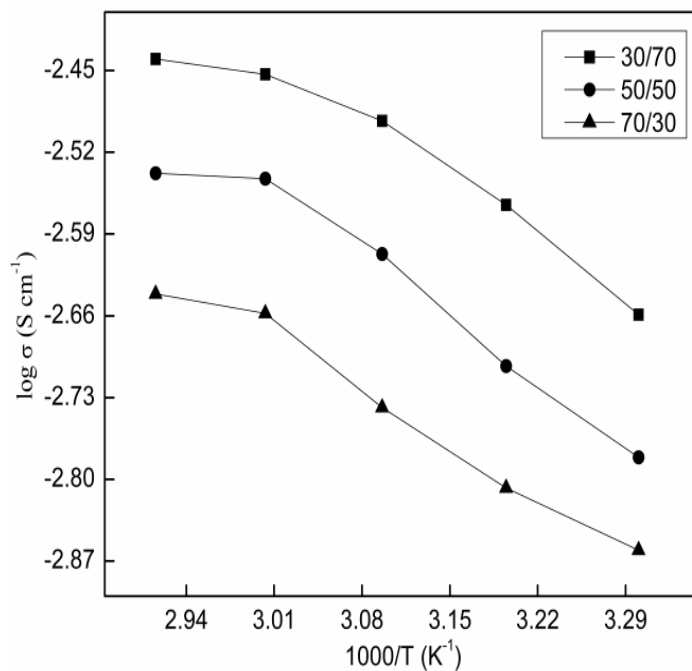


Figure 5.20 Arrhenius plots for conductivity σ of 2.5 % DPP plasticized PMMA/CAB blends.

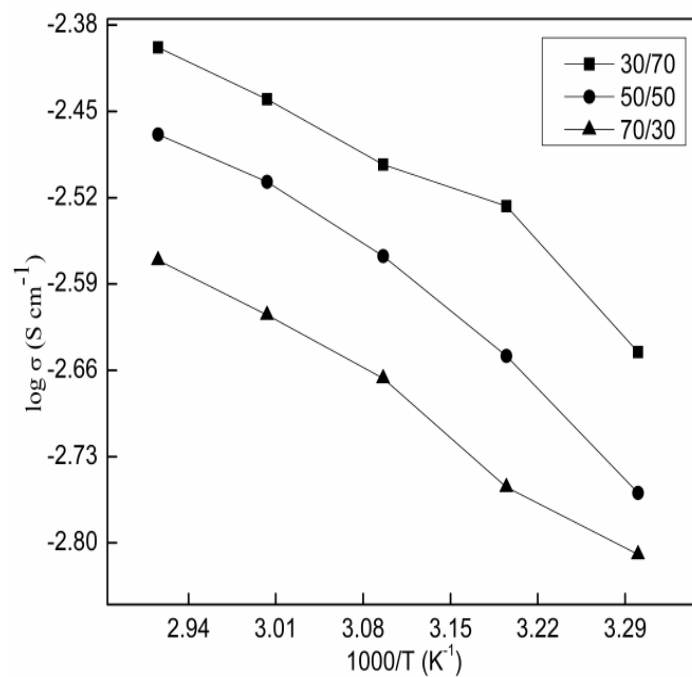


Figure 5.21 Arrhenius plots for conductivity σ of 2.5 % DPP plasticized PMMA/CAPh blends.

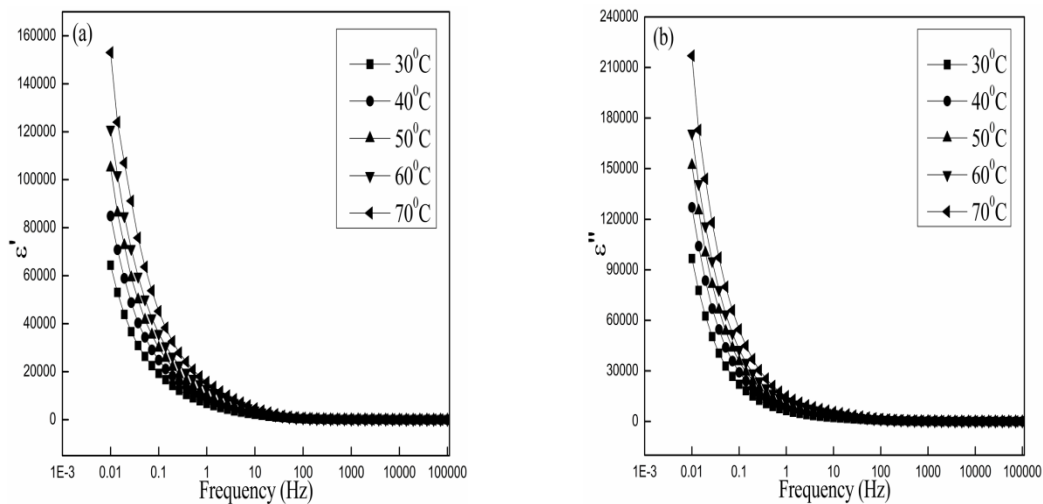


Figure 5.22 Variations of dielectric constant (a) and dielectric loss (b) with frequency at different temperatures for 2.5 % DPP plasticized 50/50 PMMA/CA blend.

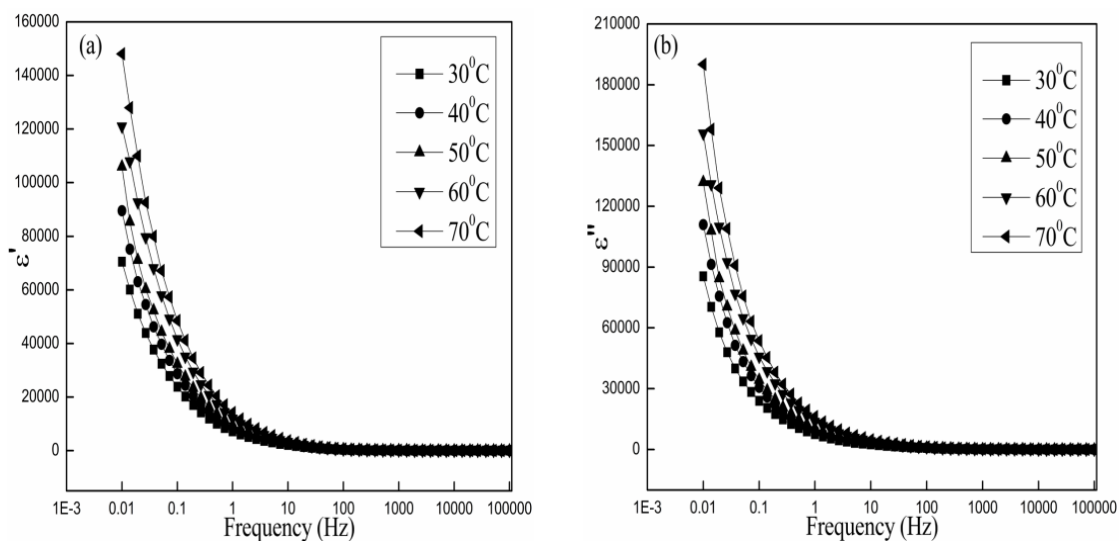


Figure 5.23 Variations of dielectric constant (a) and dielectric loss (b) with frequency at different temperatures for 5 % DPP plasticized 50/50 PMMA/CA blend.

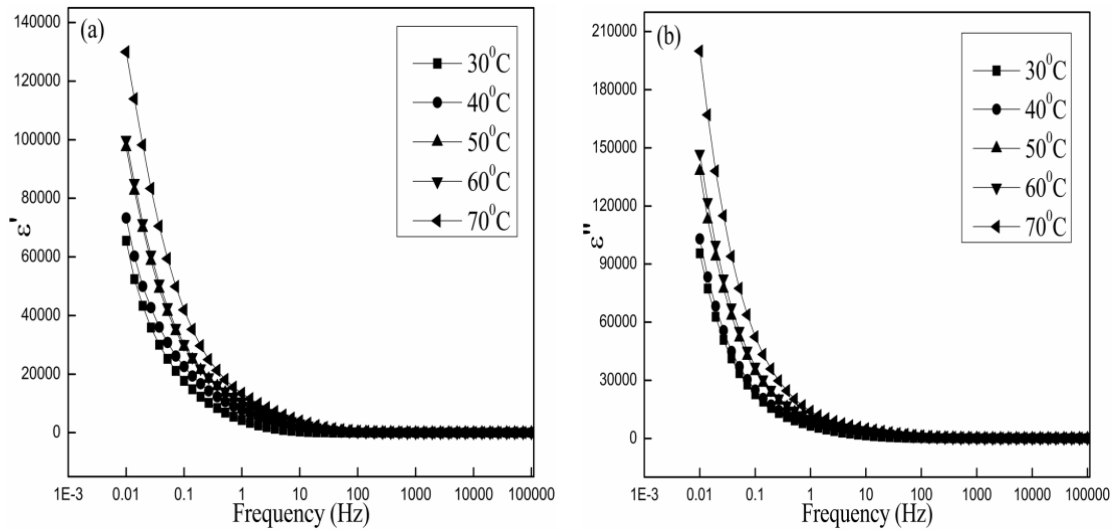


Figure 5.24 Variations of dielectric constant (a) and dielectric loss (b) with frequency at different temperatures for 7.5 % DPP plasticized 50/50 PMMA/CA blend.

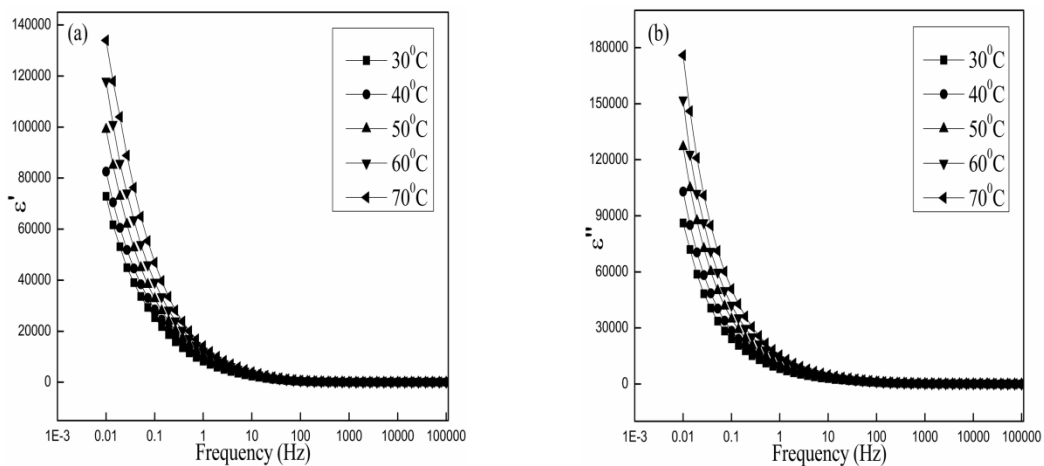


Figure 5.25 Variations of dielectric constant (a) and dielectric loss (b) with frequency at different temperatures for 10 % DPP plasticized 50/50 PMMA/CA blend.

5.4 TABLES

Table 5.1 IR stretching frequencies of DPP plasticized PMMA/CA, PMMA/CAP, PMMA/CAB and PMMA/CAPh blends.

PMMA/CA 2.5 DPP	-CO Stretching Frequencies	-OH Stretching Frequencies
0/100	1730.3	3440.3
50/50	1722.3	3444.9
PMMA/CA 5 DPP		
0/100	1732.1	3440.9
50/50	1723.1	3443.4
PMMA/CA 7.5 DPP		
0/100	1732.9	3467.3
50/50	1722.8	3437.0
PMMA/CA 10 DPP		
0/100	1732.2	3456.9
50/50	1725.6	3428.9
PMMA/CAP 2.5 DPP		
0/100	1736.4	3484.6
50/50	1722.8	3557.0
PMMA/CAP 5 DPP		
0/100	1736.5	3484.3
50/50	1724.8	3546.4
PMMA/CAP 7.5 DPP		
0/100	1737.9	3481.2
50/50	1723.7	3550.5
PMMA/CAP 10 DPP		
0/100	1736.5	3475.2
50/50	1724.9	3495.6
PMMA/CAB 2.5 DPP		
0/100	1737.3	3484.2
50/50	1722.5	3442.2
PMMA/CAB 5 DPP		
0/100	1736.9	3477.5

50/50	1723.5	3438.4
PMMA/CAB 7.5 DPP		
0/100	1737.2	3485.3
50/50	1722.7	3435.0
PMMA/CAB 10 DPP		
0/100	1737.1	3496.8
50/50	1723.0	3449.1
PMMA/CAPh 2.5 DPP		
0/100	1659.6	3405.6
50/50	1718.8	3400.5
PMMA/CAPh 5 DPP		
0/100	1652.4	3393.7
50/50	1718.3	3424.9
PMMA/CAPh 7.5 DPP		
0/100	1658.5	3424.6
50/50	1719.6	3428.5
PMMA/CAPh 10 DPP		
0/100	1653.5	3390.4
50/50	1720.0	3391.9

Table 5.2 Thermal properties of 2.5 %, 5 %, 7.5 % and 10 % DPP plasticized PMMA/CA, PMMA/CAP, PMMA/CAB and PMMA/CAPh blends.

Sample	T_g (°C)	Fox equation	k values	Gordon-Taylor equation
PMMA/CA 2.5 DPP				
0/100	182.27	182.27		182.27
30/70	124.00	150.56		123.54
50/50	114.56	134.91	0.12	115.15
70/30	111.52	122.21		110.77
100/0	107.09	107.09		107.09
PMMA/CA 5 DPP				
0/100	181.86	181.86		181.86
30/70	123.99	150.34		123.41
50/50	114.25	134.76	0.12	115.06
70/30	111.28	122.11		110.70
100/0	107.04	107.04		107.04
PMMA/CA 7.5 DPP				
0/100	180.49	180.49		180.49
30/70	123.82	149.53		122.91
50/50	114.00	134.19	0.12	114.69
70/30	110.44	121.70		110.39
100/0	106.79	106.79		106.79
PMMA/CA 10 DPP				
0/100	179.46	179.46		179.46
30/70	123.73	148.94		120.41
50/50	113.22	133.77	0.1	113.25
70/30	109.07	121.41		109.62
100/0	106.63	106.63		106.63
PMMA/CAP 2.5 DPP				
0/100	139.84	139.84		139.84
30/70	137.73	128.09		125.04
50/50	118.23	121.29	0.52	118.29
70/30	112.00	115.18		113.06
100/0	107.09	107.09		107.09
PMMA/CAP 5 DPP				
0/100	139.46	139.46		139.46
30/70	137.00	127.84		124.50
50/50	117.78	121.12	0.5	117.85
70/30	111.80	115.06		112.76

100/0	107.04	107.04		107.04
PMMA/CAP 7.5 DPP				
0/100	139.04	139.04		139.04
30/70	136.75	127.49		123.49
50/50	116.89	120.80	0.46	116.95
70/30	111.14	114.78		112.10
100/0	106.79	106.79		106.79
PMMA/CAP 10 DPP				
0/100	138.89	138.89		138.89
30/70	136.21	127.33		122.97
50/50	116.42	120.64	0.44	116.49
70/30	110.35	114.62		111.75
100/0	106.63	106.63		106.63
PMMA/CAB 2.5 DPP				
0/100	132.37	132.37		132.37
30/70	120.48	123.62		119.60
50/50	114.57	118.40	0.42	114.57
70/30	109.08	113.60		110.95
100/0	107.09	107.09		107.09
PMMA/CAB 5 DPP				
0/100	132.31	132.31		132.31
30/70	120.00	123.56		119.40
50/50	114.40	118.34	0.41	114.39
70/30	108.66	113.55		110.82
100/0	107.04	107.04		107.04
PMMA/CAB 7.5 DPP				
0/100	131.83	131.83		131.83
30/70	119.31	123.17		119.18
50/50	114.20	118.00	0.42	114.20
70/30	107.83	113.24		110.61
100/0	106.79	106.79		106.79
PMMA/CAB 10 DPP				
0/100	131.66	131.66		131.66
30/70	118.81	123.00		118.87
50/50	113.79	117.83	0.41	113.91
70/30	107.76	113.08		110.37
100/0	106.63	106.63		106.63

PMMA/CAPh 2.5 DPP				
0/100	143.45	143.45		143.45
30/70	139.05	130.19		140.29
50/50	136.72	122.63	4.5	136.84
70/30	132.12	115.90		131.03
100/0	107.09	107.09		107.09
PMMA/CAPh 5 DPP				
0/100	143.39	143.39		143.39
30/70	138.84	130.13		140.02
50/50	136.37	122.58	4.2	136.40
70/30	131.69	115.85		130.41
100/0	107.04	107.04		107.04
PMMA/CAPh 7.5 DPP				
0/100	143.25	143.25		143.25
30/70	138.13	129.94		139.27
50/50	134.98	122.36	3.5	135.15
70/30	131.27	115.62		128.67
100/0	106.79	106.79		106.79
PMMA/CAPh 10 DPP				
0/100	142.53	142.53		142.53
30/70	137.73	129.45		138.51
50/50	134.24	121.99	3.4	134.37
70/30	129.85	115.35		127.92
100/0	106.63	106.63		106.63

Chapter 6

STUDIES ON DIBUTYL PHTHALATE (DBP) PLASTICIZED BLENDS OF PMMA WITH CA, CAP, CAB AND CPh

Chapter 6 describes the study of dibutyl phthalate (DBP) plasticized blends of PMMA-CA derivatives. A brief note on DBP plasticizer has also been included in this chapter.

6.1 DIBUTYL PHTHALATE (DBP) PLASTICIZER

Dibutyl phthalate is a phthalate ester and commonly used as plasticizer. It is also used as an additive to adhesives or printing inks. It is soluble in various organic solvents, e.g. in alcohol, ether and benzene. DBP is also used as an ectoparasiticide. Dibutyl phthalate is used to help make plastics soft and flexible.

Properties:

Physical properties	
Molecular formula	C ₁₆ H ₂₂ O ₄
Molecular mass	278.34
Density	1.05 g/cm ³ at 20 °C
Boiling point	340 °C
Dielectric constant	5.99

Uses:

It is used in shower curtains, raincoats, plastic food wraps, bowls, car interiors, vinyl fabrics, floor tiles, Dibutyl phthalate is a phthalate ester with extensive use in industry in such products as plastic (PVC) piping, various varnishes and lacquers, safety glass, nail polishes, paper coatings, dental materials, pharmaceuticals and other products.

6.2 RESULTS AND DISCUSSION

6.2.1 Fourier Transform Infrared (FTIR) Spectroscopic Studies

FTIR spectra of 50/50 PMMA/CA blend plasticized with 2.5%, 5%, 7.5% and 10 % DBP are shown in Figure 6.1, Figure 6.2, Figure 6.3 and Figure 6.4 respectively. The FTIR stretching frequencies of PMMA/CA, PMMA/CAP, PMMA/CAB and PMMA/CAPh blends plasticized with DBP are also given in Tables 6.1. Carbonyl frequency of 0/100 PMMA/CA blend with 2.5 % DBP at 1734.8 cm⁻¹ decreased to 1723.2 cm⁻¹ in 50/50 PMMA/CA blend with 2.5 % DBP. Similarly, the carbonyl

frequency of 0/100 PMMA/CA blend with 5 % DBP at 1734.4 cm^{-1} decreased to 1724.2 cm^{-1} in 50/50 PMMA/CA blend with 5 % DBP, the carbonyl frequency of 0/100 PMMA/CA blend with 7.5 % DBP at 1734.4 cm^{-1} decreased to 1723.1 cm^{-1} in 50/50 PMMA/CA blend with 7.5 % DBP and 0/100 PMMA/CA blend with 10 % DBP at 1733.5 cm^{-1} decreased to 1725.1 cm^{-1} in 50/50 PMMA/CA blend with 10 % DBP.

The carbonyl frequency of 0/100 PMMA/CAP blend with 2.5 % DBP at 1735.9 cm^{-1} decreased to 1722.9 cm^{-1} in 50/50 PMMA/CAP blend with 2.5 % DBP. Similarly, the carbonyl frequency of 0/100 PMMA/CAP blend with 5 % DBP at 1735.9 cm^{-1} decreased to 1723.4 cm^{-1} in 50/50 PMMA/CAP blend with 5 % DBP, the carbonyl frequency of 0/100 PMMA/CAP blend with 7.5 % DBP at 1735.9 cm^{-1} decreased to 1722.8 cm^{-1} in 50/50 PMMA/CAP blend with 7.5 % DBP and the carbonyl frequency of 0/100 PMMA/CAP blend with 10 % DBP at 1735.5 cm^{-1} decreased to 1723.5 cm^{-1} in 50/50 PMMA/CAP blend with 10 % DBP.

The carbonyl frequency of 0/100 PMMA/CAB blend with 2.5 % DBP at 1737.7 cm^{-1} decreased to 1724.4 cm^{-1} in 50/50 PMMA/CAB blend with 2.5 % DBP. Similarly, the carbonyl frequency of 0/100 PMMA/CAB blend with 5 % DBP at 1737.1 cm^{-1} decreased to 1723.8 cm^{-1} in 50/50 PMMA/CAB blend with 5 % DBP, the carbonyl frequency at 0/100 PMMA/CAB blend with 7.5 % DBP at 1737.3 cm^{-1} decreased to 1729.0 cm^{-1} in 50/50 PMMA/CAB blend with 7.5 % DBP and the carbonyl frequency of 0/100 PMMA/CAB blend with 10 % DBP at 1736.8 cm^{-1} decreased to 1722.7 cm^{-1} in 50/50 PMMA/CAB blend with 10 % DBP.

The carbonyl frequency of 0/100 PMMA/CAPh blend with 2.5 % DBP at 1657.2 cm^{-1} shifted to 1717.9 cm^{-1} in 50/50 PMMA/CAPh blend with 2.5 % DBP. Similarly, the carbonyl frequency of 0/100 PMMA/CAPh blend with 5 % DBP at 1662.3 cm^{-1} shifted to 1719.8 cm^{-1} in 50/50 PMMA/CAPh blend with 5 % DBP, the carbonyl frequency of 0/100 PMMA/CAPh blend with 7.5 % DBP at 1661.3 cm^{-1} shifted to 1717.1 cm^{-1} in 50/50 PMMA/CAPh blend with 7.5 % DBP and the carbonyl frequency of 0/100 PMMA/CAPh blend with 10 % DBP at 1658.8 cm^{-1} shifted to 1719.6 cm^{-1} in 50/50 PMMA/CAPh blend with 10 % DBP.

Such shift in the specific vibration frequencies are ascribed to the formation of a weak hydrogen bond between component polymers in the blend. This can also be contributing to the miscibility of the blends.

The -OH stretching vibrations of hydroxyl groups occurred as broad band at 3476.5 cm^{-1} and 3437.6 cm^{-1} in 0/100 PMMA/CA blend with 2.5 % DBP and 50/50 PMMA/CA blend with 2.5 % DBP respectively. Similarly, the -OH stretching vibrations of hydroxyl groups in the case of other blends with varying compositions are given in Tables 6.1.

The intensity of the broad band decreased after blending, indicating that part of the -OH groups are involved in the hydrogen bond formation. These results indicate that specific interactions such as the hydrogen bonding forces exist in the blends and this is leading to the miscibility of the blends.

6.2.2 Differential Scanning Calorimetry (DSC) Studies

The DSC thermograms of 2.5 %, 5 %, 7.5 % and 10 % DBP plasticized 50/50 PMMA/CA blends are shown in Figure 6.5 (a), Figure 6.5 (b), Figure 6.5 (c) and Figure 6.5 (d) respectively.

From Figure 6.5 (a) to Figure 6.5 (d), it can be seen that the T_g for 2.5 %, 5 %, 7.5 % and 10 % DBP plasticized 50/50 PMMA/CA blends are $114.64\text{ }^\circ\text{C}$, $114.35\text{ }^\circ\text{C}$, $114.17\text{ }^\circ\text{C}$ and $113.31\text{ }^\circ\text{C}$ respectively. It is interesting to note here that the thermograms for the blends (Figure 6.5 (a) to Figure 6.5 (d)) exhibited single T_g and its value lies intermediate to the T_g values of 2.5 %, 5 %, 7.5 % and 10 % DBP plasticized pure PMMA and pure CA derivatives respectively. Further, the T_g values of the blend films decreased regularly on increase of PMMA content in the blends. Such a systematic variation of T_g in the blends is indicative of miscibility of the components in the blends.

Theoretical equations like Gordon-Taylor equation (Eq. (2.1)) and Fox equation (Eq. (2.2)) has been proposed for estimating the glass transition temperature of blend films from the properties of pure components. They are frequently used expressions for predicting the glass transition temperature of amorphous polymer blends.

The examination data is best fitted by this equation with $k = 0.11, 0.11, 0.11$ and 0.09 respectively for 2.5 %, 5 %, 7.5 % and 10 % DBP plasticized PMMA/CA blends. This result supports that, blends have high miscibility in the amorphous state. The thermal properties of 2.5 %, 5 %, 7.5 % and 10 % DBP plasticized PMMA/CA, PMMA/CAP, PMMA/CAB and PMMA/CAPh blends have shown single T_g and are presented in Table 6.2. Hence it can be concluded that all the blends studied are miscible in the entire composition range. The blends show a positive deviation from Fox equation implying an intermolecular interaction between the polymers.

6.2.3 Water Uptake

The water uptake capacity of the polymer blend films have been calculated using the equation 1.7. The plots of water uptake against DBP content in the PMMA/CA, PMMA/CAP, PMMA/CAB and PMMA/CAPh blends with 2.5 %, 5 %, 7.5 % and 10 % of DBP plasticizer are shown in Figure 6.6, Figure 6.7, Figure 6.8 and Figure 6.9, respectively.

As seen from the figures, the water uptake for 0/100 PMMA/CA, PMMA/CAP, PMMA/CAB and PMMA/CAPh blends with 2.5 % DBP are 0.84 wt %, 0.99 wt %, 1.18 wt % and 1.47 wt % respectively. The water uptake of the blends increased up to 50 wt % of CA derivatives concentration. The maximum water uptake was observed for the blends with 50/50 PMMA/CA, PMMA/CAP, PMMA/CAB and PMMA/CAPh blends with 2.5 % DBP are 5.38 wt %, 7.31 wt %, 7.46 wt % and 7.56 wt % respectively, which decrease on addition of further PMMA.

The water uptake for 0/100 PMMA/CA, PMMA/CAP, PMMA/CAB and PMMA/CAPh blends with 5 % DBP are 0.83 wt %, 0.97 wt %, 1.16 wt % and 1.44 wt % respectively. The water uptake of the blends increased up to 50 wt % of CA derivatives concentration. The maximum water uptake was observed for the blends with 50/50 PMMA/CA, PMMA/CAP, PMMA/CAB and PMMA/CAPh blends with 5 % DBP are 5.38 wt %, 7.02 wt %, 7.37 wt % and 7.46 wt % respectively, which decrease on addition of further PMMA.

The water uptake for 0/100 PMMA/CA, PMMA/CAP, PMMA/CAB and PMMA/CAPh blends with 7.5 % DBP are 0.83 wt %, 0.95 wt %, 1.16 wt % and 1.44 wt % respectively. The water uptake of the blends increased up to 50 wt % of CA derivatives concentration. The maximum water uptake was observed for the blends with 50/50 PMMA/CA, PMMA/CAP, PMMA/CAB and PMMA/CAPh blends with 7.5 % DBP are 5.33 wt %, 6.97 wt %, 7.13 wt % and 7.37 wt % respectively, which decrease on addition of further PMMA.

The water uptake for 0/100 PMMA/CA, PMMA/CAP, PMMA/CAB and PMMA/CAPh blends with 10 % DBP are 0.81 wt %, 0.95 wt %, 1.12 wt % and 1.43 wt % respectively. The water uptake of the blends increased up to 50 wt % of CA derivatives concentration. The maximum water uptake was observed for the blends with 50/50 PMMA/CA, PMMA/CAP, PMMA/CAB and PMMA/CAPh blends with 10 % DBP are 5.29 wt %, 6.40 wt %, 6.87 wt % and 7.13 wt % respectively, which decrease on addition of further PMMA.

The prepared polymer blends have shown a maximum water uptake in the 50 wt. % of PMMA indicating the presence of void volume in the blends and further decrease in the water uptake due to the compact structured pattern with reduction in void volumes has been discussed in chapter 3, section 3.2.3 of the thesis.

6.2.4 Ion Exchange Capacity (IEC) Measurements

Ion exchange capacity (IEC) provides an indirect approximation for the ion exchangeable groups present in the pure and blend polymers which are responsible for proton conduction. The IEC values for 2.5 %, 5 %, 7.5 % and 10 % DBP pure and PMMA/CA derivatives blends are shown graphically in Figure 6.10, Figure 6.11, Figure 6.12 and Figure 6.13.

From the figure it can be seen that the IEC values decreases for the blends with an increase in PMMA content. It is known that CA derivatives has exchangeable –OH groups. Hence it is evident that when PMMA content of the blend is increased, the number of replaceable sites available in the blend would decrease and hence the decrease in the IEC of the blends.

6.2.5 Electrochemical Impedance Spectroscopy

Electrochemical Impedance spectroscopy is recently being widely applied in determining various material properties, prime among which are permittivity and conductivity. Figure 6.14, Figure 6.15, Figure 6.16 and Figure 6.17 shows AC impedance spectra (Cole-Cole or Nyquist plots) of 2.5 %, 5 %, 7.5 % and 10 % DBP plasticized 50/50 PMMA/CA blends at different temperatures, respectively.

The impedance responses due to the bulk resistance of the electrolyte and electrolyte-electrode double layer capacitance behavior of the samples over the whole range of frequency evaluated has been discussed in the chapter 3, section 3.2.5 of the thesis. AC impedance spectra of 2.5 %, 5 %, 7.5 % and 10 % DBP plasticized 50/50 PMMA/CAP, PMMA/CAB and PMMA/CAPh blends at different temperatures, respectively have shown the similar trend for electrochemical impedance spectra.

6.2.5.1 Proton conductivity measurement

The variation of conductivity of the blends with temperature and room temperature conductivity of the blends are shown in Figure 6.18, Figure 6.19, Figure 6.20 and Figure 6.21 respectively. It has been observed that at 30 °C, among the polyblends studied the blends with 2.5 % DBP plasticized PMMA/CA, PMMA/CAP, PMMA/CAB and PMMA/CAPh 30/70 composition showed the highest proton conductivity value of $1.65 \times 10^{-3} \text{ S cm}^{-1}$, $2.14 \times 10^{-3} \text{ S cm}^{-1}$, $2.16 \times 10^{-3} \text{ S cm}^{-1}$ and $2.20 \times 10^{-3} \text{ S cm}^{-1}$, respectively. The proton conductivity increased as the temperature is increased in the measured temperature range between 30 °C to 70 °C. Also, it has been found from impedance plots that as the temperature is increased, the bulk resistance R decreased resulting in an increase in the value of proton conductivity. This may be mainly due to the fact that at higher temperature, there is an enhancement in the ion movement, favoring conductivity. Proton conductivity measurement of 5 %, 7.5 % and 10 % DBP plasticized 50/50 PMMA/CAP, PMMA/CAB and PMMA/CAPh blends at different temperatures respectively have shown the similar trend.

6.2.5.2 Temperature dependence of ionic conductivity

It has been found that the proton conductivity of the blend film increased with increasing temperature for all compositions. This may be mainly due to the fact that an increase in temperature increases the mobility of ions and this in turn increases the conductivity. Further, the vibrational motion of the polymer backbone and side chains, which becomes more vigorous with increase in temperature can also facilitate the conduction of ions. The increased amplitude of vibration brings the coordination sites closer to one another enabling the ions to hop from the occupied site to the unoccupied site with lesser energy required. Increase in amplitude of vibration of the polymer backbone and side chains can also increase the fraction of free volume in the polymer electrolyte system (Aziz et al. 2010). Druger et al. (1983) and Druger et al. (1985) have attributed the change in conductivity with temperature in solid polymer electrolyte to hopping model, which results in an increase in the free volume of the system. The hopping model either permits the ions to hop from one site to another or provides a pathway for ions to move. In other words, this facilitates translational motion of the ions. From this, it is clear that the ionic motion is due to translational motion/hopping facilitated by the polymer. The nonexistence of any unusual variation of conductivity indicates the existence of overall amorphous region (Aziz et al. 2010). This implies that coupling of the ion movement with the amorphous nature of the polymer is facilitating the conductivity in the blends.

Electrical conduction is a thermally activated process and follows the Arrhenius law

$$\sigma = \sigma_0 \exp\left[-\frac{E_a}{kT}\right] \quad (2.3)$$

where, σ is the conductivity at a particular temperature, σ_0 is the pre-exponential factor, k is the Boltzmann's constant, and T is the absolute temperature. As there is no sudden change in the value of conductivity with temperature it may be inferred that these blends do not undergo any phase transitions within the temperature range studied. The conductivity has been discussed on the basis of the increase in the CA contents along

with the ion exchange capacity and water absorption facilitating the ion hopping through the polymer structure has been detailed in chapter 3, section 3.2.5.2 of the thesis.

6.2.6 Dielectric Studies

The dielectric constant and loss of the films have been calculated using the equations 1.11 and 1.12 respectively. The conductivity behavior of polymer electrolyte can be understood from dielectric studies (Ramesh et al. 2002). The dielectric constant is a measure of stored charge. The variations of dielectric constant and dielectric loss with frequency at different temperatures have been shown in Figure 6.22, Figure 6.23, Figure 6.24 and Figure 6.25 respectively, for 2.5 %, 5 %, 7.5 % and 10 % DBP plasticized 50/50 PMMA/CA blends. Similar trends have also been seen for 2.5 %, 5 %, 7.5 % and 10 % DBP plasticized 50/50 PMMA/CAP, PMMA/CAB and PMMA/CAPh blends at different temperatures.

There are no appreciable relaxation peaks observed, indicating the electrode polarization and space charge effects have occurred confirming non-debye dependence; the increase in dielectric constant and dielectric loss at higher temperatures due to the higher charge carrier density and conductivity of the polymer blends due to hopping mechanism has been discussed in the chapter 3, section 3.2.6 in the thesis.

6.3 FIGURES

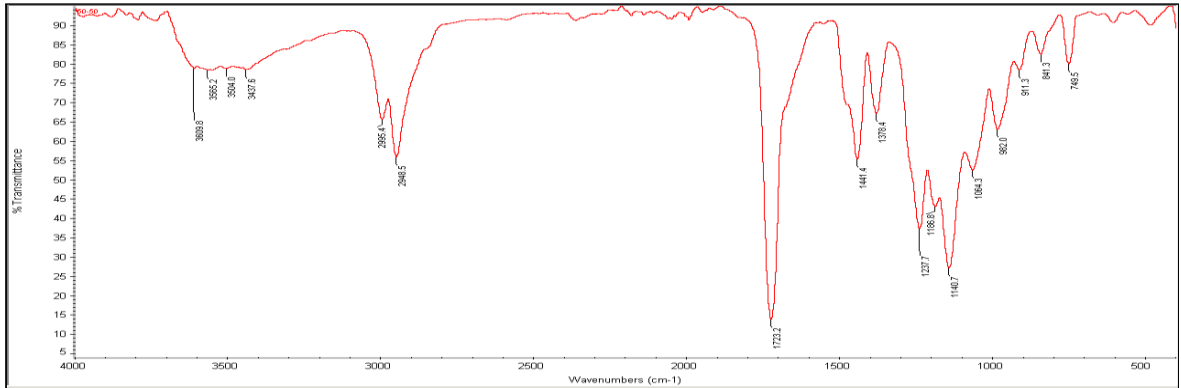


Figure 6.1 FTIR Spectrum of 2.5 % DBP plasticized 50/50 PMMA/CA blend.

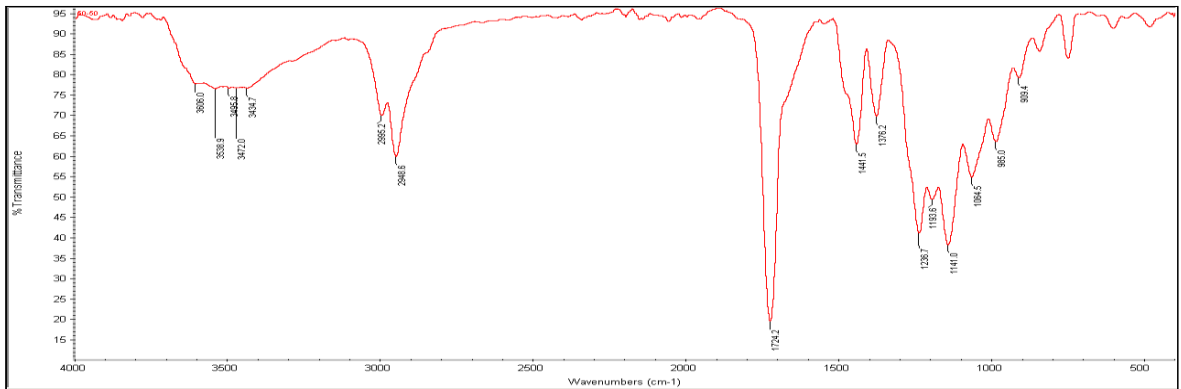


Figure 6.2 FTIR Spectrum of 5 % DBP plasticized 50/50 PMMA/CA blend.

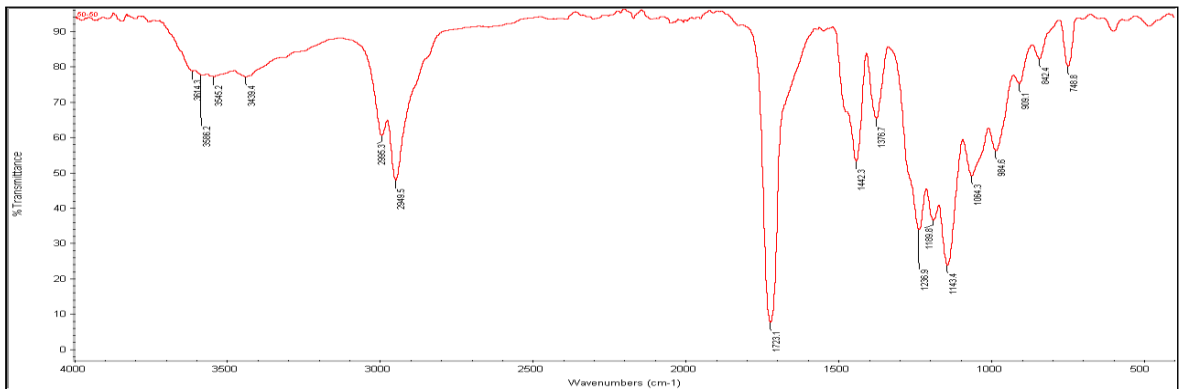


Figure 6.3 FTIR Spectrum of 7.5 % DBP plasticized 50/50 PMMA/CA blend.

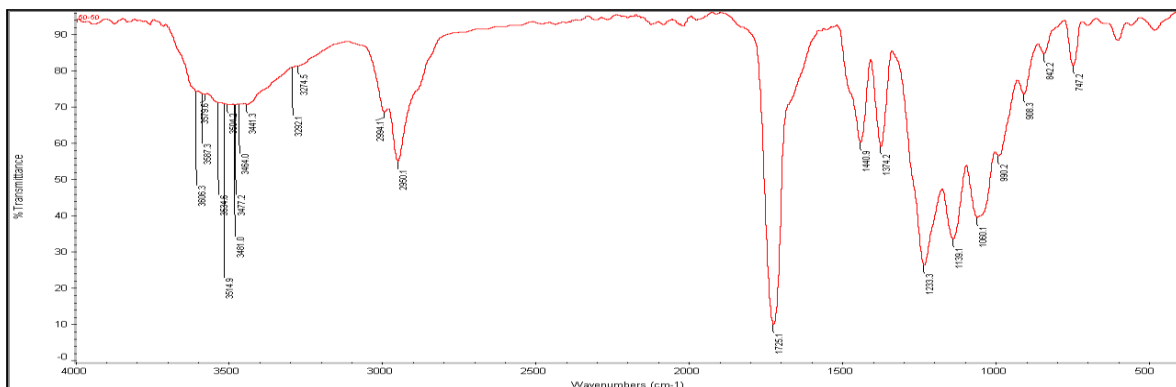


Figure 6.4 FTIR Spectrum of 10 % DBP plasticized 50/50 PMMA/CA blend.

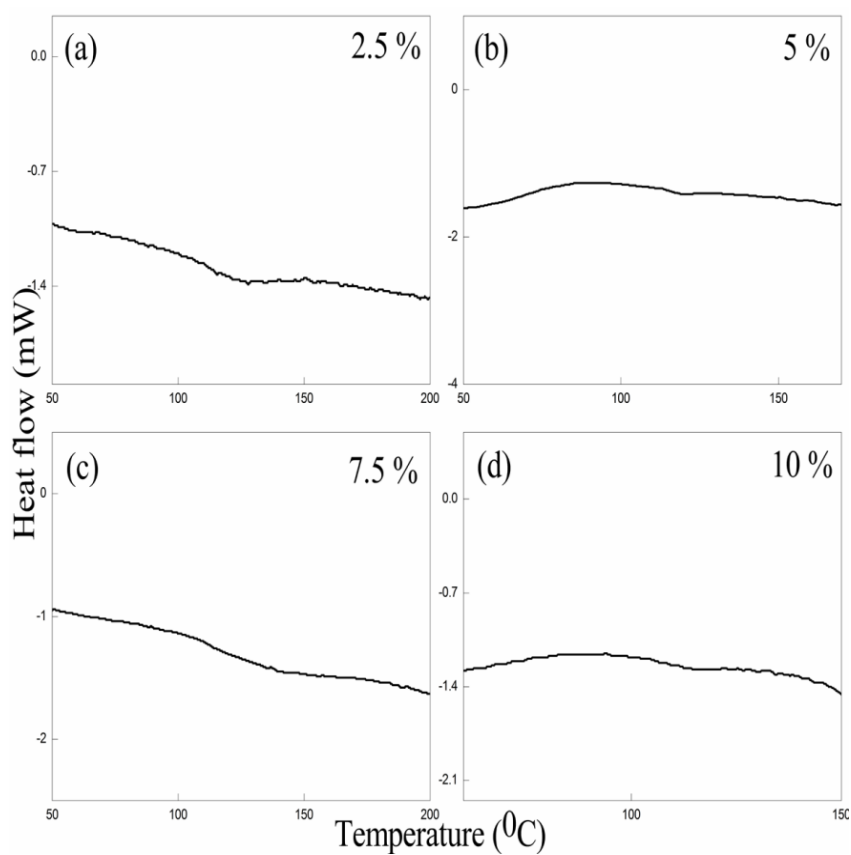


Figure 6.5 (a), (b), (c) and (d) DSC scans of 2.5 %, 5 %, 7.5 % and 10 % DBP plasticized 50/50 PMMA/CA blends.

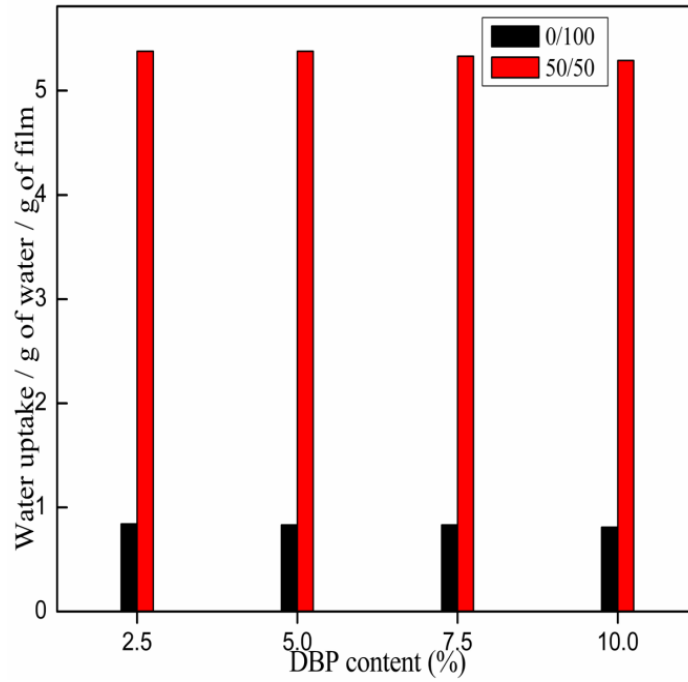


Figure 6.6 Water absorption by 2.5 %, 5 %, 7.5 % and 10 % DBP plasticized 0/100 and 50/50 PMMA/CA blends.

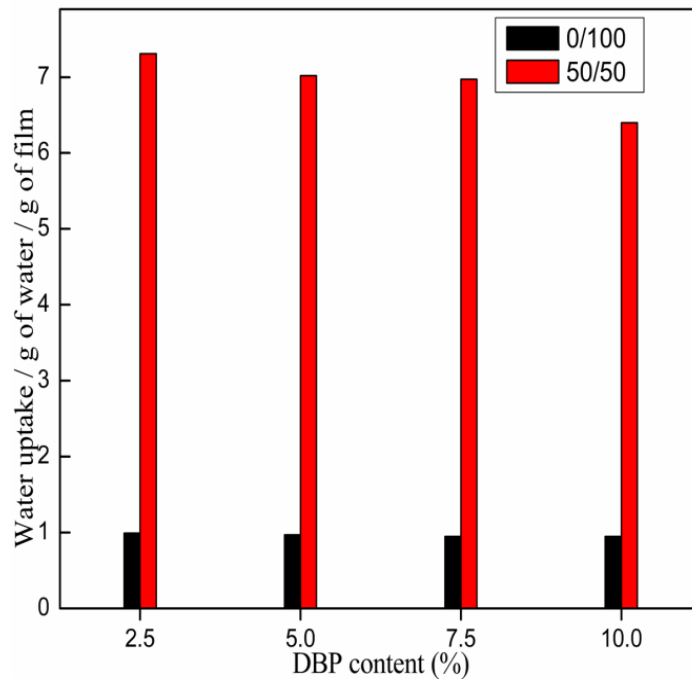


Figure 6.7 Water absorption by 2.5 %, 5 %, 7.5 % and 10 % DBP plasticized 0/100 and 50/50 PMMA/CAP blends.

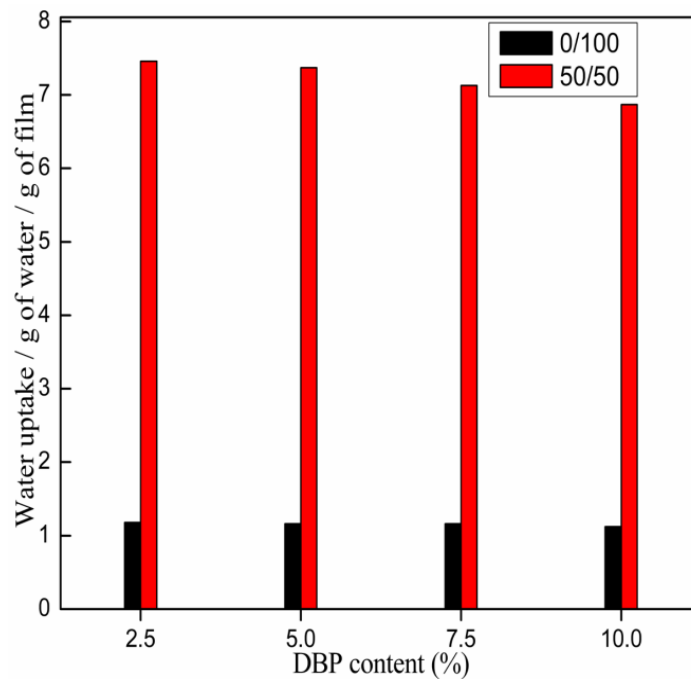


Figure 6.8 Water absorption by 2.5 %, 5 %, 7.5 % and 10 % DBP plasticized 0/100 and 50/50 PMMA/CAB blends.

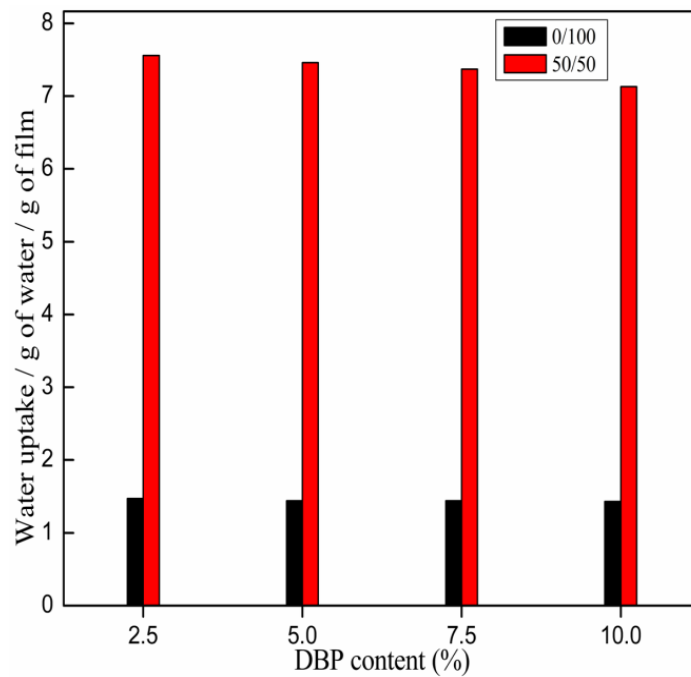


Figure 6.9 Water absorption by 2.5 %, 5 %, 7.5 % and 10 % DBP plasticized 0/100 and 50/50 PMMA/CAPh blends.

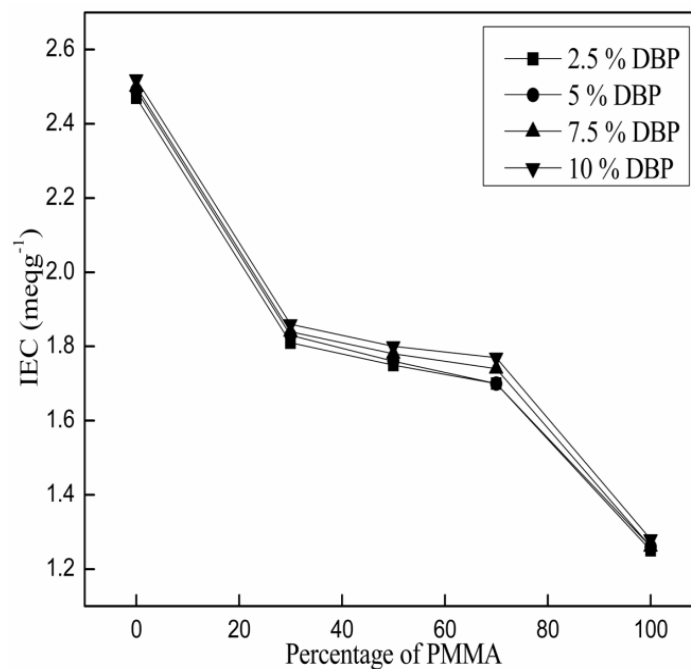


Figure 6.10 The change of IEC values in 2.5 %, 5 %, 7.5 % and 10 % DBP plasticized PMMA/CA blends.

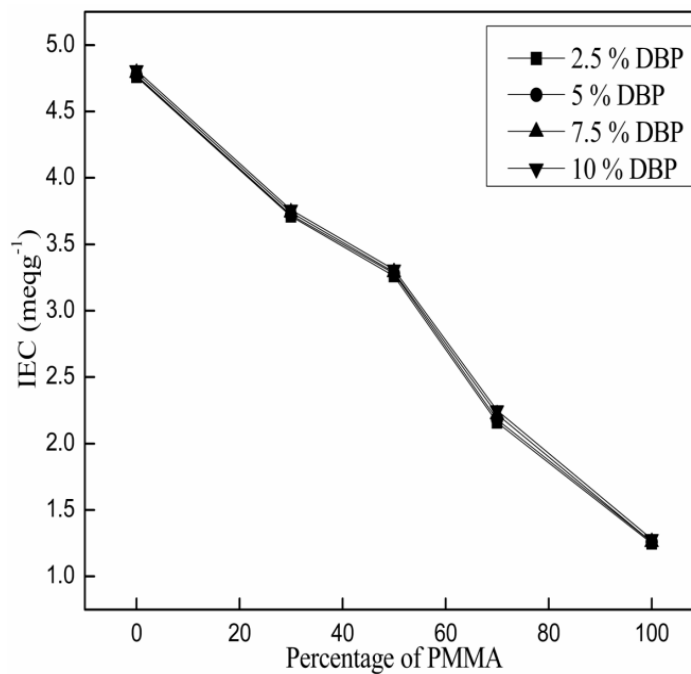


Figure 6.11 The change of IEC values in 2.5 %, 5 %, 7.5 % and 10 % DBP plasticized PMMA/CAP blends.

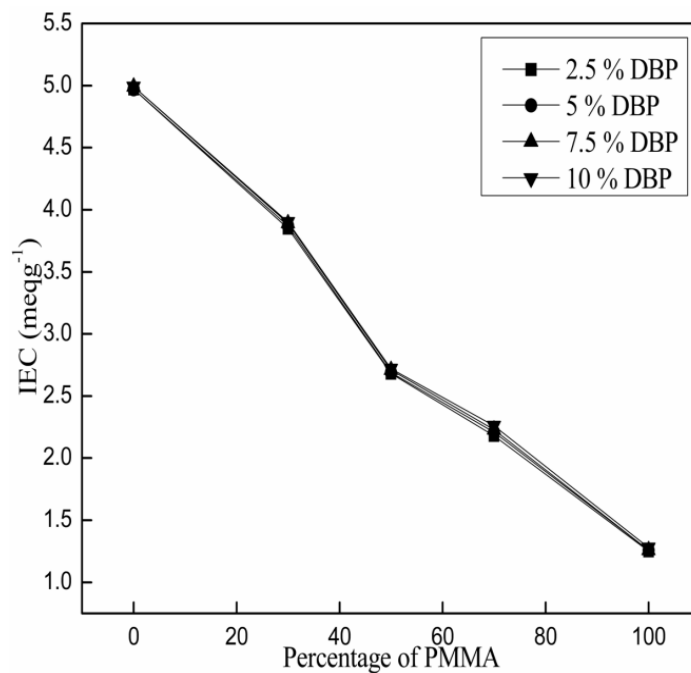


Figure 6.12 The change of IEC values in 2.5 %, 5 %, 7.5 % and 10 % DBP plasticized PMMA/CAB blends.

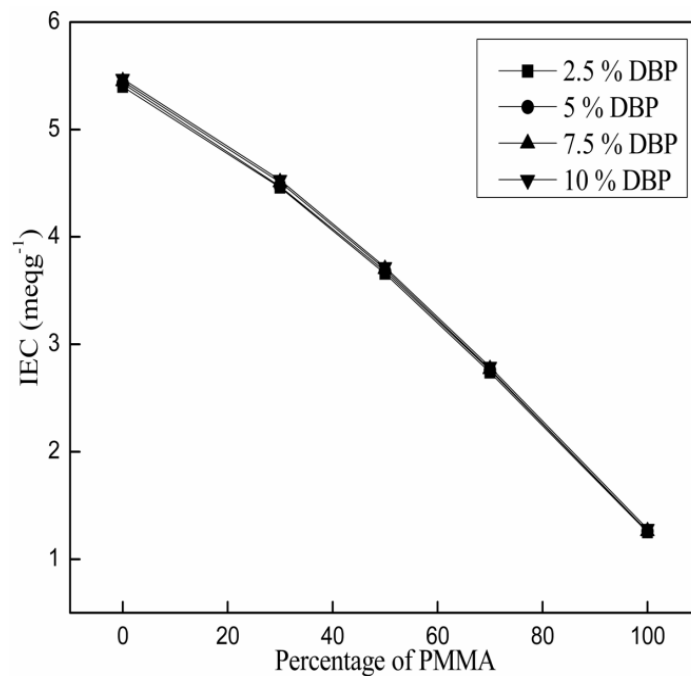


Figure 6.13 The change of IEC values in 2.5 %, 5 %, 7.5 % and 10 % DBP plasticized PMMA/CAPh blends.

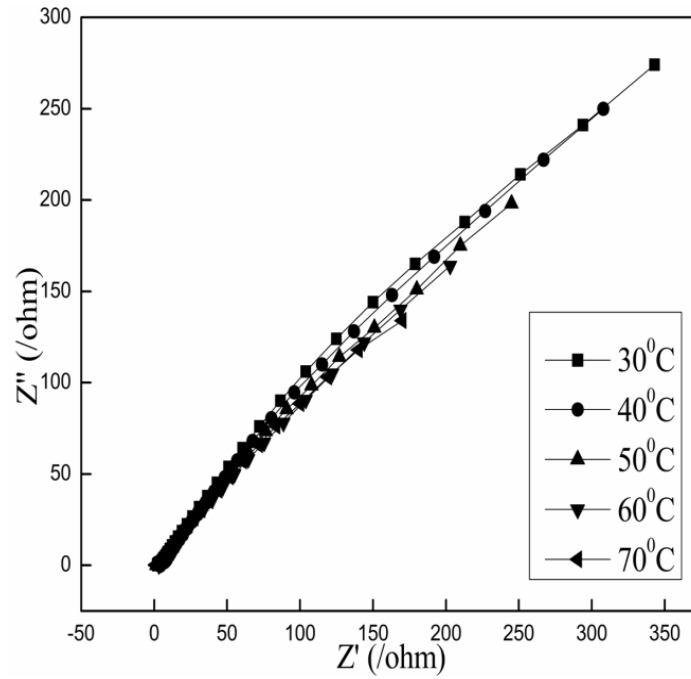


Figure 6.14 AC impedance spectrum of 2.5 % DBP plasticized 50/50 PMMA/CA blend at different temperatures.

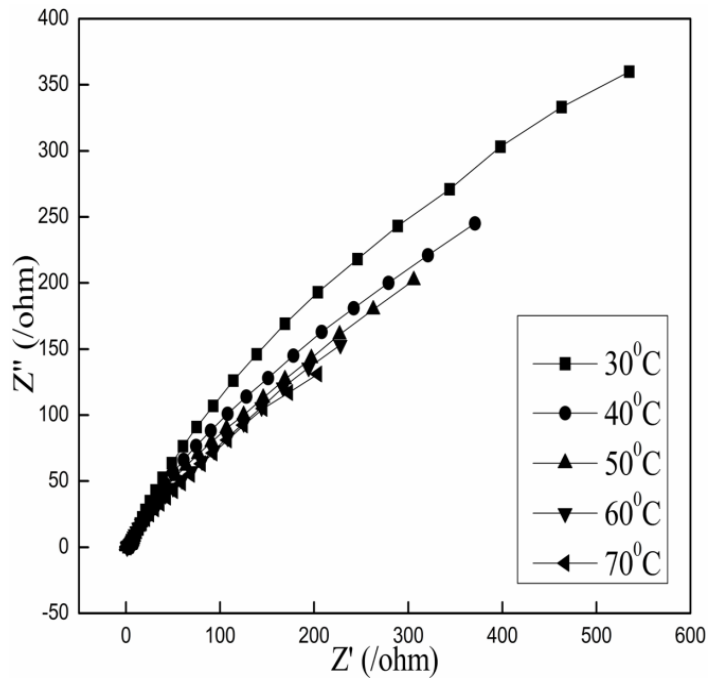


Figure 6.15 AC impedance spectrum of 5 % DBP plasticized 50/50 PMMA/CA blend at different temperatures.

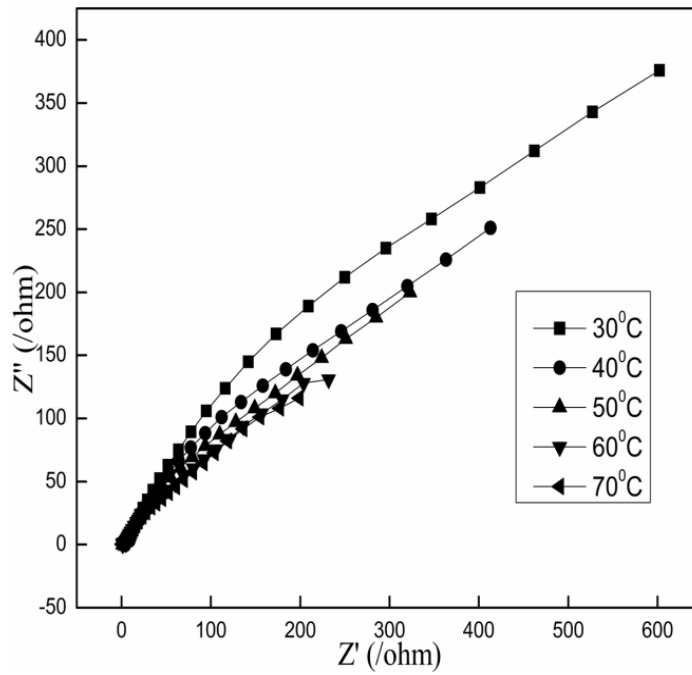


Figure 6.16 AC impedance spectrum of 7.5 % DBP plasticized 50/50 PMMA/CA blend at different temperatures.

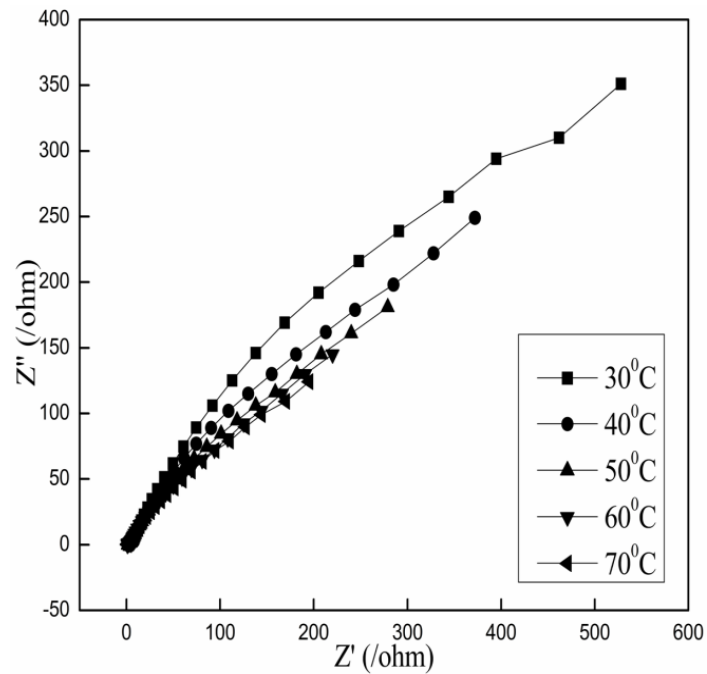


Figure 6.17 AC impedance spectrum of 10 % DBP plasticized 50/50 PMMA/CA blend at different temperatures.

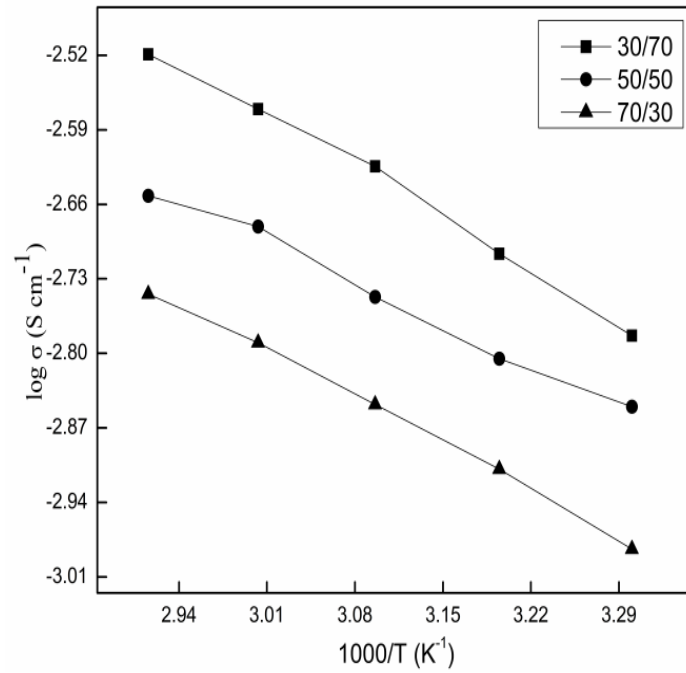


Figure 6.18 Arrhenius plots for conductivity σ of 2.5 % DBP plasticized PMMA/CA blends.

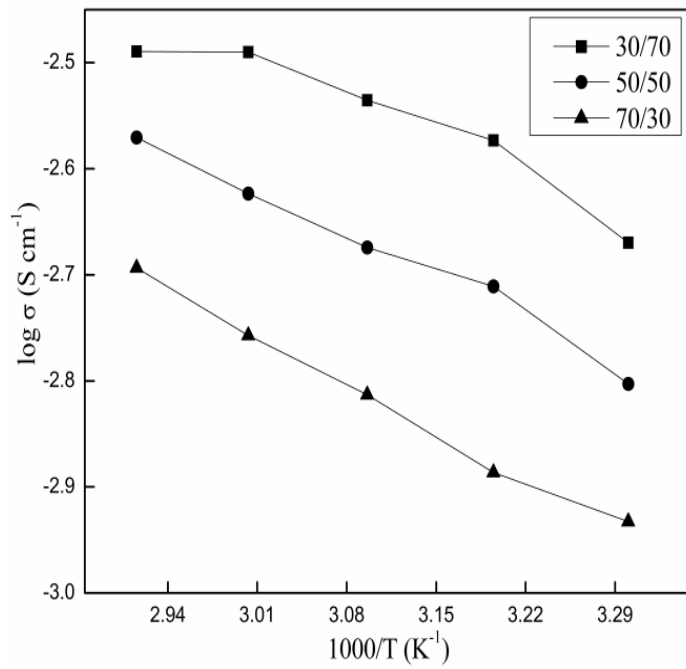


Figure 6.19 Arrhenius plots for conductivity σ of 2.5 % DBP plasticized PMMA/CAP blends.

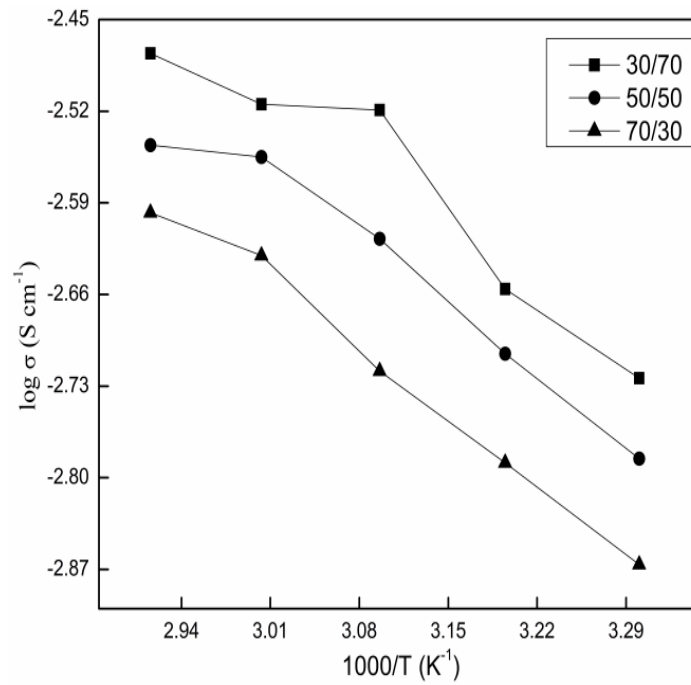


Figure 6.20 Arrhenius plots for conductivity σ of 2.5 % DBP plasticized PMMA/CAB blends.

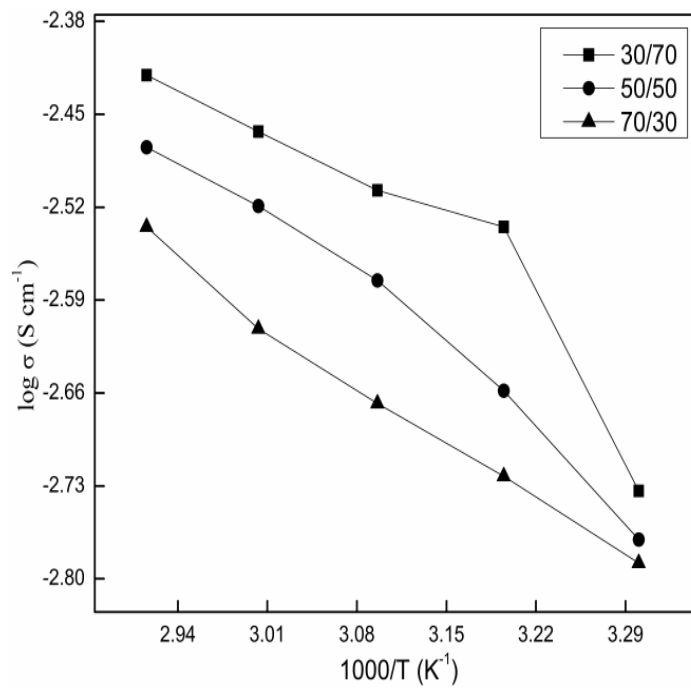


Figure 6.21 Arrhenius plots for conductivity σ of 2.5 % DBP plasticized PMMA/CAPh blends.

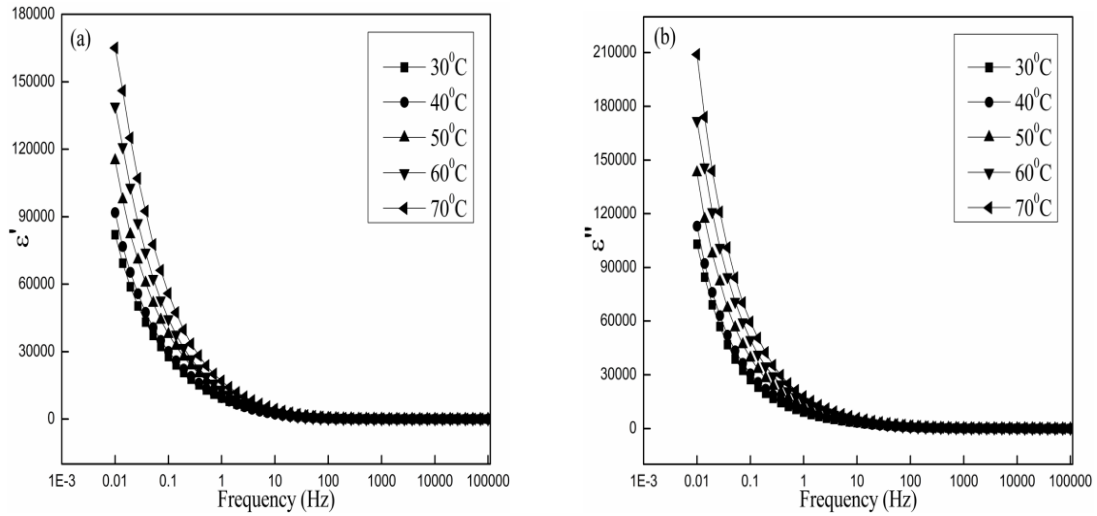


Figure 6.22 Variations of dielectric constant (a) and dielectric loss (b) with frequency at different temperatures for 2.5 % DBP plasticized 50/50 PMMA/CA blend.

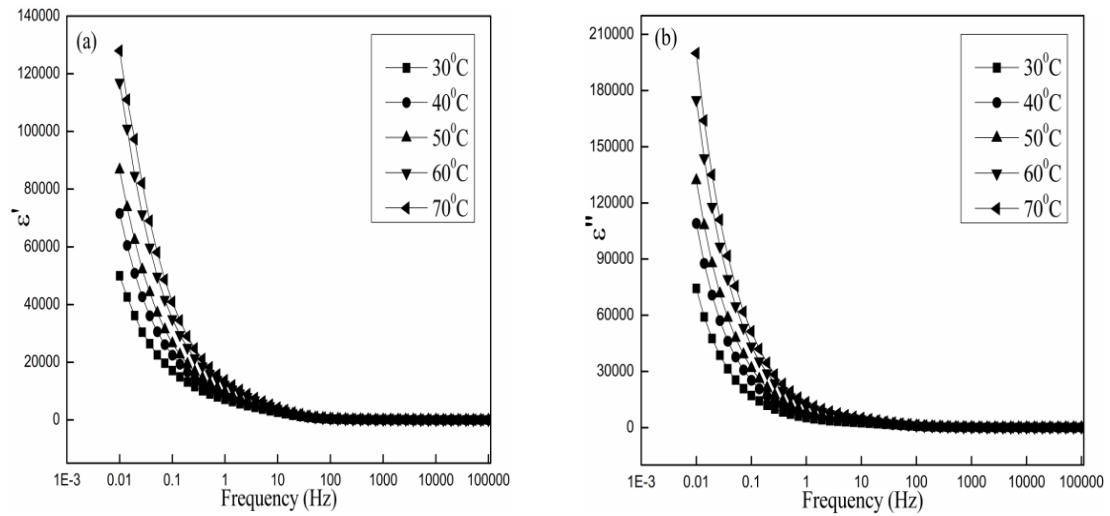


Figure 6.23 Variations of dielectric constant (a) and dielectric loss (b) with frequency at different temperatures for 5 % DBP plasticized 50/50 PMMA/CA blend.

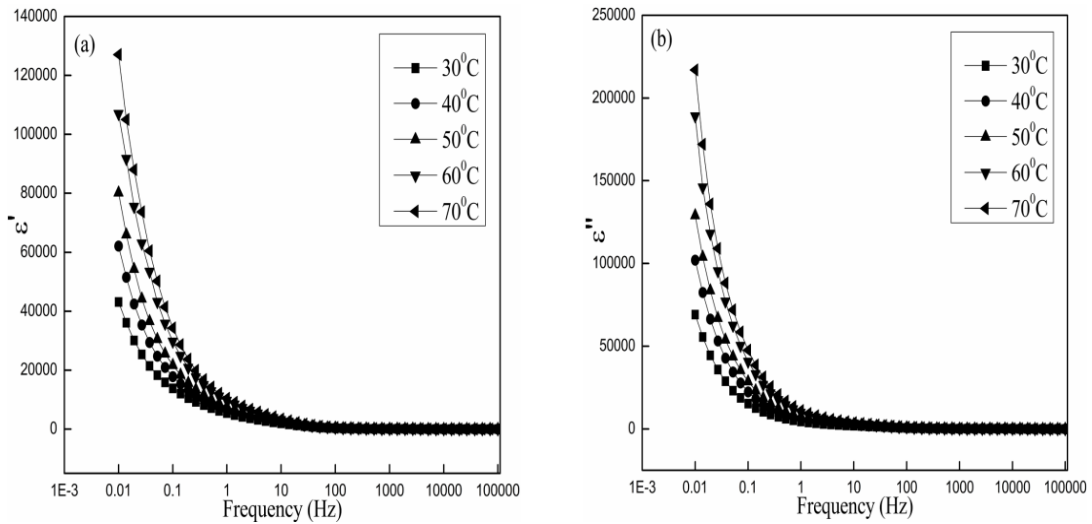


Figure 6.24 Variations of dielectric constant (a) and dielectric loss (b) with frequency at different temperatures for 7.5 % DBP plasticized 50/50 PMMA/CA blend.

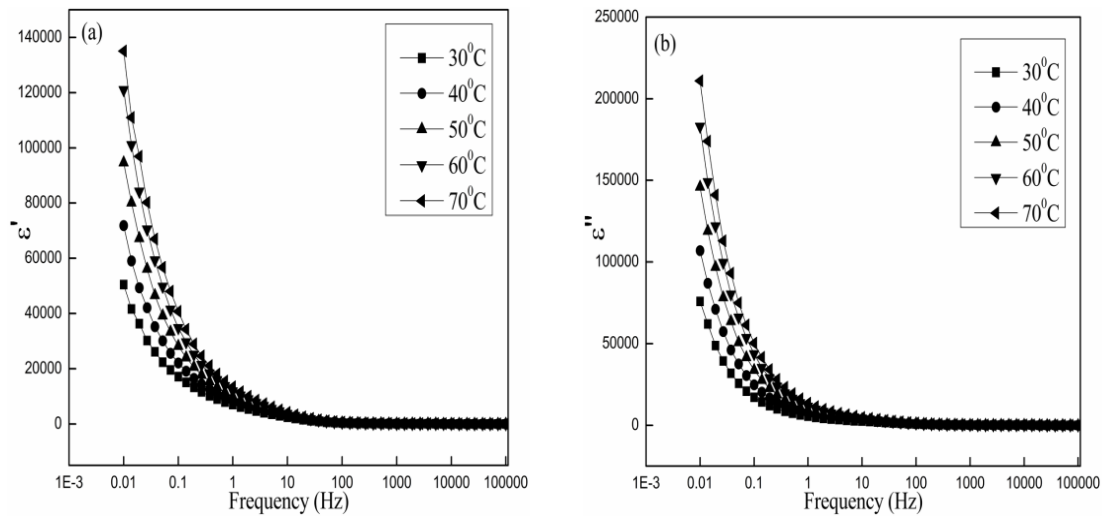


Figure 6.25 Variations of dielectric constant (a) and dielectric loss (b) with frequency at different temperatures for 10 % DBP plasticized 50/50 PMMA/CA blend.

6.4 TABLES

Table 6.1 IR stretching frequencies of DBP plasticized PMMA/CA, PMMA/CAP, PMMA/CAB and PMMA/CAPh blends.

PMMA/CA 2.5 DBP	-CO Stretching Frequencies	-OH Stretching Frequencies
0/100	1734.8	3476.5
50/50	1723.2	3437.6
PMMA/CA 5 DBP		
0/100	1734.4	3472.1
50/50	1724.2	3434.7
PMMA/CA 7.5 DBP		
0/100	1734.4	3474.0
50/50	1723.1	3439.4
PMMA/CA 10 DBP		
0/100	1733.5	3472.5
50/50	1725.1	3441.3
PMMA/CAP 2.5 DBP		
0/100	1735.9	3480.0
50/50	1722.9	3562.3
PMMA/CAP 5 DBP		
0/100	1735.9	3521.5
50/50	1723.4	3594.8
PMMA/CAP 7.5 DBP		
0/100	1735.9	3563.0
50/50	1722.8	3560.9
PMMA/CAP 10 DBP		
0/100	1735.5	3541.9
50/50	1723.5	3622.0
PMMA/CAB 2.5 DBP		
0/100	1737.7	3496.2
50/50	1724.4	3541.2
PMMA/CAB 5 DBP		
0/100	1737.1	3476.4
50/50	1723.8	3436.7

PMMA/CAB 7.5 DBP		
0/100	1737.3	3479.8
50/50	1729.0	3538.9
PMMA/CAB 10 DBP		
0/100	1736.8	3484.1
50/50	1722.7	3555.2
PMMA/CAPh 2.5 DBP		
0/100	1657.2	3411.9
50/50	1717.9	3425.0
PMMA/CAPh 5 DBP		
0/100	1662.3	3420.1
50/50	1719.8	3414.2
PMMA/CAPh 7.5 DBP		
0/100	1661.3	3421.7
50/50	1717.1	3393.1
PMMA/CAPh 10 DBP		
0/100	1658.8	3434.3
50/50	1719.6	3429.6

Table 6.2 Thermal properties of 2.5 %, 5 %, 7.5 % and 10 % DBP plasticized PMMA/CA, PMMA/CAP, PMMA/CAB and PMMA/CAPh blends.

Sample	T_g (°C)	Fox equation	k values	Gordon-Taylor equation
PMMA/CA 2.5 DBP				
0/100	191.35	191.35		191.35
30/70	124.20	154.95		124.47
50/50	114.64	137.51	0.11	115.64
70/30	111.61	123.59		111.09
100/0	107.31	107.31		107.31
PMMA/CA 5 DBP				
0/100	188.73	188.73		188.73
30/70	124.13	153.71		123.91
50/50	114.35	136.79	0.11	115.34
70/30	111.46	123.23		110.94
100/0	107.27	107.27		107.27
PMMA/CA 7.5 DBP				
0/100	188.22	188.22		188.22
30/70	124.06	153.47		123.80
50/50	114.17	136.65	0.11	115.28
70/30	110.56	123.15		110.90
100/0	107.26	107.26		107.26
PMMA/CA 10 DBP				
0/100	186.90	186.90		186.90
30/70	123.42	152.77		120.97
50/50	113.31	136.19	0.09	113.72
70/30	109.13	122.86		110.09
100/0	107.13	107.13		107.13
PMMA/CAP 2.5 DBP				
0/100	141.49	141.49		141.49
30/70	137.88	129.15		125.37
50/50	118.46	122.05	0.48	118.40
70/30	112.13	115.69		113.13
100/0	107.31	107.31		107.31
PMMA/CAP 5 DBP				
0/100	141.19	141.19		141.19
30/70	137.17	128.96		124.83
50/50	117.96	121.91	0.46	117.96
70/30	111.96	115.60		112.86

100/0	107.27	107.27		107.27
PMMA/CAP 7.5 DBP				
0/100	140.45	140.45		140.45
30/70	136.83	128.52		123.69
50/50	117.00	121.63	0.42	117.08
70/30	111.22	115.44		112.32
100/0	107.26	107.26		107.26
PMMA/CAP 10 DBP				
0/100	140.08	140.08		140.08
30/70	136.35	128.25		123.04
50/50	116.53	121.41	0.4	116.54
70/30	110.46	115.26		111.95
100/0	107.13	107.13		107.13
PMMA/CAB 2.5 DBP				
0/100	133.31	133.31		133.31
30/70	120.65	124.28		120.63
50/50	115.40	118.91	0.45	115.38
70/30	109.14	113.98		111.51
100/0	107.31	107.31		107.31
PMMA/CAB 5 DBP				
0/100	133.00	133.00		133.00
30/70	120.04	124.07		120.16
50/50	115.05	118.76	0.43	115.01
70/30	108.76	113.88		111.27
100/0	107.27	107.27		107.27
PMMA/CAB 7.5 DBP				
0/100	132.63	132.63		132.63
30/70	119.47	123.84		119.51
50/50	114.41	118.6	0.4	114.51
70/30	108.01	113.79		110.97
100/0	107.26	107.26		107.26
PMMA/CAB 10 DBP				
0/100	132.54	132.54		132.54
30/70	119.00	123.74		118.90
50/50	113.89	118.49	0.37	113.99
70/30	107.96	113.67		110.61
100/0	107.13	107.13		107.13

PMMA/CAPh 2.5 DBP

0/100	144.65	144.65		144.65
30/70	139.46	130.98		141.04
50/50	137.20	123.21	4	137.18
70/30	132.54	116.32		130.89
100/0	107.31	107.31		107.31

PMMA/CAPh 5 DBP

0/100	144.03	144.03		144.03
30/70	138.89	130.60		140.30
50/50	136.43	122.96	3.8	136.37
70/30	131.83	116.16		130.05
100/0	107.27	107.27		107.27

PMMA/CAPh 7.5 DBP

0/100	143.89	143.89		143.89
30/70	138.75	130.52		139.56
50/50	135.24	122.90	3.2	135.17
70/30	131.31	116.13		128.44
100/0	107.26	107.26		107.26

PMMA/CAPh 10 DBP

0/100	143.52	143.52		143.52
30/70	138.12	130.25		139.10
50/50	134.53	122.68	3.1	134.64
70/30	130.12	115.95		127.89
100/0	107.13	107.13		107.13

Chapter 7

STUDIES ON PROPYLENE CARBONATE (PC) PLASTICIZED BLENDS OF PMMA WITH CA, CAP, CAB AND CPh

Chapter 7 deals with the study of propylene carbonate (PC) plasticized blends of PMMA-CA derivatives. A brief note on PC plasticizer has also been included in this chapter.

7.1 PROPYLENE CARBONATE (PC) PLASTICIZER

Propylene carbonate is produced from propylene oxide and carbon dioxide with a suitable catalyst, often a zinc halide. This colorless and odorless liquid is useful as a polar, aprotic solvent. Propylene carbonate is used in a variety of syntheses and applications as a polar, aprotic solvent. It has a high molecular dipole moment (4.9 D), considerably higher than those of acetone (2.91 D) and ethyl acetate (1.78 D). It is possible, for example, to obtain potassium, sodium, and other alkali metals by electrolysis of their chlorides and other salts dissolved in propylene carbonate.

Properties:

Physical properties	
Molecular formula	C ₄ H ₆ O ₃
Molecular mass	102.09
Density	1.205 g/cm ³
Boiling point	242 °C
Dielectric constant	64

Uses:

Due to its high dielectric constant of 64, it is frequently used as a high-permittivity component of electrolytes in lithium batteries, usually together with a low-viscosity solvent (e.g. dimethoxyethane). Its high polarity allows it to create an effective solvation shell around lithium ions, thereby creating a conductive electrolyte. However, it is not used in lithium-ion batteries due to its destructive effect on graphite. Propylene carbonate can also be found in some adhesives, paint strippers, and in cosmetics. It is also used as plasticizer.

7.2 RESULTS AND DISCUSSION

7.2.1 Fourier Transform Infrared (FTIR) Spectroscopic Studies

FTIR spectra of 50/50 PMMA/CA blend plasticized with 2.5%, 5%, 7.5% and 10 % PC are shown in Figure 7.1, Figure 7.2, Figure 7.3 and Figure 7.4 respectively. The FTIR stretching frequencies of PMMA/CA, PMMA/CAP, PMMA/CAB and PMMA/CAPh blends plasticized with PC are also given in Tables 7.1. Carbonyl frequency of 0/100 PMMA/CA blend with 2.5 % PC at 1734.7 cm^{-1} decreased to 1724.1 cm^{-1} in 50/50 PMMA/CA blend with 2.5 % PC. Similarly, the carbonyl frequency of 0/100 PMMA/CA blend with 5 % PC at 1734.1 cm^{-1} decreased to 1725.0 cm^{-1} in 50/50 PMMA/CA blend with 5 % PC, the carbonyl frequency of 0/100 PMMA/CA blend with 7.5 % PC at 1734.3 cm^{-1} decreased to 1727.9 cm^{-1} in 50/50 PMMA/CA blend with 7.5 % PC and 0/100 PMMA/CA blend with 10 % PC at 1734.5 cm^{-1} decreased to 1723.4 cm^{-1} in 50/50 PMMA/CA blend with 10 % PC.

The carbonyl frequency of 0/100 PMMA/CAP blend with 2.5 % PC at 1737.6 cm^{-1} decreased to 1722.9 cm^{-1} in 50/50 PMMA/CAP blend with 2.5 % PC. Similarly, the carbonyl frequency of 0/100 PMMA/CAP blend with 5 % PC at 1737.0 cm^{-1} decreased to 1723.2 cm^{-1} in 50/50 PMMA/CAP blend with 5 % PC, the carbonyl frequency of 0/100 PMMA/CAP blend with 7.5 % PC at 1736.5 cm^{-1} decreased to 1723.1 cm^{-1} in 50/50 PMMA/CAP blend with 7.5 % PC and the carbonyl frequency of 0/100 PMMA/CAP blend with 10 % PC at 1736.9 cm^{-1} decreased to 1723.5 cm^{-1} in 50/50 PMMA/CAP blend with 10 % PC.

The carbonyl frequency of 0/100 PMMA/CAB blend with 2.5 % PC at 1737.6 cm^{-1} decreased to 1726.9 cm^{-1} in 50/50 PMMA/CAB blend with 2.5 % PC. Similarly, the carbonyl frequency of 0/100 PMMA/CAB blend with 5 % PC at 1737.9 cm^{-1} decreased to 1727.8 cm^{-1} in 50/50 PMMA/CAB blend with 5 % PC, the carbonyl frequency at 0/100 PMMA/CAB blend with 7.5 % PC at 1737.7 cm^{-1} decreased to 1722.7 cm^{-1} in 50/50 PMMA/CAB blend with 7.5 % PC and the carbonyl frequency of 0/100 PMMA/CAB blend with 10 % PC at 1737.7 cm^{-1} decreased to 1723.5 cm^{-1} in 50/50 PMMA/CAB blend with 10 % PC.

The carbonyl frequency of 0/100 PMMA/CAPh blend with 2.5 % PC at 1661.0 cm^{-1} shifted to 1714.9 cm^{-1} in 50/50 PMMA/CAPh blend with 2.5 % PC. Similarly, the carbonyl frequency of 0/100 PMMA/CAPh blend with 5 % PC at 1662.6 cm^{-1} shifted to 1716.8 cm^{-1} in 50/50 PMMA/CAPh blend with 5 % PC, the carbonyl frequency of 0/100 PMMA/CAPh blend with 7.5 % PC at 1661.7 cm^{-1} shifted to 1719.5 cm^{-1} in 50/50 PMMA/CAPh blend with 7.5 % PC and the carbonyl frequency of 0/100 PMMA/CAPh blend with 10 % PC at 1664.2 cm^{-1} shifted to 1667.8 cm^{-1} in 50/50 PMMA/CAPh blend with 10 % PC.

Such shift in the specific vibration frequencies are ascribed to the formation of a weak hydrogen bond between component polymers in the blend. This can also be contributing to the miscibility of the blends.

The -OH stretching vibrations of hydroxyl groups occurred as broad band at 3468.3 cm^{-1} and 3445.0 cm^{-1} in 0/100 PMMA/CA blend with 2.5 % PC and 50/50 PMMA/CA blend with 2.5 % PC respectively. Similarly, the -OH stretching vibrations of hydroxyl groups in the case of other blends with varying compositions are given in Tables 7.1.

The intensity of the broad band decreased after blending, indicating that part of the -OH groups are involved in the hydrogen bond formation. These results indicate that specific interactions such as the hydrogen bonding forces exist in the blends and this is leading to the miscibility of the blends.

7.2.2 Differential Scanning Calorimetry (DSC) Studies

The DSC thermograms of 2.5 %, 5 %, 7.5 % and 10 % PC plasticized 50/50 PMMA/CA blends are shown in Figure 7.5 (a), Figure 7.5 (b), Figure 7.5 (c) and Figure 7.5 (d) respectively.

From Figure 7.5 (a) to Figure 7.5 (d), it can be seen that the T_g for 2.5 %, 5 %, 7.5 % and 10 % PC plasticized 50/50 PMMA/CA blends are 112.94 °C, 112.3 °C, 112.1 °C and 111.32 °C respectively. It is interesting to note here that the thermograms for the blends (Figure 7.5 (a) to Figure 7.5 (d)) exhibited single T_g and its value lies intermediate to the T_g values of 2.5 %, 5 %, 7.5 % and 10 % PC plasticized pure PMMA and pure CA

derivatives respectively. Further, the T_g values of the blend films decreased regularly on increase of PMMA content in the blends. Such a systematic variation of T_g in the blends is indicative of miscibility of the components in the blends.

Gordon-Taylor equation (Eq. (2.1)) and Fox equation (Eq. (2.2)) are frequently used expressions for predicting the glass transition temperature of amorphous polymer blends and also for estimating the glass transition temperature of blend films from the properties of pure components.

The examination data is best fitted by this equation with $k = 0.13, 0.13, 0.13$ and 0.10 respectively for 2.5 %, 5 %, 7.5 % and 10 % PC plasticized PMMA/CA blends. This result supports that, blends have high miscibility in the amorphous state. The thermal properties of 2.5 %, 5 %, 7.5 % and 10 % PC plasticized PMMA/CA, PMMA/CAP, PMMA/CAB and PMMA/CAPh blends have shown single T_g and are presented in Table 7.2. Hence it can be concluded that all the blends studied are miscible in the entire composition range. The blends show a positive deviation from Fox equation implying an intermolecular interaction between the polymers.

7.2.3 Water Uptake

The water uptake capacity of the polymer blend films have been calculated using the equation 1.7. The plots of water uptake against PC content in the PMMA/CA, PMMA/CAP, PMMA/CAB and PMMA/CAPh blends with 2.5 %, 5 %, 7.5 % and 10 % of PC plasticizer are shown in Figure 7.6, Figure 7.7, Figure 7.8 and Figure 7.9, respectively.

As seen from the figures, the water uptake for 0/100 PMMA/CA, PMMA/CAP, PMMA/CAB and PMMA/CAPh blends with 2.5 % PC are 0.99 wt %, 1.1 wt %, 1.38 wt % and 1.59 wt % respectively. The water uptake of the blends increased up to 50 wt % of CA derivatives concentration. The maximum water uptake was observed for the blends with 50/50 PMMA/CA, PMMA/CAP, PMMA/CAB and PMMA/CAPh blends with 2.5 % PC are 6.41 wt %, 7.63 wt %, 7.66 wt % and 7.74 wt % respectively, which decrease on addition of further PMMA.

The water uptake for 0/100 PMMA/CA, PMMA/CAP, PMMA/CAB and PMMA/CAPh blends with 5 % PC are 0.97 wt %, 1.09 wt %, 1.38 wt % and 1.59 wt % respectively. The water uptake of the blends increased up to 50 wt % of CA derivatives concentration. The maximum water uptake was observed for the blends with 50/50 PMMA/CA, PMMA/CAP, PMMA/CAB and PMMA/CAPh blends with 5 % PC are 6.11 wt %, 7.56 wt %, 7.63 wt % and 7.66 wt % respectively, which decrease on addition of further PMMA.

The water uptake for 0/100 PMMA/CA, PMMA/CAP, PMMA/CAB and PMMA/CAPh blends with 7.5 % PC are 0.95 wt %, 1.07 wt %, 1.33 wt % and 1.58 wt % respectively. The water uptake of the blends increased up to 50 wt % of CA derivatives concentration. The maximum water uptake was observed for the blends with 50/50 PMMA/CA, PMMA/CAP, PMMA/CAB and PMMA/CAPh blends with 7.5 % PC are 5.94 wt %, 7.46 wt %, 7.56 wt % and 7.6 wt % respectively, which decrease on addition of further PMMA.

The water uptake for 0/100 PMMA/CA, PMMA/CAP, PMMA/CAB and PMMA/CAPh blends with 10 % PC are 0.95 wt %, 1.05 wt %, 1.32 wt % and 1.56 wt % respectively. The water uptake of the blends increased up to 50 wt % of CA derivatives concentration. The maximum water uptake was observed for the blends with 50/50 PMMA/CA, PMMA/CAP, PMMA/CAB and PMMA/CAPh blends with 10 % PC are 5.84 wt %, 7.37 wt %, 7.43 wt % and 7.52 wt % respectively, which decrease on addition of further PMMA.

The prepared polymer blends have shown a maximum water uptake in the 50 wt. % of PMMA indicating the presence of void volume in the blends and further decrease in the water uptake due to the compact structured pattern with reduction in void volumes has been discussed in chapter 3, section 3.2.3 of the thesis.

7.2.4 Ion Exchange Capacity (IEC) Measurements

Ion exchange capacity (IEC) provides an indirect approximation for the ion exchangeable groups present in the pure and blend polymers which are responsible for proton conduction. The IEC values for 2.5 %, 5 %, 7.5 % and 10 % PC pure and

PMMA/CA derivatives blends are shown graphically in Figure 7.10, Figure 7.11, Figure 7.12 and Figure 7.13.

From the figure it can be seen that the IEC values decreases for the blends with an increase in PMMA content. It is known that CA derivatives has exchangeable –OH groups. Hence it is evident that when PMMA content of the blend is increased, the number of replaceable sites available in the blend would decrease and hence the decrease in the IEC of the blends.

7.2.5 Electrochemical Impedance Spectroscopy

Electrochemical Impedance spectroscopy is recently being widely applied in determining various material properties, prime among which are permittivity and conductivity. Figure 7.14, Figure 7.15, Figure 7.16 and Figure 7.17 shows AC impedance spectra (Cole-Cole or Nyquist plots) of 2.5 %, 5 %, 7.5 % and 10 % PC plasticized 50/50 PMMA/CA blends at different temperatures, respectively.

The impedance responses due to the bulk resistance of the electrolyte and electrolyte-electrode double layer capacitance behavior of the samples over the whole range of frequency evaluated has been discussed in the chapter 3, section 3.2.5 of the thesis. AC impedance spectra of 2.5 %, 5 %, 7.5 % and 10 % PC plasticized 50/50 PMMA/CAP, PMMA/CAB and PMMA/CAPh blends at different temperatures, respectively have shown the similar trend for electrochemical impedance spectra.

7.2.5.1 Proton conductivity measurement

The variation of conductivity of the blends with temperature and room temperature conductivity of the blends are shown in Figure 7.18, Figure 7.19, Figure 7.20 and Figure 7.21 respectively. It has been observed that at 30 °C, among the polyblends studied the blends with 2.5 % PC plasticized PMMA/CA, PMMA/CAP, PMMA/CAB and PMMA/CAPh 30/70 composition showed the highest proton conductivity value of $2.07 \times 10^{-3} \text{ S cm}^{-1}$, $2.59 \times 10^{-3} \text{ S cm}^{-1}$, $2.65 \times 10^{-3} \text{ S cm}^{-1}$ and $2.77 \times 10^{-3} \text{ S cm}^{-1}$, respectively. The proton conductivity increased as the temperature is increased in the measured temperature range between 30 °C to 70 °C. Also, it has been found from impedance plots that as the temperature is increased, the bulk resistance R decreased

resulting in an increase in the value of proton conductivity. This may be mainly due to the fact that at higher temperature, there is an enhancement in the ion movement, favoring conductivity. Proton conductivity measurement of 5 %, 7.5 % and 10 % PC plasticized 50/50 PMMA/CAP, PMMA/CAB and PMMA/CAPh blends at different temperatures respectively have shown the similar trend.

7.2.5.2 Temperature dependence of ionic conductivity

It has been found that the proton conductivity of the blend film increased with increasing temperature for all compositions. This may be mainly due to the fact that an increase in temperature increases the mobility of ions and this in turn increases the conductivity. Further, the vibrational motion of the polymer backbone and side chains, which becomes more vigorous with increase in temperature can also facilitate the conduction of ions. The increased amplitude of vibration brings the coordination sites closer to one another enabling the ions to hop from the occupied site to the unoccupied site with lesser energy required. Increase in amplitude of vibration of the polymer backbone and side chains can also increase the fraction of free volume in the polymer electrolyte system (Aziz et al. 2010). Druger et al. (1983) and Druger et al. (1985) have attributed the change in conductivity with temperature in solid polymer electrolyte to hopping model, which results in an increase in the free volume of the system. The hopping model either permits the ions to hop from one site to another or provides a pathway for ions to move. In other words, this facilitates translational motion of the ions. From this, it is clear that the ionic motion is due to translational motion/hopping facilitated by the polymer. The nonexistence of any unusual variation of conductivity indicates the existence of overall amorphous region (Aziz et al. 2010). This implies that coupling of the ion movement with the amorphous nature of the polymer is facilitating the conductivity in the blends.

Electrical conduction is a thermally activated process and follows the Arrhenius law

$$\sigma = \sigma_o \exp \left[- \frac{E_a}{kT} \right] \quad (2.3)$$

where, σ is the conductivity at a particular temperature, σ_0 is the pre-exponential factor, k is the Boltzmann's constant, and T is the absolute temperature. As there is no sudden change in the value of conductivity with temperature it may be inferred that these blends do not undergo any phase transitions within the temperature range studied. The conductivity has been discussed on the basis of the increase in the CA contents along with the ion exchange capacity and water absorption facilitating the ion hopping through the polymer structure has been detailed in chapter 3, section 3.2.5.2 of the thesis.

7.2.6 Dielectric Studies

The dielectric constant and loss of the films have been calculated using the equations 1.11 and 1.12 respectively. The conductivity behavior of polymer electrolyte can be understood from dielectric studies (Ramesh et al. 2002). The dielectric constant is a measure of stored charge. The variations of dielectric constant and dielectric loss with frequency at different temperatures have been shown in Figure 7.22, Figure 7.23, Figure 7.24 and Figure 7.25 respectively, for 2.5 %, 5 %, 7.5 % and 10 % PC plasticized 50/50 PMMA/CA blends. Similar trends have also been seen for 2.5 %, 5 %, 7.5 % and 10 % PC plasticized 50/50 PMMA/CAP, PMMA/CAB and PMMA/CAPh blends at different temperatures.

There are no appreciable relaxation peaks observed, indicating the electrode polarization and space charge effects have occurred confirming non-debye dependence; the increase in dielectric constant and dielectric loss at higher temperatures due to the higher charge carrier density and conductivity of the polymer blends due to hopping mechanism has been discussed in the chapter 3, section 3.2.6 in the thesis.

7.3 FIGURES

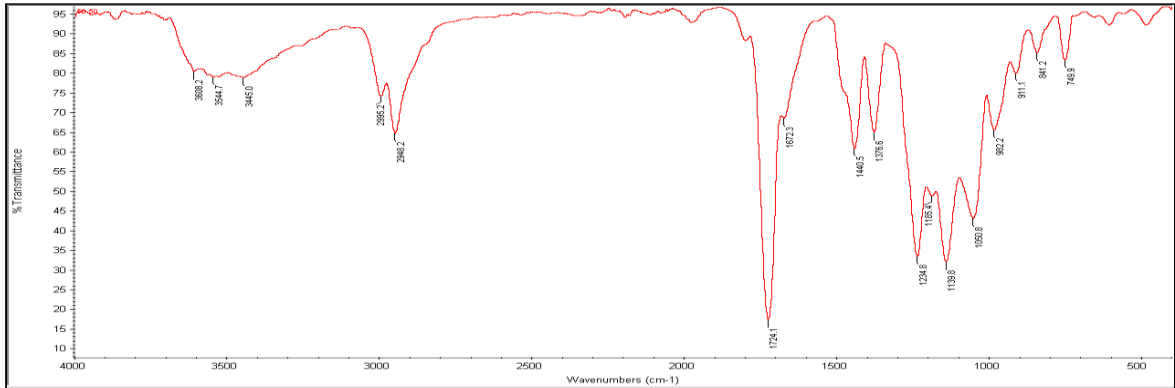


Figure 7.1 FTIR Spectrum of 2.5 % PC plasticized 50/50 PMMA/CA blend.

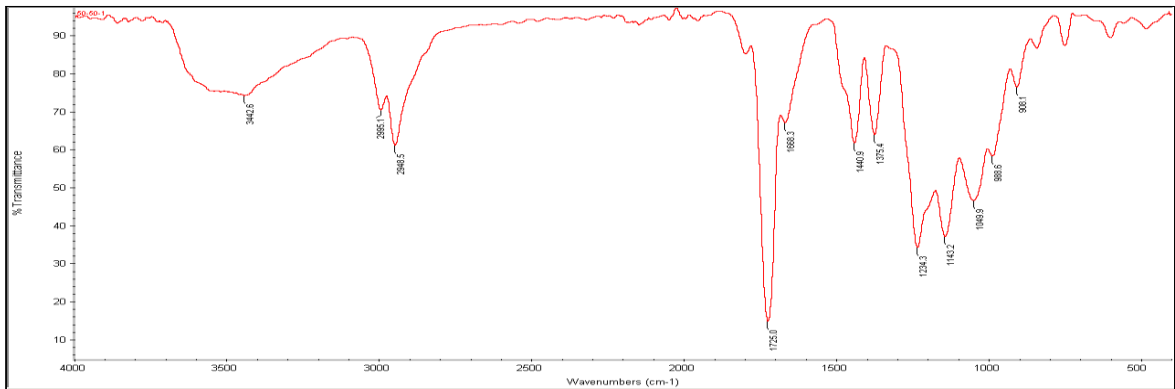


Figure 7.2 FTIR Spectrum of 5 % PC plasticized 50/50 PMMA/CA blend.

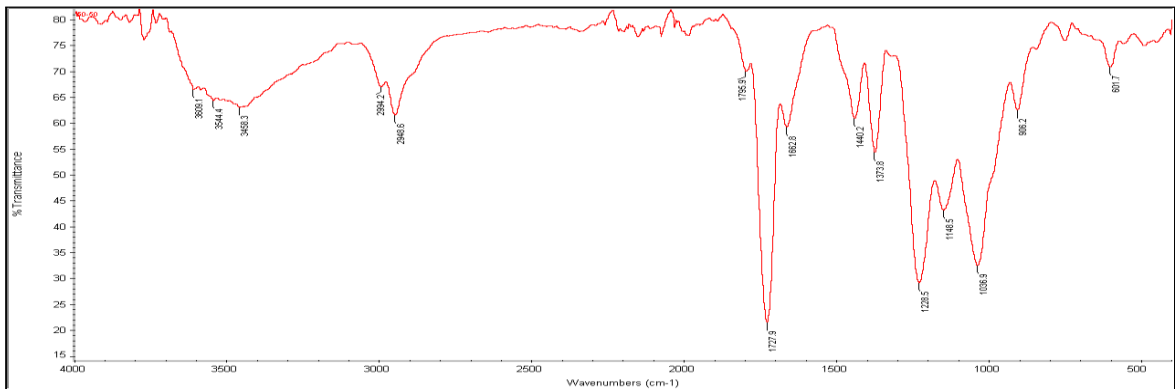


Figure 7.3 FTIR Spectrum of 7.5 % PC plasticized 50/50 PMMA/CA blend.

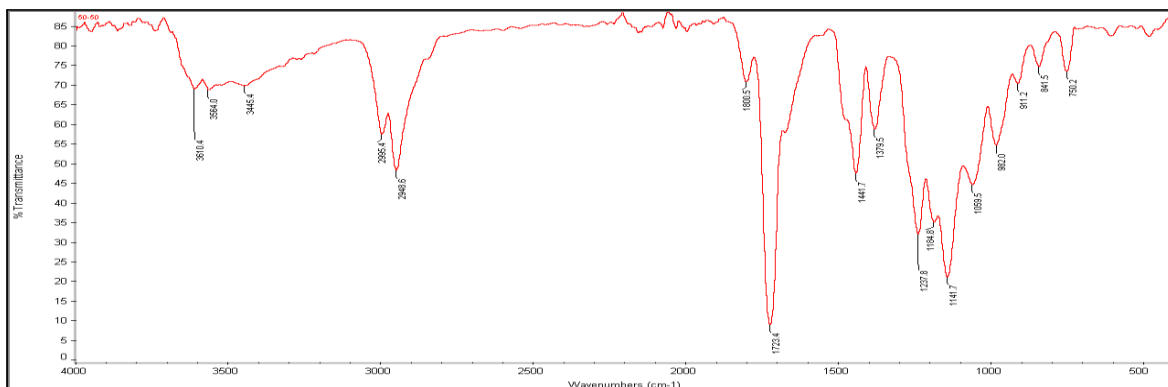


Figure 7.4 FTIR Spectrum of 10 % PC plasticized 50/50 PMMA/CA blend.

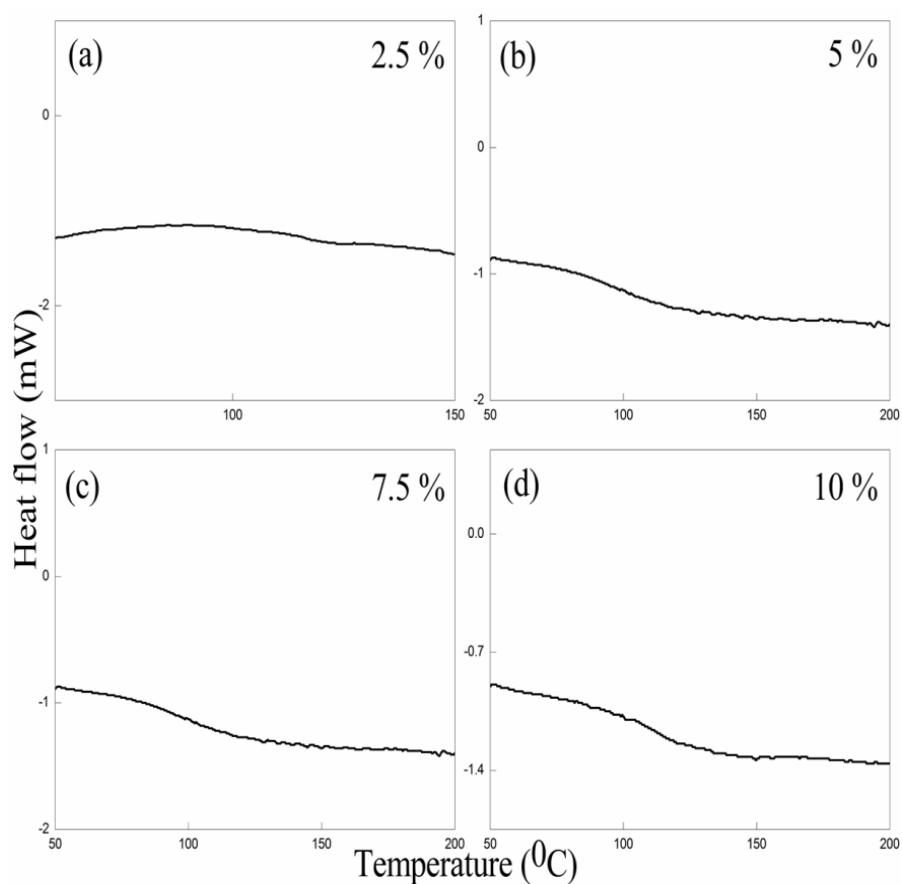


Figure 7.5 (a), (b), (c) and (d) DSC scans of 2.5 %, 5 %, 7.5 % and 10 % PC plasticized 50/50 PMMA/CA blends.

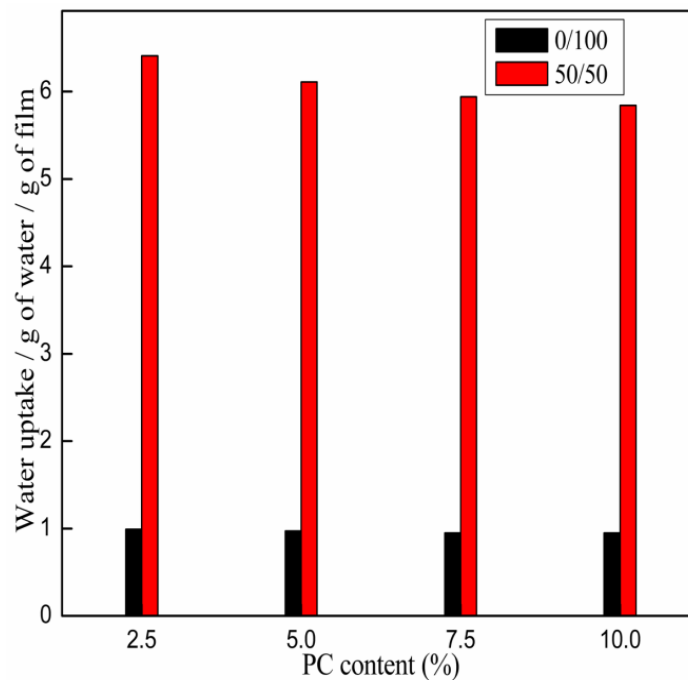


Figure 7.6 Water absorption by 2.5 %, 5 %, 7.5 % and 10 % PC plasticized 0/100 and 50/50 PMMA/CA blends.

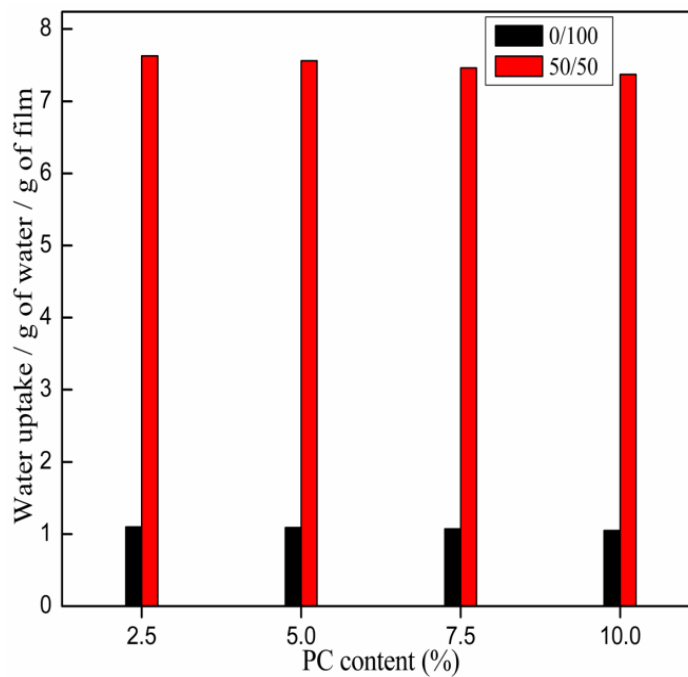


Figure 7.7 Water absorption by 2.5 %, 5 %, 7.5 % and 10 % PC plasticized 0/100 and 50/50 PMMA/CAP blends.

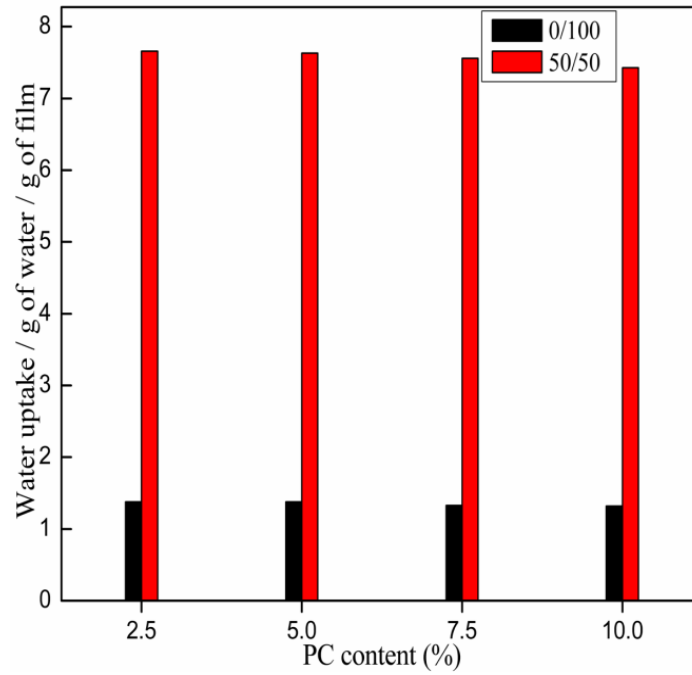


Figure 7.8 Water absorption by 2.5 %, 5 %, 7.5 % and 10 % PC plasticized 0/100 and 50/50 PMMA/CAB blends.

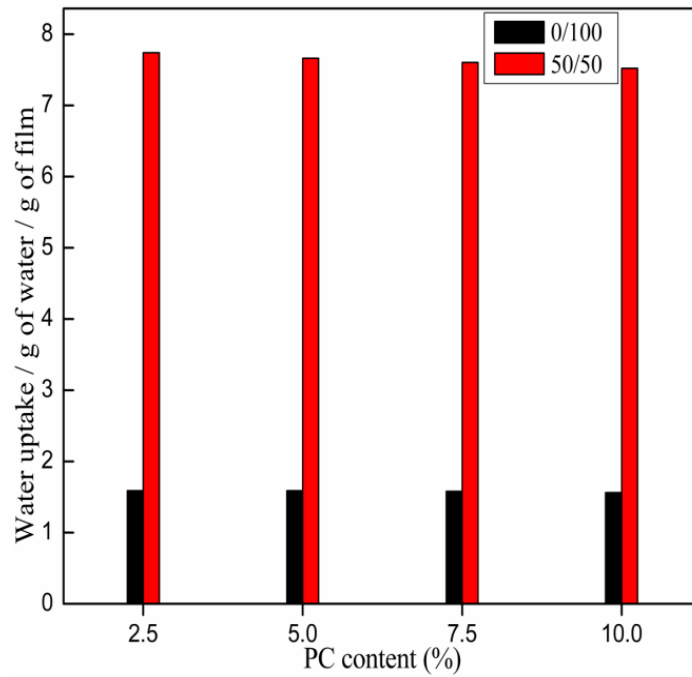


Figure 7.9 Water absorption by 2.5 %, 5 %, 7.5 % and 10 % PC plasticized 0/100 and 50/50 PMMA/CAPh blends.

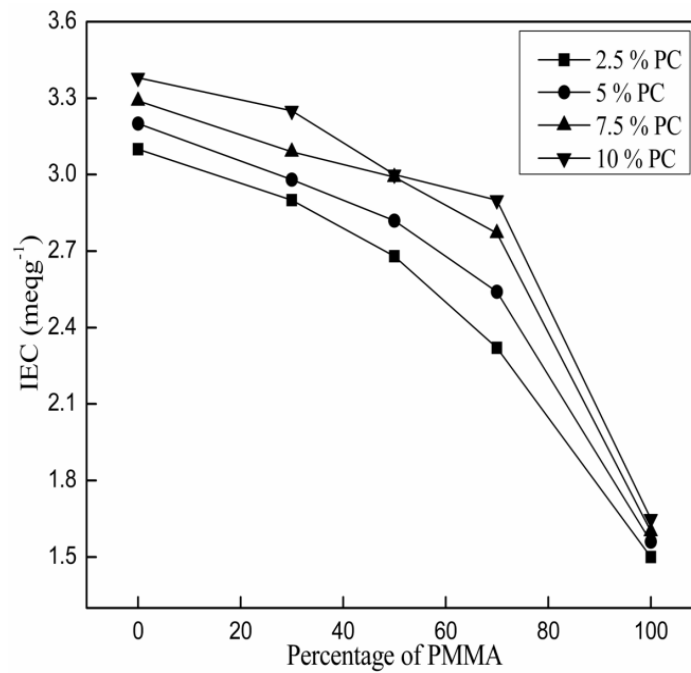


Figure 7.10 The change of IEC values in 2.5 %, 5 %, 7.5 % and 10 % PC plasticized PMMA/CA blends.

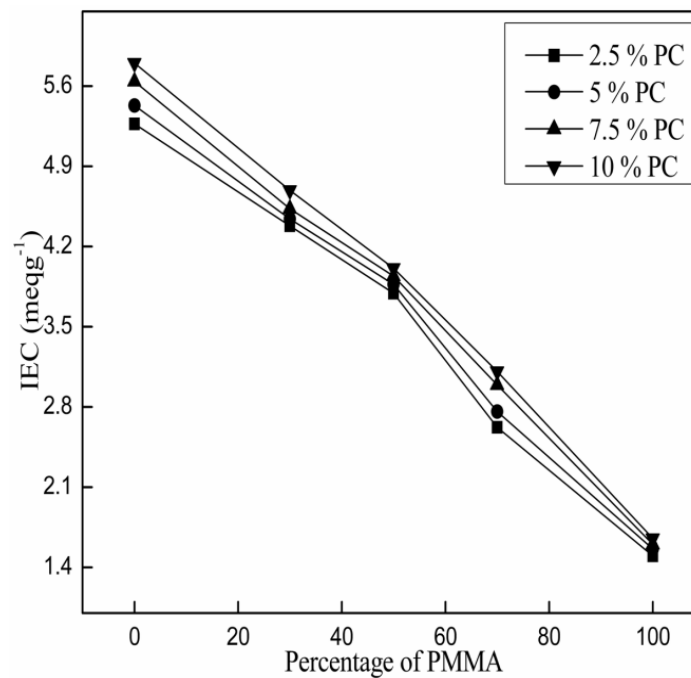


Figure 7.11 The change of IEC values in 2.5 %, 5 %, 7.5 % and 10 % PC plasticized PMMA/CAP blends.

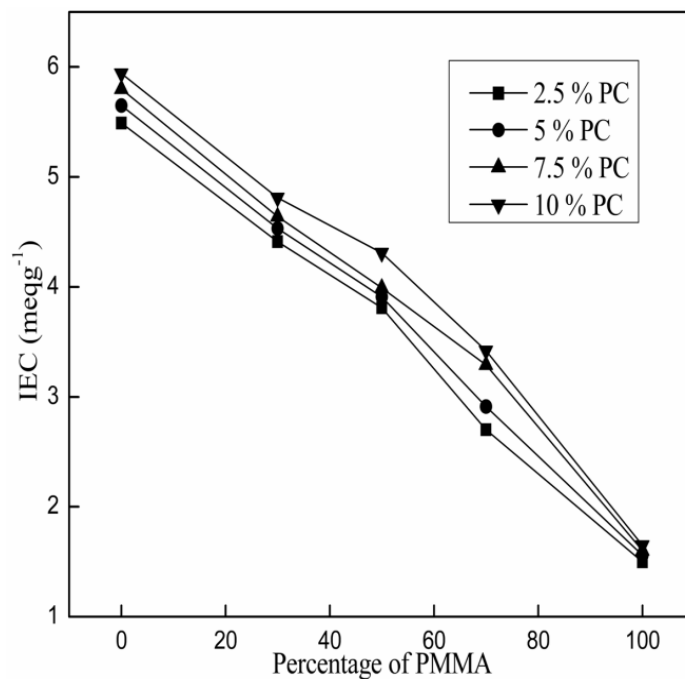


Figure 7.12 The change of IEC values in 2.5 %, 5 %, 7.5 % and 10 % PC plasticized PMMA/CAB blends.

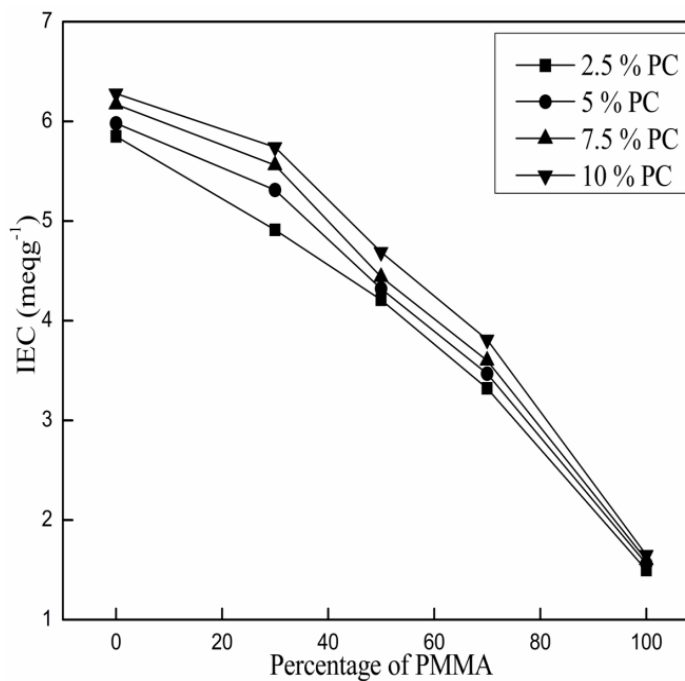


Figure 7.13 The change of IEC values in 2.5 %, 5 %, 7.5 % and 10 % PC plasticized PMMA/CAPh blends.

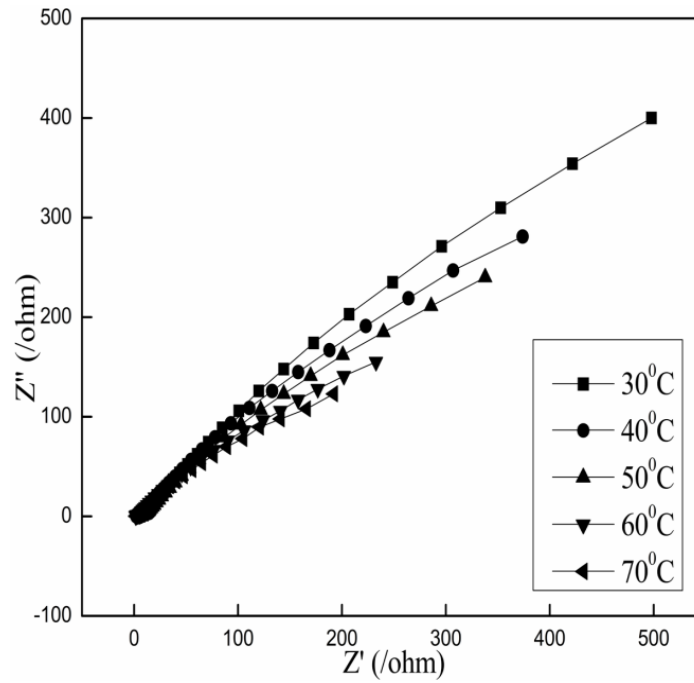


Figure 7.14 AC impedance spectrum of 2.5 % PC plasticized 50/50 PMMA/CA blend at different temperatures.

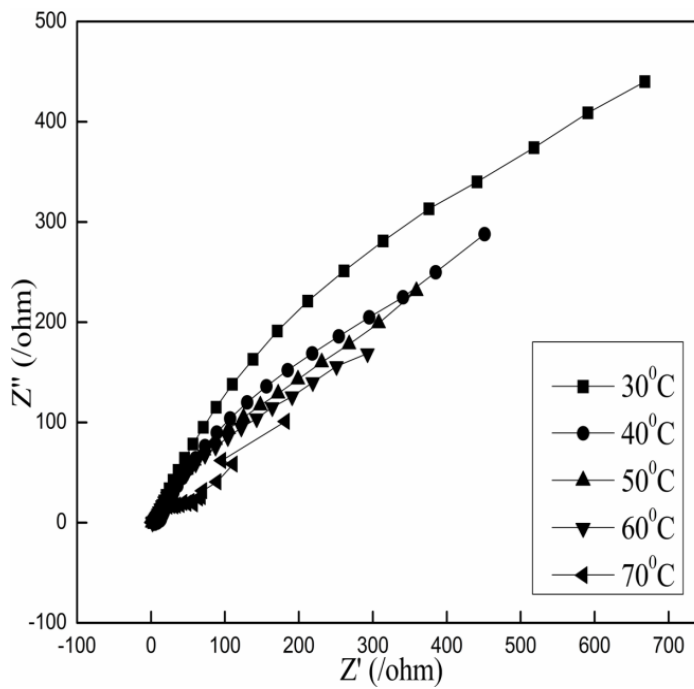


Figure 7.15 AC impedance spectrum of 5 % PC plasticized 50/50 PMMA/CA blend at different temperatures.

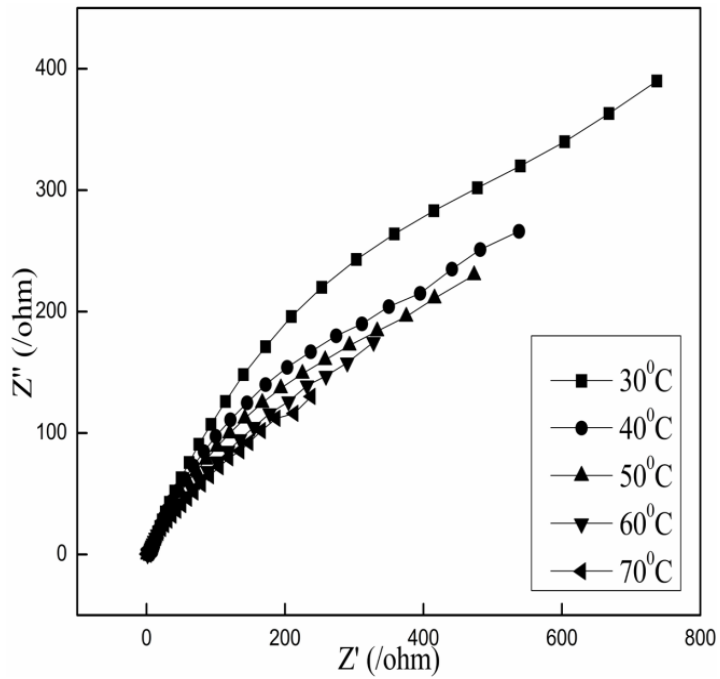


Figure 7.16 AC impedance spectrum of 7.5 % PC plasticized 50/50 PMMA/CA blend at different temperatures.

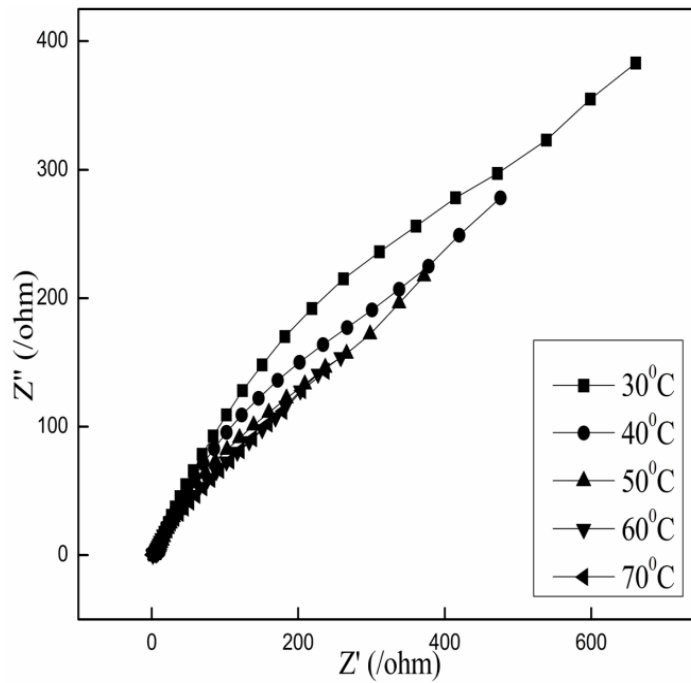


Figure 7.17 AC impedance spectrum of 10 % PC plasticized 50/50 PMMA/CA blend at different temperatures.

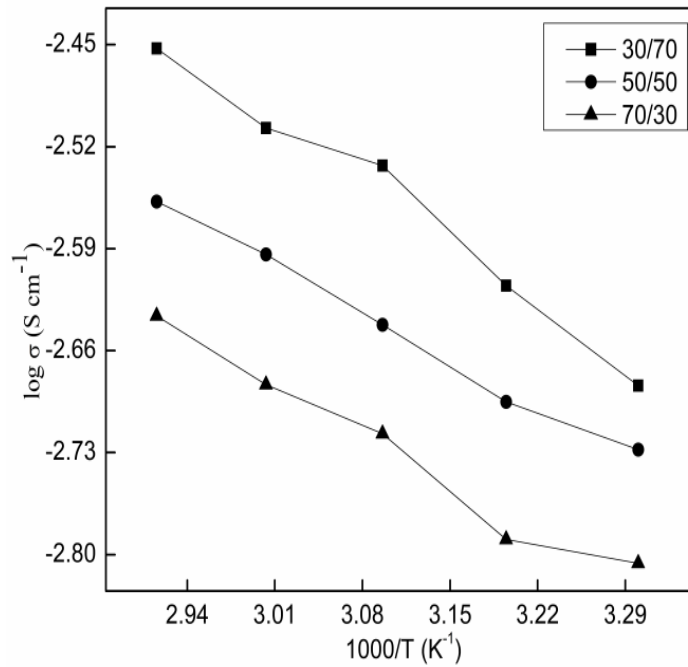


Figure 7.18 Arrhenius plots for conductivity σ of 2.5 % PC plasticized PMMA/CA blends.

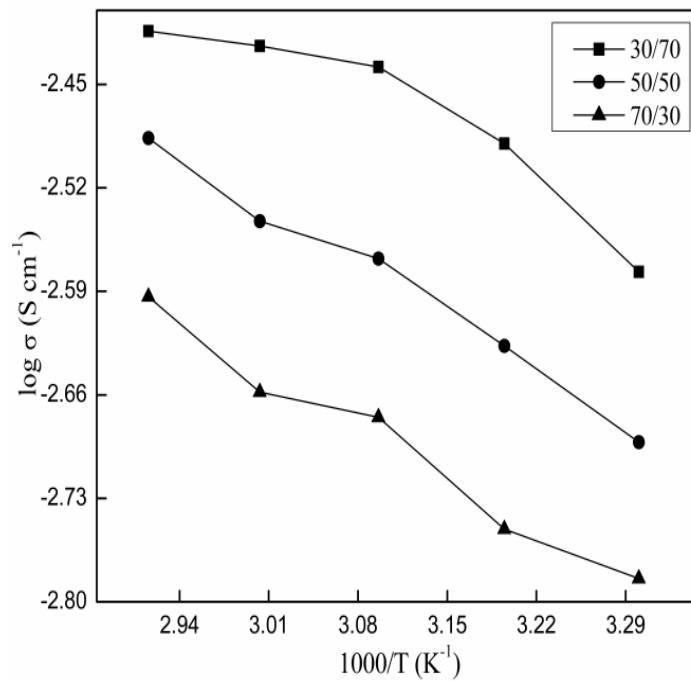


Figure 7.19 Arrhenius plots for conductivity σ of 2.5 % PC plasticized PMMA/CAP blends.

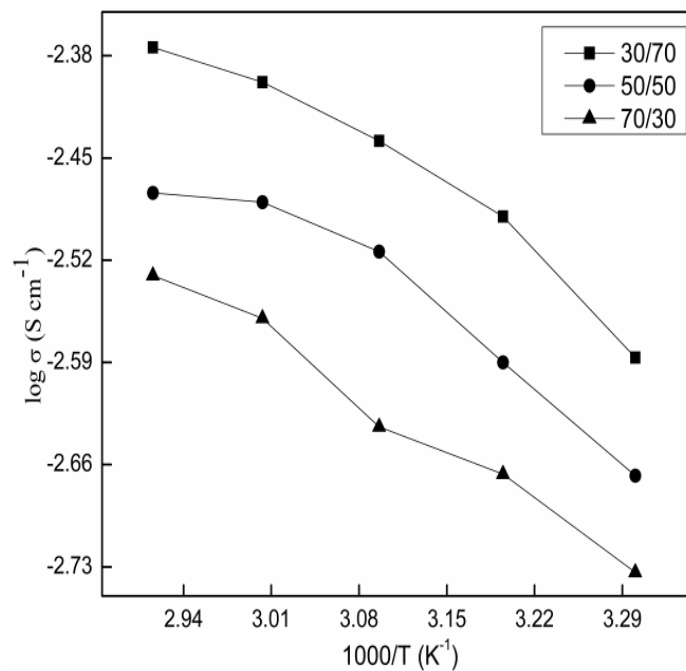


Figure 7.20 Arrhenius plots for conductivity σ of 2.5 % PC plasticized PMMA/CAB blends.

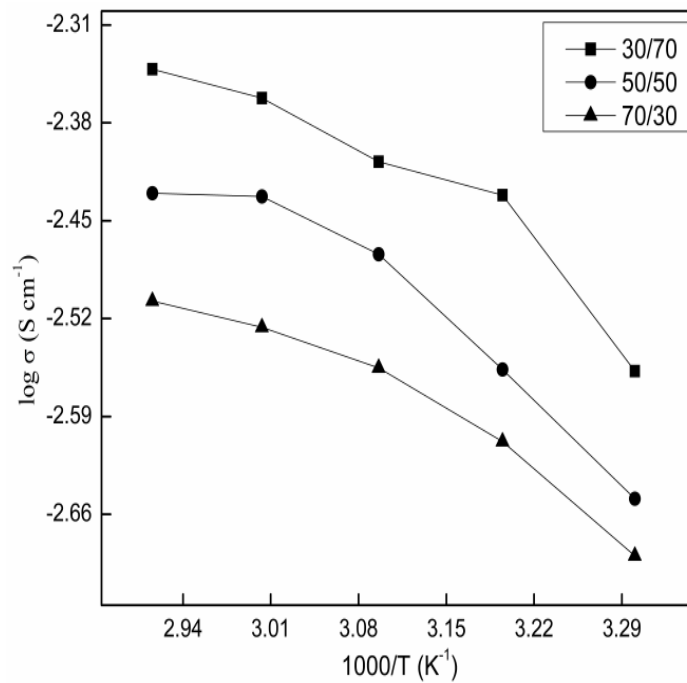


Figure 7.21 Arrhenius plots for conductivity σ of 2.5 % PC plasticized PMMA/CAPh blends.

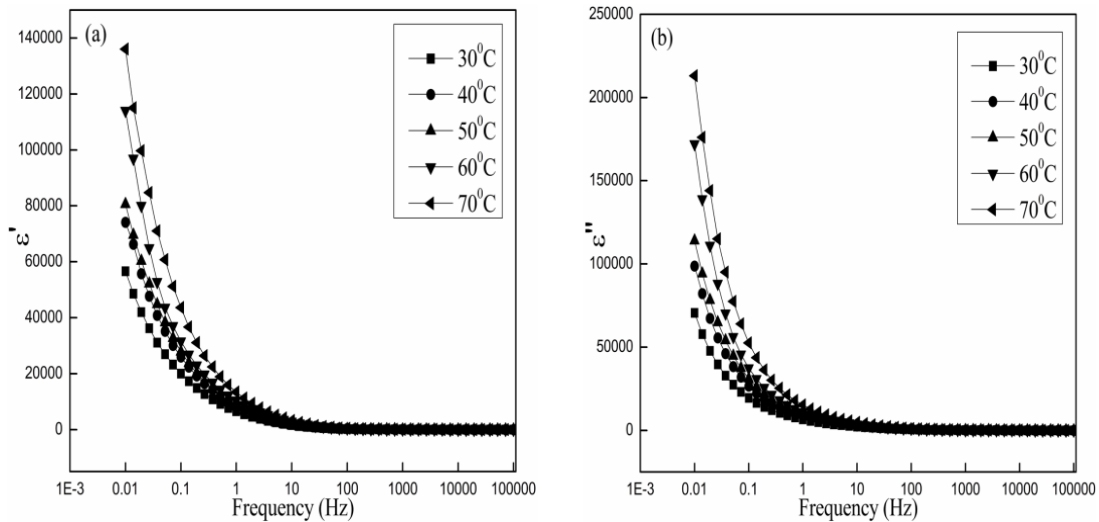


Figure 7.22 Variations of dielectric constant (a) and dielectric loss (b) with frequency at different temperatures for 2.5 % PC plasticized 50/50 PMMA/CA blend.

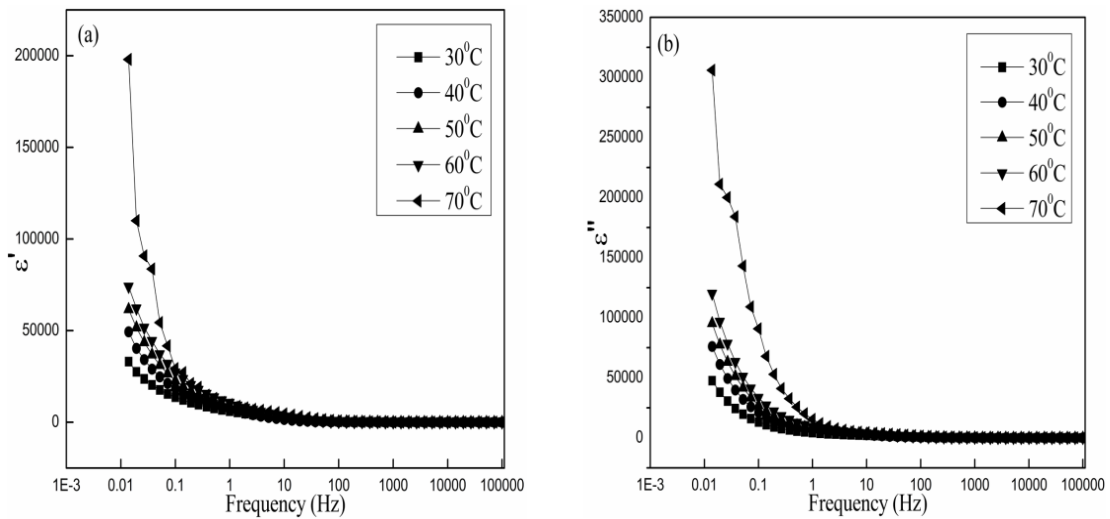


Figure 7.23 Variations of dielectric constant (a) and dielectric loss (b) with frequency at different temperatures for 5 % PC plasticized 50/50 PMMA/CA blend.

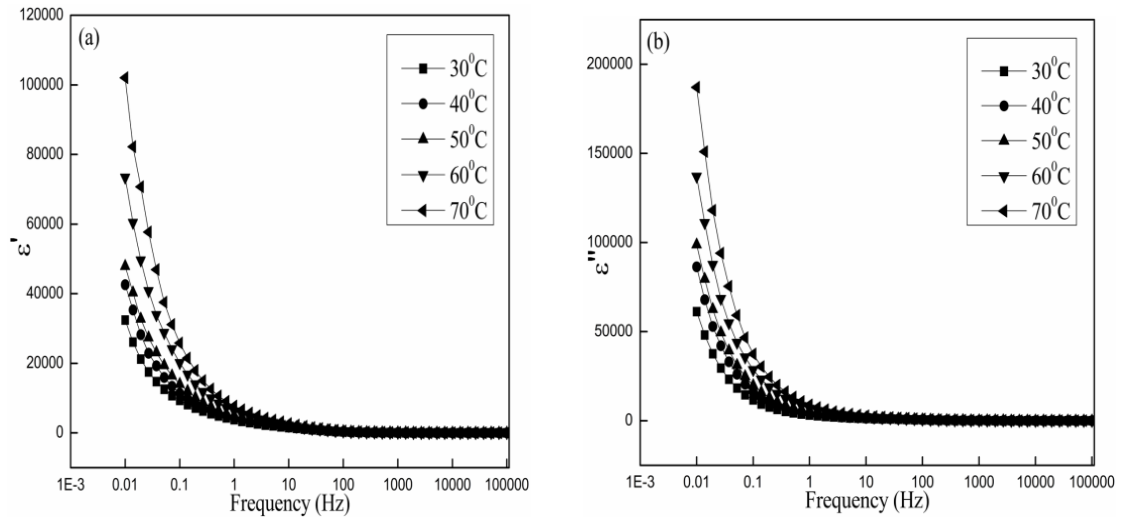


Figure 7.24 Variations of dielectric constant (a) and dielectric loss (b) with frequency at different temperatures for 7.5 % PC plasticized 50/50 PMMA/CA blend.

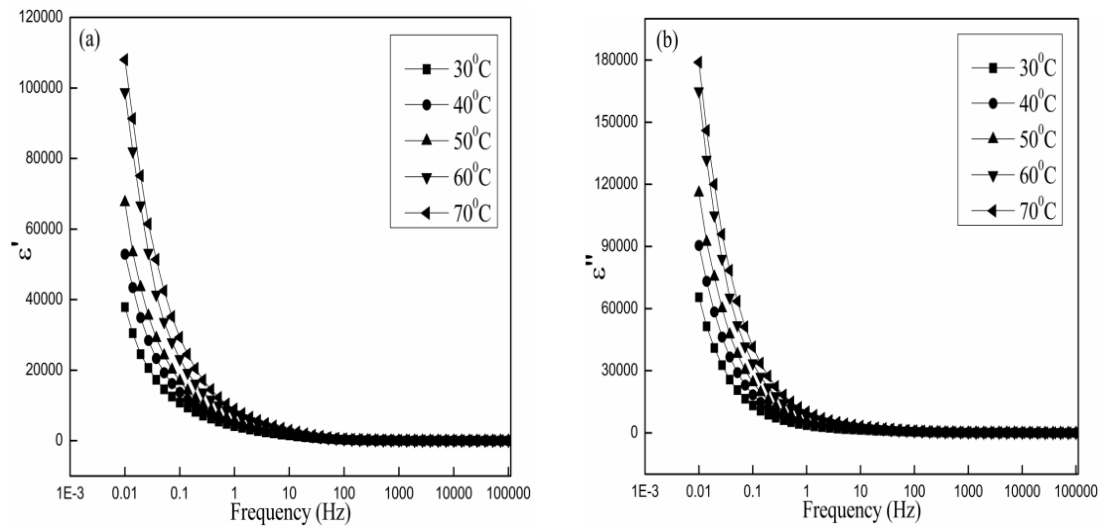


Figure 7.25 Variations of dielectric constant (a) and dielectric loss (b) with frequency at different temperatures for 10 % PC plasticized 50/50 PMMA/CA blend.

7.4 TABLES

Table 7.1 IR stretching frequencies of PC plasticized PMMA/CA, PMMA/CAP, PMMA/CAB and PMMA/CAPh blends.

PMMA/CA 2.5 PC	-CO Stretching Frequencies	-OH Stretching Frequencies
0/100	1734.7	3468.3
50/50	1724.1	3445.0
PMMA/CA 5 PC		
0/100	1734.1	3465.6
50/50	1725.0	3442.6
PMMA/CA 7.5 PC		
0/100	1734.3	3467.2
50/50	1727.9	3458.3
PMMA/CA 10 PC		
0/100	1734.5	3464.4
50/50	1723.4	3445.4
PMMA/CAP 2.5 PC		
0/100	1737.6	3470.3
50/50	1722.9	3439.9
PMMA/CAP 5 PC		
0/100	1737.0	3491.2
50/50	1723.2	3448.1
PMMA/CAP 7.5 PC		
0/100	1736.5	3473.3
50/50	1723.1	3440.5
PMMA/CAP 10 PC		
0/100	1736.9	3479.6
50/50	1723.5	3557.6
PMMA/CAB 2.5 PC		
0/100	1737.6	3481.0
50/50	1726.9	3560.0
PMMA/CAB 5 PC		
0/100	1737.9	3487.3
50/50	1727.8	3448.9

PMMA/CAB 7.5 PC		
0/100	1737.7	3494.1
50/50	1722.7	3438.3
PMMA/CAB 10 PC		
0/100	1737.7	3482.3
50/50	1723.5	3584.7
PMMA/CAPh 2.5 PC		
0/100	1661.0	3420.3
50/50	1714.9	3404.7
PMMA/CAPh 5 PC		
0/100	1662.6	3394.1
50/50	1716.8	3400.9
PMMA/CAPh 7.5 PC		
0/100	1661.7	3402.0
50/50	1719.5	3424.7
PMMA/CAPh 10 PC		
0/100	1664.2	3404.3
50/50	1667.8	3413.5

Table 7.2 Thermal properties of 2.5 %, 5 %, 7.5 % and 10 % PC plasticized PMMA/CA, PMMA/CAP, PMMA/CAB and PMMA/CAPh blends.

Sample	T_g (°C)	Fox equation	k values	Gordon-Taylor equation
PMMA/CA 2.5 PC				
0/100	172.49	172.49		172.49
30/70	121.90	145.10		121.37
50/50	112.94	131.21	0.13	113.53
70/30	109.25	119.74		109.39
100/0	105.87	105.87		105.87
PMMA/CA 5 PC				
0/100	172.43	172.43		172.43
30/70	121.66	144.78		120.96
50/50	112.30	130.79	0.13	113.07
70/30	108.94	119.27		108.89
100/0	105.35	105.35		105.35
PMMA/CA 7.5 PC				
0/100	171.92	171.92		171.92
30/70	121.34	144.35		120.61
50/50	112.10	130.41	0.13	112.74
70/30	108.25	118.93		108.58
100/0	105.05	105.05		105.05
PMMA/CA 10 PC				
0/100	171.81	171.81		171.81
30/70	121.06	144.27		117.63
50/50	111.32	130.33	0.1	111.06
70/30	107.03	118.86		107.74
100/0	104.99	104.99		104.99
PMMA/CAP 2.5 PC				
0/100	134.70	134.70		134.70
30/70	134.47	124.53		123.03
50/50	116.96	118.56	0.63	117.01
70/30	110.28	113.13		112.00
100/0	105.87	105.87		105.87
PMMA/CAP 5 PC				
0/100	134.68	134.68		134.68
30/70	133.86	124.30		122.22
50/50	116.11	118.22	0.58	116.12
70/30	109.61	112.71		111.19

100/0	105.35	105.35		105.35
PMMA/CAP 7.5 PC				
0/100	134.61	134.61		134.61
30/70	133.28	124.13		121.25
50/50	115.08	118.01	0.52	115.16
70/30	108.30	112.46		110.44
100/0	105.05	105.05		105.05
PMMA/CAP 10 PC				
0/100	134.53	134.53		134.53
30/70	132.44	124.06		120.28
50/50	114.22	117.94	0.46	114.30
70/30	107.58	112.39		109.85
100/0	104.99	104.99		104.99
PMMA/CAB 2.5 PC				
0/100	128.71	128.71		128.71
30/70	119.10	120.89		116.90
50/50	112.36	116.18	0.4	112.40
70/30	107.29	111.82		109.21
100/0	105.87	105.87		105.87
PMMA/CAB 5 PC				
0/100	127.81	127.81		127.81
30/70	118.18	120.13		116.47
50/50	112.06	115.50	0.42	111.99
70/30	106.82	111.21		108.78
100/0	105.35	105.35		105.35
PMMA/CAB 7.5 PC				
0/100	127.29	127.29		127.29
30/70	117.24	119.96		116.44
50/50	111.96	115.11	0.45	111.95
70/30	106.09	110.86		108.65
100/0	105.05	105.05		105.05
PMMA/CAB 10 PC				
0/100	126.43	126.43		126.43
30/70	116.55	119.13		115.60
50/50	111.27	114.72	0.42	111.33
70/30	105.92	110.62		108.26
100/0	104.99	104.99		104.99

PMMA/CAPh 2.5 PC				
0/100	138.90	138.90		138.90
30/70	137.50	127.01		137.14
50/50	135.10	120.16	7.6	135.06
70/30	130.25	114.00		131.14
100/0	105.87	105.87		105.87
PMMA/CAPh 5 PC				
0/100	137.20	137.20		137.20
30/70	136.80	125.79		135.69
50/50	134.02	119.18	8.6	133.88
70/30	129.43	113.24		130.40
100/0	105.35	105.35		105.35
PMMA/CAPh 7.5 PC				
0/100	136.40	136.40		136.40
30/70	135.85	125.19		134.98
50/50	133.31	118.69	9	133.27
70/30	129.07	112.83		129.95
100/0	105.05	105.05		105.05
PMMA/CAPh 10 PC				
0/100	136.40	136.40		136.40
30/70	135.30	125.17		134.59
50/50	130.00	118.65	7	132.47
70/30	128.39	112.78		128.55
100/0	104.99	104.99		104.99

Chapter 8

SUMMARY AND CONCLUSIONS

Chapter 8 presents the summary of the work discussed in this thesis along with the conclusions drawn. Scope for the future work has also been included here at the end.

8.1 SUMMARY AND CONCLUSIONS

The work presented in this thesis has been broadly divided into eight chapters with subsections in each chapter. The **first chapter** titled “**Introduction**” gives introduction to the subject of polymer blends, factors influencing miscibility/immiscibility, concept of glass-transition temperature, followed by methodology and characterization techniques. Subsequent sections brief about review of literature, scope and objectives of the present work along with materials and methods adopted in the present investigation.

Chapter 2 describes the **miscibility, water uptake, ion exchange capacity, conductivity and dielectric studies of non-plasticized blends of PMMA with CA, CAP, CAB and CAPH**. A brief account on polymers used has been included in this chapter. The blends of PMMA with CA derivatives have been prepared by solution casting method. The non-plasticized PMMA with CA derivatives blends has been characterized by FTIR and DSC to study the miscibility of the prepared blends. The membrane properties like water uptake and ion exchange capacity has been studied for the prepared blends. The conductivity and dielectric studies have been carried out for the prepared non-plasticized blends at different temperatures.

FTIR spectrum of the individual and blend polymer films have been measured at room temperature to identify the presence of hydrogen bonding in the blends and hence the miscibility of blends in the solid state. FTIR spectra of most of the blends showed a considerable shift in their carbonyl and hydroxyl vibration frequencies. DSC scans have also been measured for prepared blends. It is interesting to note here that the thermograms for the blends exhibited single T_g . Further, the T_g values of the blend films decreased regularly on increase of PMMA content in the blends. T_g of the blend films was generally found to be intermediate of the T_g values of the component polymers. Such a systematic variation of T_g in the blends is indicative of miscibility of the components in the blends. The T_g values have further been confirmed with Fox and Gordon-Taylor

equations. The values calculated from the theoretical equations are well matching with the experimentally obtained data.

The water uptake study revealed that the prepared non-plasticized PMMA with CA derivatives blends have considerable water absorption capacity. Among the prepared blends 50% blends have shown maximum water uptake. At this composition the structure of the blends formed may be with maximum amount of voids. The hydrogen bonding between the components of the blends at this composition may be facilitating maximum voids. At other compositions the component polymers may be blending in a gradually more compact structured pattern with reduction in voids and hence in turn reducing the water absorption.

The IEC values decrease for the blends with an increase in PMMA content. It is known that CA derivatives has exchangeable –OH groups. Hence it is evident that when PMMA content of the blend is increased, the number of replaceable sites available in the blend would decrease and hence the decrease in the IEC of the blends.

The electrochemical impedance spectroscopic studies have been carried out from 30 °C to 70 °C in order to get the R, bulk resistance values. The proton conductivity values have been calculated using the R values. With increase in temperature, the R, bulk resistance decreased intern increase in the proton conductivity values has been observed. The proton conductivities of the blends were in the order of 10^{-3} S cm⁻¹. This may be mainly due to the fact that at higher temperature, there is an enhancement in the ion movement, favoring conductivity. The dielectric constant and dielectric loss studies have been done on the prepared non-plasticized blends. There are no appreciable relaxation peaks observed in the frequency range employed in this study. Both dielectric constant and dielectric loss rise sharply at low frequencies indicating that electrode polarization and space charge effects have occurred confirming non-debye dependence. The dielectric constant and dielectric loss increases at higher temperatures due to the higher charge carrier density.

In conclusion, the results of this study indicated that the prepared non-plasticized blends are miscible in the entire composition range. The FTIR studies of the blend films

also indicated the presence of weak hydrogen bonding interactions, supporting the miscibility of the blends. DSC study of the blends also supports that the blends are miscible. The water uptake study supports the voids present in the prepared blends, which intern supports the hydrogen bonding interactions between the components polymers during blending. The IEC test suggests the exchangeable –OH groups in the blend matrix. The conductivity and dielectric studies supports the conductivity of the blend films under suitable ionic environment.

Chapters 3, 4, 5, 6 and 7 present miscibility, water uptake, ion exchange capacity, conductivity and dielectric studies of blends of PMMA with CA, CAP, CAB and CAPH plasticized with Dimethyl phthalate (DMP), Diethyl phthalate (DEP), Dipropyl phthalate (DPP), Dibutyl phthalate (DBP) and Propylene carbonate (PC) respectively. Each chapter includes a brief account of plasticizers used during the studies. The plasticized blends were prepared by solution casting method. The dried blends films were subjected to different characterization techniques. Miscibility of the blends was studied using FTIR and DSC techniques. The water uptake and ion exchange capacity tests have been performed on the prepared plasticized blends. The conductivity and dielectric studies have been done by using electrochemical impedance spectroscopy at different temperatures.

FTIR spectrum of plasticized pure and blend polymer films have been measured to study the presence of hydrogen bonding and hence miscibility in the blends. FTIR spectra of most of the blends showed an acceptable shift in their carbonyl and hydroxyl vibration frequencies. Such shift in the specific vibration frequencies are ascribed to the formation of a weak hydrogen bond between component polymers in the blend. This can also be contributing to the miscibility of the blends. DSC scans have also been measured for prepared plasticized blends. The addition of plasticizers introduces more free volume to the polymer, which lowers the glass transition temperature. This effect is due to the reduction in cohesive forces of attraction between the polymer chains. The studied blends have shown single T_g and are intermediate of the T_g values of the component plasticized polymers, further indicating the miscibility of the components in the blends. The T_g

values of the plasticized blends have shown the decrease in the trend when compared to the non-plasticized blends, indicating the action of plasticizers. Incorporation of the plasticizers decreases the T_g of the component as well as blends films to considerable extent. Among the plasticizers studied, DBP plasticized blends has shown highest values of T_g for all the series of blends studied compared to PC plasticized blends. This may attributed due to the molecular weight of the plasticizers. The T_g values are well comparable with Fox and Gordon-Taylor equations.

The water uptake study has been conducted on plasticized PMMA with CA derivatives blends. Among the prepared plasticized blends 50 % blends have shown maximum water uptake. This may be due to the voids present in the blends and which is indicative of weak hydrogen bond formation during the blend formation. Since the molecular weight of PC polymer is low, the PC plasticized series has shown maximum water absorption compared to DBP plasticized series.

The IEC test has been conducted for plasticized PMMA with CA derivatives blends. In each plasticized series, the IEC values decreases with an increase in PMMA content, respectively. The polymer blend series with PC plasticizer has shown highest ion exchange capacity compared with DMP, DEP, DPP and DBP plasticized blend series. Since the molecular weight of the PC is low compared to other plasticizers, it can easily penetrate into the bulk of the polymer matrix, establishing the exchange of ions with medium.

The proton conductivity and dielectric studies have been calculated using electrochemical impedance spectroscopy at different temperatures (30 °C to 70 °C). The proton conductivities of the plasticized blends were in the order of 10^{-3} S cm^{-1} . Plasticizers molecules being relatively small in size compared with polymer molecules penetrate in to the polymer matrix and establish attractive force between the plasticizer molecule and polymer chain. These attractive forces reduce the cohesive force between the polymer chains and increase the ionic conduction thus enhancing the conductivity i.e., the plasticizer can interrupt polymer-polymer interactions by occupying inter and intra chain free volume. In the present study plasticizer PC has shown maximum conductivity

compared to DMP, DEP, DPP and DBP plasticizers. The parameters like low molecular weight, small size and high dielectric constant of plasticizer PC enabling it to show high conductivity compared with other plasticizers.

The dielectric constant and dielectric loss studies have been done on the prepared plasticized blends. There are no appreciable relaxation peaks observed in the frequency range employed in this study indicating non-debye dependence. The dielectric constant and dielectric loss increases at higher temperatures due to the higher charge carrier density.

With increasing plasticizer content and for a fixed frequency, the conductivity value of the polymer blends increases. This shows that the plasticizer has increased the conductivity of the polymer blends. Therefore the number of mobile ions in the sample increases and since the conductivity is proportional to the number of mobile ions, the conductivity is therefore increased. It is quite obvious that salt is the agent responsible for conductivity of the polymer blends as other components of the blends do not have such species. The role of the plasticizer here is to increase the mobility of the ions so that the conductivity of polymer blend increases. Alternatively, plasticization can also increase ionic mobility by reducing the potential barrier to ionic motion as a result of the decreasing cation-anion coordination of the salt. Since no significant relaxation peaks have been observed in the dielectric constant and dielectric loss-frequency spectrum, it is inferred that the bulk electrolyte does not contribute much towards conductivity enhancement. This indicates that the polymer blends have shown conductivity due to hopping mechanism.

In conclusion, the results of this study indicated that the prepared plasticized blends are miscible in the entire composition range. The FTIR studies of the blend films also indicated the presence of weak hydrogen bonding interactions, supporting the miscibility of the blends. DSC study of the blends also supports that the blends are miscible. The T_g values of the plasticized blends have shown the decrease in the trend when compared to the non-plasticized blends, indicating the action of plasticizers. The water uptake study supports the voids present in the prepared blends, which intern

supports the hydrogen bonding interactions between the components polymers during blending. The water uptake trend in plasticized blends decreased compared to non-plasticized blends. The IEC test has shown increasing trend compared to non-plasticized blends, indicating the action of plasticizers. The conductivity and dielectric studies supports the conductivity of the blend films under suitable ionic environment.

Based on the above discussion and summary, the following conclusions can be drawn.

- Plasticized and non-plasticized PMMA/CA derivatives blends can be successfully prepared by solution casting method.
- The results suggest that homogeneous polymer blend films are formed over all the blend compositions.
- FTIR spectral bands of the plasticized and non-plasticized blends have been assigned to different specific frequencies.
- A single glass transition temperature was observed for all the plasticized and non-plasticized PMMA/CA derivatives blends. The T_g value increased upon decreasing the content of PMMA.
- The order of T_g among plasticized series is as follows: PC<DMP<DEP<DPP<DBP.
- FTIR and DSC results suggest that these blend systems are compatible and miscible.
- The increase in PMMA content reduced water uptake of the plasticized and non-plasticized blends significantly. Particularly a sudden drop in water uptake was observed after 50 wt. % of PMMA in the blend. This may be due to unfavorable structure formation at these compositions.
- The order of water uptake in plasticized series is: DBP<DPP<DEP<DMP<PC.
- The ion exchange capacity decreases, for the blends with an increase in PMMA content for plasticized and non-plasticized PMMA/CA derivatives blends, indicating exchangeable –OH groups in the blend matrix.

- For plasticized series, ion exchange capacity increases in the order: DBP<DPP<DEP<DMP<PC.
- AC impedance spectroscopy was used to measure the conductivity and dielectric studies of the plasticized and non-plasticized PMMA and CA derivatives blends, at different temperatures (30 °C to 70 °C).
- For plasticized and non-plasticized PMMA and CA derivatives blends the proton conductivities of the blends were in the order of 10^{-3} S cm⁻¹.
- For plasticized blends of PMMA and CA derivatives, the proton conductivities of the blends are in the order: DBP<DPP<DEP<DMP<PC.
- The dielectric constant and dielectric loss studies have been done on the prepared plasticized and non-plasticized blends. There are no appreciable relaxation peaks observed in the frequency range employed in this study indicating non-debye dependence. The dielectric constant and dielectric loss increases at higher temperatures due to the higher charge carrier density.

Finally, summary and conclusions of the above study along with scope for future work have been given in **Chapter 8**. The plasticized and non-plasticized polymer blends have been prepared by solution casting method. Miscibility of the blends has been analyzed by FTIR and DSC. It is confirm that the blends are miscible in the entire composition range. Membrane properties have been studied by water uptake and ion exchange capacity tests. Electrochemical impedance spectroscopy study has been carried out in order to calculate the proton conductivity as well as dielectric studies. The plasticized blends have shown increased proton conductivity and dielectric study measurement compared to non-plasticized blends. This further confirms that the plasticized blends have shown enhanced hopping mechanism compared to non-plasticized blends.

8.2 SCOPE FOR THE FUTURE WORK

In the present era, polymer blends have become the focus of study for material scientists. Since polymer blending is effective and more economical route to design the article of interest, which may have the similar properties of that of existing material. Presently, the preparation of polymer blends and characterization is rapidly being taken up by many material scientists around the globe. As per the requirement, the polymers can be chosen and tailored into a blends material with exciting novel properties and functionalities. The study can be further improved by the addition of additives like plasticizers, metal oxides and nanoparticles in to the polymer blends matrix. Keeping in view of these factors, the scope of the present work can be extended but not limited to the following experiments.

- Studies on the effect of employing different polymers and additives in the preparation of polymer blends.
- Miscibility of the polymer blends can be further studied by extensive use of DSC and FTIR, for solid films as well as liquid blend solutions.
- The membrane properties can be further studied by using techniques such as, pure water flux, heavy metal rejection and desalination studies.
- The study can be further continued by incorporating various plasticizers, metal oxides and nanoparticles.
- A detailed study of proton conductivity and dielectric properties of the polymer blend films would be of great interest.
- A detailed study of mechanical properties of these polymer blends are of major interest.
- The study can be further continued by plasticizing and doping various materials in to the polymer matrix, which will further enhance the proton conductivity and dielectric properties.

Since the quest for novel materials is never ending, the field of polymer blends is incredibly large and scope for the present work in future is bright.

REFERENCES

- Adoor, S.G., Manjeshwar, L.S., Rao, K.S.V.K., Naidu, B.V.K. and Aminabhavi, T.M. (2006). "Solution and Solid-State Blend Compatibility of Poly(vinyl alcohol) and Poly(methyl methacrylate)." *J. Appl. Polym. Sci.*, 100, 2415–2421.
- Aoki, D., Teramoto, Y. and Nishio, Y. (2011). "Cellulose acetate/poly(methyl methacrylate) interpenetrating networks: synthesis and estimation of thermal and mechanical properties." *Cellulose*, 18, 1441–1454.
- Artyushkova, K., Wall, B., Koenig, J. and Fulghum, J.E. (2001). "Direct correlation of x-ray photoelectron spectroscopy and Fourier transform infrared spectra and images from poly(vinyl chloride)/poly(methyl methacrylate) polymer blends." *J. Vac. Sci. Technol. A.*, 19, 2791-2799.
- Aziz, S.B., Abidin, Z.H.Z. and Arof, A.K. (2010). "Effect of silver nanoparticles on the DC conductivity in chitosan-silver triflate polymer electrolyte." *Physica B*, 405, 4429-4433.
- Badmapriya, D. and Rajalakshmi, A.N. (2011). "New polymeric film coating for colon targeting and its evaluation." *Int. J. Pharm.*, 2(7), 136-140.
- Barsoukov, E. and Macdonald, J.R. (2005). "Impedance Spectroscopy Theory, Experiment, and Applications." John Wiley & Sons, Inc., Hoboken, New Jersey, *Fundamentals of Impedance Spectroscopy*, 1-4.
- Bhat, D.K. and Kumar, M.S. (2006). "Biodegradability of PMMA blends with some cellulose derivatives." *J. Polym. Environ.*, 14, 385-392.
- Bichuch, N.A., Izvozchikova, V.A., Zaitsev, S.D., Kronman, A.G. and Semchikov, Y.D. (2004). "Behavior of Binary and Ternary Systems Based on Poly(Vinyl Chloride), Poly(Methyl Methacrylate), and Their Copolymers." *Russ. J. Appl. Chem+*, 77(8), 1345-1350.
- Billmeyer, W.F.Jr. (1970). "Textbook of Polymer Science." John Wiley & Sons, New York, *The Science of large molecules, Polymer processing*, 3-4, 458.
- Buchanan, C.M., Pearcy, B.G., White, A.W. and Wood, M.D. (1997). "The relationship between blend miscibility and biodegradation of cellulose acetate and poly(ethylene succinate) blends." *J. Environ. Polym. Degr.*, 5, 209-223.

- Chand, N. and Vashushtha, S.R. (2000). "Development, structure and strength properties of PP/PMMA/FA blends." *Bull. Mater. Sci.*, 23(2), 103-107.
- Chang, L. and Woo, E.M. (2009). "Effect of a Miscible Polymeric Diluent on Complex Formation between Isotactic and Syndiotactic Poly(methyl methacrylate)." *Ind. Eng. Chem. Res.*, 48, 3432–3440.
- Deka, M. and Kumar, A. (2010). "Enhanced ionic conductivity in novel nanocomposite gel polymer electrolyte based on intercalation of PMMA into layered LiV_3O_8 ." *J. Solid State Electrochem.*, 14, 1649–1656.
- Druger, S.D., Nitzam, A. and Ratner, M.A. (1983). "Dynamic bond percolation theory: A microscopic model for diffusion in dynamically disordered systems. I. Definition and one-dimensional case." *J. Chem. Phys.*, 79, 3133-3142.
- Druger, S.D., Nitzam, A. and Ratner, M.A. (1985). "Generalized hopping model for frequency-dependent transport in a dynamically disordered medium, with applications to polymer solid electrolytes." *Phys. Rev. B*, 31, 3939-3947.
- Durães, J.A., Drummond, A.L., Pimentel, T.A.P.F., Murta, M.M., Moreira, S.G.C. and Sales, M.J.A. (2008). "Thermal and structural behavior of buriti oil/poly(methyl methacrylate) and buriti oil/polystyrene materials." *J. Therm. Anal. Calorim.*, 92(2), 529–534.
- Eguiburu, J.L., Iruin, J.J., Berridi, M.J.F. and Roman, J.S. (1998). "Blends of amorphous and crystalline polylactides with poly(methyl methacrylate) and poly(methyl acrylate): a miscibility study." *Polymer*, 39(26), 6891–6897.
- Fox, T.G. (1956). "Influence of diluents and of copolymer composition on the glass temperature of a polymer system." *Bull. Am. Phys. Soc.*, 1, 123.
- Fu, W., Zhang, R., Li, B. and Chen, L. (2013). "Hydrogen bond interaction and dynamics in PMMA/PVPh polymer blends as revealed by advanced solid-state NMR." *Polymer*, 54, 472-479.
- Gordon, M. and Taylor, J. (1952). "Ideal copolymers and the second-order transitions of synthetic rubbers. i. non-crystalline copolymers." *J. Appl. Chem.*, 2, 493-500.
- Govindaraj, G., Baskaran, N., Shahi, K. and Monoravi, P. (1995). "Preparation, conductivity, complex permittivity and electric modulus in $\text{AgI-Ag}_2\text{O-}\text{SeO}_3\text{-}\text{MoO}_3$ glasses." *Solid State Ionics*, 76, 47-55.

Gowariker, V.R., Viswanathan, N.V. and Sreedhar, J. (2008). "Polymer Science." New age international (P) limited, Publishers, New Delhi, *The Genesis of Polymers, Glass Transition Temperature, Individual Polymers, Polymer Processing*, 9-12, 150-172, 220-221, 260, 450-475.

Hatakeyama, T. and Liu, Z. (1998). "Handbook of thermal analysis." John Wiley & Sons, England, Introduction, *The application of molecular spectroscopy to characterization of polymers*, 4-5, 387.

He, Y., Zhu, B. and Inoue, Y. (2004). "Hydrogen bonds in polymer blends." *Prog. Polym. Sci.*, 29, 1021-1051.

Hou, X. and Siow, K.S. (2001). "Electrochemical characterization of plasticized polymer electrolytes based on ABS/PMMA blends." *J. Solid State Electrochem.*, 5, 293-299.

Jeon, G.W., An, J.-E. and Jeong, Y.G. (2012). "High performance cellulose acetate propionate composites reinforced with exfoliated graphene." *Composites: Part B*, 43, 3412-3418.

Kalyanasundaram, S., Gopalan, A., Muniyandi, N., Renganathan, N.G., Saito, Y., Kataoka, H., Stephan, A.M. and Elizabeth, R.N. (2001). "Ionic Conductivity, Thermal Stability and FT-IR Studies on Plasticized PVC/PMMA Blend Polymer Electrolytes Complexed with LiAsF₆ and LiPF₆." *Ionics*, 7, 44-52.

Karlou, K. and Schneider, H.A. (2000). "DSC and p-V-T study of PVC/PMMA blends." *J. Therm. Anal. Calorim.*, 59, 59-69.

Kumar, M.S. and Bhat, D.K. (2011). "Miscibility of Poly(vinylidene fluoride) and Cellulose Acetate Blends in Dimethyl Formamide." *Asian J. Chem.*, 23, 4, 1474-1478.

Kuriacose, J.C. and Rajaram, J. (1998). "Chemistry in Engineering Technology." Tata Mc Graw-Hill Publishing Company Limited, New Delhi, *High Polymers*, 598.

Li, R., Yu, W. and Zhou, C. (2006). "Phase behavior and its viscoelastic responses of poly(methyl methacrylate) and poly(styrene-co-maleic anhydride) blend systems." *Polym. Bull.*, 56, 455-466.

Macossay, J., Marruffo, A., Rincon, R., Eubanks, T. and Kuang, A. (2007). "Effect of needle diameter on nanofiber diameter and thermal properties of electrospun poly(methyl methacrylate)." *Polymer Adv. Tech.*, 18, 180-183.

Mahendran, O. and Rajendran, S. (2003). "Ionic Conductivity Studies in PMMA / PVdF Polymer blend Electrolyte with Lithium Salts." *Ionics*, 9, 282-288.

Mahendran, O., Chen, S.Y., Yang, Y.W.C., Lee, J.Y. and Rajendran, S. (2005). "Investigations on PMMA-PVdF polymer blend electrolyte with esters of Dibenzoic acids as plasticizers." *Ionics*, 11, 251-258.

Mark, J., Ngai, K., Graessley, W., Mandelkern, L., Samulski, E., Koenig, J. and Wignall, G. (2004). "Physical properties of Polymers." Cambridge University Press, United Kingdom, *The glass transition and the glassy state, Some characterization techniques*, 72-75, 101-114, 387-397.

Mijovic, J., Luo, H.-L. and Han, C.D. (2004). "Property-morphology relationships of polymethylmethacrylate/polyvinylidene fluoride blends." *Polym. Eng. Sci.*, 22, 234-240.

Miyashita, Y., Suzuki, T. and Nishio, Y. (2002). "Miscibility of cellulose acetate with vinyl polymers." *Cellulose*, 9, 215-223.

Nicotera, I., Coppola, L., Oliviero, C. and Ranieri, G.A. (2005). "Rheological properties and impedance spectroscopy of PMMA-PVDF blend and PMMA gel polymer electrolytes for advanced lithium batteries." *Ionics*, 11, 87-94.

Oldak, D., Kaczmarek, H., Buffeteau, T. and Sourisseau, C. (2005). "Photo- and biodegradation processes in polyethylene, cellulose and their blends studied by ATR-FTIR and Raman spectroscopies." *J. Mater. Sci.*, 40, 4189-4198.

Olmos, D. and Benito, J.G. (2006). "Cure process and reaction-induced phase separation in a diepoxy-diamine/PMMA blend. Monitoring by steady-state fluorescence and FT-IR (near and medium range)." *Colloid. Polym. Sci.*, 284, 654-667.

Osman, Z., Ansor, N.M., Chew, K.W. and Kamarulzaman, N. (2005). "Infrared and conductivity studies on blends of PMMA/PEO based polymer electrolytes." *Ionics*, 11, 431-435.

Othman, L., Chew, K.W. and Osman, Z. (2007). "Impedance spectroscopy studies of poly (methyl methacrylate)-lithium salts polymer electrolyte systems." *Ionics*, 13, 337-342.

Park, M.S., Kim, J.K., Ahn, S. and Sung, H.J. (2001). "Water-soluble binder of cellulose acetate butyrate/poly(ethylene glycol) blend for powder injection molding." *J. Mater. Sci.*, 36, 5531-5536.

Pillai, S.O., (2006). "Solid State Physics." New Age International (P) Limited, Publishers, New Delhi, *Dielectrics and Related Properties*, 625-626, 664-666, 681-682.

Puls, S., Wilson, S.A. and Holter, D. (2011). "Degradation of Cellulose Acetate-Based Materials: A Review." *J. Polym. Environ.*, 19, 152-165.

Qian, X., Gu, N., Cheng, Z., Yang, X., Wang, E. and Dong, S. (2001). "Impedance study of (PEO)₁₀LiClO₄-Al₂O₃ composite polymer electrolyte with blocking electrodes." *Electrochim. Acta*, 46, 1829-1836.

Quintana, R., Persenaire, O., Lemmouchi, Y., Sampson, J., Martin, S., Bonnaud, L. and Dubois, P. (2013). "Enhancement of cellulose acetate degradation under accelerated weathering by plasticization with eco-friendly plasticizers." *Polym. Degrad. Stabil.*, 98, 1556-1562.

Rajendran, S. and Mahendran, O. (2001). "Experimental investigations on plasticized PMMA/PVA polymer blend electrolytes." *Ionics*, 7, 463-468.

Rajendran, S. and Uma, T. (2000). "Effect of ZrO₂ on conductivity of PVC-PMMA-LiBF₄-DBP polymer electrolytes." *Bull. Mater. Sci.*, 23(1), 31-34.

Rajendran, S., Bama, V.S. and Prabhu, M.R. (2009). "Effect of lithium salt concentration in PVAc/PMMA-based gel polymer electrolytes." *Ionics*, 16, 27-32.

Rajendran, S., Bama, V.S. and Prabhu, M.R. (2010). "Preparation and characterization of PVAc-PMMA-based solid polymer blend electrolytes." *Ionics*, 16, 283-287.

Ramesh, S. and Arof, A.K. (2001). "Structural, thermal and electrochemical cell characteristics of poly(vinyl chloride)-based polymer electrolytes." *J. Power Sources*, 99, 41-47.

Ramesh, S. and Chao, L.Z. (2011). "Investigation of dibutyl phthalate as plasticizer on poly (methyl methacrylate)-lithium tetraborate based polymer electrolytes." *Ionics*, 17, 29-34.

Ramesh, S., Yahaya, A.H. and Arof, A.K. (2002). "Miscibility studies of PVC blends (PVC/PMMA and PVC/PEO) based polymer electrolytes." *Solid State Ionics*, 148, 483-486.

Ramesh, S., Yahya, A.H. and Arof, A.K. (2002). "Dielectric behavior of PVC-based polymer electrolytes." *Solid State Ionics*, 152, 291-294.

- Rao, V., Ashokan, P.V. and Shridhar, M.H. (1999). "Studies on the compatibility and specific interaction in cellulose acetate hydrogen phthalate (CAP) and poly methyl methacrylate (PMMA) blend." *Polymer*, 40, 7167–7171.
- Rao, V., Ashokan, P.V., Shridhar, M.H. (2000). "Miscible Blends of Cellulose Acetate Hydrogen Phthalate and Poly(vinyl pyrrolidone) Characterization by Viscometry, Ultrasound, and DSC." *J. Appl. Polym. Sci.*, 76, 859–867.
- Salazar, J.M., Camara, J.C.C. and Calleja, F.J.B. (1991). "Mechanical study of poly(vinylidene fluoride) – poly(methyl methacrylate) amorphous blends." *J. Mater. Sci.*, 26, 2579-2582.
- Saq'an, S., Ramadin, Y., Ahmad, M., Zihlif, A., Pavlovska, F.P. and Trajkovska, A. (2001). "Optical and dielectric properties of polyvinylchloride/polymethylmethacrylate blends." *Polym. Test.*, 20, 919–923.
- Schroeder, F.W., Borrajo, J. and Aranguren, I.M. (2007). "Poly(methyl methacrylate)-modified vinyl ester thermosets: Morphology, volume shrinkage, and mechanical properties." *J. Appl. Polym. Sci.*, 106, 4007-4017.
- Selvakumar, M. (2009). "Biodegradation, Electrochemical and Solution Properties of some Polymer systems." Doctoral dissertation, National Institute of Technology Karnataka, Surathkal, India.
- Selvakumar, M. and Bhat, D.K. (2008). "LiClO₄ Doped Cellulose Acetate as Biodegradable Polymer Electrolyte for Supercapacitors." *J. Appl. Polym. Sci.*, 110, 594–602.
- Selvakumar, M. and Bhat, D.K. (2008). "Miscibility of poly(methyl methacrylate) and cellulose acetate butyrate blends in dimethyl formamide." *Indian J. Chem. Techn.*, 15, 547-554.
- Selvakumar, M., Bhat, D.K. and Renganathan, N.G. (2009). "Miscibility of Polymethylmethacrylate and Polyethyleneglycol Blends in Tetrahydrofuran." *J. Appl. Polym. Sci.*, 111, 452-460.
- Shafee, E.E., Saad, G.R. and Fahmy, S.M. (2001). "Miscibility, crystallization and phase structure of poly(3-hydroxybutyrate)/cellulose acetate butyrate blends." *Eur. Polym. J.*, 37, 2091-2104.
- Shonaike, O.G. and Simon, P.G. (1999). "Polymer blends and alloys." Marcel Dekker, Inc., New York, Basel, *Compatibilization of polymer blends, Compounding and*

compatibilization of High-performance polymer alloys and blends, Developments in poly(vinyl chloride)/epoxidized natural rubber blends, 2-3, 23-24, 695.

Sobral, M.C.C.M., Sobral, A.J.F.N., Guthrie, J.T. and Gil, M.H. (2008). "Ketotifen controlled release from cellulose acetate propionate and cellulose acetate butyrate membranes." *J. Mater. Sci.: Mater. Med.*, 19, 677–682.

Soldera, A., Metatla, N., Beaudoin, A., Said, S. and Grohens, Y. (2010). "Heat capacities of both PMMA stereomers: Comparison between atomistic simulation and experimental data." *Polymer*, 51, 2106-2111.

Song, M., Park, M.S., Kim, J.K., Cho, I.B., Kim, K.H., Sung, H.J. and Ahn, S. (2005). "Water-soluble binder with high flexural modulus for powder injection molding." *J. Mater. Sci.*, 40, 1105-1109.

Sperling, L.H. (2001). "Introduction to physical polymer science." John Wiley & Sons, Inc., New York, *Introduction to polymer science*, 1, 17.

Stephan, A.M., Kumar, T.K., Renganathan, N.G., Pitchumani, S., Thirunakaran, R. and Muniyandi, N. (2000). "Ionic conductivity and FT-IR studies on plasticized PVC/PMMA blend polymer electrolytes." *J. Power Sources*, 89, 80–87.

Tanwar, A., Gupta, K.K., Singh, P.J. and Vijay, Y.K. (2006). "Dielectric parameters and A.C. conductivity of pure and doped poly(methyl methacrylate) films at microwave frequencies." *Bull. Mater. Sci.*, 29, 397-401.

Torres, H.V.-. and Ramos, C.A.C.-. (1994). "Poly(vinylidene fluoride)/cellulose acetate-butyrates blends: Characterization by DSC, WAXS, and FTIR." *Polym. Bull.*, 33, 673-680.

Uma, T., Mahalingam, T., Rajendran, S. and Stimming, U. (2003). "Structural and Ionic Conductivity Studies of Solid Polymer Electrolytes Based on Poly (vinylchloride) and Poly (methylemethacrylate) Blends." *Ionics*, 9, 274-281.

Unemoria, M., Matsuya, Y., Matsuya, S., Akashi, A. and Akamine, A. (2003). "Water absorption of poly(methyl methacrylate) containing 4-methacryloxyethyl trimellitic anhydride." *Biomaterials*, 24, 1381–1387.

Utracki, L.A. (2002). "Polymer Blends Handbook." Kluwer Academic Publishers, Dordrecht, Netherlands, *Introduction to polymer blends*, 11-12.

Vallejos, M.E., Peresin, M.S. and Rojas, O.J. (2012). "All-Cellulose Composite Fibers Obtained by Electrospinning Dispersions of Cellulose Acetate and Cellulose Nanocrystals." *J. Polym. Environ.*, 20, 1075-1083.

Yamaguchi, M. and Masuzawa, K. (2008). "Transparent polymer blends composed of cellulose acetate propionate and poly(epichlorohydrin)." *Cellulose*, 15, 17-22.

Yarovoy, Y.K., Wang, H.P. and Wunder, S.L. (1999). "Dynamic mechanical spectroscopy and conductivity studies of gel electrolytes based on stereocomplexed poly(methyl methacrylate)." *Solid State Ionics*, 118, 301–310.

Yoshida, H. (1997). "Structure formation of PVDF/PMMA blends studied simultaneous DSC/FT-IR measurement." *J. Therm. Anal.*, 49, 101-105.

Yuan, X.Y., Zou, L.L., Liao, C.C. and Dai, J.W. (2012). "Improved properties of chemically modified graphene/poly(methyl methacrylate) nanocomposites via a facile in-situ bulk polymerization." *eXPRESS Polymer Letters*, 6(10), 847–858.

LIST OF PUBLICATIONS

1. Sreekantha Jois H. S. and D. Krishna Bhat, (2013). "Miscibility, water uptake, ion exchange capacity, conductivity and dielectric studies of poly(methyl methacrylate) and cellulose acetate blends." J. Appl. Polym. Sci., 130(5), 3074-3081.
2. Denthaje Krishna Bhat and H. S. Sreekantha Jois, (2013). "Miscibility, Conductivity and Dielectric Studies of Poly(methyl methacrylate) and Cellulose acetate propionate Blends." International Journal of Chemical Studies, 1(4), 12-21.
3. Sreekantha Jois H. S. and D. Krishna Bhat, (2013). "Miscibility and conductivity studies of Poly(methyl methacrylate) and Cellulose acetate phthalate blends." Procedia Materials Science, 5, 995-1004.
4. Sreekantha Jois H. S. and D. Krishna Bhat, "Miscibility and conductivity studies of Dimethyl phthalate plasticized Poly(methyl methacrylate) and Cellulose acetate derivatives blends." (Communicated).
5. Sreekantha Jois H. S. and D. Krishna Bhat, "Study on thermal, spectral and electrical properties of Poly(methyl methacrylate) and Cellulose acetate derivatives blends plasticized with Diethyl phthalate." (Communicated).
6. Sreekantha Jois H. S. and D. Krishna Bhat, "Effect of Phthalate plasticizers (DPP and DBP) on Poly(methyl methacrylate) and Cellulose acetate derivatives blends." (Communicated).
7. Sreekantha Jois H. S. and D. Krishna Bhat, "Effect of the addition of Propylene carbonate on the miscibility and conductivity of Poly(methyl methacrylate)/Cellulose derivatives blends." (Communicated).

LIST OF CONFERENCE PRESENTATIONS

1. Sreekantha Jois H. S. and D. Krishna Bhat (2009). "Thermal and microhardness studies of PMMA blends with Cellulose acetate derivatives." National Conference on Recent trends in advanced materials, "RTAM – 2009" held at KVG College of Engineering, Sullia, 18th December 2009.

2. Sreekantha Jois H. S. and D. Krishna Bhat (2010). "Thermal and spectral studies of PMMA and Cellulose acetate derivative blends." International Conference on Emerging Trends in Chemistry, "ETIC-2010" held at Dept. of Chemistry, University of Pune, Pune-411007, Maharashtra, India, 5th – 7th January 2010.
3. Sreekantha Jois H. S. and D. Krishna Bhat (2010). "Spectral and DSC study of Poly(methyl methacrylate) and Cellulose acetate propionate blends." National on Recent Trends in Chemical Research, "NCRTCRC 2010" held at NITK, Surathkal, 8th – 10th March 2010.
4. Sreekantha Jois H. S. and D. Krishna Bhat (2010). "Spectral, Microhardness and Thermal studies of Poly(methyl methacrylate) and Cellulose acetate propionate blends." National Conference on Recent Trends in Chemical and Biological Sciences, "NCRTCBS-2010" held at Kuvempu University, Jnana Sahyadri, Shankaraghatta, 30th – 31st March 2010.
5. Supriya S., Sreekantha Jois H. S. and D. Krishna Bhat (2010). "Spectral and Microhardness studies of Poly(methyl methacrylate) and Ethyl cellulose blends." National Conference on Recent Trends in Chemical and Biological Sciences, "NCRTCBS-2010" held at Kuvempu University, Jnana Sahyadri, Shankaraghatta, 30th – 31st March 2010.
6. Sreekantha Jois H. S. and D. Krishna Bhat (2010). "Differential Scanning Calorimetry and Spectral studies of Poly(methyl methacrylate) and Cellulose acetate butyrate blends." National Conference organized by Indian Council of Chemistry, "ICC-2010" held at Panjab University, Chandigarh, 19th-21st December 2010.
7. Sreekantha Jois H. S. and D. Krishna Bhat (2013). "Miscibility, Spectral and Conductivity studies of Dimethyl phthalate plasticized Poly(methyl methacrylate) and Cellulose acetate blends." International Conference on Recent advances in Material Science and Technology – 2013, "ICRAMST-2013" held at NITK, Surathkal, 17th – 19th January 2013.

CURRICULUM VITAE

SREEKANTHA JOIS H. S.

M.I.G-II, #13, 1st Main, 3rd Phase, KHB colony, Ph: +91-9449542026
Jyothinagar, Chikmagalur-577102. Karnataka, India. sreekanthajois@gmail.com

EDUCATIONAL QUALIFICATIONS

Course	Institute or University	Division	Year
M.Sc.,	Kuvempu University	First	2002-2004
M.Phil.	Alagappa University	First	2007-2008
Ph.D.	National Institute of Technology (NITK), Surathkal	-	2008-

TEACHING EXPERIENCE

College	Year
Tunga Mahavidyalaya, Thirthahalli	2004-2005
Sri Dharmasthala Manjunatheshwara College (Autonomous), Ujire	2005-2008
National Institute of Technology Karnataka, Surathkal	2013-2014 (one semester)

LIST OF PUBLICATIONS

1. Sreekantha Jois H. S. and D. Krishna Bhat, (2013). "Miscibility, water uptake, ion exchange capacity, conductivity and dielectric studies of poly(methyl methacrylate) and cellulose acetate blends." J. Appl. Polym. Sci., 130(5), 3074-3081.
2. Denthaje Krishna Bhat and H. S. Sreekantha Jois, (2013). Miscibility, Conductivity and Dielectric Studies of Poly(methyl methacrylate) and Cellulose acetate propionate Blends." International Journal of Chemical Studies, 1(4), 12-21.
3. Sreekantha Jois H. S. and D. Krishna Bhat, (2013). "Miscibility and conductivity studies of Poly(methyl methacrylate) and Cellulose acetate phthalate blends." Procedia Materials Science, 5, 995-1004.
4. Sreekantha Jois H. S. and D. Krishna Bhat, "Miscibility and conductivity studies of Dimethyl phthalate plasticized Poly(methyl methacrylate) and Cellulose acetate derivatives blends." (Communicated).

-
5. Sreekantha Jois H. S. and D. Krishna Bhat, "Study on thermal, spectral and electrical properties of Poly(methyl methacrylate) and Cellulose acetate derivatives blends plasticized with Diethyl phthalate." (Communicated).
 6. Sreekantha Jois H. S. and D. Krishna Bhat, "Effect of Phthalate plasticizers (DPP and DBP) on Poly(methyl methacrylate) and Cellulose acetate derivatives blends." (Communicated).
 7. Sreekantha Jois H. S. and D. Krishna Bhat, "Effect of the addition of Propylene carbonate on the miscibility and conductivity of Poly(methyl methacrylate)/Cellulose derivatives blends." (Communicated).
-

LIST OF CONFERENCE PRESENTATIONS

1. Sreekantha Jois H. S. and D. Krishna Bhat (2009). "Thermal and microhardness studies of PMMA blends with Cellulose acetate derivatives." National Conference on Recent trends in advanced materials, "RTAM – 2009" held at KVG College of Engineering, Sullia, 18th December 2009.
 2. Sreekantha Jois H. S. and D. Krishna Bhat (2010). "Thermal and spectral studies of PMMA and Cellulose acetate derivative blends." International Conference on Emerging Trends in Chemistry, "ETIC-2010" held at Dept. of Chemistry, University of Pune, Pune-411007, Maharashtra, India, 5th – 7th January 2010.
 3. Sreekantha Jois H. S. and D. Krishna Bhat (2010). "Spectral and DSC study of Poly(methyl methacrylate) and Cellulose acetate propionate blends." National on Recent Trends in Chemical Research, "NCRTCR 2010" held at NITK, Surathkal, 8th – 10th March 2010.
 4. Sreekantha Jois H. S. and D. Krishna Bhat (2010). "Spectral, Microhardness and Thermal studies of Poly(methyl methacrylate) and Cellulose acetate propionate blends." National Conference on Recent Trends in Chemical and Biological Sciences, "NCRTCBS-2010" held at Kuvempu University, Jnana Sahyadri, Shankaraghatta, 30th – 31st March 2010.
 5. Supriya S., Sreekantha Jois H. S. and D. Krishna Bhat (2010). "Spectral and
-

-
- Microhardness studies of Poly(methyl methacrylate) and Ethyl cellulose blends.” National Conference on Recent Trends in Chemical and Biological Sciences, “NCRTCBS-2010” held at Kuvempu University, Jnana Sahyadri, Shankaraghatta, 30th – 31st March 2010.
6. Sreekantha Jois H. S. and D. Krishna Bhat (2010). “Differential Scanning Calorimetry and Spectral studies of Poly(methyl methacrylate) and Cellulose acetate butyrate blends.” National Conference organized by Indian Council of Chemistry, “ICC-2010” held at Panjab University, Chandigarh, 19th-21st December 2010.
 7. Sreekantha Jois H. S. and D. Krishna Bhat (2013). “Miscibility, Spectral and Conductivity studies of Dimethyl phthalate plasticized Poly(methyl methacrylate) and Cellulose acetate blends.” International Conference on Recent advances in Material Science and Technology – 2013, “ICRAMST-2013” held at NITK, Surathkal, 17th – 19th January 2013.
-

COMPUTER SKILLS

Windows and MS-office, ‘C’, MS-Access, Networking and internet, Web development with lab practical from Lakhotia Computer Centre (LCC).

Senior Typewriting Certification (in English) from Karnataka Education Examination Board.

DECLARATION

I hereby declare that the information given by me is true, complete and correct to the best of my knowledge and belief and that nothing has been concealed or distorted.

Place: NITK

Date:

(Sreekantha Jois H. S.)